UNIVERSIDAD EAFIT

Vigilada Mineducación

A Class of Conservative Lagrangian-Eulerian Methods on Triangular Grids for Hyperbolic Problems: Design, Analysis and Applications

Jorge Eliécer Agudelo Quiceno.

Thesis

Advisor: Prof. John Alexander Pérez Sepúlveda, PhD (ITM, Colombia)
Co-Advisor: Prof. Eduardo Abreu (IMECC-UNICAMP, Brazil)
Co-Advisor: Prof. Jose Albeiro Sánchez (EAFIT, Colombia)

UNIVERSIDAD EAFIT
Escuela de Ciencias Aplicadas e Ingeniería
Doctorado en Ingeniería Matemática

Medellín
2024

Abstract

In this thesis, we construct, analyze and implement a class of fully-discrete and semi-discrete schemes on triangular grids intended to numerically solve initial value problems involving multidimensional hyperbolic conservation and balance laws, both scalar and systems. Firstly, the construction of this novel class of schemes is based on the no-flow surface/curve concept and introduces an effective class of numerical fluxes that do not require constructing or evaluating the Jacobian matrix of the respective flux functions. Secondly, the analysis of these new schemes includes the following theoretical results: *i*) convergence proof of fully-discrete and semi-discrete schemes towards the entropy solution of $u_t(\mathbf{x},t)+\mathrm{div}(f(u(\mathbf{x},t)))=0$ with $u_0 \in L^\infty(\mathbb{R}^2)$ following, for fully-discrete schemes, the theoretical results for the uniqueness and regularity properties of the *entropy process solutions* in the $L^\infty_t(L^1_{\mathbf{x}})-$norm introduced by Eymard, Gallouët and Herbin [87,88], and using, for semi-discrete schemes, the *weak asymptotic analysis* developed by Abreu, Colombeau and Panov [17], *ii*) optimal convergence rate for fully-discrete schemes on equilateral triangular grids from the results of Cockburn, Gremaud, and Yang [64], and *iii*) l^2-norm stability of the solutions of the schemes proving that, in the more general context of multidimensional hyperbolic systems of conservation laws, the fully-discrete and semi-discrete Lagrangian-Eulerian schemes on triangular grids satisfy the desired *positivity principle* proposed by Lax and Liu [130, 131], and *the weak positivity principle* introduced in E. Abreu, J. François, W. Lambert and J. Pérez [3]. Finally, the implementation of the new fully-discrete and semi-discrete Lagrangian-Eulerian schemes, using a weak CFL-type stability condition that is independent of the eigenvalues (exact and approximate values) of the relevant Jacobian of the numerical flux functions, and without the need for high-resolution reconstruction procedures, in the solution of nontrivial scalar and systems problems, such as 2D scalar equations with convex and non-convex flux functions (e.g. the sonic point for the inviscid Burgers' equation, and the Buckley-Leverett equation with gravity), the non-classical 2 by 2 three-phase flow system of nonstrictly hyperbolic conservation laws (with resonance/umbilic point), the 2D system of compressible Euler equations (Double Mach Reflection problem and Mach 3 wind tunnel flow), the 3 by 3 shallow-water system (with and without bottom topography), and the 8 by 8 system of Magnethohydrynamic equations (the Orzs-Tang problem), demonstrates their robustness and their capability of capturing accurate qualitative solutions.

Key words: Systems of conservation laws, no-flow surface/curve, Entropy measure-valued solutions, Entropy process solution, Weak asymptotic analisys, Error estimates, Positive Lagrangian-Eulerian method.

List of Figures

List of Tables

Contents

1. Introduction

This thesis is concerned with the construction, analysis and implementation of a new fully-discrete and semi-discrete Lagrangian-Eulerian schemes on triangular grids intended to numerically solve initial value problems involving multidimensional hyperbolic conservation and balance laws, both scalar and systems.

First-order systems of nonlinear hyperbolic conservation laws assume the generic form:

$$\begin{cases} \mathbf{u}_t(\mathbf{x},t) + \nabla \cdot \mathbf{f}(\mathbf{u}(\mathbf{x},t)) &= 0, & \forall \mathbf{x} \in \Omega,\, \forall t \in (0,T], \\ \mathbf{u}(\mathbf{x},0) &= \mathbf{u}_0(\mathbf{x}), & \forall \mathbf{x} \in \Omega, \end{cases} \tag{1.1}$$

where $\Omega \subset \mathbb{R}^d$, $T > 0$, $\mathbf{u}(\mathbf{x},t) : \mathbb{R}^d \times \mathbb{R}_+ \to \mathbb{R}^m$ denotes the vector of dependent (unknown) conserved variables, $\mathbf{f} : \mathbb{R}^m \to \mathbb{R}^{m\times d}$ denotes the flux vector, $u(\mathbf{x},0)$ denotes the initial data vector function, and ∇ denotes the partial derivative operator with respect to space variable $\mathbf{x}$. System (1.1) is called hyperbolic if the flux Jacobian, $\mathbf{Jf}$, is diagonalizable.

Conservation laws express the idea that the change of the total amount of $\mathbf{u}$ in any region is equal to the flux of $\mathbf{u}$, $\mathbf{f}(\mathbf{u})$, across the boundary of that region and they are typically described as multiscale, multiphysics models for a range of complex flow and nonlinear transport phenomena that should be efficiently and accurately modeled.

1.1 Motivating Examples of Systems of Conservation Laws

The theoretical study of nonlinear multidimensional hyperbolic problems, complemented by numerical simulation, has been one of the fascinating subjects in mathematical modeling, since insights can be gained into various natural phenomena modeled through the inviscid equations of hydrodynamics, incompressible Euler flows, relativistic magnetohydrodynamics equations, 3D vorticity equation, Orszag-Tang vortex system, vortex sheet models, vortex street problems, flow in porous media, dynamics of the interface between two fluids, and 2D quasi-geostrophic equations, isentropic system of gas dynamics, shallow water equations with discontinuous bathymetry among other non-trivial multidimensional systems [4, 7, 59, 61, 90, 94, 97, 109, 123, 131, 150–153, 159].

Next, we describe some of these important problems that will be discussed, along with others, in Chapters 2.3 and 3.5 of this work.

1.1.1 3×3 Shallow Water System

The shallow water system [7, 150, 159] is one of the most important models of hyperbolic systems. These equations have many applications, e.g. in hydraulic jumps, tsunamis, riverbeds channels, and reservoirs. The shallow water system is especially useful in numerical methods for weather forecasting and climate modelling.

In this work we consider the shallow water equations in the presence of non-constant bottom topography, given by the system of hyperbolic balance laws:

$$\partial_t \begin{pmatrix} h \\ hu \\ hv \end{pmatrix} + \partial_x \begin{pmatrix} hu \\ hu^2 + \frac{1}{2}gh^2 \\ huv \end{pmatrix} + \partial_y \begin{pmatrix} hv \\ huv \\ hv^2 + \frac{1}{2}gh^2 \end{pmatrix} = \begin{pmatrix} 0 \\ -ghZ_x \\ -ghZ_y \end{pmatrix}, \tag{1.2}$$

where quantity $h = h(x,y,t)$ denotes water height measured from the bottom topography, $Z = Z(x,y)$, with the total height given by $H = h + Z$. Constant g is the gravitational acceleration. The fluid velocities in the $x-$ and $y-$ directions are given by $u = u(x,y,t)$ and $v = v(x,y,t)$ respectively.

These equations, being quasi-linear and hyperbolic, admit discontinuous and piecewise continuous solutions which are called shocks and rarefaction waves, respectively.

The main difficulty often encountered at the simulation of system (1.2), coming from the preservation of steady state solutions and the preservation of water height positivity, in the treatment of the source terms. An essential part for the shallow water system and other conservation laws with source terms is that they often admit steady-state solutions in which the flux gradients are exactly balanced by the source terms. Traditional numerical schemes with a straightforward handling of the source term cannot balance the effect of the source term and the flux, and usually fail to capture the steady state well [96]. They will introduce spurious oscillations near the steady state. The well-balanced schemes are specially designed to preserve exactly these steady-state solutions up to machine error with relatively coarse grids, and therefore it is desirable to design numerical methods which have the well-balanced property [159]. The numerical tests presented in Sections 2.3.8 and 3.5.3 show that fully-discrete and semi-discrete Lagrangian-Eulerian schemes are suitable for dealing with hyperbolic balance laws, showing that they have the well-balanced property.

1.1.2 8×8 System of Magnetohydrodynamic Equations and the equation $\nabla \cdot \mathbf{B} = 0$

Many interesting problems in astrophysics, space physics and engineering, such as gamma-ray bursts, formation of black holes, astrophysical jets, blast waves of supernova, explosions, gravitational collapse and accretion, among others, can be described by magnetohydrodynamic (MHD) equations [32,98,139,147,152,155], and therefore it is of great importance to design accurate and robust numerical methods for such equations. These equations consist of a set of nonlinear hyperbolic conservation laws. Besides the standard difficulty in solving nonlinear hyperbolic equations, one complexity in simulating the MHD system is associated with the interrelation of the performance of schemes and the numerical divergence of the magnetic field. Though the divergence of the exact magnetic field is always zero when it is zero initially, numerical evidence and some analysis indicate that the nonzero divergence of the computed magnetic field can be responsible for numerical instability or nonphysical features in approximated solutions. This has been driving the development of various divergence-cleaning or divergence-free numerical algorithms for MHD equations (see [128] and references therein).

The ideal MHD equations arise when relativistic, viscous, and resistive effects can be neglected and consist of a system of nonlinear hyperbolic equations

$$\partial_t \rho = -\nabla \cdot (\rho \mathbf{v}), \tag{1.3}$$

$$\partial_t (\rho \mathbf{v}) = -\nabla \cdot \left[\rho \mathbf{v}\mathbf{v}^t + \left(p + \frac{1}{2} B^2 \right) \mathrm{I}_{3\times 3} - \mathbf{B}\mathbf{B}^t \right], \tag{1.4}$$

$$\partial_t \mathbf{B} = \nabla \times (\mathbf{v} \times \mathbf{B}), \tag{1.5}$$

$$\partial_t e = -\nabla \cdot \left[\left(\frac{\gamma}{\gamma - 1} p + \frac{1}{2} \rho v^2 \right) \mathbf{v} - (\mathbf{v} \times \mathbf{B}) \times \mathbf{B} \right], \tag{1.6}$$

where, ρ and e represent, respectively, the mass density and the total internal energy, $\mathbf{v} = (v_x, v_y, v_z)^t$ is the velocity field, $v^2 := \|\mathbf{v}\|^2$ and $\mathbf{B} = (B_x, B_y, B_z)^t$ and $B^2 := \|\mathbf{B}\|^2$ represent the magnetic field and its norm. The pressure, p, is coupled to the internal energy, $e = \frac{1}{2}\rho v^2 + \frac{1}{2} B^2 + \frac{p}{\gamma - 1}$, where γ is the (fixed) ratio of specific heats.

The system is augmented by the divergence-free constraint,

$$\nabla \cdot \mathbf{B} = 0, \tag{1.7}$$

that is, if the condition (1.7) is satisfied initially at $t = 0$, then by (1.5) it remains invariant in time.

It is important to point out that one of the main difficulties in numerically solving MHD equations is the non-compliance with the divergence-free constraint (1.7), which can lead to multiple

numerical problems, such as nonlinear instabilities leading to non-physical pressure and density values. In physics, these two quantities are always non-negative. Numerically, their positivity is very important but not always satisfied by the numerical solutions. Non-positivity of density or pressure in MHD simulations turns the discrete problem into an ill-posed problem, causing code breaking [155]. In general, the effects of not controlling the numerical errors arising from the discrete form of the divergence-free constraint have been well-documented in the literature (see [147] and references therein for more details). As shown in Sections 2.3.10 and 3.5.4, the fully-discrete and semi-discrete Lagrangian-Eulerian schemes satisfy both, the divergence-free constraint and the positivity of density and pressure without the need of using correction techniques.

1.1.3 4×4 System of Compressible Euler Equations

In fluid dynamics, the Euler equations [111, 130, 151] for a gas are a set of quasilinear partial differential equations governing adiabatic and inviscid flow. These equations model the evolution of the density, momentum and total energy of a gas and take the form

$$\partial_t \begin{pmatrix} \rho \\ \rho u \\ \rho v \\ E \end{pmatrix} + \partial_x \begin{pmatrix} \rho u \\ \rho u^2 + p \\ \rho uv \\ u(E+p) \end{pmatrix} + \partial_y \begin{pmatrix} \rho v \\ \rho uv \\ \rho v^2 + p \\ v(E+p) \end{pmatrix} = 0, \tag{1.8}$$

where ρ is the density of the gas, p is the pressure, u and v are the $x-$ and $y-$ velocities, respectively, and E is the total energy.

To make the system closed, an equation relating the internal energy e, density and pressure of the fluid is needed. This equation is called, equation of state (EoS). In its general form, the EoS must consider the composition of the gas. Therefore, the EoS should be written as a function

$$e(\rho, p). \tag{1.9}$$

For an ideal gas, the EoS reads

$$p = (\gamma - 1)\left[E - \frac{\rho}{2}(u^2 + v^2)\right], \tag{1.10}$$

where γ is the adiabatic constant of the gas.

The Euler equations model fluid flows with strong shocks, that is, shocks in which there is a substantial entropy production. For flows containing such strong shocks, a careful treatment of these complicated flow discontinuities is of greatest importance in obtaining accurate numerical results.

In particular, there are two important problems modeled by the Euler equations that have been extensively studied because the complicated flow structures and interacting shocks appearing in their solutions make the computing of these flows difficult. These are, the double Mach reflection problem and the Mach 3 wind tunnel problem with a step. The boundary conditions of the double mach reflection problem and, the corner of the step, which is a singularity of the domain boundary and the center of a rarefaction fan, i.e., a singular point of the flow in Mach 3 wind tunnel problem with a step, become important difficulties in these problems. As shown in Section 2.3.9, the main aspects in the simulation of these two problems are well captured by the fully-discrete Lagrangian-Eulerian scheme .

1.1.4 2×2 nonstrictly conservation law in three-phase flow in porous media

Modeling three-phase flows of immiscible fluids in porous media [18, 19, 53, 135] is important in many scientific and industrial areas, including petroleum engineering and hydrogeology, chemical engineering, and nuclear safety.

Oil recovery processes where gases are injected into reservoirs containing oil and water or the remediation of polluted aquifers, among others, are modeled using the equations of three-phase flow in porous media.

Three-phase flow is described by the following system of partial differential equations:

$$\begin{cases} \dfrac{\partial S_w}{\partial t} + \dfrac{\partial f_w^1(S_w,S_g)}{\partial x} + \dfrac{\partial f_g^1(S_w,S_g)}{\partial y} &= 0, \\ \dfrac{\partial S_g}{\partial t} + \dfrac{\partial f_w^2(S_w,S_g)}{\partial x} + \dfrac{\partial f_g^2(S_w,S_g)}{\partial y} &= 0, \\ S_o + S_w + S_g &= 1. \end{cases} \tag{1.11}$$

System (1.11), which generalizes the classical Buckley-Leverett equation and express the conservation of mass of water, oil, and gas, is composed of a pressure equation expressing Darcy's law of force coupled to two saturation equations. S_i is the phase saturation and subscripts w, o, and g refer to the water, oil, and gas phases, respectively. The phase saturation of one of them can be directly obtained from the phase saturations of the others. In this paper, we choose, for convenience purposes, to work with the saturations of water and gas as the primary variables.

In (1.11), f_w and f_g are the flux functions whose components are given by

$$f_w^1 = f_w^2 = \frac{S_w^2}{S_w^2 + \frac{5}{3}S_g^2 + \frac{1}{2}(1-S_w-S_g)^2} \text{ and } f_g^1 = f_g^2 = \frac{S_g^2}{0.6S_w^2 + S_g^2 + 0.3(1-S_w-S_g)^2},$$

respectively.

System (1.11) has solutions that propagate as waves. The propagation speeds of continuous waves are the eigenvalues of the Jacobian derivative matrix $\partial(\mathbf{f}_w, \mathbf{f}_g)/\partial(S_w, S_g)$, provided that these eigenvalues are real. There are two eigenvalues corresponding to each pair of saturations; the smaller is called the slow characteristic speed, and the larger is called the fast characteristic speed. Both are nonnegative in the saturation triangle $\{(S_w, S_g) :\ 0 \le S_w \le 1,\ 0 \le S_g \le 1,\ S_w + S_g \le 1\}$.

If the characteristic speeds coincide or resonate, strict hyperbolicity is lost (i.e., the characteristic speeds fail to be real and distinct) in a particular state in the interior of the saturation triangle called *umbilic point*. On the other hand, if the characteristic speeds are always distinct, a Riemann solution for a system of two equations contains precisely two groups of waves, associated with the slow and fast characteristic speeds. Because the characteristic speeds are not always distinct for three-phase flow, a Riemann solution can have another kind of wave structure, involving a third (transitional) wave group between the slow and the fast wave groups. The occurrence of this third wave group is a remarkable and unusual feature when solving system (1.11). So, correctly capturing the umbilic point and/or the kind of nonclassical shock wave becomes a major challenge and makes the three-phase flow problem mathematically rich [135]. Simulations in Section 2.3.7 show that the fully-discrete Lagrangian-Eulerian scheme correctly capture the complicated structure of the solutions of this problem.

1.2 Notions of Solution for Hyperbolic Equations

The notion of a solution for a hyperbolic partial differential equation is a key part of its study and is closely related to understanding the physics of the problem it models. In this section, we will cover the traditional notions of strong (classical) solution, weak entropy solution and the more modern notions of entropy process solution and weak asymptotic solution.

1.2.1 Strong (Classical) Solution

Definition 1 *A function* $\mathbf{u} : \mathbb{R}^d \times \mathbb{R}_+ \to \mathbb{R}^m$ *is a* ***strong (classical) solution*** *of (1.1) if* $\mathbf{u}$ *is a* C^1-*function that verifies (1.1) pointwise.*

In general, there are no solutions for (1.1) in the classical sense, since solutions of (1.1) with discontinuities may arise in a finite time interval, even if the initial condition of (1.1) is a smooth function [100, 126].

1.2.2 Weak Solution

When solutions of (1.1) form discontinuities such as shock waves, these solutions are sought in the sense of distributions. The existence of these discontinuous solutions leads to the introduction of the concept of *weak solutions* [100, 126] defined bellow.

Definition 2 *Assume that* $\mathbf{u}_0 \in L^\infty_{\text{loc}}(\mathbb{R}^d)^m$, *and* $0 < T < \infty$. *A function* $\mathbf{u} \in L^\infty_{\text{loc}}(\mathbb{R}^d \times (0,T))^m$ *is a* ***weak solution*** *of (1.1) if it satisfies*

$$\int_0^T \int_{\mathbb{R}^d} (\mathbf{u}(\mathbf{x},t)\ \partial_t \varphi(\mathbf{x},t) + \mathbf{f}(\mathbf{u}(\mathbf{x},t)) \cdot \nabla \varphi(\mathbf{x},t))\ d\mathbf{x}\ dt + \int_{\mathbb{R}^d} \mathbf{u}_0(\mathbf{x}) \cdot \varphi(\mathbf{x})\ d\mathbf{x} = 0, \tag{1.12}$$

for any function $\varphi \in C_0^1(\mathbb{R}^d \times (0,T))^m$, *where* C_0^1 *denotes the set of functions* C^1 *with compact support.*

Remark 1 *By construction, any classical solution of (1.1) is also a weak solution. Conversely, by choosing* $\varphi \in C_0^\infty(\mathbb{R}^d \times (0,T))^m$, *we obtain that any weak solution* $\mathbf{u}$ *satisfies (1.1) in the sense of distributions on* $\mathbb{R}^d \times (0,\infty)$. *Moreover, if* $\mathbf{u}$ *happens to be a* C^1 *function, then it is a classical solution.*

1.2.3 Entropy Weak Solution

The weak solution of a conservation law is not necessarily unique. The uniqueness of these weak solutions depends on additional admissibility criteria, termed *entropy conditions*, which guarantee the physically relevant solution. *Entropy solutions*, i.e., weak solutions along with entropy conditions, are widely regarded as the standard solution model for conservation law systems [100, 126, 136] and are defined as follows:

Definition 3 *A function* $\mathbf{u}(\mathbf{x},t) \in L^\infty((0,T) \times \mathbb{R}^d)$ *is a* ***entropy weak solution*** *of (1.1) if it satisfies*

$$\begin{aligned} \int_0^T \int_{\mathbb{R}^d} (\eta(\mathbf{u}(\mathbf{x},t))\ \partial_t \varphi(\mathbf{x},t) + \Phi(\mathbf{u}(\mathbf{x},t)) \cdot \nabla \varphi(\mathbf{x},t))\ d\mathbf{x}\ dt \\ + \int_{\mathbb{R}^d} \eta(\mathbf{u}_0(\mathbf{x}))\varphi(\mathbf{x},0))\ d\mathbf{x} \geq 0, \end{aligned} \tag{1.13}$$

for all $\varphi \in C_0^1(\mathbb{R}^d \times (0,T))$, $\varphi \geq 0$, *for any convex function* $\eta \in C^1(\mathbb{R}^m, \mathbb{R})$, *and* $\Phi \in C^1(\mathbb{R}^m, \mathbb{R}^d)$ *such that* $\Phi_j'(\mathbf{u}) = \mathbf{f}_j'(\mathbf{u})\eta_j'(\mathbf{u})$, $1 \leq j \leq d$.

1.2.4 Entropy Process Solution

The concept of *entropy process solution* was introduced by Eymard, Gallouët and Herbin [87, 89] (see also Barth, Herbin and Ohlberger (2018) [33]) and generalizes the concept of *measure valued-solution* established by DiPerna [79].

The existence of entropy weak solution to problems similar to (1.1) was already proven by passing to the limit on solutions of an appropiate numerical scheme on a uniform rectangular grid, and requires that the initial condition $\mathbf{u}_0$ have locally bounded variation in the sense of Tonelli-Cesaro. In this work, we assume $\mathbf{u}_0 \in L^\infty(\mathbb{R}^d \times (0,T))$ and use triangular grids. Therefore, the bounded variation framework is no longer applicable. Instead, we have to work with the weak

star convergence in L^∞ of a family of approximate solutions. The passage to the limit on the solutions given by a finite volume numerical scheme leads to the existence of a *entropy process solution* to problem (1.1) [89]. This new concept of solution is defined as follows:

Definition 4 *A function $\mathbf{v} \in L^\infty(\mathbb{R}^d \times \mathbb{R}_+ \times (0,1), \mathbb{R}^m)$ is an **entropy process solution** to (1.1) if it satisfies*

$$\int_0^T \int_{\mathbb{R}^d} \int_0^1 (\eta(\mathbf{v}(\mathbf{x},t,\alpha))\, \partial_t \varphi(\mathbf{x},t) + \Phi(\mathbf{v}(\mathbf{x},t,\alpha)) \cdot \nabla \varphi(\mathbf{x},t))\, d\alpha\, d\mathbf{x}\, dt + \int_{\mathbb{R}^d} \eta(\mathbf{u}_0(\mathbf{x}))\varphi(\mathbf{x},0))\, d\mathbf{x} \geq 0, \tag{1.14}$$

for all $\varphi \in C_0^1(\mathbb{R}^d \times (0,T), \mathbb{R}_+)$, for any convex function $\eta \in C^1(\mathbb{R}^m, \mathbb{R})$, and $\Phi \in C^1(\mathbb{R}^m, \mathbb{R}^d)$ such that $\Phi' = \mathbf{f}'\eta'$.

Remark 2 *From an entropy weak solution $\mathbf{u}(\mathbf{x},t)$ to (1.1), one may construct an entropy process solution to (1.1) by setting $\mathbf{v}(\mathbf{x},t,\alpha) = \mathbf{u}(\mathbf{x},t)$ for any $\alpha \in (0,1)$. On the other hand, if $\mathbf{v}$ is entropy process solution to (1.1) such that there exists $\mathbf{u} \in L^\infty((0,T) \times \mathbb{R}^d)$ such that $\mathbf{v}(\mathbf{x},t,\alpha) = \mathbf{u}(\mathbf{x},t)$, for a.e $(\mathbf{x},t,\alpha) \in \mathbb{R}^d \times \mathbb{R}_+ \times (0,1)$, then $\mathbf{u}$ is an entropy weak solution to (1.1).*

1.2.5 Weak Asymptotic Solution

The weak asymptotic method (WAM), introduced by V. Danilov et al. [74, 75] in the framework of the Maslov-Whitham approach, as an efficient mathematical tool to study fully-discrete and semi-discrete schemes, consists of constructing sequences of continuous functions which tend to satisfy asymptotically scalar equations and systems when a small parameter tends to 0. WAM leads to the concept of *weak asymptotic solution* defined bellow.

Definition 5 *For $\boldsymbol{\epsilon} = (\epsilon_1, \epsilon_2) \in (0,\infty)^2$, a weak asymptotic solution for the scalar problem*

$$\begin{cases} u_t(\mathbf{x},t) + \nabla \cdot \mathbf{f}(u(\mathbf{x},t)) = 0, & (\mathbf{x},t) \in \mathbb{R}_+ \times \mathbb{T}^2 \\ u(\mathbf{x},0) = u_0(\mathbf{x}), & \mathbf{x} \in \mathbb{T}^2, \end{cases} \tag{1.15}$$

where $\mathbb{T}^2 = \mathbb{R}^2/\mathbb{Z}^2$, $u : \mathbb{R}_+ \times \mathbb{T}^2 \to \mathbb{R}$, $\mathbf{f} : \mathbb{R} \to \mathbb{R}^2$, and $u_0 \in L^\infty(\mathbb{T}^2)$, is a sequence $u^{\boldsymbol{\epsilon}}(\mathbf{x},t) = u(\mathbf{x},t,\boldsymbol{\epsilon})$ of functions of class $\mathcal{C}^1$ in t and of class L^∞ in $\mathbf{x}$ such that $\forall \psi \in \mathcal{C}_c^\infty\left(\mathbb{R}^2\right)$ and $\forall t$,

$$\lim_{\boldsymbol{\epsilon} \to \mathbf{0}} \int_\Omega [\partial_t u^{\boldsymbol{\epsilon}} \psi - \mathbf{f}(u^{\boldsymbol{\epsilon}}) \cdot \nabla \psi]\, d\mathbf{x} = 0, \tag{1.16}$$

with $\Omega = \text{Supp}\ \psi$, and that satisfies the initial condition $u(\mathbf{x},0,\boldsymbol{\epsilon}) = u_{0,\boldsymbol{\epsilon}}(\mathbf{x})$.

1.3 Some Considerations about Entropy Weak Solutions

Global well-posedness (existence, uniqueness and continuous dependence on initial data) of entropy solutions of scalar conservation laws ($m = 1$ in (1.1)), was established in the pioneering work of Kruzhkov [116]. For one-dimensional systems ($d = 1$, $m > 1$ in (1.1)), global existence, under the assumption of small initial total variation, was shown by Glimm [99] and by Bianchini and Bressan [37]. Uniqueness and stability of entropy-weak solutions (depending Lipschitz continuously on the initial data in the L^1–norm) for one-dimensional systems has also been shown; see [23,47,72] and references therein. As pointed out in [43], in discussing global well-posedness of entropy solutions a very relevant issue is the stability and convergence of several types of approximate solutions.

However, as observed in [43], one major remaining open problem is the convergence of fully-discrete schemes for general hyperbolic systems. In fact, for generic systems of conservation

laws in several spatial dimensions, well-posedness results are more difficult to obtain and global existence and uniqueness (stability) results are not currently available [90, 92, 136]. For instance, the convergence results known for fully-discrete numerical algorithms, such as the Lax-Friedrichs or the Godunov scheme, rely on compensated compactness [158]. They apply only to 2×2 systems, and do not yield information about uniqueness or convergence rates. We mention that in [121], the authors proved a rigorous result of convergence of the approximate solutions via compensated compactness techniques of the approximate solutions toward an entropy solution for one-dimensional $n \times n$ hyperbolic systems of conservation laws, but under the assumptions existence of convex positively invariant domains, genuine nonlinearity and together with the subcharacteristic condition as in [113]. The compensated-compactness approach was used in [107] to prove existence and uniqueness of solutions for one-dimensional $n \times n$ systems of conservation laws which belong to the Temple class, which is heavly dependent on Riemann invariants. However, for general hyperbolic systems, it is known that the Godunov scheme [46] is unstable with respect to the BV norm.

1.4 State of the Art

1.4.1 About the Theoretical Analysis of Numerical Schemes for Hyperbolic Systems of Conservation Laws

Except in some very special cases, there are no explicit formulas for the solution of system (1.1), and therefore it is needed to devise numerical schemes to obtain qualitative solutions of systems of conservation laws.

In spite of the remarkable success of numerical methods in approximating solutions of systems of conservation laws, the fundamental question about the convergence of the numerical schemes approximating (1.1), on grid refinement, is largely unanswered, particularly for several space dimensions. There is no rigorous proof of convergence for any kind of finite volume (difference) and finite element method for the entropy solutions of conservation law systems in both one and several spatial dimensions. Even the stability of numerical approximations to conservation law systems is largely open [136]. Consequently, due to the lack of rigorous stability and convergence results for systems of conservation laws, it has become customary to rely on numerical benchmark tests to demonstrate the convergence of the scheme empirically [92].

On the other hand, the convergence of numerical methods for the scalar problem in one space dimension has been obtained by several authors using some kind of L^∞-stability and "BV-stability" (Total variation diminishing schemes, for instance). In particular, the BV-stability is used to obtain the relative compactness in L^1_{loc} of a family of approximate solutions. This method can be generalized to problems in two spatial dimensions for first order schemes on rectangular grids. Technical difficulties appear when non-rectangular grids are used (i.e triangles or irregular quadrangles). Indeed, the L^∞ result still holds, but it seems that the BV-stability result is no longer valid. The L^∞-stability is not sufficient to prove convergence. Another estimate on the spatial derivatives of the approximate solution (weaker than BV-stability) must be used to prove convergence [57].

Several authors [35, 57, 69], by using the uniqueness result of Diperna [79] to measure-valued solutions of the multi-dimensional scalar equation ($m = 1$ in (1.1)), get some convergence results for finite volume schemes [148].

In [87], using the notions of "Entropy process solution" and "nonlinear weak-$\star$ convergence", the authors proved the existence and uniqueness of an "entropy solution" to the nonlinear scalar hyperbolic equation in d space dimensions ($d \geq 1$):

$$\begin{cases} u_t(\mathbf{x},t) + \operatorname{div}(\mathbf{v}f(u))(\mathbf{x},t) = & 0, & \mathbf{x} \in \mathbb{R}^d,\ t \in \mathbb{R}_+ \\ u(\mathbf{x},0) = & u_0(\mathbf{x}), & \mathbf{x} \in \mathbb{R}^d, \end{cases}$$

where $\mathbf{v} \in C^1(\mathbb{R}^d \times \mathbb{R}_+, \mathbb{R}^d)$ and $f \in C(\mathbb{R}, \mathbb{R})$, by passing to the limit of the approximate solutions

given by a finite volume schemes on general grids in two or three space dimensions.

In [56], using the ideas developed in [87], the author proved the convergence of a family of approximate solutions given by a finite volume schemes on general grids in several space dimensions towards the entropy solution to the scalar problem:

$$\begin{cases} u_t(\mathbf{x},t) + \operatorname{div}(\mathbf{f}(\mathbf{x},t,u(\mathbf{x},t))) = & 0, & \mathbf{x} \in \mathbb{R}^d,\ t \in \mathbb{R}_+ \\ u(\mathbf{x},0) = & u_0(\mathbf{x}), & \mathbf{x} \in \mathbb{R}^d. \end{cases}$$

Additionally, it was widely believed [136] that well-designed numerical methods for approximating the problem (1.1) in several space dimensions also converge to the entropy solution on grid refinement. However, the appearance of oscillations in the solution at finer and finer scales under grid refinement, the unstable behaviour of these oscillations with respect to grid resolution, the numerical method and the small initial perturbations may prevent convergence of the scheme [94] to an entropy solution of the multi-dimensional system (1.1). So, in order to characterize the limits of numerical schemes for (1.1), an alternative solution paradigm is required [94].

Another issue of significant importance with respect to (1.1) is that finding non-smooth solutions to nonlinear equations such as certain asymptotic problems, the description of shock waves and vorticities is not easy since, due to the nonlinearity, the search for such solutions eventually reduces to the problem of multiplying distributions (generalized functions) [76].

An analytical approach to finding generalized strongly singular solutions to nonlinear equations is the so-called *weak asymptotic method* (WAM). The WAM, introduced by V. Danilov et al. [74,75] in the framework of the Maslov-Whitham approach, allows to investigate the dynamics of propagation of various types of singularities of quasilinear differential equations and hyperbolic first order systems.

WAM was used for constructing sequences of continuous functions which tend to satisfy asymptotically scalar equations (one dimensional hyperbolic equation [17] and multidimensional degenerate parabolic equation [14]) when a small parameter tends to 0. Specifically, WAM allowed to show that these sequences tend to satisfy the equation(s) in the strong sense in time and in the weak sense in space.

Regarding the theory of error estimates for scalar conservation laws, its historical development begins with the seminal work of Kuznetsov [117]. In this work, Kuztnezov, considering monotone schemes in uniform Cartesian grids, proved that the total variation and the uniform norm are uniformly bounded with respect to Δx, and concluded that such schemes converge as $(\Delta x)^{1/2}$ to the entropy solution in the $L^\infty(L^1)$-norm. This pioneering work strongly influenced the subsequent studies for numerical schemes for the problem (1.1) (see [66] and references cited therein).

It soon became apparent that progress along the above approach was going to be very hard to achieve since even the simplest schemes, the monotone schemes, could not be proven to generate approximate solutions with uniformly bounded total variation when defined in general triangulations [66]. Therefore, to overcome this drawback, in [67], using a suitable modification of Kuznetsov's approximation result, the authors proved that monotone schemes defined in general triangulations converge to the entropy solution with a rate of no less than $(\Delta x)^{1/4}$ in the $L^\infty(L^1)$-norm.

On the other hand, estimates on the convergence rate for a deterministic version of the Glimm scheme [99, 129] were derived in [48], and more recently in [24, 137] for a wider class of flux functions. Based on the techniques introduced by Bressan and Yang in [45] for systems of conservation laws, rate of convergence for vanishing viscosity approximations to strictly hyperbolic and genuinely nonlinear systems of balance laws in one space dimension was established in [62]. Additional convergence results were proved by Bianchini for approximate solutions constructed by the semi-discrete (upwind) Godunov scheme [38], and by the Jin-Xin relaxation model [36]

In [66], the authors construct a general theory of *a priori* error estimates for multidimensional

scalar conservation laws by suitably modifying the original Kuznetsov approximation theory. In [65], applying this theory and using a suitable definition of *consistency*, they obtain the optimal rate of convergence of $(\Delta x)^{\frac{1}{2}}$ in $L^{\infty}(L^{1})$-norm for one dimensional flux-splitting consistent monotone schemes in nonuniform Cartesian grids. In [64], they consider multidimensional flux-splitting consistent monotone schemes on non-Cartesian grids multidimensional, identify those schemes which are consistent and prove that the $L^{\infty}(L^{1})$-norm of the error goes to zero as $(\Delta x)^{\frac{1}{2}}$ when the parameter Δx goes to zero.

Finally, it is important to highlight that, besides the approach used in this work to numerically solve multi–dimensional systems of conservation laws, there exist other alternative solution paradigms. One of such paradigms used a statistical approach based on the notion of entropy statistical solutions. Entropy statistical solutions, which were first proposed by Foias in the context of the incompressible Navier-Stokes equations of fluid dynamics, are time–parametrized probability measures on a given infinite-dimensional function space. Under additional entropy conditions, the existence and uniqueness of this kind of solutions can be demonstrated. For more details, see [93] and reference therein.

1.4.2 About the Lagrangian-Eulerian schemes on Cartesian Grids for Hyperbolic Equations

A variety of efficient numerical schemes for hyperbolic conservation laws – scalar and systems – in one and several spatial dimensions have been developed in the recent past for different problem settings [23, 30, 35, 87, 102, 115, 126, 127, 144]. These schemes evolved following the natural understanding of fundamental concepts from the theory of nonlinear hyperbolic conservation laws concerning the properties of the characteristic surfaces, existence, uniqueness, and solution of the Riemann problem.

As an important development in the context of accurate numerical methods that reduce numerical diffusion and eliminate oscillations in the numerical solutions, different Eulerian-Lagrangian schemes, for the time discretization of advection-dominated diffusion equations, have been developed: Modified Method of Characteristics (MMOC) [86], Modified Method of Adjusted Advection Characteristics (MMOCAA) [22, 83], Eulerian-Lagrangian Localized Adjoint Methods (ELLAM) [29, 39, 54, 55, 73, 106, 142, 149] and Locally Conservative Eulerian-Lagrangian Methods (LCELM) [10, 12, 15, 80–82, 134].

In an effort to develop fast, accurate and stable versions of MMOC methods for transport dominated broadcasting systems, in [81] was identified the region in the space-time domain where the mass conservation takes place, but linked to a scalar convection-dominated nonlinear parabolic problem, which models the immiscible incompressible two-phase flow in a porous medium. The key ingredient in finding this conservative region was the use of an Eulerian-Lagrangian framework.

In [81, 112], the authors applied the LCELM to both linear [25, 26, 112] and nonlinear [81, 84, 85] flow and transport problems showing that this Eulerian-Lagrangian approach provides a very precise solution to purely advection problems, practically free of numerical diffusion. Later on, in a sequel paper [27] - see also [25] and the references cited therein -, the authors discussed a formal presentation, without rigorous mathematical proof of convergence, of a new type of Lagrangian formulation for solving purely linear hyperbolic radionuclide transport problems in which, in turn, the space-time integral curves coincide with the characteristic equations. This new scheme was named Forward Integral Tube Tracking. A similar but different approach can be found in [28, 112].

With the aim to numerically solve transport models with source terms and balance law systems and related applications, the above innovative ideas were explored in the PhD thesis [140] to give a rigorous construction of a new class of accurate Lagrangian-Eulerian schemes. These new schemes were constructed using a spatial-time region, where the local conservation takes place, called *the no-flow region*. This novel concept, substantially different from the concept of *integral tube* discussed in [25–27, 81, 84, 85], was supported by theoretical foundations. Besides, as a significant contribution of this work, the proof of convergence of this novel class of Lagragian-Eulerian schemes towards entropy solution of nonlinear scalar hyperbolic conservation was carried out using the

Harten's theory and the Majda and Crandall's theory.

In [12, 15], the authors used the Lagrangian-Eulerian approach developed in [140] to construct a fully-discrete scheme to study scalar conservation law problems in one and two dimensions and hyperbolic equation systems in one spatial variable. In particular, in [15], a fully-discrete Lagrangian-Eulerian scheme was used to discuss the hard case of a one-dimensional balance law with discontinuous source term in the space variable. The one-dimensional fully-discrete Lagrangian-Eulerian scheme used in [15] was extended in [10] to solve systems of balance laws and hyperbolic problems in two dimensions. This new Lagrangian-Eulerian scheme was embedded in the classical theory of monotone schemes allowing to show that the scheme converges to entropy solutions linked to the purely hyperbolic counterpart. The application of this new class of Lagrangian-Eulerian schemes in several nontrivial problems in one and two spatial dimensions on Cartesian grids throughout these works showed that these schemes capture qualitatively correct solutions with accurate resolution.

Unlike existing classical methods, which are based on the strong form of the problem and track back in time the characteristic curves at each time interval, the Lagrangian-Eulerian methods dynamically track forward the no-flow region (by step of time). This is the key to avoid altogether the use of Riemann solvers. Furthermore, in the method of the characteristics, widely used in the construction of numerical schemes, the backward-projected characteristic curves do not necessarily intersect the surface of the known solution at prespecified grid points (by time step). Therefore, the initial data on the backward-projected features must be determined by [81] interpolation, and since hyperbolic problems are not, in general, reversible systems, this situation for multidimensional conservation law systems is not well understood. Consequently, the definition of the backward projected characteristics is extremely complicated or simply impossible given the nonlinear and focused interaction of the waves. Also, since the method of characteristics is based on the strong form of the differential equation, it is not valid after shock formation or wave breaking, which is common in hyperbolic problems. The Lagrangian-Eulerian methods do not suffer from these drawbacks, which represents a substantial contribution to the current state of knowledge in the hyperbolic equations area.

On the other hand, as a way to improve/reduce the diffusion effects that occur in fully-discrete schemes, in recent decades different semi-discrete schemes have been designed to numerically solve problems associated with hyperbolic conservation law systems and related problems dominated by convection. Some of these schemes include Runge-Kutta discontinuous Galerkin method [70], central semi-discrete scheme [118, 120] and Godunov type semi-discrete central scheme [119], spectral methods for hyperbolic problems [103], semi-Lagrangian methods [138] and arbitrary Lagrangian-Eulerian methods [132], among others. Due to the separation of time and space discretization processes, semi-discrete schemes are very flexible and their construction becomes a suitable strategy for deriving higher-order schemes. In fact, the semi-discrete formulation can separately increase the order of spatial and temporal precision, and thus the semi-discrete schemes can be used efficiently using as small time steps as necessary [120].

Inspired by the advantages of semi-discrete schemes, in [3], based on the novel concept of *no-flow curves* (no-flow region lateral boundaries), a new semi-discrete Lagrangian-Eulerian scheme was introduced and analyzed to solve initial value problems associated with scalar conservation laws in one dimension. In [4], a new semi-discrete Lagrangian-Eulerian scheme on Cartesian grids was designed and discussed for solving scalar hyperbolic problems and hyperbolic systems in several dimensions. In both papers, the weak asymptotic method was successfully used to prove the convergence and stability of the solutions from the semi-discrete Lagrangian-Eulerian schemes for scalar problems and systems of conservation laws in one and two dimensions on Cartesian grids, giving a new sense of definition for the solution. In addition, several numerical tests for nontrivial and nonlinear hyperbolic problems arising in fluid dynamics were discussed. These numerical experiments confirmed robustness of this class of positive semi-discrete schemes and showed their feasibility in a wide range of applications.

In short, the Lagrangian-Eulerian schemes [3, 4, 8, 10–12, 15–17] have been successfully employed in a number of non-trivial problems and has also been theoretically developed with its link to several

transport models and interesting engineering studies such as Euler's System of Compressible Gas Dynamics, Hydrogen Energy, Chemical Engineering, Biology and Medicine, and molecular liquids, thus showing that it is able to compute qualitatively correct (entropy) solutions involving intricate nonlinear wave interactions of rarefaction and shock waves (see [14] and references cited therein).

1.5 Motivation and Significance of the Thesis

As discussed in the preceding section, the theory for multidimensional scalar equations and systems of strictly hyperbolic conservation laws in one space variable is well developed and understood [72, 102, 124–126, 146]. However, for general multidimensional systems, the issue of existence, uniqueness and continuous dependence on initial data is not well stablished, and is still in full progress with several open questions, and only partial results are avaliable for certain non-trivial special cases. [21, 23, 43, 51, 59, 60, 71, 77, 78, 90, 108, 136, 143].

On the other hand, due to the complexity of wave interactions that make evolution complicated, in general, it is not possible to derive exact solutions to these equations, and therefore numerical methods are needed to simulate their approximate solutions, which besides being enormously useful quantitatively, there is the possibility that they can be used to demonstrate the existence of solutions [124]. In this sense, the numerical study of the systems of conservation laws in some depth is justified because [21, 43, 59, 77, 108, 127, 143]:

- Many practical problems in science and engineering involve conserved quantities and lead to systems of conservation laws.
- There are special difficulties associated with solving these systems (e.g. shock formation) that are not seen elsewhere and must be dealt with carefully in developing numerical methods.
- Although few exact solutions are known, much is known about the mathematical structure of these equations and their solution. This theory can be exploited to develop special methods that overcome some of the numerical difficulties encountered with a more naive approach.

In consequence, the design of new and feasible schemes for multidimensional systems are crucial to improve the understanding of the qualitative structure of their solutions, and to acquire new knowledge and new techniques to obtain advances regarding the existence, uniqueness, and continuous dependence on the initial data of hyperbolic systems of conservation laws.

According to the reasons explained, and motivated by the robustness, precision, and effectiveness of the Lagrangian-Eulerian approach in the construction of efficient numerical schemes for one-dimensional and multidimensional hyperbolic problems mentioned above, and based on the improved concept of no-flow curves presented and studied with a solid mathematical foundation for fully-discrete and semi-discrete Lagrangian-Eulerian schemes on Cartesian grids [3, 4, 7, 8, 10], in this thesis, following a Lagrangian-Eulerian approach, we propose a new class of fully-discrete and semi-discrete schemes on triangular grids for numerically solve scalar hyperbolic conservation laws and systems, in two dimensions. As in [10], the space-time no-flow surfaces (two-dimensional extension of no-flow curves) construction, per time step, is the key ingredient for the fully-discrete and semi-discrete schemes on triangular grids.

The construction of the new fully-discrete Lagrangian-Eulerian scheme on triangular grids is based on the approximation of the flux integral,

$$\int_{\partial\Re} [\mathbf{f}(u) \;\; u]^{\top} \cdot \mathbf{n}_{KL}\, d(\partial\Re). \tag{1.17}$$

Eq. (1.17) arises from integrating $\nabla_{\mathbf{x},t} \cdot [\mathbf{f}(u) \;\; u]^{\top} = 0$ over a *non-rigid space-time* control volume, after applying the divergence theorem in a *suitable space-time region*, $\Re$, for each element K in the triangulation $\mathcal{T}$ of the domain $\Omega \in \mathbb{R}^2$ [10, 14]. The vector, $\mathbf{n}_{KL}$, is an outward unit normal vector to the interface between the elements K and L of $\mathcal{T}$. That is, the new fully-discrete and semi-discrete schemes on triangular grids are based on the divergent form of the equation and

preserves certain integral identities satisfied by the solution of the differential system governing the considered flow problem.

As in [3, 4], in this thesis, the new concept of the no-flow surface/curve is used to replace, in the numerical flux function, a quantity of numerical dissipation that depends on $\mathcal{O}([h/\Delta t])$ by stability estimates of the type $\mathcal{O}([\mathrm{Sup}\,|\mathbf{f}(u)/u\cdot\mathbf{n}|])$, where h is the grid spatial step, $\mathbf{n}$ is an outward unit normal vector to each element of the triangulation, and the "Sup" is taken on the values of u and $\mathbf{n}$. An interesting feature of construction of the the Lagrangian-Eulerian no-flow surfaces/curves is that, for a general class of hyperbolic flux for scalar problems and systems, the matrices are symmetric for free (actually, they are diagonal). Besides, they allow to obtain an accurate approximation of the local speeds of wave propagation in the control volumes.

Thanks to the fact that the stability coefficient of the Lagrangian-Eulerian numerical flux function, i.e., $\underset{u,\mathbf{n}}{\mathrm{Sup}}\,|\mathbf{f}(u)/u\cdot\mathbf{n}|$, does not depend on $\mathcal{O}(1/\Delta t)$ and therefore, does not have a blow-up singularity as Δt goes to 0, the new semi-discrete Lagrangian-Eulerian scheme on triangular grids is constructed from the fully-discrete scheme taking the limit as $\Delta t \to 0^+$ over this. This allows us to show the robustness and effectiveness of the no-flow surfaces/curves.

The extension of the fully-discrete and semi-discrete Lagrangian-Eulerian schemes on triangular grids to systems is carried out through a straightforward componentwise application of the multidimensional scalar space-time no flow surfaces/curves construction.

As can be seen, the construction of the fully-discrete and semi-discrete Lagrangian-Eulerian schemes on triangular grids, via no-flow surfaces/curves, is free of field-to-field constraints, does not require the use of eigenvalues (exact or approximate), and leads to the design of an effective and computationally stable numerical flux function in the conservative form and of a weaker CFL stability condition. Computationally speaking, such schemes appear to be useful both for solving hyperbolic systems with complex eigenvalues or weak hyperbolic multidimensional systems, and for obtaining information about the behavior of the solutions.

The main advantages of these new Lagrangian-Eulerian schemes are: *i*) independence of their numerical fluxes from the Jacobian matrix of the flux function of the hyperbolic equation involved, *ii*) simple implementation, since no (local) Riemann problems are solved and hence, time-consuming field-by-field decompositions to trace the direction of the wind (particularly in the case of systems) are avoided, *iii*) low complexity in the algorithm design, since no high-resolution non-oscillating interpolation reconstructions (widely used in central differentiation schemes) are performed, *iv*) easy component-wise extension from the scalar framework to multidimensional conservation law systems thanks to the no-flow surfaces, and *v*) validity for higher dimensions.

It is also important to emphasize that, the new Lagrangian-Eulerian schemes on triangular grids to numerically solve nonlinear multidimensional systems of conservation/balance laws are substantially different from other classical numerical schemes, such as the *Osher-Solomon Numerical Flow*, the *Roe Flow*, the *Steger-Heating flux vector division*, and *local Lax-Friedrichs flux* (see, for example, Section 6.1.2 in [33] as well as in the vast literature [101, 114, 126, 146] for comparison purposes) since the numerical fluxes only depend on the flux functions and therefore, the flux functions Jacobian matrix is neither constructed nor evaluated.

Finally, the Lagrangian-Eulerian schemes are ideally suited to address the difficulties arising in Gudonov-type Finite Volume or Discontinuous Galerkin discretization approaches due to the non-autonomous flux functions that appear in balance law systems caused by the presence of spatially dependent geometric information [41,141] (see also [2,52] and the references cited therein) and source terms containing flux (discontinuous) variables. In particular, source terms containing flux (discontinuous) variables yield to discontinuous local Riemann problems (for schemes based on Riemann solvers (exact or approximate), the handling of non-autonomous fluxes is still an open question) and complicate the identification of the correct wave structure and interaction that is needed in these approaches. The Lagrangian evolution and Eulerian remapping steps, in Lagrangian-Eulerian schemes, automatically handle the non-autonomous fluxes, avoiding the use of moving grids, and allowing the use of a single mesh while maintaining local conservation (see [2] and references therein).

1.6 Meaningful Contributions of the Thesis

In this thesis, using the novel concept of *the no-flow surface/curve*, we propose a new class of fully discrete and semi-discrete Lagrangian-Eulerian schemes on triangular grids to numerically solve multidimensional hyperbolic conservation and balance laws, both scalar and systems, whose numerical fluxes do not require constructing or evaluating the Jacobian matrix of the respective flux functions. The originality and novelty of this thesis lie in the following aspects:

1. Design of a new class of fully-discrete Lagrangian-Eulerian schemes on triangular grids as a natural extension of the one-dimensional fully-discrete Lagrangian-Eulerian scheme previously introduced in [140] and studied for specialized settings in [7, 10, 12, 15].

2. The *no-flow surface/curve* as a key ingredient to design, from the new fully-discrete scheme on triangular grids, a new class of semi-discrete schemes on triangular grids.

3. Theoretical analysis of the fully-discrete schemes supported by the convergence proof of the numerical solutions given by the family of schemes towards the entropy solution of $u_t(\mathbf{x},t)+\text{div}(f(u(\mathbf{x},t)))=0$ with $u_0 \in L^\infty(\mathbb{R}^2)$, being analyzed in the setting of uniqueness and regularity properties of the *entropy process solutions*, and the obtaining of an optimal error estimate in the $L^\infty_t(L^1_{\mathbf{x}})$-norm as $\mathcal{O}(h^{\frac{1}{2}})$ on equilateral triangular grids using the general theory of a priori error estimates for scalar conservation laws, developed by Cockburn et al.

4. Theoretical analysis of the semi-discrete schemes supported by the convergence proof of the scheme towards the entropy solution of $u_t(\mathbf{x},t)+\text{div}(f(u(\mathbf{x},t)))=0$ with $u_0 \in L^\infty(\mathbb{R}^2)$, using the *weak asymptotic analysis*.

5. l^2 norm stability of solutions of the schemes guaranteed by the proof that fully-discrete and semi-discrete schemes satisfy the *positivity principle* [130, 131] and the *weak positivity principle*, introduced in [4].

6. Use of a CFL-type stability condition in the implementation of the schemes, which does not require the need to employ the eigenvalues (exact and approximate values), avoiding the calculation of the Jacobian of the numerical flux functions.

7. The robustness, ease of implementation, and the capability of the new locally conservative Lagrangian-Eulerian schemes on triangular grids of capturing correct solutions for scalar and systems nontrivial multidimensional models such as 2D scalar equations with convex and non-convex flux functions (e.g. the sonic point for the inviscid Burgers' equation, and the Buckley-Leverett equation with gravity), the non-classical 2 by 2 three-phase flow system of nonstrictly hyperbolic conservation laws (with resonance/umbilic point), the 2D system of compressible Euler equations (Double Mach Reflection problem and Mach 3 wind tunnel flow), the 3 by 3 shallow-water system (with and without bottom topography), and the 8 by 8 system of Magnethohydrynamic equations (the Orzs-Tang problem).

1.7 Objectives

1.7.1 General Objective

Analyze a class of fully-discrete and semi-discrete locally conservative Lagrangian-Eulerian schemes on triangular grids, constructed from the novel concept of no-flow surface/curve, to numerically solve two-dimensional hyperbolic problems of conservation and balance laws, both scalar and systems, which contribute to a broader understanding of the multidimensional hyperbolic problems both from the numerical and theoretical point of view.

1.7.2 Specific Objectives

1. Improve the concept of no-flow surface in triangular grids from its concept in Cartesian grids.
2. Construct, using the no-flow surface/curve concept, a new class of fully-discrete and semi-discrete locally conservative Lagrangian-Eulerian schemes to numerically solve conservation laws and systems of conservation laws in two spatial dimensions on triangular grids.
3. Justify, theoretically, the schemes. This includes, convergence proof for the fully-discrete and semi-discrete scheme, convergence order of the fully-discrete scheme, and proof that both schemes (fully and semi-discrete) satisfy the principles of *positivity* and *weak positivity*.
4. Implement the new class of locally conservative Lagrangian-Eulerian schemes to solve nontrivial scalar problems numerically.
5. Extend the constructed schemes to two-dimensional hyperbolic law systems, and implement them to solve related nontrivial problems numerically.

1.8 Thesis Content and Structure

The theoretical study of (1.1) complemented by numerical simulation has been one of the fascinating subjects in mathematical modeling as one can gain insights into several natural phenomena [4, 7, 59, 61, 90, 94, 97, 109, 123, 131, 150–153, 159]. Thus, the construction of novel approaches and the design of new numerical methods, to extract useful features from nonlinear multidimensional hyperbolic problems, is naturally challenging, and the research, in the field during the past few decades to the present, is progressing (see, e.g., [4, 7, 33, 34, 40, 42, 58, 90, 92–94, 97, 101, 110, 114, 126, 146, 152, 153, 156, 157] and the references cited therein).

In this context, in this thesis, we design, analyze, and implement a class of positive fully-discrete and semi-discrete Lagrangian-Eulerian schemes on triangular grids for initial value problems involving two-dimensional hyperbolic conservation laws and related problems. These schemes are designed from a novel Lagrangian-Eulerian approach for space-time discretization based on the concept of *no-flow surface/curve* (see Figure 1.1), that has been previously presented and analyzed for fully-discrete monotone-type schemes [7–10, 12] and semi-discrete schemes [3, 4] in Cartesian grids. In those works, the concept of *no-flow surface/curve* is clarified and improved by establishing the connection between a generalized system of ordinary differential equations related to it (the *no-flow surface*) and a new way to construct/extract a numerical flux function for triangular grids that satisfies the properties of monotony, conservativity, and consistency related to finite volume schemes.

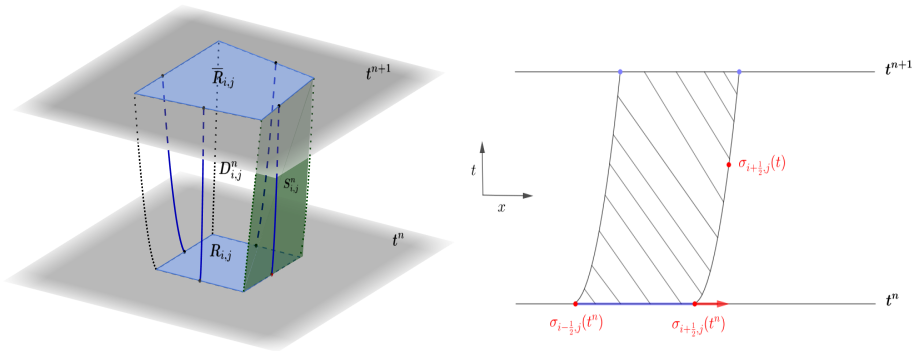

Figure 1.1: 2D no-flow surfaces (left); the projection of one of them on the $x-t$ plane (right).

This thesis is organized as follows. In Chapter 2, we discuss the construction, theoretical analysis, and implementation of a fully-discrete Lagrangian-Eulerian scheme on triangular grids

from the novel concept of *non-flow surface/curve*, as the main ingredient for the construction of the Lagrangian-Eulerian schemes. Through the *theory of the entropy process solution*, a rigorous convergence proof of the fully-discrete Lagrangian-Eulerian scalar scheme is carried out. We obtain its order of convergence and prove that it satisfies the desired *positivity principle*, both in the strong and the weak sense. Additionally, nontrivial numerical tests are presented. Chapter 3 deals with the construction of a semi-discrete Lagrangian-Eulerian scheme from the fully-discrete scheme, its convergence via the *weak asymptotic method*, and the proof that it satisfies the *positivity principle* in both the strong and weak senses, and its implementation in several scalar hyperbolic problems and systems. Chapter 4 concludes the work and gives an outlook on further research questions.

1.9 Publications

During the development of this thesis, the following outputs were achieved:

1. Abreu, E., Agudelo, J., Lambert, W., & Pérez, J. A Lagrangian–Eulerian Method on Regular Triangular Grids for Hyperbolic Problems: Error Estimates for the Scalar Case and a Positive Principle for Multidimensional Systems. Journal of Dynamics and Differential Equations, 1-66, 2023.
2. Abreu, E., Agudelo, J., & Pérez, J. A triangle-based positive semi-discrete Lagrangian–Eulerian scheme via the weak asymptotic method for scalar equations and systems of hyperbolic conservation laws. Journal of Computational and Applied Mathematics, 437, 115465, 2024.

In addition, the following lectures were presented:

1. J. Agudelo (Presenter), Una formulación naturalmente conservativa para leyes de Conservación Hiperbólicas en dos dimensiones. IV Encuentro Internacional de Matemáticas, Estadística y Educación Matemática. Tunja, 2019.
2. J. Agudelo (Presenter), A Lagragian-Eulerian scheme on triangular grids for Hyperbolic Problems with source terms. Challenges in Numerical Analysis and Scientific Computing. University of Minho, Braga, Portugal, 2022.

2. The Fully-Discrete Lagrangian-Eulerian Schemes on Triangular Grids: Theoretical Foundations, Design, Analysis, and Implementation

This chapter introduces the Lagrangian-Eulerian framework for the construction of locally conservative fully-discrete schemes to numerically solve Hyperbolic Conservation Laws that do not require the calculation of eigenvalues of the Jacobian matrix of the hyperbolic equation flux function, and all possible theoretical results including: convergence proof to the entropy solution for scalar problems, convergence rates on equilateral grids, and posivity principle for systems.

2.1 Theoretical Foundations of the Fully-Discrete Lagrangian-Eulerian schemes on Triangular Grids

For the sake of a clear understanding, we restrict the explanation of the approach to one spatial dimension. A more in-depth study of the mathematical foundations of the Lagrangian-Eulerian approach can be consulted in [10, 14, 16, 20].

2.1.1 Presentation of the No-Flow Curves

Let us consider the initial value problem

$$\begin{cases} u_t(x,t) + f(u(x,t))_x &= 0, & \forall x \in (-\infty,\infty),\ \forall t > 0, \\ u(x,0) &= u_0(x), & \forall x \in (-\infty,\infty). \end{cases} \tag{2.1}$$

We first consider Eq. (2.1) written in locally conservative space-time generalized divergence form, along with $u(0,x) = u_0(x)$,

$$\nabla_{x,t} \cdot \begin{bmatrix} f(u) \\ u \end{bmatrix} = 0, \quad t > 0, \quad x \in (-\infty,\infty). \tag{2.2}$$

For the finite dimensional function spaces on which the problem associated with (2.1) is numerically solved, we introduce the standard notation presented below. Space region $\mathbb{R} \times \overline{\mathbb{R}} = \{(x,t) : -\infty < x < \infty,\ t > 0\}$ is replaced by lattice $\mathbb{Z} \times \mathbb{N} = \{(j,n) : j = 0, \pm 1, \pm 2, \ldots;\ n = 0, 1, 2, \cdots\}$. In addition, we consider sequence $U^n = (U_j^n)$ for a given grid, $\Delta x > 0$, and the following time level:

$$t^n = \sum_{j=0}^{n} \Delta t^j, \quad \text{with } t^0 = 0, \tag{2.3}$$

for a non-constant time step, Δt^j, that is subject to a new weak Courant-Friedrichs-Lewy (CFL) condition.

As shown in figure 2.1, at time level t^n, on the uniform local grid —or primary grid —, we have $x_j^n = ih$ and $x_{j\pm\frac{1}{2}}^n = j\Delta x \pm \frac{\Delta x}{2}$, where x_j^n are the centers of the cells $\left[x_{j-1/2}, x_{j+1/2}\right]$ of lenght $h = \Delta x = h_j^n = x_{j+\frac{1}{2}}^n - x_{j-\frac{1}{2}}^n$ and, at time level t^{n+1}, on the non-uniform grid —or induced grid —composed by the cells $\left[\overline{x}_{j-1/2}, \overline{x}_{j+1/2}\right]$, we have $h_j^{n+1} = \overline{\Delta x}^{n+1} = \overline{x}_{j+\frac{1}{2}}^{n+1} - \overline{x}_{j-\frac{1}{2}}^{n+1}$.

For all $j \in \mathbb{Z},\ n \in \mathbb{N}$, the approximate solution of u to (2.1) in each cell of both grids (the uniform and the non–uniform grid) is, respectively, defined by

$$U(x_j, t^n) = U_j^n \equiv \frac{1}{h} \int_{x_{j-\frac{1}{2}}^n}^{x_{j+\frac{1}{2}}^n} u(x, t^n)\, dx. \tag{2.4}$$

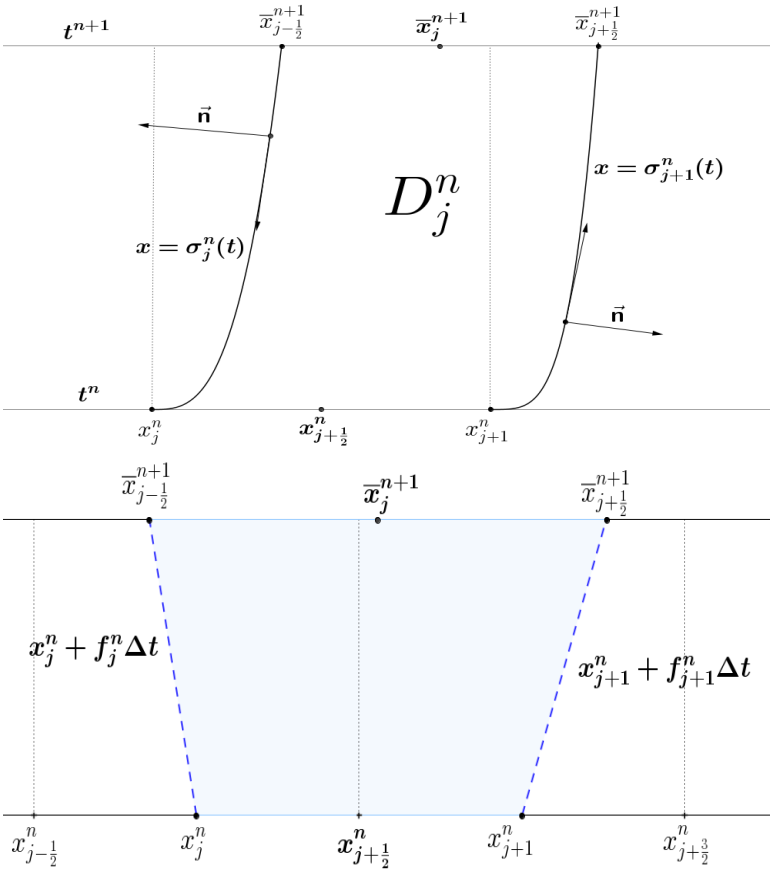

Figure 2.1: Lagrangian-Eulerian space-time control-volume (top) and its first order approximation (bottom).

$$\overline{U}(x_j, t^{n+1}) = \overline{U}^{n+1}_j \equiv \frac{1}{h^{n+1}_j} \int_{\overline{x}^{n+1}_{j-\frac{1}{2}}}^{\overline{x}^{n+1}_{j+\frac{1}{2}}} u(x, t^{n+1})\, dx \tag{2.5}$$

along with the initial condition, $U(x^0_j, t^0) = U^0_j$, in cells $\left[x^0_{j-\frac{1}{2}}, x^0_{j+\frac{1}{2}}\right]$.

The Lagrangian-Eulerian approach considers the cell-centered finite-volume (see figure 2.1),

$$D^n_j = \left\{(x,t)/\ t^n \le t \le t^{n+1},\ \sigma^n_j(t) \le x \le \sigma^n_{j+1}(t)\right\}, \tag{2.6}$$

where $\sigma^n_j(t)$ is a parameterized curve such that $\sigma^n_j(t^n) = x^n_j$.

Remark 3 *The parameterized curves $\sigma^n_j(t)$ and $\sigma^n_{j+1}(t)$ are called **the no-flow curves**, and they are naturally impervious zero-flux boundaries.*

The construction of *the no-flow curves* $\sigma^n_j(t)$, limiting the space-time control volume D^n_j, and which are the key point of the Lagrangian-Eulerian approach, is as follows.

The impermeability of *the no-flow curves* $\sigma^n_j(t)$ implies that

$$\int_{\sigma^n_j(t)} \begin{bmatrix} f(u) \\ u \end{bmatrix} \cdot \mathbf{n}\, ds = 0 \Rightarrow \begin{bmatrix} f(u) \\ u \end{bmatrix} \cdot \mathbf{n} = 0, \text{ over the curve } \sigma^n_j(t). \tag{2.7}$$

It is easy to show that the vector $\left(1, -\dfrac{d\sigma^n_j(t)}{dt}\right)^T$ is normal to the curve $\sigma^n_j(t)$. Therefore, assuming that $\lim\limits_{u\to 0} \dfrac{f(u)}{u} < \infty$, from Eq. (2.7), substituting the normal vector $\mathbf{n}$ by $\left(1, -\dfrac{d\sigma^n_j(t)}{dt}\right)^T$,

we get

$$\frac{d\sigma_j^n(t)}{dt} = \frac{f(u)}{u}, \;\; \sigma_j^n(t^n) = x_j^n, \;\; t^n \leq t \leq t^{n+1}, \tag{2.8}$$

which defines the generalized system of ordinary differential equations for the no-flow curves $\sigma_j^n(t)$.

The existence and uniqueness of the no-flow curves were proved in [1], that now they are viewed as vector fields with bounded directional variation [49, 50].

Remark 4 *It is important to highlight that thanks to the Lagrangian-Eulerian framework and by performing a dimensionless analysis of the flux function from Eq. (2.1), one can see that*

$$\left[\frac{h}{\Delta t}\right] \alpha \left[\left|\frac{f(u)}{u}\right|\right]. \tag{2.9}$$

In addition, the quantity $\dfrac{f(u)}{u}$ *corresponds to* ***the no-flow curve derivative****, and controls the speed of the interface tracking problem (2.1), yielding an accurate approximation of the local speed of propagation in the space-time control volumes built in the* $Q-$*forms, without the need to calculate the eigenvalues of* f*. As can be seen, it is related to the unknown solution* u*, so one cannot find the exact trace lines of the fluid particles. However, the fairly simple explicit approximation* $\dfrac{f(u)}{u} \approx \dfrac{f(u_j^n)}{u_j^n} := f_j^n$ *provides quite good results, for both hyperbolic and balance equations, which is advantageous to the numerical analysis.*

Now, integrating Eq. (2.2) over the cell-centered finite-volume D_j^n and applying the divergence theorem, we get

$$\int_{D_j^n} \nabla_{x,t} \cdot \begin{bmatrix} f(u) \\ u \end{bmatrix} \, dA = \oint_{\partial D_j^n} \begin{bmatrix} f(u) \\ u \end{bmatrix} \cdot \mathbf{n} \, ds = 0. \tag{2.10}$$

As a consequence of Eq. (2.7), Eq. (2.10) leads to the (natural) local conservation,

$$\int_{x_j^n}^{x_{j+1}^n} u(x, t^n) \, dx = \int_{\overline{x}_{j-\frac{1}{2}}^{n+1}}^{\overline{x}_{j+\frac{1}{2}}^{n+1}} u(x, t^{n+1}) \, dx, \tag{2.11}$$

where $\overline{x}_{j-\frac{1}{2}}^{n+1} = \sigma_j^n(t^{n+1})$ and $\overline{x}_{j+\frac{1}{2}}^{n+1} = \sigma_{j+1}^n(t^{n+1})$.

Remark 5 *Eq. (2.11) expresses that the amount of* u *entering the space–time control volume* D_j^n *at* $t = t^n$ *is equal to the amount of* u *leaving that volume at* $t = t^{n+1}$*. That is, Eq. (2.11) indicates that the scheme is locally conservative. The global conservation of schemes constructed using the Lagrangian-Eulerian approach is achieved by discrete local conservation Eq. (2.11) in each of the control volumes* D_j^n *which fill-up the space-time domain.*

In summary, the concept of *no-flow curve* allows to reduce problem (2.1), in the weak distributional sense, to the equivalent problem:

$$\begin{cases} \dfrac{d\sigma_j^n(t)}{dt} = \dfrac{f(u)}{u}, \quad t^n < t \leq t^{n+1}, \qquad \sigma_j(t^n) = x_j^n. \\ \dfrac{1}{h_j^{n+1}} \displaystyle\int_{\overline{x}_{j-\frac{1}{2}}^{n+1}}^{\overline{x}_{j+\frac{1}{2}}^{n+1}} u(x, t^{n+1}) \, dx = \frac{1}{h_j^{n+1}} \int_{x_j^n}^{x_{j+1}^n} u(x, t^n) dx, \quad h_j^{n+1} = \sigma_{j+1}^n(t^{n+1}) - \sigma_j^{n+1}(t^{n+1}), \\ u(x, t_0) = u_0(x), \;\; -\infty < x < \infty. \end{cases} \tag{2.12}$$

2.1.2 The Lagrangian-Eulerian Building Block

From Eqs. (2.5) and (2.11), we have

1. **Lagrangian Evolution Stage.** Forward tracking of the no-flow curves leads to

$$\begin{aligned}\overline{U}_j^{n+1} &= \frac{1}{h_j^{n+1}} \int_{\overline{x}_{j-\frac{1}{2}}^{n+1}}^{\overline{x}_{j+\frac{1}{2}}^{n+1}} u(x,t^{n+1})\,dx \\ &= \frac{1}{h_j^{n+1}} \int_{x_j^n}^{x_{j+1}^n} u(x,t^n)\,dx \\ &= \frac{h}{h_j^{n+1}} \left[\frac{1}{h} \int_{x_j^n}^{x_{j+\frac{1}{2}}^n} u(x,t^n)\,dx + \frac{1}{h} \int_{x_{j+\frac{1}{2}}^n}^{x_{j+1}^n} u(x,t^n)\,dx \right] \\ &= \frac{h}{h_j^{n+1}} \left(\frac{1}{2} U_j^n + \frac{1}{2} U_{j+1}^n \right),\end{aligned} \tag{2.13}$$

   $h = h_j^n = x_{j+\frac{1}{2}}^n - x_{j-\frac{1}{2}}^n$ and, $h_j^{n+1} = \overline{x}_{j+\frac{1}{2}}^{n+1} - \overline{x}_{j-\frac{1}{2}}^{n+1}$.

2. **Eulerian Remaping Stage.** The resulting local approximations $U_j^{n+1},\ j \in \mathbb{Z}$ over the original grid are defined as

$$U_j^{n+1} = \frac{1}{h} \left[c_{0j} \overline{U}_{j-1}^{n+1} + c_{1j} \overline{U}_j^{n+1} \right], \tag{2.14}$$

   where $c_{0j} = \dfrac{h}{2} + f_j^n \Delta t^n$, $c_{1j} = \dfrac{h}{2} - f_j^n \Delta t^n$ and $\Delta t^n = t^{n+1} - t^n$ (see figure 2.1 right) satisfying the weak CFL condition:

$$\frac{\Delta t^n}{\Delta x} \operatorname*{Sup}_u \left| \frac{f(u)}{u} \right| \leq \frac{1}{2}, \tag{2.15}$$

Remark 6 *Eqs. (2.8), (2.13) and (2.14) form* ***the basic building block*** *of the Lagrangian-Eulerian schemes used in this work to numerically solve hyperbolic conservation laws with or without source term.*

Plugging (2.13) into (2.14), and taking into account (2.9), the 1-D Fully-Discrete Lagrangian-Eulerian scheme in conservation form, for numerically solving Eq. (2.1), is given by:

$$U_j^{n+1} = U_j^n - \frac{\Delta t}{\Delta x} \left(\mathcal{F}(U_j^n, U_{j+1}^n) - \mathcal{F}(U_{j-1}^n, U_j^n) \right), \tag{2.16}$$

where,

$$\mathcal{F}(U_j^n, U_{j+1}^n) = \operatorname*{Sup}_u \left| \frac{f(u)}{u} \right| \left(U_j^n - U_{j+1}^n \right) + \frac{1}{2} \Big(f(U_j^n) + f(U_{j+1}^n) \Big). \tag{2.17}$$

2.2 The Fully-Discrete Lagrangian-Eulerian Schemes on Triangular Grids

In this section, we construct the fully-discrete Lagrangian-Eulerian schemes on triangular grids as a natural extension of the 1D fully-discrete scheme (2.16)-(2.17), we prove their convergence towards the entropic solution of $u_t(\mathbf{x},t) + \operatorname{div}(f(u(\mathbf{x},t))) = 0$ with $u_0 \in L^\infty(\mathbb{R}^2)$ following the

theoretical results for the uniqueness and regularity properties of the *entropy process solutions* in the $L_t^\infty(L_{\mathbf{x}}^1)-$norm introduced by Eymard, Gallouët and Herbin (1995, [88,89]; 2000, [87]), and we show that, for systems, they also satisfy the desired *positivity principle* proposed by Lax and Liu (1996, [131]; 2003, [130]), and *the weak positivity principle* introduced in E. Abreu, J. François, W. Lambert and J. Pérez (2022, [4]).

2.2.1 Construction of the Fully-Discrete Lagrangian-Eulerian Schemes on Triangular Grids

Let $\mathcal{T}$ be a family of triangulations of $\mathbb{R}^2$ such that the common face between two cells of $\mathcal{T}$ is included in a plane of $\mathbb{R}^2$. For any control volume K, we denote by $m(K)$ its 2-dimensional measure, by $m(\partial K)$ its perimeter, by $\delta(K)$ its diameter and by $N(K)$, the set of its neighbors. For $L \in N(K)$, $m(K|L)$ denotes the 1-dimensional measure of $K|L$.

From previous work [7, 9] we find that, the Lagrangian-Eulerian framework (*over non-rigid space-time control volumes*) is a general discretization method in which a Finite Volume formulation can be recovered, with the *numerical flux* fully defined on the common face $K|L$ between the K and L cells of $\mathcal{T}$ such that K can be viewed as a rigid control volume.

Denoting by $h = \underset{K}{\text{Sup}}\{\delta(K)\}$ the *spatial step size* and assuming that, for some $\alpha > 0$ and for all $K \in \mathcal{T}$,

$$\alpha h^2 \leq m(K), \qquad m(\partial K) \leq \frac{1}{\alpha} h, \tag{2.18}$$

the new *2D fully-discrete Lagrangian-Eulerian scheme on triangular grids* is given by

$$\begin{cases} u_K^0 = \dfrac{1}{m(K)} \displaystyle\int_K u(x,y,0)dA, \\ \\ u_K^{n+1} = u_K^n - \dfrac{\Delta t}{m(K)} \displaystyle\sum_{L \in N(K)} \mathcal{F}(u_K^n, u_L^n), \end{cases} \tag{2.19}$$

where $\mathcal{F}(u_K^n, u_L^n)$ is the numerical flux (2.17) of the 1D fully-discrete scheme (2.16) used for solving the 1D scalar conservation law $\partial_t u + \partial_{\mathbf{n}_{KL}}(\mathbf{f}(\mathbf{u}(\mathbf{x},t)) \cdot \mathbf{n}_{KL}) = 0$. That is,

$$\mathcal{F}(u_K^n, u_L^n) = \left[\frac{1}{2}(\mathbf{f}(u_K^n) + \mathbf{f}(u_L^n)) \cdot \mathbf{n}_{KL} - \underset{u,K,L}{\text{Sup}} \left|\frac{\mathbf{f}(u)}{u} \cdot \mathbf{n}_{KL}\right| (u_L^n - u_K^n)\right] m(K|L). \tag{2.20}$$

where $\mathbf{n}_{KL}$ denotes the outward unit normal vector to the face $K|L$ of the finite volume K and h, a grid parameter that will be defined in the next section.

The numerical flux $\mathcal{F}(u_K^n, u_L^n; \mathbf{n}_{KL})$ approximates the flux integral $\displaystyle\int_{\partial K} \mathbf{f}(u) \cdot \mathbf{n}_{KL}\, d(\partial K)$ at the common face $(K|L)$ between cells K and L of $\mathcal{T}$. In other words,

$$\int_{\partial K} \mathbf{f}(u) \cdot \mathbf{n}_{KL}\, d(\partial K) \approx \sum_{L \in N(K)} \mathcal{F}(u_K^n, u_L^n). \tag{2.21}$$

Furthermore, as in the 1-D Lagrangian-Eulerian scheme (2.16)-(2.17), in (2.20), the no-flow curves dependent stability coefficient, that is, $\underset{u,\mathbf{n}}{\text{Sup}} \left|\dfrac{\mathbf{f}(u)}{u} \cdot \mathbf{n}\right|$, produces accurate approximations of the local speeds in the space-time control volumes in the fully-discrete Lagrangian-Eulerian schemes.

It is noteworthy that the Lagrangian-Eulerian flux (2.20) is distintic to that of *monotone flux functions* and *E-flux* functions –for scalar problems – and in particular for its counterpart numerical flux functions for nonlinear systems of conservation laws, for instance, the *system local*

Lax-Friedrichs flux as well as the Osher-Solomon numerical flux (see, e.g., [33, 95, 100, 145] for a comprehensive survey). Moreover, the Lagrangian-Eulerian flux (2.20) does not require solving local Riemannian problems or calculating/evaluating the associated Jacobian matrix or using its eigenvalues (exact or approximate) and, therefore, field-to-field decompositions are avoided.

We point out that the Lagrangian-Eulerian flux (2.20) may be generalized as

$$\mathcal{F}(u_K^n, u_L^n) = \left[\frac{1}{2}(\mathbf{f}(u_K^n) + \mathbf{f}(u_L^n)) \cdot \mathbf{n}_{KL} - Q_{LE}\left(\frac{\mathbf{f}(u_K^n)}{u_K^n}, \frac{\mathbf{f}(u_L^n)}{u_L^n}\right)(u_L^n - u_K^n)\right] m(K|L), \tag{2.22}$$

where Q_{LE} stands for the numerical viscosity of the scheme that is independent of the eigenvalues (exact and approximate) of the Jacobian matrix of the flux functions of the hyperbolic equation [10] (indeed, one can evaluate the vector-valued function at a specific value in a straightforward manner, that is, by simply evaluating each component function at that grid value) and correctly approximates the local speed of propagation in the space-time control volumes. For instance, in (2.20), $Q_{LE} = \underset{u,K,L}{\text{Sup}} \left|\frac{\mathbf{f}(u)}{u} \cdot \mathbf{n}_{KL}\right|$.

It is important to emphasize that, from the previous works for Cartesian grids [7,9,10,14,15], the scalar quantities $\frac{\mathbf{f}(u_K^n)}{u_K^n} \cdot \mathbf{n}_{KL}$ and $\frac{\mathbf{f}(u_L^n)}{u_L^n} \cdot \mathbf{n}_{KL}$ are the derivatives of the so-called *no-flow curves* motivated by the flux integral, $\int_{\partial K} [u \;\; \mathbf{f}(u)]^\top \cdot \mathbf{n}_{KL}\, ds$, in a natural componentwise extension for systems.

The Lagrangian-Eulerian *no-flow surfaces/curves*, which are independent of the flux function Jacobian matrix, play a key role in the fully-discrete Lagrangian-Eulerian scheme (2.19)-(2.20), and their numerically stable construction requires that the following condition, called *weak CFL–condition*, be fulfilled:

$$\frac{\Delta t}{h} \underset{u,K,L}{\text{Sup}} \left|\frac{\mathbf{f}(u)}{u} \cdot \mathbf{n}_{KL}\right| \leq \frac{1}{2}, \;\; \forall u \in [-r, r], \;\forall\, (K, L) \in \mathcal{T}^2. \tag{2.23}$$

Weak CFL–condition (2.23) guarantees the numerical stability of the Lagrangian-Eulerian schemes on triangular grids.

Finally, the approximate solution to problem (1.1) given by the fully-discrete Lagrangian-Eulerian scheme (2.19)-(2.20) is the piecewise-constant function:

$$U_{\mathcal{T}}(\mathbf{x}, t) = u_K^n, \; \forall \mathbf{x} \in K, \; \forall t \in [n\Delta t, (n+1)\Delta t). \tag{2.24}$$

The Lagrangian-Eulerian flux (2.20) is a *monotone numerical flux*. That is, it satisfies the following properties:

$$\begin{cases} (i) \;\textbf{Monotonicity}\text{: } \mathcal{F}(u, v) \text{ is nondecreasing with respect to } u \text{ and} \\ \qquad\qquad\qquad\quad \text{nonincreasing with respect to } v \text{ for } (u, v) \in [-r, r]^2, \\ \qquad\qquad\qquad\quad \text{provided that (2.26) is fulfilled.} \\ (ii) \;\textbf{Conservativity}\text{: } \mathcal{F}(u, v) = -\mathcal{F}(v, u), \; \forall (u, v) \in [-r, r]^2. \\ (iii)\; \mathcal{F}(u, v) \text{ is } \textbf{Lipschitz continuous} \text{ over } [-r, r]^2. \\ (iv) \;\textbf{Consistency}\text{: } \mathcal{F}(s, s) = \mathbf{f}(s) \cdot \mathbf{n}_{KL} \text{ for all } s \in [-r, r]. \end{cases} \tag{2.25}$$

It can be easily proven that the monotonicity is guaranteed by the condition:

$$\frac{1}{2}\left|\mathbf{f}'(u) \cdot \mathbf{n}_{KL}\right| \leq \underset{u,K,L}{\text{Sup}} \left|\frac{\mathbf{f}(u)}{u} \cdot \mathbf{n}_{KL}\right|, \;\; \forall u \in [-r, r], \;\forall\, (K, L) \in \mathcal{T}^2, \tag{2.26}$$

which indicates that the characteristic wave velocities are bounded by the no-flow curves and implies that if the weak CFL-condition (2.23) is satisfied, the classical (strong) CFL-condition

is also satisfied. Therefore, the Lagrangian-Eulerian schemes are independent of the eigenvalues (exact or approximate) of the Jacobian matrix of the numerical flux functions.

On the other hand, property (iii) is satisfied by taking the same Lipschitz constant, $m(K|L)M$, with respect u and v where

$$\mathrm{M} \geq \operatorname*{Sup}_{u} \|\mathbf{f}'(u)\|_{l^\infty} + \operatorname*{Sup}_{u,K,L} \left| \frac{\mathbf{f}(u)}{u} \cdot \mathbf{n}_{KL} \right|. \tag{2.27}$$

In addition, defining the function

$$\bar{f}(x, y, t, s) = f(s),\ \forall (x, y) \in K,\ \forall t \in [n\Delta t,\ (n+1)\Delta t),\ \forall s \in \mathbb{R},$$

we have to

$$(f(s) \cdot n_{KL}) m(K|L) = \frac{1}{\Delta t} \int_{t^n}^{t^{n+1}} \int_{K|L} \bar{f}(\gamma, t, s) \cdot n_{KL} d\gamma dt,$$

where γ is a parameterization of $K|L$.

Then, by the divergence theorem, it follows that

$$\sum_{L \in N(K)} \mathcal{F}(s, s) = 0,\ \forall K \in \mathcal{T},\ \forall n \in \mathbb{N},\ \forall s \in \mathbb{R}. \tag{2.28}$$

2.2.2 Convergence Proof of the Fully-Discrete Lagrangian-Eulerian Scheme on Triangular Grids via Entropy Process Solution

In this section, following [56, 88, 89], we show that any sequence of solutions given by the 2D fully-discrete Lagrangian-Eulerian scheme (2.19)–(2.20) converges to the unique entropy solution of the problem (1.1). For this, the following hypotheses on the data must be satisfied:

$$\begin{cases} -u_0 \in L^\infty(\mathbb{R}^2) : \exists r \in \mathbb{R}_+ \text{ such that } \|u_0\|_\infty \leq r \text{ almost everywhere,} \\ -\mathbf{f} \in C^1(\mathbb{R}), \text{ and } \mathbf{f}'(s) \text{ is locally Lipschitz continuous,} \\ - \text{ for all compact set } \kappa \subset \mathbb{R}, \text{ there exists } V_\kappa < \infty \text{ such that } |\mathbf{f}'(s)| \leq V_\kappa \\ \quad \text{for almost every } s \in \kappa, \end{cases} \tag{2.29}$$

In addition, to support the theoretical stability and convergence results, we require that the time step be chosen such that:

$$\Delta t \leq \frac{(1-\xi)\alpha^2 h}{2\mathrm{M}},\ \xi \in (0, 1). \tag{2.30}$$

The convergence analysis of the Lagrangian-Eulerian scheme discussed in this work requires the following definition.

Definition 6 *Let $\mathbb{P}(\mathbb{R})$ be the set of probability measures on $\mathbb{R}$. A Young measure is a weak $*$ measurable map $m : \mathbb{R}^2 \times (0, T) \to \mathbb{P}(\mathbb{R})$, which means that mapping $(\mathbf{x}, t) \mapsto \langle m_{(\mathbf{x},t)}, g \rangle$ is Borel measurable for every $g \in C_0(\mathbb{R})$.*

Furthermore, before to stablish the theorem of existence and uniqueness of the solution, we show several properties of the scheme as crucial points in the proof, and we collect some results related to the probability measures which are its fundamental core.

Lagrangian-Eulerian scheme properties

The Lagrangian-Eulerian scheme satisfies the following properties, which are proven following the proofs done in [56].

L^∞–stability

Lemma 1 *Assume (2.29), (2.18) and (2.30) hold. Then, the approximate solution U_h of the problem (1.1) defined by (2.24) verifies:*

$$-r \leq u_K^n \leq r,\ \forall n \in \mathbb{N},\ \forall K \in \mathcal{T}, \tag{2.31}$$

and

$$\|U_h\|_\infty \leq \|u_0\|_\infty \tag{2.32}$$

Proof. We prove (2.31) by induction. From the hypothesis on data, (2.31) holds for $n = 0$. We assume that it holds for n. That is, $u_K^n \in [-r, r],\ \forall K \in \mathcal{T}$.

Thanks to (2.28) and (2.19), we have:

$$u_K^{n+1} = u_K^n - \frac{\Delta t}{m(K)} \sum_{L \in N(K)} \mathcal{G}(u_K^n, u_L^n)(u_K^n - u_L^n),$$

where

$$\mathcal{G}(u_K^n, u_L^n) = \frac{\mathcal{F}(u_K^n, u_L^n) - \mathcal{F}(u_K^n, u_K^n)}{u_K^n - u_L^n}.$$

Since $\mathcal{F}$ is nonincresing w.r.t u_L^n then, $\mathcal{F}(u_K^n, u_L^n) \geq \mathcal{F}(u_K^n, u_K^n)$ if $u_K^n > u_L^n$ and $\mathcal{F}(u_K^n, u_L^n) \leq \mathcal{F}(u_K^n, u_K^n)$ if $u_K^n < u_L^n$. Therefore, $\mathcal{G}(u_K^n, u_L^n) \geq 0,\ \forall K,\ \forall L$ and $\forall n$.

Additionally, $\mathcal{G}(u_K^n, u_L^n) \leq m(K|L)\mathrm{M}$ because $\mathcal{F}$ is Lipschitz continuous. Thus,

$$\begin{aligned}
1 - \frac{\Delta t}{m(K)} \sum_{L \in N(K)} \mathcal{G}(u_K^n, u_L^n) &\geq 1 - \frac{\Delta t}{m(K)} \sum_{L \in N(K)} m(K|L)\mathrm{M} \\
&\geq 1 - \frac{\mathrm{M}\, m(\partial K)\, \Delta t}{m(K)} \\
&\geq 1 - \mathrm{M}\left(\frac{h}{\alpha}\right)\left(\frac{1}{\alpha h^2}\right)\left(\frac{(1-\xi)\alpha^2 h}{2\mathrm{M}}\right) \\
&= \frac{1+\xi}{2} > 0.
\end{aligned}$$

Accordingly, by rewritting u_K^{n+1} as:

$$u_K^{n+1} = \left(1 - \frac{\Delta t}{m(K)} \sum_{L \in N(K)} \mathcal{G}(u_K^n, u_L^n)\right) u_K^n + \frac{\Delta t}{m(K)} \sum_{L \in N(K)} \mathcal{G}(u_K^n, u_L^n) u_L^n,$$

we observe that u_K^{n+1} is a convex combination of u_K^n and u_L^n, $L \in N(K)$ and with that, $u_K^{n+1} \in [-r, r],\ \forall K \in \mathcal{T}$.

(2.32) is a consequence of (2.31). It concludes the proof.

Estimate of the temporal and spatial derivatives of the approximate solution

Lemma 2 *Assume (2.29), (2.18) and (2.30) hold. Let U_h be the approximate solution of the problem (1.1) defined by (2.20) and (2.19) and let $T > 0$ and $R > 0$. Then, there exists $C_{bv} \in \mathbb{R}$ depending only on f, u_0, α, ξ, R and T such that:*

$$\begin{aligned}
\sum_{n=0}^{N_T} \Delta t \sum_{(K,L) \in \varepsilon_R^n} &\Big[\max_{u_L^n \leq c \leq d \leq u_K^n} (\mathcal{F}(d,c) - \mathcal{F}(d,d)) \\
&+ \max_{u_L^n \leq c \leq d \leq u_K^n} (\mathcal{F}(d,c) - \mathcal{F}(c,c)) \Big] \leq \frac{C_{bv}}{\sqrt{h}}
\end{aligned} \tag{2.33}$$

and

$$\sum_{n=0}^{N_T}\sum_{K\in\tau_R} m(K)|u_K^{n+1}-u_K^n| \le \frac{C_{bv}}{\sqrt{h}} \tag{2.34}$$

where,

$N_T = \max\left\{n\in\mathbb{N}, n\le \frac{T}{\Delta t}+1\right\}$

$\tau_R = \{K\in\mathcal{T}, K\subset B(0,R)\}$

$\varepsilon^n = \left\{(K,L)\in\mathcal{T}^2, L\in N(K),\ u_K^n > u_L^n\right\}$

$\varepsilon_R^n = \left\{(K,L)\in\mathcal{T}^2, K \text{ or } L\in\mathcal{T}_R, L\in N(K), K|L\subset B(0,R) \text{ and } u_K^n > u_L^n\right\}$

Proof. In this proof we denote by $(C_i)_{i\in\mathbb{N}}$ various quantities only depending on $F,\ u_0,\ M,\ \alpha,\ \xi,\ R$ and T.

Multiplying (2.19) by $\Delta t\, u_K^n$ and summing the result over $K\in\mathcal{T}_R$ and $n\in\{0,...,N_T\}$ yields

$$B_1 + B_2 = 0, \tag{2.35}$$

where

$$B_1 = \sum_{n=0}^{N_T}\sum_{K\in\tau_R} m(K)u_K^n(u_K^{n+1}-u_K^n),$$

and

$$B_2 = \sum_{n=0}^{N_T}\Delta t\sum_{K\in\tau_R}\sum_{L\in N(K)}[u_K^n(\mathcal{F}(u_K^n,u_L^n)-\mathcal{F}(u_K^n,u_K^n)) - u_L^n(\mathcal{F}(u_K^n,u_L^n)-\mathcal{F}(u_L^n,u_L^n))].$$

Let us define B_3 by

$$B_3 = \sum_{n=0}^{N_T}\Delta t\sum_{(K,L)\in\varepsilon_R^n}[u_K^n(\mathcal{F}(u_K^n,u_L^n)-\mathcal{F}(u_K^n,u_K^n)) - u_L^n(\mathcal{F}(u_K^n,u_L^n)-\mathcal{F}(u_L^n,u_L^n))].$$

The expression $|B_3-B_2|$ is reduced to a sum of terms each of which corresponds to the boundary of a control volume which is included in $B(0,R+h)\setminus B(0,R-h)$. Denoting by N_Δ the number of such terms, since the measure of $B(0,R+h)\setminus B(0,R-h)$ is less than C_1h and greater than $N_\Delta m(K),\ K\in B(0,R+h)\setminus B(0,R-h)$, for n fixed, N_Δ is lower than $C_1h/\alpha h^2 = C_2/h$.
Thanks to $u_K^n\in[-r,r],\forall K,\forall n$, that $\mathcal{F}$ is Lipschitz continuous, and that $m(K|L)\le\frac{1}{\alpha}h$ we have that

$$\begin{aligned}|u_K^n(\mathcal{F}(u_K^n,u_L^n)-\mathcal{F}(u_K^n,u_K^n))| &= |u_K^n|\,|\mathcal{F}(u_K^n,u_L^n)-\mathcal{F}(u_K^n,u_K^n)|\\ &\le |u_K^n|m(K|L)\mathrm{M}|u_K^n-u_L^n|\\ &\le 8r^2\left(\frac{1}{\alpha}h\right)\mathrm{M} = C_3h.\end{aligned}$$

Thus,

$$|B_3-B_2| \le \sum_{n=0}^{N_T}\Delta t\sum_{(K,L)\in\varepsilon_R^n} C_3h \le \sum_{n=0}^{N_T}\Delta t\Big[C_3h(C_2/h)\Big] = C_2C_3\sum_{n=0}^{N_T}\Delta t = C_2C_3t^{N_T}.$$

Therefore,

$$|B_3-B_2|\le C_4. \tag{2.36}$$

For all $K\in\mathcal{T},\ L\in N(K)$ and $n\in\mathbb{N}$ we denote by Ψ_{KL}^n the function

$$\Psi_{KL}^n(x) = \int_0^x s\frac{d}{ds}(\mathcal{F}(s,s))ds.$$

An integration by parts yields, for all $(a,b) \in \mathbb{R}^2$,

$$\begin{aligned}\Psi^n_{KL}(b) - \Psi^n_{KL}(a) &= \int_a^b s\frac{d}{ds}(\mathcal{F}(s,s))ds \\ &= b\mathcal{F}(b,b) - a\mathcal{F}(a,a) - \int_a^b \mathcal{F}(s,s)ds \\ &= b(\mathcal{F}(b,b) - \mathcal{F}(a,b)) - a(\mathcal{F}(a,a) - \mathcal{F}(a,b)) \\ &\qquad - \int_a^b (\mathcal{F}(s,s) - \mathcal{F}(a,b))ds.\end{aligned}$$

Using this equality, B_3 may be descomposed as

$$B_3 = B_4 - B_5, \tag{2.37}$$

with

$$B_4 = \sum_{n=0}^{N_T} \Delta t \sum_{(K,L)\in\varepsilon^n_R} \int_{u^n_L}^{u^n_K} (\mathcal{F}(u^n_K, u^n_L) - \mathcal{F}(s,s))ds$$

and

$$B_5 = \sum_{n=0}^{N_T} \Delta t \sum_{(K,L)\in\varepsilon^n_R} (\Psi^n_{KL}(u^n_K) - \Psi^n_{KL}(u^n_L)).$$

Because of (2.28), $\sum_{L\in N(K)} \Psi^n_{KL}(x) = 0$, $\forall K \in \tau$, $\forall x \in [-r,r]$ and with that, B_5 is again reduced to a sum of terms corresponding to control volumes included in $B(0,R+h)\setminus B(0,R-h)$. Therefore, as for (2.36), there exists a constant C_5 such that

$$|B_5| \le C_5. \tag{2.38}$$

Let us now turn to an estimate of B_4. We now use the following technical lemma which will be proved after completion of the present proof.

Lemma 3 *Let $f : \mathbb{R} \to \mathbb{R}$ be a monotonic, Lipschitz continuous function, with a Lipschitz constant $L > 0$. Then,*

$$\left|\int_c^d (f(s) - f(c))ds\right| \ge \frac{1}{2L}(f(d) - f(c))^2, \forall c,d \in \mathbb{R}.$$

Thanks to the monotonicity of $\mathcal{F}$, from Lemma 3 with $f(s) = \mathcal{F}(d,s)$ first and then, with $f(s) = \mathcal{F}(s,c)$, we have:

$$\begin{aligned}\int_c^d (\mathcal{F}(d,c) - \mathcal{F}(s,s))ds &\ge \int_c^d (\mathcal{F}(d,c) - \mathcal{F}(d,s))ds \\ &\ge \frac{1}{2m(K|L)\mathrm{M}}(\mathcal{F}(d,c) - \mathcal{F}(d,d))^2\end{aligned}$$

and

$$\begin{aligned}\int_c^d (\mathcal{F}(d,c) - \mathcal{F}(s,s))ds &\ge \int_c^d (\mathcal{F}(d,c) - \mathcal{F}(s,c))ds \\ &\ge \frac{1}{2m(K|L)\mathrm{M}}(\mathcal{F}(d,c) - \mathcal{F}(c,c))^2.\end{aligned}$$

Taking the maximum for $(c,d) \in \left\{(r,t) \in [u^n_L, u^n_K]^2, K, L \in \varepsilon^n_R \,:\, r \le t\right\}$ and adding the two above inequalities, we obtain

$$\begin{aligned}\int_{u^n_L}^{u^n_K} (\mathcal{F}(u^n_K, u^n_L) - \mathcal{F}(s,s))ds \ge \frac{1}{4m(K|L)\mathrm{M}}\Bigg(&\max_{u^n_L \le c \le d \le u^n_K} (\mathcal{F}(d,c) - \mathcal{F}(d,d))^2 \\ &+ \max_{u^n_L \le c \le d \le u^n_K} (\mathcal{F}(d,c) - \mathcal{F}(c,c))^2\Bigg).\end{aligned}$$

Then,

$$B_4 \geq \frac{1}{4\mathrm{M}}\sum_{n=0}^{N_T}\Delta t\sum_{(K,L)\in\varepsilon_R^n}\left[\frac{1}{m(K|L)}\max_{u_L^n\leq c\leq d\leq u_K^n}(\mathcal{F}(d,c)-\mathcal{F}(d,d))^2 + \frac{1}{m(K|L)}\max_{u_L^n\leq c\leq d\leq u_K^n}(\mathcal{F}(d,c)-\mathcal{F}(c,c))^2\right]. \tag{2.39}$$

Let us now to get an estimate of B_1. Taking into account that

$$\begin{aligned}(u_K^{N_T+1})^2-(u_K^0)^2 &= \sum_{n=0}^{N_T}\left[(u_K^{n+1})^2-(u_K^n)^2\right]\\ &= \sum_{n=0}^{N_T}(u_K^{n+1}+u_K^n)(u_K^{n+1}-u_K^n)\\ &= \sum_{n=0}^{N_T}u_K^{n+1}(u_K^{n+1}-u_K^n)+\sum_{n=0}^{N_T}u_K^n(u_K^{n+1}-u_K^n),\end{aligned}$$

we have that:

$$\begin{aligned}\sum_{n=0}^{N_T}u_K^n(u_K^{n+1}-u_K^n) &= \sum_{n=0}^{N_T}(u_K^n-u_K^{n+1}+u_K^{n+1})(u_K^{n+1}-u_K^n)\\ &= -\sum_{n=0}^{N_T}(u_K^{n+1}-u_K^n)^2+\sum_{n=0}^{N_T}u_K^{n+1}(u_K^{n+1}-u_K^n)\\ &= -\sum_{n=0}^{N_T}(u_K^{n+1}-u_K^n)^2+(u_K^{N_T+1})^2-(u_K^0)^2-\sum_{n=0}^{N_T}u_K^n(u_K^{n+1}-u_K^n).\end{aligned}$$

This is,

$$\sum_{n=0}^{N_T}u_K^n(u_K^{n+1}-u_K^n)=\frac{1}{2}\left[-\sum_{n=0}^{N_T}(u_K^{n+1}-u_K^n)^2+(u_K^{N_T+1})^2-(u_K^0)^2\right].$$

Thus,

$$B_1=-\frac{1}{2}\sum_{n=0}^{N_T}\sum_{K\in\mathcal{T}_R}m(K)(u_K^{n+1}-u_K^n)^2+\frac{1}{2}\sum_{K\in\mathcal{T}_R}m(K)(u_K^{N_T+1})^2-\frac{1}{2}\sum_{K\in\mathcal{T}_R}m(K)(u_K^0)^2.$$

From (2.25) and (2.19) we have:

$$\begin{aligned}u_K^{n+1}-u_K^n &= -\frac{\Delta t}{m(K)}\sum_{L\in N(K)}\mathcal{F}(u_K^n,u_L^n)\\ &= -\frac{\Delta t}{m(K)}\sum_{L\in N(K)}\sqrt{m(K|L)}\left[\frac{1}{\sqrt{m(K|L)}}(\mathcal{F}(u_K^n,u_L^n)-\mathcal{F}(u_K^n,u_K^n))\right].\end{aligned}$$

The Cauchy-Shwarz inequality applying to this equation yields:

$$\begin{aligned}(u_K^{n+1}-u_K^n)^2 &\leq \frac{\Delta t^2}{[m(K)]^2}\sum_{L\in N(K)}m(K|L)\sum_{L\in N(K)}\frac{1}{m(K|L)}(\mathcal{F}(u_K^n,u_L^n)-\mathcal{F}(u_K^n,u_K^n))^2\\ &= \frac{\Delta t^2}{[m(K)]^2}m(\partial(K))\sum_{L\in N(K)}\frac{1}{m(K|L)}(\mathcal{F}(u_K^n,u_L^n)-\mathcal{F}(u_K^n,u_K^n))^2.\end{aligned}$$

Using (2.18) and (2.30) in this inequality gives:

$$m(K)(u_K^{n+1}-u_K^n)^2 \leq \frac{1-\xi}{2\mathrm{M}}\Delta t \sum_{L\in N(K)} \frac{1}{m(K|L)}(\mathcal{F}(u_K^n,u_L^n)-\mathcal{F}(u_K^n,u_K^n))^2. \tag{2.40}$$

Summing equation (2.40) over $K \in \mathcal{T}_R$ and over $n = 0, \dots, N_T$, and reordering the summation lead to:

$$\begin{aligned}\frac{1}{2}\sum_{n=0}^{N_T}\sum_{K\in\mathcal{T}_R} m(K)(u_K^{n+1}-u_K^n)^2 \leq \frac{1-\xi}{4\mathrm{M}}\sum_{n=0}^{N_T}\Delta t \sum_{(K,L)\in\varepsilon_R^n} \\ \left[\frac{1}{m(K|L)}\max_{u_L^n\leq c\leq d\leq u_K^n}(\mathcal{F}(d,c)-\mathcal{F}(d,d))^2\right. \\ \left. + \frac{1}{m(K|L)}\max_{u_L^n\leq c\leq d\leq u_K^n}(\mathcal{F}(d,c)-\mathcal{F}(c,c))^2\right].\end{aligned} \tag{2.41}$$

Since $\sum_{K\in\mathcal{T}_R} m(K)(u_K^{N_T+1})^2 \geq 0$ and $\frac{1}{2}\sum_{K\in\mathcal{T}_R} m(K)(u_K^0)^2 \leq C_6$, from (2.41) we have:

$$\begin{aligned}B_1 \geq -C_6 - \frac{1-\xi}{4\mathrm{M}}\sum_{n=0}^{N_T}\Delta t \sum_{(K,L)\in\varepsilon_R^n}\left[\frac{1}{m(K|L)}\max_{u_L^n\leq c\leq d\leq u_K^n}(\mathcal{F}(d,c)-\mathcal{F}(d,d))^2\right. \\ \left. + \frac{1}{m(K|L)}\max_{u_L^n\leq c\leq d\leq u_K^n}(\mathcal{F}(d,c)-\mathcal{F}(c,c))^2\right].\end{aligned} \tag{2.42}$$

From (2.35), (2.36) and (2.37) we get $|B_1 + B_4 - B_5| \leq C4$. From this and from (2.38), (2.39) and (2.42), we can then deduce:

$$\begin{aligned}\sum_{n=0}^{N_T}\Delta t \sum_{(K,L)\in\varepsilon_R^n}\left[\frac{1}{m(K|L)}\max_{u_L^n\leq c\leq d\leq u_K^n}(\mathcal{F}(d,c)-\mathcal{F}(d,d))^2\right. \\ \left. + \frac{1}{m(K|L)}\max_{u_L^n\leq c\leq d\leq u_K^n}(\mathcal{F}(d,c)-\mathcal{F}(c,c))^2\right] \leq C_7,\end{aligned} \tag{2.43}$$

where $C_7 = \frac{4\mathrm{M}}{\xi}(C_4 + C_5 + C_6)$.

Applying the Cauchy-Shwarz inequality to the expression

$$\sum_{n=0}^{N_T}\Delta t \sum_{(K,L)\in\varepsilon_R^n}\frac{1}{m(K|L)}\max_{u_L^n\leq c\leq d\leq u_K^n}(\mathcal{F}(d,c)-\mathcal{F}(d,d))$$

and using the monotonicity of $\mathcal{F}$, one gets:

$$\begin{aligned}&\left[\sum_{n=0}^{N_T}\Delta t \sum_{(K,L)\in\varepsilon_R^n}\frac{1}{m(K|L)}\max_{u_L^n\leq c\leq d\leq u_K^n}(\mathcal{F}(d,c)-\mathcal{F}(d,d))\right]^2 \\ &= \left(\sum_{n=0}^{N_T}\Delta t\right)^2\left[\sum_{(K,L)\in\varepsilon_R^n}\sqrt{m(K|L)}\left(\frac{1}{\sqrt{m(K|L)}}\max_{u_L^n\leq c\leq d\leq u_K^n}(\mathcal{F}(d,c)-\mathcal{F}(d,d))\right)\right]^2 \\ &\leq \left(\sum_{n=0}^{N_T}\Delta t\right)^2\sum_{(K,L)\in\varepsilon_R^n} m(K|L)\sum_{(K,L)\in\varepsilon_R^n}\frac{1}{m(K|L)}\left(\max_{u_L^n\leq c\leq d\leq u_K^n}(\mathcal{F}(d,c)-\mathcal{F}(d,d))\right)^2 \\ &\leq (N_T+1)\Delta t\sum_{(K,L)\in\varepsilon_R^n} m(K|L)\sum_{n=0}^{N_T}\Delta t\sum_{(K,L)\in\varepsilon_R^n}\frac{1}{m(K|L)}\left(\max_{u_L^n\leq c\leq d\leq u_K^n}(\mathcal{F}(d,c)-\mathcal{F}(d,d))\right. \\ &\qquad \left. + \max_{u_L^n\leq c\leq d\leq u_K^n}(\mathcal{F}(d,c)-\mathcal{F}(c,c))\right)^2.\end{aligned} \tag{2.44}$$

Let $N_\Delta^{\mathcal{T}_{R+h}}$ be the number of control volumes included in $B(0,R+h)$. Noting that

$$\begin{aligned}\sum_{(K,L)\in\varepsilon_R^n} m(K|L) &\le \sum_{K\in\mathcal{T}_{R+h}} m(K|L) \le N_\Delta^{\mathcal{T}_{R+h}} \sum_{L\in N(K)} m(K|L)\\ &\le \frac{m(B(0,R+h))}{m(K)} m(\partial K) \le C_8\left(\frac{1}{\alpha h^2}\right)\left(\frac{1}{\alpha}h\right)\\ &= \frac{C_9}{h}\end{aligned}$$

and that $(N_T+1)\Delta t$ is bounded, from (2.43) and (2.44) one obtains:

$$\sum_{n=0}^{N_T}\Delta t \sum_{(K,L)\in\varepsilon_R^n} \frac{1}{m(K|L)} \max_{u_L^n\le c\le d\le u_K^n} (\mathcal{F}(d,c)-\mathcal{F}(d,d)) \le \frac{C_{10}}{\sqrt{h}}. \tag{2.45}$$

Similarly we have:

$$\sum_{n=0}^{N_T}\Delta t \sum_{(K,L)\in\varepsilon_R^n} \frac{1}{m(K|L)} \max_{u_L^n\le c\le d\le u_K^n} (\mathcal{F}(d,c)-\mathcal{F}(c,c)) \le \frac{C_{10}}{\sqrt{h}}. \tag{2.46}$$

Adding equations (2.45) and (2.46) one obtains (2.33).

Finally, since (2.19) yields

$$m(K)|u_K^{n+1}-u_K^n| \le \Delta t \sum_{L\in N(K)} |\mathcal{F}(u_K^n,u_L^n)-\mathcal{F}(u_K^n,u_K^n)|,$$

inequality (2.34) immediately follows from (2.33). This completes the proof of Lemma 2.

It remains to prove Lemma 3.

We assume that f is nondecreasing and $c<d$ (the other cases are similar). Let $q=\frac{f(d)-f(c)}{L}$ and

$$h(s)=\begin{cases} f(c), & s\in[c,d-q]\\ f(c)+(s-d+q)L, & s\in[d-q,d]\end{cases}.$$

Thanks to f is a nondecreasing Lipschitz continuous function, $0<q\le d-c$.

Now, $c-(d-q) = c-d+q \le c-d+d-c = 0$. This is, $c\le d-q$. Hence, h is well defined.

On the other hand, it is clear that $f(s)\ge h(s)$, for all $s\in[c,d-q]$. Furthermore, for all $s\in[d-q,d]$,

$$h(s)=f(c)+(s-d+q)L = f(c)+qL+(s-d)L = f(d)+(s-d)L \le f(s),$$

because $f(d)-f(s)\le L(d-s)$. So, $f(s)\ge h(s),\ \forall s\in[c,d]$.

Then,

$$\begin{aligned}\int_c^d (f(s)-f(c))ds &\ge \int_c^d (h(s)-f(c))ds\\ &= \int_{d-q}^d (s-d+q)Lds = \frac{1}{2}(q^2L)\\ &= \frac{1}{2}\left(\frac{f(d)-f(c)}{L}\right)(f(d)-f(c))\\ &= \frac{1}{2L}(f(d)-f(c))^2.\end{aligned}$$

This completes the proof of Lemma 3.

Discrete entropy inequality for the approximate solution

Lemma 4 *Assume (2.18), (2.25) and (2.30). Let U_h be the approximate solution of the problem (1.1) defined by (2.20) and (2.19). Then, for all $k \in \mathbb{R}, K \in \mathcal{T}$ and $n \in \mathbb{N}$, the following inequality holds:*

$$|u_K^{n+1} - k| - |u_K^n - k| + \frac{\Delta t}{m(K)} \sum_{L \in N(K)} (\mathcal{F}(u_K^n \top k, u_L^n \top k) - \mathcal{F}(u_K^n \bot k, u_L^n \bot k)) \leq 0, \tag{2.47}$$

where $a \top b = \max\{a, b\}$ and $a \bot b = \min\{a, b\}$.

Proof. The scheme (2.19) writes

$$u_K^{n+1} = u_K^n - \frac{\Delta t}{m(K)} \sum_{L \in N(K)} \mathcal{F}(u_K^n, u_L^n) = G(u_K^n, u_L^n),$$

where G is a nondecreasing function w.r.t u_L^n, $L \in N(K)$, and u_K^n when Δt satisfies (2.30) and such that $G(k, k) = k$, $\forall k \in \mathbb{R}$. Therefore, $\forall k \in \mathbb{R}$

$$u_K^{n+1} = G(u_K^n, u_L^n) \leq G(u_K^n \top k, u_L^n) \leq G(u_K^n \top k, u_L^n \top k),$$

and

$$k = G(k, k) \leq G(u_K^n \top k, k) \leq G(u_K^n \top k, u_L^n \top k),$$

which yields

$$u_K^{n+1} \top k \leq G(u_K^n \top k, u_L^n \top k) = u_K^n \top k - \frac{\Delta t}{m(K)} \sum_{L \in N(K)} \mathcal{F}(u_K^n \top k, u_L^n \top k). \tag{2.48}$$

In the same manner, we get

$$u_K^{n+1} \bot k \geq u_K^n \bot k - \frac{\Delta t}{m(K)} \sum_{L \in N(K)} \mathcal{F}(u_K^n \bot k, u_L^n \bot k) \tag{2.49}$$

Taking into account that $|a - b| = (a \top b) - (a \bot b)$, the difference between (2.48) and (2.49) leads directly to (2.47).

Continuous entropy estimate for the approximate solution

For $\Omega = \mathbb{R}^2$ or $\Omega = \mathbb{R}^2 \times \mathbb{R}_+$, we denote by $\mathfrak{M}(\Omega)$ the set of measures on Ω, i.e, the set of positive continuous linear forms on $C_c(\Omega)$. If $\mu \in \mathfrak{M}(\Omega)$, we set $\langle \mu, g \rangle = \int_\Omega g d\mu$ for all $g \in C_c(\Omega)$.

Lemma 2 allows to obtain the following result which corresponds to a kind of Kruzkov's entropy inequality.

Theorem 2.2.1 *Assume (2.18), (2.25) and (2.30). Let U_h be the approximate solution of the problem (1.1) defined by (2.20) and (2.19). Then, there exist $\mu_{\mathcal{T}} \in \mathfrak{M}(\mathbb{R}^2)$ and $\mu_{\mathcal{T},\Delta t} \in \mathfrak{M}(\mathbb{R}^2 \times \mathbb{R}_+)$ such that, $\forall k \in \mathbb{R}$, $\forall \varphi \in C_c^\infty(\mathbb{R}^2 \times \mathbb{R}_+, \mathbb{R}_+)$:*

$$\begin{aligned} \int_{\mathbb{R}^2 \times \mathbb{R}_+} [|U_h(x,y,t) - k| \varphi_t(x,y,t) + \operatorname{sign}(U_h(x,y,t) - k)(f(U_h(x,y,t)) - f(k)) \cdot \\ \nabla \varphi(x,y,t)] dx dy dt + \int_{\mathbb{R}^2} |u_0(x,y) - k| \varphi(x,y,0) dx dy \\ + \int_{\mathbb{R}^2 \times \mathbb{R}_+} (|\varphi_t(x,y,t)| + |\nabla \varphi(x,y,t)|) d\mu_{\mathcal{T},\Delta t}(x,y,t) \\ + \int_{\mathbb{R}^2} \varphi(x,y,0) d\mu_{\mathcal{T}}(x,y) \geq 0. \end{aligned} \tag{2.50}$$

Furthermore, the measures $\mu_{\mathcal{T},\Delta t}$ and $\mu_{\mathcal{T}}$ verify the following properties:

1. For all $R > 0$ and $T > 0$, there exists C_m depending only on $F, u_0, M, \alpha, \xi, R$ and T such that

$$\mu_{\mathcal{T},\Delta t}(B(0,R)\times[0,T]) \leq C_m\sqrt{h} \tag{2.51}$$

2. The measure $\mu_{\mathcal{T}}$ is the measure of density $|u_0 - u_{\mathcal{T},0}|$ with respect to the Lebesgue measure. For all $R > 0$, we have:

$$\lim_{h\to 0}(\mu_{\mathcal{T}}(B(0,R))) = 0. \tag{2.52}$$

Proof. Let $\varphi \in C_c^\infty(\mathbb{R}^2\times\mathbb{R}_+,\mathbb{R}_+)$ and $k \in \mathbb{R}$. Let $T > 0$ and $R > 0$ such that $\varphi(x,y,t) \neq 0$ implies $\|(x,y)\| \leq R - h$ and $t \in [0,T]$. Let us multiply (2.47) by $\frac{1}{\Delta t}\int_{t^n}^{t^{n+1}}\int_K \varphi(x,y,t)dxdydt$ and sum the result for all K and n. It yields:

$$T_1 + T_2 \leq 0 \tag{2.53}$$

with

$$T_1 = \sum_{n=0}^{N_T}\sum_{K\in\mathcal{T}_R}\frac{|u_K^{n+1}-k| - |u_K^n - k|}{\Delta t}\int_{t^n}^{t^{n+1}}\int_K \varphi(x,y,t)dxdydt \tag{2.54}$$

and

$$\begin{aligned} T_2 = \sum_{n=0}^{N_T}\sum_{K\in\mathcal{T}_R}\frac{1}{m(K)}\int_{t^n}^{t^{n+1}}\int_K \varphi(x,y,t)dxdydt \\ \Big[\sum_{L\in N(K)}(\mathcal{F}(u_K^n\top k, u_L^n\top k) - \mathcal{F}(u_K^n\top k, u_K^n\top k) \\ - \mathcal{F}(u_K^n\perp k, u_L^n\perp k) + \mathcal{F}(u_K^n\perp k, u_K^n\perp k))\Big] \end{aligned} \tag{2.55}$$

We introduce T_{10} and T_{20} defined by

$$\begin{aligned} T_{10} &= -\int_{\mathbb{R}^2\times\mathbb{R}_+}|U_h(x,y,t)-k|\varphi_t(x,y,t)dxdydt - \int_{\mathbb{R}^2}|u_0(x,y)-k|\varphi(x,y,0)dxdy, \\ T_{20} &= -\int_{\mathbb{R}^2\times\mathbb{R}_+}(f(U_h(x,y,t)\top k) - f(U_h(x,y,t)\perp k))\cdot\bigtriangledown\varphi(x,y,t)dxdydt. \end{aligned}$$

In order to prove (2.50) we just need to prove that

$$T_{10} + T_{20} \leq \int_{\mathbb{R}^2\times\mathbb{R}_+}(|\varphi_t(x,y,t)| + |\nabla\varphi(x,y,t)|)d\mu_{\mathcal{T},\Delta t}(x,y,t) + \int_{\mathbb{R}^2}\varphi(x,y,0)d\mu_{\mathcal{T}}(x,y).$$

To do it, we compare T_1 to T_{10} and T_2 to T_{20}.

Comparison between T_1 and T_{10}

Since supp $\varphi \subset B(0,R)\times[0,T]$, using the definition of $U_h(x,y,t)$ given by (2.24) and

introducing the function $U_h(x,y,0) = U_K^0, \forall (x,y) \in \mathcal{T}$, we obtain:

$$\begin{aligned}
-\int_{\mathbb{R}^2\times\mathbb{R}_+} |U_h(x,y,t)-k|\varphi_t(x,y,t)dxdydt &= -\sum_{n=0}^{N_T}\sum_{K\in\mathcal{T}_R}\int_{t^n}^{t^{n+1}}\int_K |u_K^n-k|\varphi_t(x,y,t)dxdydt \\
&= -\sum_{K\in\mathcal{T}_R}\int_K \sum_{n=0}^{N_T}|u_K^n-k|(-\varphi(x,y,t^n)+\varphi(x,y,t^{n+1}))dxdy \\
&= -\sum_{K\in\mathcal{T}_R}\int_K [-|u_K^0-k|\varphi(x,y,0) \\
&\qquad -\sum_{n=0}^{N_T}(|u_K^{n+1}-k|-|u_K^n-k|)\varphi(x,y,t^{n+1})]dxdy \\
&= \int_{\mathbb{R}^2}(|U_h(x,y,0)-k|\varphi(x,y,0)dxdy \\
&+\sum_{n=0}^{N_T}\sum_{K\in\mathcal{T}_R}\frac{|u_K^{n+1}-k|-|u_K^n-k|}{\Delta t}\int_{t^n}^{t^{n+1}}\int_K \varphi(x,y,t^{n+1})dxdydt.
\end{aligned}$$

So, we get:

$$\begin{aligned}
T_{10} = \sum_{n=0}^{N_T}\sum_{K\in\mathcal{T}_R}\frac{|u_K^{n+1}-k|-|u_K^n-k|}{\Delta t}\int_{t^n}^{t^{n+1}}\int_K \varphi(x,y,t^{n+1})dxdydt \\
+\int_{\mathbb{R}^2}(|U_h(x,y,0)-k|-|u_0(x,y)-k|)\varphi(x,y,0)dxdy
\end{aligned}$$

which leads to

$$\begin{aligned}
|T_1-T_{10}| &= \Big|\sum_{n=0}^{N_T}\sum_{K\in\mathcal{T}_R}(|u_K^{n+1}-k|-|u_K^n-k|)\int_{t^n}^{t^{n+1}}\int_K \frac{\varphi(x,y,t^{n+1})-\varphi(x,y,t)}{\Delta t}dxdydt \\
&\qquad -\int_{\mathbb{R}^2}(|U_h(x,y,0)-k|-|u_0(x,y)-k|)\varphi(x,y,0)dxdy\Big| \\
&\le \sum_{n=0}^{N_T}\sum_{K\in\mathcal{T}_R}|u_K^{n+1}-u_K^n|\int_{t^n}^{t^{n+1}}\int_K |\varphi_t(x,y,t)|dxdydt \\
&\qquad +\int_{\mathbb{R}^2}|u_0(x,y)-U_h(x,y,0)|\varphi(x,y,0)dxdy.
\end{aligned} \tag{2.56}$$

We define two measures $\lambda_{\mathcal{T},\Delta t}$ and $\mu_{\mathcal{T}}$ defined by their action on $C_c(\mathbb{R}^2)$ and $C_c(\mathbb{R}^2\times\mathbb{R}_+)$ as:

$$\langle \mu_{\mathcal{T}}, g\rangle = \int_{\mathbb{R}^2} g(x,y)d\mu_{\mathcal{T}}(x,y) = \int_{\mathbb{R}^2}|u_0(x,y)-u_{\mathcal{T},0}(x,y)|g(x,y)dxdy,\ \forall g\in C_c(\mathbb{R}^2)$$

and

$$\begin{aligned}
\langle \lambda_{\mathcal{T},\Delta t}, g\rangle &= \int_{\mathbb{R}^2} g(x,y)d\lambda_{\mathcal{T},\Delta t}(x,y) \\
&= \sum_{n=0}^{N_T}\sum_{K\in\mathcal{T}}|u_K^{n+1}-u_K^n|\int_{t^n}^{t^{n+1}}\int_K g(x,y,t)dxdydt,\ \forall g\in C_c(\mathbb{R}^2\times\mathbb{R}_+).
\end{aligned}$$

Next, we prove (2.52) and that

$$\lambda_{\mathcal{T},\Delta t}(B(0,R)\times[0,T]) \le D\sqrt{h},$$

where D is a constant depending on $F, u_0, M, \alpha, \xi, R$ and T.

Let $\mathbf{x}, \overline{\mathbf{y}} \in K$ with $\mathbf{x} = (x, y)$ and $\overline{\mathbf{y}} = (\overline{x}, \overline{y})$. It is clear that $\|\mathbf{x} - \overline{\mathbf{y}}\| \leq h$. Let $u_0 \in C_c^\infty(\mathbb{R}^2)$. Since K is a compact and u_0 is continuous in K, u_0 is uniformly continuous in K. So, for all $\epsilon > 0$, there exists $\delta > 0$ such that, for all $\mathbf{x}, \overline{\mathbf{y}} \in K$

$$|u_0(\mathbf{x}) - u_0(\overline{\mathbf{y}})| < \epsilon \text{ provided that } \|\mathbf{x} - \overline{\mathbf{y}}\| \leq \delta.$$

Since $u_K^0 = \frac{1}{m(K)} \int_K u_0(\overline{\mathbf{y}}) d\overline{\mathbf{y}}$, for $h \leq \delta$ we have:

$$\begin{aligned}
\int_K |u_0(\mathbf{x}) - u_K^0| d\mathbf{x} &= \int_K \left| u_0(\mathbf{x}) - \frac{1}{m(K)} \int_K u_0(\overline{\mathbf{y}}) d\overline{\mathbf{y}} \right| d\mathbf{x} \\
&= \frac{1}{m(K)} \int_K \left| \int_K (u_0(\mathbf{x}) - u_0(\overline{\mathbf{y}})) d\overline{\mathbf{y}} \right| d\mathbf{x} \\
&\leq \frac{1}{m(K)} \int_K \int_K |u_0(\mathbf{x}) - u_0(\overline{\mathbf{y}})| d\overline{\mathbf{y}} d\mathbf{x} \\
&< m(K)\epsilon.
\end{aligned}$$

Let $u_0 \in L^\infty(\mathbb{R}^2)$. By density, for all $\epsilon > 0$, there exists $\overline{u}_0 \in C_c^\infty(\mathbb{R}^2)$ such that $|u_0 - \overline{u}_0| \leq \|u_0 - \overline{u}_0\|_{L^\infty} < \epsilon/3$. Set $\overline{u}_K^0 = \frac{1}{m(K)} \int_K \overline{u}(\mathbf{x}, 0) d\mathbf{x}$.

For h small enough, for all $K \in \mathcal{T}$ and for all $\mathbf{x} \in K$, the above inequality leads to

$$\int_K |\overline{u}_0(\mathbf{x}) - \overline{u}_K^0| d\mathbf{x} < m(K)\epsilon/3.$$

Furthermore,

$$|\overline{u}_K^0 - u_K^0| = \frac{1}{m(K)} \left| \int_K (\overline{u}_0(\mathbf{x}) - u_0(\mathbf{x})) \right| d\mathbf{x} \leq \frac{1}{m(K)} \int_K |\overline{u}_0(\mathbf{x}) - u_0(\mathbf{x})| d\mathbf{x} < \epsilon/3.$$

Therefore,

$$\begin{aligned}
\mu_{\mathcal{T}}(B(0,R)) &= \langle \mu_{\mathcal{T}}, 1_{B(0,R)} \rangle \\
&= \int_{\mathbb{R}^2} |u_0(\mathbf{x}) - u_{\mathcal{T},0}(\mathbf{x})| 1_{B(0,R)}(\mathbf{x}) d\mathbf{x} \\
&= \sum_{K \in \mathcal{T}_R} \int_K |u_0(\mathbf{x}) - u_K^0| d\mathbf{x} \\
&\leq \sum_{K \in \mathcal{T}_R} \int_K (|u_0(\mathbf{x}) - \overline{u}_0(\mathbf{x})| + |\overline{u}_0(\mathbf{x}) - \overline{u}_K^0| + |\overline{u}_K^0 - u_K^0|) d\mathbf{x} \\
&< \left(\sum_{K \in \mathcal{T}_R} m(K) \right) \epsilon
\end{aligned}$$

In consequence, $\lim_{h \to 0} (\mu_{\mathcal{T}}(B(0,R))) = 0$, for all $u_0 \in L^\infty(\mathbb{R}^2)$.

Furthermore, thanks to (2.30) and (2.34), for all $R > 0$ and $T > 0$, we have:

$$\begin{aligned}
\lambda_{\mathcal{T},\Delta t}(B(0,R) \times [0,T]) &= \langle \lambda_{\mathcal{T},\Delta t}, 1_{B(0,R)\times[0,T]} \rangle \\
&= \sum_{n \in \mathbb{N}} \sum_{K \in \mathcal{T}} |u_K^{n+1} - u_K^n| \int_{t^n}^{t^{n+1}} \int_K 1_{B(0,R)\times[0,T]}(\mathbf{x}, t) d\mathbf{x} dt \\
&\leq \sum_{n=0}^{N_T} \sum_{K \in \mathcal{T}_R} |u_K^{n+1} - u_K^n| \int_{t^n}^{t^{n+1}} \int_K d\mathbf{x} dt \\
&= \sum_{n=0}^{N_T} \sum_{K \in \mathcal{T}_R} m(K) |u_K^{n+1} - u_K^n| \Delta t.
\end{aligned}$$

That is:

$$\begin{aligned}\lambda_{\mathcal{T},\Delta t}(B(0,R)\times[0,T]) &\leq C_{\xi,\alpha,f}h\sum_{n=0}^{N_T}\sum_{K\in\mathcal{T}_R} m(K)|u_K^{n+1}-u_K^n| \\ &\leq C_{\xi,\alpha,f}h\left(\frac{C_{bv}}{\sqrt{h}}\right)=D\sqrt{h}\end{aligned} \tag{2.57}$$

where D is a constant depending on f, u_0, α, ξ, R and T.

With these two measures defined, inequality (2.56) equals:

$$|T_1 - T_{10}| \leq \int_{\mathbb{R}^2\times\mathbb{R}^+} |\varphi_t(x,y,t)|d\lambda_{\mathcal{T},\Delta t}(x,y,t) + \int_{\mathbb{R}^2}\varphi(x,y,0)d\mu_{\mathcal{T}}(x,y) \tag{2.58}$$

Comparison between T_2 and T_{20}

In T_2 we gather the terms by edges. Thus, $T_2 = T_{21} - T_{22}$, with:

$$\begin{aligned}T_{21} = \sum_{n=0}^{N_T}\sum_{(K,L)\in\varepsilon_R^n}\frac{1}{m(K)}\int_{t^n}^{t^{n+1}}\int_K \varphi(x,y,t)dxdydt[\mathcal{F}(u_K^n\top k, u_L^n\top k) - \mathcal{F}(u_K^n\top k, u_K^n\top k) \\ - \mathcal{F}(u_K^n\perp k, u_L^n\perp k) + \mathcal{F}(u_K^n\perp k, u_K^n\perp k))]\end{aligned}$$

and

$$\begin{aligned}T_{22} = \sum_{n=0}^{N_T}\sum_{(K,L)\in\varepsilon_R^n}\frac{1}{m(L)}\int_{t^n}^{t^{n+1}}\int_L \varphi(x,y,t)dxdydt[\mathcal{F}(u_K^n\top k, u_L^n\top k) - \mathcal{F}(u_L^n\top k, u_L^n\top k) \\ - \mathcal{F}(u_K^n\perp k, u_L^n\perp k) + \mathcal{F}(u_L^n\perp k, u_L^n\perp k))]\end{aligned}$$

Remark 7 *By the definition of ε_R^n, T_{21} includes $L\in\mathcal{T}$ that are not completely contained in $\mathcal{T}_R$ and T_{22} is the sum of the $L\in\mathcal{T}$ which have one edge contained in $\mathcal{T}_R$.*

Taking into account the function $\bar{f}$ defined above and that $\mathrm{div}(\varphi\bar{f}) = \varphi\mathrm{div}\bar{f} + \bar{f}\cdot\bigtriangledown\varphi$, using the fact that $\mathrm{div}_{(x,y)}\bar{f} = 0$ and applying the divergence theorem we can also gather the terms of T_{20} by edges:

$$\begin{aligned}T_{20} &= -\int_{\mathbb{R}^2\times\mathbb{R}_+}\nabla\cdot[(f(U_h(x,y,t)\top k) - f(U_h(x,y,t)\perp k))\varphi(x,y,t)]dxdydt \\ &= -\sum_{n=0}^{N_T}\sum_{(K,L)\in\varepsilon_R^n}\int_{t^n}^{t^{n+1}}\int_{K|L}(f(u_K^n\top k) - f(u_K^n\perp k) \\ &\qquad - f(u_L^n\top k) + f(u_L^n\perp k))\cdot n_{KL}\varphi(\gamma,t)d\gamma dt\end{aligned}$$

As T_2, T_{20} may be decomposed as $T_{201} - T_{202}$ with:

$$\begin{aligned}T_{201} = \sum_{n=0}^{N_T}\sum_{(K,L)\in\varepsilon_R^n}\int_{K|L}\int_{t^n}^{t^{n+1}}\Bigg(\frac{1}{m(K|L)}\mathcal{F}(u_K^n\top k, u_L^n\top k) - f(u_K^n\top k)\cdot n_{KL} \\ - \frac{1}{m(K|L)}\mathcal{F}(u_K^n\perp k, u_L^n\perp k) + f(u_K^n\perp k)\cdot n_{KL}\Bigg)\varphi(\gamma,t)dtd\gamma\end{aligned}$$

$$\begin{aligned}T_{202} = \sum_{n=0}^{N_T}\sum_{(K,L)\in\varepsilon_R^n}\int_{K|L}\int_{t^n}^{t^{n+1}}\Bigg(\frac{1}{m(K|L)}\mathcal{F}(u_K^n\top k, u_L^n\top k) - f(u_L^n\top k)\cdot n_{KL} \\ - \frac{1}{m(K|L)}\mathcal{F}(u_K^n\perp k, u_L^n\perp k) + f(u_L^n\perp k)\cdot n_{KL}\Bigg)\varphi(\gamma,t)dtd\gamma\end{aligned}$$

We now want to compare T_{21} and T_{201}. It is with this aim in view that we add and substract in T_{201} terms like

$$\int_{K|L}\int_{t^n}^{t^{n+1}} \frac{1}{m(K|L)}(\mathcal{F}(u_K^n \top k, u_K^n \top k) - \mathcal{F}(u_K^n \perp k, u_K^n \perp k))\varphi(\gamma,t)d\gamma dt.$$

Then we can see that these terms in T_{201} and T_{21} are the same if we replace the mean value of φ over a cell by the mean value over the edge of the cell. The other terms depend on f.

Taking into account that

$$\begin{aligned}
&\frac{1}{\Delta t\, m(K)}\int_{t^n}^{t^{n+1}}\int_K \varphi(x,y,t)dxdydt - \frac{1}{\Delta t\, m(K|L)}\int_{t^n}^{t^{n+1}}\int_{K|L}\varphi(\gamma,s)d\gamma ds\\
&= \frac{1}{(\Delta t)^2 m(K)m(K|L)}\Big(\int_{t^n}^{t^{n+1}}\int_K \varphi(x,y,t)\Delta t m(K|L)dxdydt - \Delta t m(K)\int_{t^n}^{t^{n+1}}\int_{K|L}\varphi(\gamma,s)d\gamma ds\Big)\\
&= \frac{1}{(\Delta t)^2 m(K)m(K|L)}\int_{t^n}^{t^{n+1}}\int_{K|L}\Big(\int_{t^n}^{t^{n+1}}\int_K \varphi(x,y,t)dxdydt - \Delta t m(K)\varphi(\gamma,s)\Big)d\gamma ds\\
&= \frac{1}{(\Delta t)^2 m(K)m(K|L)}\int_{t^n}^{t^{n+1}}\int_K\int_{t^n}^{t^{n+1}}\int_{K|L}(\varphi(x,y,t)-\varphi(\gamma,s))dxdyd\gamma ds
\end{aligned}$$

we get,

$$\begin{aligned}
T_{21} - T_{201} = \sum_{n=0}^{N_T}\sum_{(K,L)\in\varepsilon_R^n}\Delta t\Big[&\mathcal{F}(u_K^n\top k, u_L^n\top k) - \mathcal{F}(u_K^n\top k, u_K^n\top k)\\
&- \mathcal{F}(u_K^n\perp k, u_L^n\perp k) + \mathcal{F}(u_K^n\perp k, u_K^n\perp k)\Big]\\
&\left(\frac{1}{(\Delta t)^2 m(K)m(k|L)}\int_{t^n}^{t^{n+1}}\int_K\int_{t^n}^{t^{n+1}}\int_{K|L}(\varphi(x,y,t)-\varphi(\gamma,s))dxdyd\gamma ds\right)
\end{aligned} \tag{2.59}$$

Lemma 5 *Let $\mathbf{x}=(x,y)$ and let $\varphi\in C_c^\infty(\mathbb{R}^2\times\mathbb{R}_+,\mathbb{R}_+)$. For all $(\mathbf{x},\gamma,t,s)\in K\times K|L\times[t^n,t^{n+1})^2$, we have:*

$$|\varphi(\mathbf{x},t)-\varphi(\gamma,s)| \le \int_0^1 (h+\Delta t)(|\nabla\varphi| + |\varphi_t|)(\gamma+\theta(\mathbf{x}-\gamma), s+\theta(t-s))d\theta \tag{2.60}$$

Proof. For $z\in\mathbb{R}^2\times\mathbb{R}_+$, let $\widetilde{\varphi}(z)=\varphi(\mathbf{x},t)$. Then, $\frac{d}{dz}(\widetilde{\varphi}(z)) = \nabla_z\widetilde{\varphi} = (\nabla\varphi,\varphi_t)$. So,

$$\varphi(\mathbf{x},t)-\varphi(\gamma,s) = \int_{(\gamma,s)}^{(\mathbf{x},t)}\frac{d}{dz}(\widetilde{\varphi}(z))\cdot dz.$$

Now, defining $z(\theta)=(\gamma,s)+\theta(\mathbf{x}-\gamma,t-s)$, $\forall\,\theta\in[0,1]$, we get:

$$\begin{aligned}
|\varphi(\mathbf{x},t)-\varphi(\gamma,s)| &= \left|\int_0^1 \frac{d}{dz}(\widetilde{\varphi}(\gamma+\theta(\mathbf{x}-\gamma), s+\theta(t-s)))\cdot(\mathbf{x}-\gamma,t-s)\right|\\
&= \left|\int_0^1 [\nabla\varphi(\gamma+\theta(\mathbf{x}-\gamma),s+\theta(t-s))\cdot(\mathbf{x}-\gamma) + \varphi_t(\gamma+\theta(\mathbf{x}-\gamma),s+\theta(t-s))(t-s)]\,d\theta\right|\\
&\le \int_0^1 (|\nabla\varphi(\gamma+\theta(\mathbf{x}-\gamma),s+\theta(t-s))|\,\|\mathbf{x}-\gamma\| + |\varphi_t(\gamma+\theta(\mathbf{x}-\gamma),s+\theta(t-s))|\,|t-s|)\,d\theta\\
&\le \int_0^1 (h\,|\nabla\varphi(\gamma+\theta(\mathbf{x}-\gamma),s+\theta(t-s))| + \Delta t\,|\varphi_t(\gamma+\theta(\mathbf{x}-\gamma),s+\theta(t-s))|)\,d\theta.
\end{aligned}$$

That is,

$$|\varphi(\mathbf{x},t)-\varphi(\gamma,s)| \leq \int_0^1 (h+\Delta t)(|\nabla\varphi|+|\varphi_t|)(\gamma+\theta(\mathbf{x}-\gamma), s+\theta(t-s))d\theta.$$

For all $K \in \mathcal{T}, L \in N(K), n \in \mathbb{N}$, we define the measure $\mu_{K,L}^n \in \mathfrak{M}(\mathbb{R}^2)$ by its action on $C_c(\mathbb{R}^2)$ as:

$$\langle \mu_{K,L}^n, g\rangle = \frac{1}{(\Delta t)^2 m(K) m(k|L)} \int_{t^n}^{t^{n+1}} \int_K \int_{t^n}^{t^{n+1}} \int_{K|L} \int_0^1 (h+\Delta t) g(\gamma+\theta(\mathbf{x}-\gamma), s+\theta(t-s)) d\theta d\gamma dt d\mathbf{x} ds$$

Then, the expressions (2.59) and (2.60) along with the definition of the measure $\mu_{K,L}^n$ lead to:

$$\begin{aligned} |T_{21}-T_{201}| \leq \sum_{n=0}^{N_T} \sum_{(K,L)\in\varepsilon_R^n} \Delta t \Big[& \mathcal{F}(u_K^n \top k, u_L^n \top k) - \mathcal{F}(u_K^n \top k, u_K^n \top k) \\ & + \mathcal{F}(u_K^n \perp k, u_L^n \perp k) - \mathcal{F}(u_K^n \perp k, u_K^n \perp k) \Big] \langle \mu_{K,L}^n, |\bigtriangledown\varphi| + |\varphi_t| \rangle \end{aligned} \tag{2.61}$$

Proceeding in a similar way, we obtain as well:

$$\begin{aligned} |T_{22}-T_{202}| \leq \sum_{n=0}^{N_T} \sum_{(K,L)\in\varepsilon_R^n} \Delta t \Big[& \mathcal{F}(u_K^n \top k, u_L^n \top k) - \mathcal{F}(u_L^n \top k, u_L^n \top k) \\ & + \mathcal{F}(u_K^n \perp k, u_L^n \perp k) - \mathcal{F}(u_L^n \perp k, u_L^n \perp k) \Big] \langle \mu_{L,K}^n, |\bigtriangledown\varphi| + |\varphi_t| \rangle \end{aligned} \tag{2.62}$$

The monotony of $\mathcal{F}$ implies that $\forall (K,L) \in \varepsilon_R^n$, $\forall k \in \mathbb{R}$,

$$\begin{aligned} 0 \leq \mathcal{F}(u_K^n \top k, u_L^n \top k) - \mathcal{F}(u_K^n \top k, u_K^n \top k) &\leq \max_{u_L^n \leq c \leq d \leq u_K^n} (\mathcal{F}(d,c) - \mathcal{F}(d,d)) \\ 0 \leq \mathcal{F}(u_K^n \top k, u_L^n \top k) - \mathcal{F}(u_L^n \top k, u_L^n \top k) &\leq \max_{u_L^n \leq c \leq d \leq u_K^n} (\mathcal{F}(d,c) - \mathcal{F}(c,c)) \end{aligned} \tag{2.63}$$

and these properties are always true if we replace $\top$ by $\perp$. Then, we can finally define $\mu_{\mathcal{T},\Delta t} \in \mathfrak{M}(\mathbb{R}^2 \times \mathbb{R}_+)$ by its action on $C_c(\mathbb{R}^2 \times \mathbb{R}_+)$ as:

$$\begin{aligned} \langle \mu_{\mathcal{T},\Delta t}, g\rangle = \langle \lambda_{\mathcal{T},\Delta t}, g\rangle + 2 \sum_{n\in\mathbb{N}} \sum_{(K,L)\in\varepsilon^n} \Delta t \Big[& \max_{u_L^n \leq c \leq d \leq u_K^n} (\mathcal{F}(d,c) - \mathcal{F}(d,d)) \langle \mu_{K,L}^n, g\rangle \\ & + \max_{u_L^n \leq c \leq d \leq u_K^n} (\mathcal{F}(d,c) - \mathcal{F}(c,c)) \langle \mu_{L,K}^n, g\rangle \Big] \end{aligned}$$

Thanks to (2.33), (2.57) and the definition of the measure $\mu_{K,L}^n$, we have the bound (2.51).

Taking into account (2.53) and that $T_2 = T_{21} - T_{22}$ and $T_{20} = T_{201} - T_{202}$, we have:

$$\begin{aligned} T_{10} + T_{20} &\leq |T_{10} + T_{20}| \\ &\leq |T_{10} - T_1| + |T_1 + T_{20}| \\ &\leq |T_{10} - T_1| + |-T_2 + T_{20}| \\ &\leq |T_{10} - T_1| + |T_{201} - T_{202} - T_{21} + T_{22}| \\ &\leq |T_{10} - T_1| + |T_{201} - T_{21}| + |T_{22} - T_{202}| \end{aligned}$$

From (2.58), (2.61), (2.62), (2.63) and the definition of the measure $\mu_{\mathcal{T},\Delta t}$, it follows that:

$$\begin{aligned}
-T_{10}-T_{20} \geq & -\int_{\mathbb{R}^2\times\mathbb{R}_+} |\varphi_t(x,y,t)| d\lambda_{\mathcal{T},\Delta t}(x,y,t) - \int_{\mathbb{R}^2} \varphi(x,y,0) d\mu_{\mathcal{T}}(x,y) \\
& - 2\sum_{n\in\mathbb{N}} \sum_{(K,L)\in\varepsilon^n} \Delta t[\max_{u_L^n\leq c\leq d\leq u_K^n} (\mathcal{F}(d,c)-\mathcal{F}(d,d))\langle \mu_{K,L}^n, |\varphi_t|+|\nabla\varphi|\rangle \\
& + \max_{u_L^n\leq c\leq d\leq u_K^n} (\mathcal{F}(d,c)-\mathcal{F}(c,c))\langle \mu_{L,K}^n, |\varphi_t|+|\nabla\varphi|\rangle] \\
\geq & -\int_{\mathbb{R}^2\times\mathbb{R}_+} (|\varphi_t(x,y,t)|+|\nabla\varphi(x,y,t)|) d\lambda_{\mathcal{T},\Delta t}(x,y,t) - \int_{\mathbb{R}^2} \varphi(x,y,0) d\mu_{\mathcal{T}}(x,y) \\
& - 2\sum_{n\in\mathbb{N}} \sum_{(K,L)\in\varepsilon^n} \Delta t[\max_{u_L^n\leq c\leq d\leq u_K^n} (\mathcal{F}(d,c)-\mathcal{F}(d,d))\langle \mu_{K,L}^n, |\varphi_t|+|\nabla\varphi|\rangle \\
& + \max_{u_L^n\leq c\leq d\leq u_K^n} (\mathcal{F}(d,c)-\mathcal{F}(c,c))\langle \mu_{L,K}^n, |\varphi_t|+|\nabla\varphi|\rangle] \\
\geq & -\int_{\mathbb{R}^2\times\mathbb{R}_+} (|\varphi_t(x,y,t)|+|\nabla\varphi(x,y,t)|) d\mu_{\mathcal{T},\Delta t}(x,y,t) - \int_{\mathbb{R}^2} \varphi(x,y,0) d\mu_{\mathcal{T}}(x,y)
\end{aligned}$$

This concludes the proof of theorem 4.1.

A property of probability measures

Proposition 1 *Let $\mathbb{P}(\mathbb{R})$ be the set of probability measures on $\mathbb{R}$ and let $m \in \mathbb{P}(\mathbb{R})$. For any $g \in C_b(\mathbb{R},\mathbb{R})$, where $C_b(\mathbb{R},\mathbb{R})$ is the space of bounded continuous functions from $\mathbb{R}$ to $\mathbb{R}$, define $m(g) = \langle m, g\rangle = \int_{\mathbb{R}} g(z)dm(z)$. Then, there exists $\mu \in L^\infty(\mathbb{R}^2\times\mathbb{R}_+\times(0,1),\mathbb{R})$ such that*

$$\langle m, g\rangle = \int_0^1 g(\mu(x,y,t,\alpha))d\alpha, \ \ a.e\ (x,y,t)\in\mathbb{R}^2\times(0,T). \tag{2.64}$$

Proof. Let $F_m : \mathbb{R}\to[0,1]$ be the repartition function of the measure m, defined for any $x\in\mathbb{R}$ by:

$$F_m(x) = \mathrm{Sup}\left\{m(g),\ g\in C_b(\mathbb{R},\mathbb{R}),\ g\leq 1_{(-\infty,x)}\right\}.$$

Let $M_m : (0,1)\to\mathbb{R}$ be the function defined by:

$$M_m(\alpha) = \mathrm{Inf}\left\{x\in\mathbb{R},\ F_m(x)>\alpha\right\},\ \text{for any } \alpha\in(0,1).$$

Since the function F_m is nondecreasing and left-continuous, it is easily seen that:

$$\mathrm{Sup}\left\{\alpha\in(0,1),\ M_m(\alpha)<x\right\} = F_m(x),\ \text{for any } x\in\mathbb{R} \text{ such that } F_m(x)>0.$$

Hence the function M_m is nondecreasing, right-continuous, and it is the reciprocal of the function F_m if it is continuous. Therefore,

$$\int_0^1 1_{(-\infty,x)}\left(M_m(\alpha)\right)d\alpha = F_m(x),\ \text{for any } x\in\mathbb{R} \text{ such that } F_m(x)>0.$$

In consequence, the repartition function of the measure defined by $g\to\int_0^1 g\left(M_m(\alpha)\right)d\alpha$ is also the function F_m. Then, the measure $g\to\int_0^1 g\left(M_m(\alpha)\right)d\alpha$ is identical to the measure m.

The proof ends by defining μ by $\mu(\mathbf{x},t,\alpha) = M_{m_{(\mathbf{x},t)}}(\alpha)$ for $(\mathbf{x},t,\alpha)\in\mathbb{R}^2\times\mathbb{R}_+\times(0,1)$.

A classical result on Young measures

Young measures were introduced in the context of PDEs by Tartar in order to represent weak* limits of L^∞-bounded sequences of highly oscillatory functions.

Definition 7 *A Young measure is a map $m : \mathbb{R}^2 \times (0,T) \to \mathbb{P}(\mathbb{R})$, such that for every $g \in C_0(\mathbb{R})$ the map $\langle\, m, g\rangle\,(x,y,t) := \langle\, m(x,y,t), g\rangle$ is measurable.*

Theorem 2.2.2 *Let $(u_n)_{n\in\mathbb{N}}$ be a bounded sequence of $L^\infty(\mathbb{R}^2 \times (0,T))$ with $\|u_n\|_\infty \leq r$, $r > 0$. Then, a subsequence of $(u_n)_{n\in\mathbb{N}}$ (which will still be denoted by $(u_n)_{n\in\mathbb{N}}$) and a Young measure $m_{(x,y,t)}$ exist, such that $\operatorname{supp} m_{(x,y,t)} \subset [-r,r]$ and $\forall g \in C(\mathbb{R},\mathbb{R})$, $g(u_n(x,y,t)) \overset{*}{\rightharpoonup} \overline{g}(x,y,t) = \int_{\mathbb{R}} g dm_{(x,y,t)}$ in the following sense:*

For all $\varphi \in L^1(\mathbb{R}^2 \times (0,T))$,

$$\lim_{n\to\infty} \int_{\mathbb{R}^2\times(0,T)} g(u_n(x,y,t))\varphi(x,y,t)dxdydt = \int_{\mathbb{R}^2\times(0,T)} \overline{g}(x,y,t)\varphi(x,y,t)dxdydt. \tag{2.65}$$

Proof. Let $(u_n)_{n\in\mathbb{N}}$ be a bounded sequence of $L^\infty(\mathbb{R}^2 \times (0,T))$ and $r \geq 0$ such that $\|u_n\|_\infty \leq r,\ \forall n \in \mathbb{N}$.

Thanks to the separability of the set of continuous functions defined from $[-r,r]$ into $\mathbb{R}$ (endowed with the supremum norm) and the sequential weak star relative compactness of the bounded sets of $L^\infty(\mathbb{R}^2 \times (0,T))$, there exists (using a diagonal process) a subsequence (which will still be denoted by $(u_n)_{n\in\mathbb{N}}$) such that for any function $g \in C(\mathbb{R},\mathbb{R})$, the sequence $(g(u_n))_{n\in\mathbb{N}}$ converges in $L^\infty(\mathbb{R}^2 \times (0,T))$ for the weak star topology towards a function $U_g \in L^\infty(\mathbb{R}^2 \times (0,T))$.

Let $\mathbf{y} = (\mathbf{x},t) \in \mathbb{R}^2 \times (0,T)$ and $F_{\mathbf{y}} = \left\{ g \in C([-r,r]) : \lim_{h\to 0} \frac{1}{m(B(\mathbf{y},h))} \int_{B(\mathbf{y},h)} U_g(z)dz \text{ exists} \in \mathbb{R} \right\}$.

If $g \in F_{\mathbf{y}}$, we set $\overline{U}_g(\mathbf{y}) = \lim_{h\to 0} \frac{1}{m(B(\mathbf{y},h))} \int_{B(\mathbf{y},h)} U_g(z)dz$. We define $T_{\mathbf{y}}$ from $F_{\mathbf{y}}$ in $\mathbb{R}$ by $T_{\mathbf{y}}(g) = \overline{U}_g(\mathbf{y})$. It is easily seen that $F_{\mathbf{y}}$ is a vector space which contains the constants and $T_{\mathbf{y}}$ is a linear positive form over $F_{\mathbf{y}}$. Hence using a modified version of Hanh-Banach's theorem, one can prolongue $T_{\mathbf{y}}$ into a positive linear form $\overline{T}_{\mathbf{y}}$ defined over $C([-r,r],\mathbb{R})$. By Riesz' theorem, there exists a (positive) measure $\nu_{\mathbf{y}}$ on the borelian sets of $[-r,r]$ such that:

$$T_{\mathbf{y}}(g) = \overline{U}_g(\mathbf{y}) = \int_{-r}^{r} g d\nu_{\mathbf{y}},\ \forall g \in C([-r,r],\mathbb{R}). \tag{2.66}$$

The function $g \equiv 1$ is in $F_{\mathbf{y}}$, and for $g \equiv 1$, $\overline{U}_g(1) = 1$. Therefore, from (2.66) $\nu_{\mathbf{y}}$ is a probability over $[-r,r]$, and thus a probability over $\mathbb{R}$ by prolonging it by 0 outside $[-r,r]$. It is important to remark that if $g \in C(\mathbb{R},\mathbb{R})$, then for a.e. $\mathbf{y} \in \mathbb{R}^2 \times (0,T)$, $U_g(\mathbf{y}) = \overline{U}_g(\mathbf{y})$.

From Proposition 1, one has

$$m_{(\mathbf{x},t)}(g) = \int_0^1 g(\mu(\mathbf{x},t,\alpha))d\alpha,\ \forall g \in C(\mathbb{R},\mathbb{R}),$$

and for any function $g \in C(\mathbb{R},\mathbb{R})$, $\int_0^1 g(\mu(\mathbf{x},t,\alpha))d\alpha = U_g(\mathbf{x},t)$ for almost any $(\mathbf{x},t) \in \mathbb{R}^2 \times (0,T)$.

Existence of an entropy process solution

Definition 4 along with Theorems 2.2.1 and 2.2.2 and Proposition 1 are essential for the proof of the existence of the solution to problem (1.1).

This is not a new result. It simply collects sufficient conditions which allow to prove the convergence of the fully-discrete Lagrangian-Eulerian scheme (2.19)-(2.20).

Next, we prove the following existence result:

Theorem 2.2.3 *Assume (2.29), then there exists an entropy process solution to the problem (1.1).*

Proof. Under assumptions (2.29), Lemma 1 allows, by means of the scheme defined by (2.20) and (2.19), to construct a bounded sequence $U_h(x,y,t) = u_K^n,\ (x,y) \in K,\ n \in \mathbb{N},\ t \in (0,T)$ of $L^\infty(\mathbb{R}^2 \times (0,T))$.

Therefore, from Theorem 2.2.2 and Proposition 1, there exists $\mu \in L^\infty(\mathbb{R}^2 \times (0,T) \times (0,1))$ and a subsequence of $U_h(x,y,t)$ (which will still be denoted by $U_h(x,y,t)$) such that $\forall g \in C(\mathbb{R},\mathbb{R})$ and $\forall \psi \in L^1(\mathbb{R}^2 \times (0,T))$,

$$\lim_{n\to\infty} \int_{\mathbb{R}^2\times(0,T)} g(U_h(x,y,t))\psi(x,y,t)dxdydt = \int_{\mathbb{R}^2\times(0,T)\times(0,1)} g(\mu(x,y,t,\alpha))\psi(x,y,t)dxdydtd\alpha \tag{2.67}$$

Let $\varphi \in C_c^\infty(\mathbb{R}^2 \times \mathbb{R}_+, \mathbb{R}_+)$ and $k \in \mathbb{R}$. Let $R > 0$ and $T > 0$ such that $\text{supp}\varphi \subset B(0,R) \times [0,T]$.

Taking $g(\cdot) = |\cdot - k|$ and $\psi(x,y,t) = \varphi_t(x,y,t)$ in (2.67), it follows that

$$\lim_{n\to\infty} \int_{\mathbb{R}^2\times\mathbb{R}_+} |U_h(x,y,t) - k|\varphi_t(x,y,t)dxdydt = \int_{\mathbb{R}^2\times\mathbb{R}_+\times(0,1)} |\mu(x,y,t,\alpha) - k|\varphi_t(x,y,t)dxdydtd\alpha \tag{2.68}$$

Now, taking $g_i(\cdot) = \text{sign}(\cdot - k)(f_i(\cdot) - f_i(k)), i = 1,2, f = (f_1,f_2), g = (g_1,g_2)$ and $\psi(x,y,t) = \nabla\varphi(x,y,t)$ in (2.67), we have

$$\lim_{n\to\infty} \int_{\mathbb{R}^2\times\mathbb{R}_+} \text{sign}(U_h(x,y,t) - k)(f(U_h(x,y,t)) - f(k)) \cdot \nabla\varphi(x,y,t)dxdydt = \int_{\mathbb{R}^2\times\mathbb{R}_+\times(0,1)} \text{sign}(\mu(x,y,t,\alpha) - k)(f(\mu(x,y,t,\alpha) - f(k)) \cdot \nabla\varphi(x,y,t)dxdydtd\alpha. \tag{2.69}$$

From (2.51) one can deduce that:

$$\int_{\mathbb{R}^2\times\mathbb{R}_+} (|\varphi_t(x,y,t)| + |\nabla\varphi(x,y,t)|)d\mu_{\mathcal{T},\Delta t}(x,y,t) \le (\|\varphi_t\|_\infty + \|\nabla\varphi\|_\infty)C_m\sqrt{h}. \tag{2.70}$$

Furthermore,

$$\int_{\mathbb{R}^2} \varphi(x,y,0)d\mu_{\mathcal{T}}(x,y) = \int_{B(0,R)} \varphi(x,y,0)d\mu_{\mathcal{T}}(x,y) \le \|\varphi(\cdot,0)\|_\infty \mu_{\mathcal{T}}(B(0,R). \tag{2.71}$$

Passing to the limit (as $h \to 0$) in (2.50), the expressions (2.68), (2.69), (2.70), (2.71) and (2.52) lead to $\mu(x,y,t,\alpha)$ being an entropy process solution in the sense of definition 4.

Uniqueness of the entropy process solution

Theorem 2.2.4 *Under the assumptions (2.29), the entropy process solution to (1.1) is unique and it is the unique entropy solution to (1.1).*

Proof. Assume that there exist two entropy process solutions $v \in L^\infty(\mathbb{R}^2 \times \mathbb{R}_+ \times (0,1))$ and $w \in L^\infty(\mathbb{R}^2 \times \mathbb{R}_+ \times (0,1))$. It means that, $\forall k \in \mathbb{R}, \forall \varphi \in C_c^1(\mathbb{R}^2 \times \mathbb{R}_+, \mathbb{R}_+)$,

$$\int_{\mathbb{R}^2\times\mathbb{R}_+} \int_0^1 [|v(x,y,t,\alpha) - k|\varphi_t(x,y,t) + \text{sign}(v(x,y,t,\alpha) - k)(f(v(x,y,t,\alpha)) - f(k)) \cdot \nabla\varphi(x,y,t)]d\alpha dtdxdy + \int_{\mathbb{R}^2} |u_0(x,y) - k|\varphi(x,y,0)dxdy \ge 0, \tag{2.72}$$

and

$$\int_{\mathbb{R}^2\times\mathbb{R}_+}\int_0^1 [|w(\overline{x},\overline{y},s,\beta)-k|\varphi_s(\overline{x},\overline{y},t)+\text{sign}(w(\overline{x},\overline{y},s,\beta)-k)(f(w(\overline{x},\overline{y},s,\beta))-f(k)) \cdot\nabla\varphi(\overline{x},\overline{y},s)]d\beta ds d\overline{x}d\overline{y}+\int_{\mathbb{R}^2}|u_0(\overline{x},\overline{y})-k|\varphi(\overline{x},\overline{y},0)d\overline{x}d\overline{y}\geq 0. \tag{2.73}$$

Considering two functions $\rho_2\in C_c^\infty(\mathbb{R}^2,\mathbb{R})$ and $\overline{\rho}_1\in C_c^\infty(\mathbb{R},\mathbb{R})$ that satisfy:

$$\begin{cases}\text{Supp}(\rho_2)\subset\left\{(x,y)\in\mathbb{R}^2;|(x,y)|\leq 1\right\}, & \text{Supp}(\overline{\rho}_1)\subset[-1,0],\\ \rho_2(x,y)\geq 0,\forall(x,y)\in\mathbb{R}^2, & \overline{\rho}_1(x)\geq 0,\forall x\in\mathbb{R},\\ \int_{\mathbb{R}^2}\rho_2(x,y)dA=1, & \int_{\mathbb{R}}\overline{\rho}_1(x)dx=1.\end{cases} \tag{2.74}$$

For all $r\geq 1$, we define $\rho_{2,r}:(x,y)\to r^2\rho_2(rx,ry)$ and $\overline{\rho}_{1,r}:x\to r\overline{\rho}_1(rx)$. We have:

$$\int_{\mathbb{R}^2\times\mathbb{R}_+}\rho_{2,r}(x-\overline{x},y-\overline{y})\overline{\rho}_{1,r}(t-s)d\overline{x}d\overline{y}ds=1,\ \forall(x,y)\in\mathbb{R}^2,\ \forall t\in\mathbb{R}^+. \tag{2.75}$$

Let $\psi\in C_c^\infty(\mathbb{R}^2\times\mathbb{R}_+,\mathbb{R}_+)$, we set

$$\varphi(x,y,t,\overline{x},\overline{y},s)=\psi(x,y,t)\rho_{2,r}(x-\overline{x},y-\overline{y})\overline{\rho}_{1,r}(t-s).$$

We rewrite (2.72) for the function $\varphi(\cdot,\cdot,\cdot,\overline{x},\overline{y},s)$ and $k=w(\overline{x},\overline{y},s,\beta)$ and we integrate with respect to $\overline{x},\overline{y},s$ and β. For this case, we have:

$\varphi(x,y,0)=\psi(x,y,0)\rho_{2,r}(x-\overline{x},y-\overline{y})\overline{\rho}_{1,r}(-s)$,

$\varphi_t(x,y,t)=\psi_t(x,y,t)\rho_{2,r}(x-\overline{x},y-\overline{y})\overline{\rho}_{1,r}(t-s)+\psi(x,y,t)\rho_{2,r}(x-\overline{x},y-\overline{y})\overline{\rho}'_{1,r}(t-s)$

and

$\nabla\varphi(x,y,t)=\nabla\psi(x,y,t)\rho_{2,r}(x-\overline{x},y-\overline{y})\overline{\rho}_{1,r}(t-s)+\psi(x,y,t)\nabla\rho_{2,r}(x-\overline{x},y-\overline{y})\overline{\rho}_{1,r}(t-s)$

It yields:

$$A_1+A_2+A_3+A_4+A_5\geq 0 \tag{2.76}$$

with

$$A_1=\int_{(\mathbb{R}^2\times\mathbb{R}_+\times(0,1))^2}|v(x,y,t,\alpha)-w(\overline{x},\overline{y},s,\beta)|\psi_t(x,y,t)\rho_{2,r}(x-\overline{x},y-\overline{y}) \overline{\rho}_{1,r}(t-s)dxdydtd\alpha d\overline{x}d\overline{y}dsd\beta$$

$$A_2=\int_{(\mathbb{R}^2\times\mathbb{R}_+\times(0,1))^2}|v(x,y,t,\alpha)-w(\overline{x},\overline{y},s,\beta)|\psi(x,y,t)\rho_{2,r}(x-\overline{x},y-\overline{y}) \overline{\rho}'_{1,r}(t-s)dxdydtd\alpha d\overline{x}d\overline{y}dsd\beta$$

$$A_3=\int_{(\mathbb{R}^2\times\mathbb{R}_+\times(0,1))^2}(f(v(x,y,t,\alpha)\top w(\overline{x},\overline{y},s,\beta))-f(v(x,y,t,\alpha)\bot w(\overline{x},\overline{y},s,\beta)))\cdot \nabla\psi(x,y,t)\rho_{2,r}(x-\overline{x},y-\overline{y})\overline{\rho}_{1,r}(t-s)dxdydtd\alpha d\overline{x}d\overline{y}dsd\beta$$

$$A_4=\int_{(\mathbb{R}^2\times\mathbb{R}_+\times(0,1))^2}(f(v(x,y,t,\alpha)\top w(\overline{x},\overline{y},s,\beta))-f(v(x,y,t,\alpha)\bot w(\overline{x},\overline{y},s,\beta)))\cdot \nabla\rho_{2,r}(x-\overline{x},y-\overline{y})\psi(x,y,t)\overline{\rho}_{1,r}(t-s)dxdydtd\alpha d\overline{x}d\overline{y}dsd\beta$$

$$A_5=\int_{(\mathbb{R}^2)^2\times\mathbb{R}_+\times(0,1)}|u_0(x,y)-w(\overline{x},\overline{y},s,\beta)|\psi(x,y,0)\rho_{2,r}(x-\overline{x},y-\overline{y}) \overline{\rho}_{1,r}(-s)dxdyd\overline{x}d\overline{y}dsd\beta$$

Let us denote by S the support of ψ and by S_0 the support of $\psi(\cdot,\cdot,0)$.

First, let us prove that for all $\psi\in C_c^\infty(\mathbb{R}^2\times\mathbb{R}_+,\mathbb{R}_+)$

$$\int_{\mathbb{R}^2\times\mathbb{R}_+\times(0,1)^2}(|v(x,y,t,\alpha)-w(x,y,t,\beta)|\psi_t(x,y,t)+(f(v(x,y,t,\alpha)\top w(x,y,t,\beta)) -f(v(x,y,t,\alpha)\bot w(x,y,t,\beta))\cdot\nabla\psi(x,y,t))dxdydtd\alpha d\beta\geq 0. \tag{2.77}$$

The following result will be used to prove it.

Lemma 6 *Let $g \in L^\infty(\mathbb{R}^q)$. For all compact set $K \subset \mathbb{R}^q$:*

$$\int_{\mathbb{R}^q} |g(\mathbf{x}+\mathbf{h}) - g(\mathbf{x})| 1_K(\mathbf{x}) d\mathbf{x} \overset{\mathbf{h}\to 0}{\longrightarrow} 0$$

Proof. Let $K \subset \mathbb{R}^q$ be a compact, let $g \in L^\infty(\mathbb{R}^q)$ and let $\mathbf{x}, \mathbf{h} \in \mathbb{R}^q$. Since

$$|g(\mathbf{x}+\mathbf{h}) - g(\mathbf{x})| \leq |g(\mathbf{x}+\mathbf{h})| + |g(\mathbf{x})| \leq 2\,\|g\|_{L^\infty} \text{ a.e } \mathbb{R}^q$$

then,

$$\int_{\mathbb{R}^q} |g(\mathbf{x}+\mathbf{h}) - g(\mathbf{x})| 1_K(\mathbf{x}) d\mathbf{x} \leq 2\,\|g\|_{L^\infty}\, m(K) < \infty.$$

By density of $C_c^\infty(\mathbb{R}^q)$ in $L^\infty(\mathbb{R}^q)$, there exists $\overline{g} \in C_c^\infty(\mathbb{R}^q)$ such that for all $\epsilon > 0$ and for all $x \in \mathbb{R}^q$,

$$|g(\mathbf{x}) - \overline{g}(\mathbf{x})| \leq \|g - \overline{g}\|_{L^\infty} < \epsilon/3$$

Furthermore, by the continuity of $\overline{g}$, there exists $\delta > 0$ such that,

$$|\overline{g}(\mathbf{x}+\mathbf{h}) - \overline{g}(\mathbf{x})| < \epsilon/3 \text{ provided that } \|\mathbf{h}\| < \delta$$

By the triangular inequality we have, for all $h \in \mathbb{R}^q$ such that $\|\mathbf{h}\| < \delta$:

$$|g(\mathbf{x}+\mathbf{h}) - g(\mathbf{x})| \leq |g(\mathbf{x}+\mathbf{h}) - \overline{g}(\mathbf{x}+\mathbf{h})| + |\overline{g}(\mathbf{x}+\mathbf{h}) - \overline{g}(\mathbf{x})| + |\overline{g}(\mathbf{x}) - g(\mathbf{x})| < \epsilon.$$

Hence,

$$\begin{aligned}\int_{\mathbb{R}^q} |g(\mathbf{x}+\mathbf{h}) - g(\mathbf{x})| 1_K(\mathbf{x}) d\mathbf{x} &< \int_K \epsilon\, d\mathbf{x} \\ &= \epsilon\, m(K), \text{ provided that } \|\mathbf{h}\| < \delta.\end{aligned}$$

So, $\int_{\mathbb{R}^q} |g(\mathbf{x}+\mathbf{h}) - g(\mathbf{x})| 1_K(\mathbf{x}) d\mathbf{x} \overset{\mathbf{h}\to 0}{\longrightarrow} 0$, for all $g \in L^\infty(\mathbb{R}^q)$.

Let us introduce

$$A_{10} = \int_{\mathbb{R}^2\times\mathbb{R}_+\times(0,1)^2} |v(x,y,t,\alpha) - w(x,y,t,\beta)| \psi_t(x,y,t) dx dt d\alpha d\beta$$

which, thanks to (2.75) can be written as:

$$\begin{aligned}A_{10} = \int_{(\mathbb{R}^2\times\mathbb{R}_+\times(0,1))^2} &|v(x,y,t,\alpha) - w(x,y,t,\beta)| \psi_t(x,y,t) \rho_{2,r}(x-\overline{x}, y-\overline{y}) \\ &\overline{\rho}_{1,r}(t-s) dx dy dt d\alpha d\overline{x} d\overline{y} ds d\beta.\end{aligned}$$

With the triangular inequality we get:

$$\begin{aligned}|A_1 - A_{10}| = \Big| \int_{(\mathbb{R}^2\times\mathbb{R}_+\times(0,1))^2} &(|v(x,y,t,\alpha) - w(x,y,t,\beta)| - |v(x,y,t,\alpha) - w(\overline{x},\overline{y},t,\beta)|) \\ &\psi_t(x,y,t) \rho_{2,r}(x-\overline{x}, y-\overline{y}) \overline{\rho}_{1,r}(t-s) dx dy dt d\alpha d\overline{x} d\overline{y} ds d\beta \Big| \\ \leq \int_S \int_{\mathbb{R}^2} \int_{\mathbb{R}_+} \int_0^1 &|w(x,y,t,\beta) - w(\overline{x},\overline{y},t,\beta)| \\ &|\psi_t(x,y,t)| \rho_{2,r}(x-\overline{x}, y-\overline{y}) \overline{\rho}_{1,r}(t-s) dx dy dt d\overline{x} d\overline{y} ds d\beta.\end{aligned}$$

Let

$$\varepsilon(r, S, w) = \text{Sup}\left\{ \int_S \int_0^1 |w(x,y,t,\beta) - w((x,y)+\eta, t+\tau, \beta)| dx dy dt d\beta, \|\eta\| \leq \frac{1}{r}, 0 \leq \tau \leq \frac{1}{r} \right\},$$

and let $(\overline{x},\overline{y}) = (x,y) + \eta$ and $s = t + \tau$. Then,

$$\begin{aligned}|A_1 - A_{10}| &\leq \|\psi_t\|_\infty \int_S \int_{B(0,\frac{1}{r})} \int_0^{\frac{1}{r}} \int_0^1 |w(x,y,t,\beta) - w((x,y)+\eta, t+\tau, \beta)| \\ &\qquad \rho_{2,r}(-\eta)\overline{\rho}_{1,r}(-\tau) dx dy dt d\eta d\tau d\beta \\ &\leq \|\psi_t\|_\infty \int_{B(0,\frac{1}{r})} \int_0^{\frac{1}{r}} \rho_{2,r}(-\eta)\overline{\rho}_{1,r}(-\tau) \\ &\qquad \left(\int_S \int_0^1 |w(x,y,t,\beta) - w((x,y)+\eta, t+\tau, \beta)| dx dy dt d\beta \right) d\eta d\tau \\ &\leq \|\psi_t\|_\infty \varepsilon(r,S,w) \int_{B(0,\frac{1}{r})} \int_0^{\frac{1}{r}} \rho_{2,r}(-\eta)\overline{\rho}_{1,r}(-\tau) d\tau d\eta.\end{aligned}$$

Whereupon,

$$|A_1 - A_{10}| \leq \|\psi_t\|_\infty \varepsilon(r,S,w)$$

and, as $\varepsilon(r,S,w) \overset{r\to\infty}{\longrightarrow} 0$ (Lemma 6), we get $A_1 \overset{r\to\infty}{\longrightarrow} A_{10}$, i.e,

$$A_1 \overset{r\to\infty}{\longrightarrow} \int_{\mathbb{R}^2\times\mathbb{R}_+\times(0,1)^2} |v(x,y,t,\alpha) - w(x,y,t,\beta)| \psi_t(x,y,t) dx dy dt d\alpha d\beta \tag{2.78}$$

Proceeding in the same way, let us introduce

$$\begin{aligned}A_{30} = \int_{\mathbb{R}^2\times\mathbb{R}_+\times(0,1)^2} &(f(v(x,y,t,\alpha)\top w(x,y,t,\beta)) - f(v(x,y,t,\alpha)\bot w(x,y,t,\beta))) \cdot \\ &\nabla\psi(x,y,t) dx dy dt d\alpha d\beta\end{aligned}$$

which, thanks to (2.75) can be written as:

$$\begin{aligned}A_{30} = \int_{\mathbb{R}^2\times\mathbb{R}_+\times(0,1)^2} &(f(v(x,y,t,\alpha)\top w(x,y,t,\beta)) - f(v(x,y,t,\alpha)\bot w(x,y,t,\beta)) \cdot \\ &\nabla\psi(x,y,t)\rho_{2,r}(x-\overline{x}, y-\overline{y})\overline{\rho}_{1,r}(t-s) dx dy dt d\alpha d\overline{x} d\overline{y} ds d\beta.\end{aligned}$$

Since $f \in C^1(\mathbb{R})$, for all $x \leq y$,

$$f(y) - f(x) \leq \operatorname*{Sup}_{\xi\in(x,y)} \{f'(\xi)\} (y-x), \tag{2.79}$$

and taking into account that

$$\begin{aligned}A_3 - A_{30} = \int_{(\mathbb{R}^2\times\mathbb{R}_+\times(0,1)^2)^2} &(f(v(x,y,t,\alpha)\top w(\overline{x},\overline{y},t,\beta)) - f(v(x,y,t,\alpha)\bot w(\overline{x},\overline{y},t,\beta)) \\ &- f(v(x,y,t,\alpha)\top w(x,y,t,\beta)) + f(v(x,y,t,\alpha)\bot w(x,y,t,\beta))) \cdot \\ &\nabla\psi(x,y,t)\rho_{2,r}(x-\overline{x}, y-\overline{y})\overline{\rho}_{1,r}(t-s) dx dy dt d\alpha d\overline{x} d\overline{y} ds d\beta,\end{aligned}$$

following the procedure used to the estimate $|A_1 - A_{10}|$, there exists $C_{f,\psi,v,w}$ that only depends on $f, \psi, \|v\|_\infty$ and $\|w\|_\infty$ such that,

$$\begin{aligned}|A_3 - A_{30}| &\leq C_{f,v,w} \|\nabla\psi\|_\infty \int_{(\mathbb{R}^2\times\mathbb{R}_+\times(0,1))^2} |w(x,y,t,\beta) - w(\overline{x},\overline{y},t,\beta)| \\ &\qquad \rho_{2,r}(x-\overline{x}, y-\overline{y})\overline{\rho}_{1,r}(t-s) dx dy dt d\overline{x} d\overline{y} ds d\beta \\ &\leq C_{f,\psi,v,w}\varepsilon(r,S,w)\end{aligned}$$

and again, due to Lemma 6 $A_3 \overset{r\to\infty}{\longrightarrow} A_{30}$, i.e,

$$\begin{aligned}A_3 \overset{r\to\infty}{\longrightarrow} \int_{\mathbb{R}^2\times\mathbb{R}_+\times(0,1)^2} &(f(v(x,y,t,\alpha)\top w(x,y,t,\beta)) - f(v(x,y,t,\alpha)\bot w(x,y,t,\beta))) \cdot \\ &\nabla\psi(x,y,t) dx dy dt d\alpha d\beta.\end{aligned} \tag{2.80}$$

Taking into account that,

$$\varphi_s(\overline{x},\overline{y},s) = -\psi(x,y,t)\rho_{2,r}(x-\overline{x},y-\overline{y})\overline{\rho}'_{1,r}(t-s),$$

$$\nabla\varphi(\overline{x},\overline{y},s) = -\psi(x,y,t)\nabla\rho_{2,r}(x-\overline{x},y-\overline{y})\overline{\rho}_{1,r}(t-s)$$

and $\varphi(\overline{x},\overline{y},0) = \psi(x,y,t)\rho_{2,r}(x-\overline{x},y-\overline{y})\overline{\rho}_{1,r}(t) = 0$ because supp $\overline{\rho}_{1,r} \subset [-1,0]$ and $t \in (0,1)$, we rewrite (2.73) with the test function $\varphi(x,y,t,\cdot,\cdot,\cdot)$ and $k = v(x,y,t,\alpha)$, and we integrate w.r.t x, y and t. It yields,

$$\begin{aligned}
&-\int_{(\mathbb{R}^2\times\mathbb{R}_+\times(0,1))^2} |v(x,y,t,\alpha) - w(\overline{x},\overline{y},s,\beta)|\psi(x,y,t)\rho_{2,r}(x-\overline{x},y-\overline{y}) \\
&\qquad\qquad \overline{\rho}'_{1,r}(t-s)dxdydtd\alpha d\overline{x}d\overline{y}dsd\beta \\
&-\int_{(\mathbb{R}^2\times\mathbb{R}_+\times(0,1))^2} (f(v(x,y,t,\alpha)\top w(\overline{x},\overline{y},s,\beta)) - f(v(x,y,t,\alpha)\bot w(\overline{x},\overline{y},s,\beta))) \\
&\qquad\qquad \cdot\nabla\rho_{2,r}(x-\overline{x},y-\overline{y})\psi(x,y,t)\overline{\rho}_{1,r}(t-s)dxdydtd\alpha d\overline{x}d\overline{y}dsd\beta \geq 0.
\end{aligned}$$

Therefore, for all $r \geq 1$,

$$A_2 + A_4 \leq 0. \tag{2.81}$$

On the other hand, taking $\varphi(\overline{x},\overline{y},s) = \psi(x,y,0)\rho_{2,r}(x-\overline{x},y-\overline{y})\int_s^\infty \overline{\rho}_{1,r}(-\lambda)d\lambda$ we have,

$$\varphi_s(\overline{x},\overline{y},s) = -\psi(x,y,0)\rho_{2,r}(x-\overline{x},y-\overline{y})\overline{\rho}_{1,r}(-\lambda),$$

$$\nabla\varphi(\overline{x},\overline{y},s) = -\psi(x,y,0)\nabla\rho_{2,r}(x-\overline{x},y-\overline{y})\int_s^\infty \overline{\rho}_{1,r}(-\lambda)d\lambda$$

and $\varphi(\overline{x},\overline{y},0) = -\psi(x,y,0)\rho_{2,r}(x-\overline{x},y-\overline{y})\int_0^\infty \overline{\rho}_{1,r}(-\lambda)d\lambda$.

Rewriting (2.73) with $\varphi(\overline{x},\overline{y},s)$ and $k = u_0(x,y)$, and integrating w.r.t (x,y) we get

$$-A_5 \geq -A_6 - A_7, \tag{2.82}$$

where

$$\begin{aligned}
A_6 = -\int_{(\mathbb{R}^2)^2\times\mathbb{R}_+\times(0,1)} &(f(w(\overline{x},\overline{y},s,\beta)\top u_0(x,y)) - f(w(\overline{x},\overline{y},s,\beta)\bot u_0(x,y)))\cdot \\
&\nabla\rho_{2,r}(x-\overline{x},y-\overline{y})\psi(x,y,0)\int_s^\infty \overline{\rho}_{1,r}(-\lambda)d\lambda dxdyd\overline{x}d\overline{y}dsd\beta
\end{aligned}$$

and

$$A_7 = \int_{(\mathbb{R}^2)^2} |u_0(\overline{x},\overline{y}) - u_0(x,y)|\psi(x,y,0)\rho_{2,r}(x-\overline{x},y-\overline{y})\int_0^\infty \overline{\rho}_{1,r}(-\lambda)d\lambda dxdyd\overline{x}d\overline{y}.$$

Let

$$\varepsilon(r,S_0,u_0) = \mathrm{Sup}\left\{\int_{S_0} |u_0(x,y) - u_0((x,y)+\eta)|dxdy,\ \eta\in\mathbb{R}^2,\ \|\eta\| \leq \frac{1}{r}\right\},$$

and let $(\overline{x},\overline{y}) = (x,y) + \eta$. Then,

$$\begin{aligned}
|A_7| &\leq \int_{B(0,\frac{1}{r})}\int_{S_0} |u_0((x,y)+\eta) - u_0(x,y)|\,\|\psi(\cdot,\cdot,0)\|_\infty \rho_{2,r}(-\eta)dxdyd\eta\int_0^\infty \overline{\rho}_{1,r}(-\lambda)d\lambda \\
&\leq \|\psi(\cdot,\cdot,0)\|_\infty \int_{B(0,\frac{1}{r})}\left(\int_{S_0} |u_0((x,y)+\eta) - u_0(x,y)|dxdy\right)\rho_{2,r}(-\eta)d\eta\int_0^\infty \overline{\rho}_{1,r}(-\lambda)d\lambda \\
&\leq \|\psi(\cdot,\cdot,0)\|_\infty\, \varepsilon(r,S_0,u_0)\int_{B(0,\frac{1}{r})}\rho_{2,r}(-\eta)d\eta\int_0^\infty \overline{\rho}_{1,r}(-\lambda)d\lambda \\
&\leq \|\psi(\cdot,\cdot,0)\|_\infty\, \varepsilon(r,S_0,u_0).
\end{aligned}$$

Thus, with the Lemma 6, we have

$$A_7 \overset{r\to\infty}{\longrightarrow} 0. \tag{2.83}$$

Replacing $u_0(x,y)$ by $u_0(\overline{x},\overline{y})$ in A_6, we get

$$A_{60} = -\int_{(\mathbb{R}^2)^2\times\mathbb{R}_+\times(0,1)} (f(w(\overline{x},\overline{y},s,\beta)\top u_0(\overline{x},\overline{y})) - f(w(\overline{x},\overline{y},s,\beta)\perp u_0(\overline{x},\overline{y})))\cdot \nabla\rho_{2,r}(x-\overline{x},y-\overline{y})\psi(x,y,0)\int_s^\infty \overline{\rho}_{1,r}(-\lambda)d\lambda dxdyd\overline{x}d\overline{y}dsd\beta.$$

Taking into account that $\psi \in C_c^\infty$, $\int_{\mathbb{R}} \rho\psi_{x_i}dx_i = -\int_{\mathbb{R}} \rho_{x_i}\psi dx_i$. Then, integrating by parts w.r.t x and y the previous integral, we have:

$$A_{60} = \int_{(\mathbb{R}^2)^2\times\mathbb{R}_+\times(0,1)} (f(w(\overline{x},\overline{y},s,\beta)\top u_0(\overline{x},\overline{y})) - f(w(\overline{x},\overline{y},s,\beta)\perp u_0(\overline{x},\overline{y})))\cdot \rho_{2,r}(x-\overline{x},y-\overline{y})\nabla\psi(x,y,0)\int_s^\infty \overline{\rho}_{1,r}(-\lambda)d\lambda dxdyd\overline{x}d\overline{y}dsd\beta.$$

From (2.79) and since $|w(\overline{x},\overline{y},s,\beta) - u_0(\overline{x},\overline{y})| \leq \frac{1}{r}$ because w is an entropy process solution, we have:

$$\begin{aligned}
|A_{60}| &\leq C_{f,w,u_0}\left\|\nabla\psi(\cdot,\cdot,0)\right\|_\infty \int_{\mathbb{R}^2\times\mathbb{R}_+\times(0,1)} |w(\overline{x},\overline{y},s,\beta) - u_0(\overline{x},\overline{y})|\rho_{2,r}(x-\overline{x},y-\overline{y}) \\
&\qquad \int_s^\infty \overline{\rho}_{1,r}(-\lambda)d\lambda dxdyd\overline{x}d\overline{y}dsd\beta \\
&\leq \frac{C_{f,w,u_0}\left\|\nabla\psi(\cdot,\cdot,0)\right\|_\infty}{r} \int_{\mathbb{R}^2\times\mathbb{R}_+}\int_s^\infty \rho_{2,r}(x-\overline{x},y-\overline{y})\overline{\rho}_{1,r}(-\lambda)d\lambda d\overline{x}d\overline{y}ds \\
&\leq \frac{C_{f,w,u_0}\left\|\nabla\psi(\cdot,\cdot,0)\right\|_\infty}{r} \int_{\mathbb{R}^2}\int_0^\infty\int_0^\lambda \rho_{2,r}(x-\overline{x},y-\overline{y})\overline{\rho}_{1,r}(-\lambda)dsd\lambda d\overline{x}d\overline{y} \\
&\leq \frac{C_{f,w,u_0}\left\|\nabla\psi(\cdot,\cdot,0)\right\|_\infty}{r} \int_{\mathbb{R}^2}\int_0^1 \lambda\rho_{2,r}(x-\overline{x},y-\overline{y})\overline{\rho}_{1,r}(-\lambda)d\lambda d\overline{x}d\overline{y}.
\end{aligned}$$

Then,

$$|A_{60}| \leq \frac{C_{f,\psi,w,u_0}}{r}.$$

Furthermore, taking into account that

$$\begin{aligned}
A_6 - A_{60} = \int_{(\mathbb{R}^2)^2\times\mathbb{R}_+\times(0,1)} &(f(w(\overline{x},\overline{y},s,\beta)\top u_0(x,y)) - f(w(\overline{x},\overline{y},s,\beta)\perp u_0(x,y)) \\
&- f(w(\overline{x},\overline{y},s,\beta)\top u_0(\overline{x},\overline{y})) + f(w(\overline{x},\overline{y},s,\beta)\perp u_0(\overline{x},\overline{y})))\cdot \\
&\rho_{2,r}(x-\overline{x},y-\overline{y})\nabla\psi(x,y,0)\int_s^\infty \overline{\rho}_{1,r}(-\lambda)d\lambda dxdyd\overline{x}d\overline{y}dsd\beta,
\end{aligned}$$

following the procedure used to the estimate A_7, there exists C'_{f,ψ,w,u_0} depending on $f,\psi,\|w\|_\infty$ and $\|u_0\|_\infty$ such that

$$|A_6 - A_{60}| \leq C'_{f,\psi,w,u_0}\varepsilon(r,S_0,u_0).$$

Thus, given that $|A_6| \leq |A_6 - A_{60}| + |A_{60}|$, with the Lemma 6, we have

$$A_6 \overset{r\to\infty}{\longrightarrow} 0. \tag{2.84}$$

From (2.83) and (2.84) we get

$$A_5 \leq 0. \tag{2.85}$$

By passing to the limit in the inequality (2.76), the expressions (2.78), (2.80), (2.81) and (2.85) lead to (2.77).

Secondly, we prove that for all compact set $\Omega \subset \mathbb{R}^2 \times \mathbb{R}_+$:

$$\int_{\Omega\times(0,1)^2} |v(x,y,t,\alpha) - w(x,y,t,\beta)| dxdydtd\alpha d\beta = 0.$$

Let Ω be a compact set of $\mathbb{R}^2 \times \mathbb{R}_+$. Let $\omega \in \mathbb{R}, R > 0$ and $T \in (0, \frac{R}{\omega})$ such that

$$\Omega \subset \bigcup_{0\le t\le T} (B(0, R-\omega t) \times \{t\})$$

Let $\rho \in C_c^\infty(\mathbb{R}^+, [0,1])$ be a function verifying:

$$\begin{aligned} \rho(r) &= 1 \text{ if } r \in [0, R], \\ \rho(r) &= 0 \text{ if } r \in [R+1, +\infty], \\ \rho'(r) &\le 0 \text{ for all } r \in \mathbb{R}_+ \end{aligned}$$

with $\omega = V_\kappa$ where $\kappa = [-(\|v\|_\infty \top \|w\|_\infty), (\|v\|_\infty \top \|w\|_\infty)]$, taking ψ in (2.77), the function defined by:

$$\psi(x,y,t) = \begin{cases} \rho(\|(x,y)\| + \omega t)\frac{T-t}{T} & \text{if} \quad (x,y) \in \mathbb{R}^2 \qquad \text{and } t \in [0,T] \\ 0 & \text{if} \quad (x,y) \in \mathbb{R}^2 \qquad \text{and } t \ge T \end{cases}, \tag{2.86}$$

we get

$$\begin{aligned} \int_{\mathbb{R}^2\times\mathbb{R}_+\times(0,1)^2} \Bigg[|v(x,y,t,\alpha) - w(x,y,t,\beta)| \Big(\frac{T-t}{T}\omega\rho'(\|(x,y)\| + \omega t) - \frac{1}{T}\rho(\|(x,y)\| + \omega t) \Big) \\ + (f(v(x,y,t,\alpha)\top w(x,y,t,\beta)) - f(v(x,y,t,\alpha)\perp w(x,y,t,\beta)) \cdot \\ \frac{(x,y)}{\|(x,y)\|} \frac{T-t}{T} \rho'(\|(x,y)\| + \omega t) \Bigg] dxdydtd\alpha d\beta \ge 0. \end{aligned}$$

Now, since for all $(x,y,t) \in \Omega$, $\|(x,y)\| + \omega t \le R$. Then, $\rho(\|(x,y)\| + \omega t) = 1$, $\forall (x,y,t) \in \Omega$ and therefore $\rho'(\|(x,y)\| + \omega t) = 0$. Thus, from the above inequality we get:

$$\int_{\Omega\times(0,1)^2} |v(x,y,t,\alpha) - w(x,y,t,\beta)| dxdydtd\alpha d\beta \le 0.$$

This result implies:

$$v(x,y,t,\alpha) = w(x,y,t,\beta) \text{ for almost all } (x,y,t,\alpha,\beta) \in \mathbb{R}^2 \times \mathbb{R}_+ \times (0,1)^2$$

Therefore $v(x,y,t,\alpha)$ and $w(x,y,t,\beta)$ do not respectively depend on α and β. Thus, the entropy process solution is unique and it is the unique entropy solution u.

2.2.3 Convergence Order of the Fully-Discrete Lagrangian-Eulerian Scheme on Triangular Grids

This section is devoted to the error estimate for the scheme defined by (2.19) and (2.20), and it is based on the paper of Cockburn et al. [64]. In all the proof, we use the notation $\mathbf{x} = (x,y)$ and assume that the entropy solution v is smooth since the general case can be obtained by a standard density argument.

We begin by expressing the numerical flux in the form:

$$F_{KL}(v,w) = F_{cent;KL}(v,w) - F_{visc;KL}(v,w), \tag{2.87}$$

with

$$F_{cent;KL}(v,w) = a_{KL} f(v) \cdot n_{KL} + b_{KL} f(w) \cdot n_{KL},$$

and

$$F_{visc;KL}(v,w) = \alpha_{K|L}(N_{K|L}(w) - N_{K|L}(v)),$$

where,

$$a_{KL} = b_{KL} = \frac{1}{2},\ \alpha_{K|L} = 1 \text{ and } N_{K|L}(s) = \operatorname*{Sup}_{\substack{w\in[-r,r]\\K,L\in\mathcal{T}}} \left|\frac{\mathbf{f}(w)}{w}\cdot\mathbf{n}_{KL}\right| s. \tag{2.88}$$

Remark 8 *The consistency and conservativity of the 2D extension of the Lagrangian-Eulerian scheme defined by (2.20) and (2.19) are equivalent to the following conditions:*

$$a_{KL} + b_{KL} = 1,\ \ a_{LK} = b_{KL} \ \text{ and } \ b_{LK} = a_{KL}. \tag{2.89}$$

Furthermore, the following condition regarding the size of time step Δt:

$$\frac{\Delta t\, m(\partial K)}{m(K)} \operatorname*{Sup}_{w,K,L} \left|\frac{\mathbf{f}(w)}{w}\cdot\mathbf{n}_{KL}\right| \le 1,\ w\in[-r,r],\ K,L\in\mathcal{T}, \tag{2.90}$$

ensures the monotonicity of the fully-discrete Lagrangian-Eulerian scheme (2.19)-(2.20). That is, (2.90) guarantees that $\dfrac{\partial u_K^{n+1}}{\partial u_K^n} \ge 0$ and $\dfrac{\partial u_K^{n+1}}{\partial u_L^n} \ge 0$. Importantly, condition (2.90), which depends on the no-flow curves, is fulfilled when Δt satisfies (2.30).

Next, to state Theorem 2.2.5, which gives an upper bound for the error estimate of the fully-discrete Lagrangian-Eulerian scheme (2.19)-(2.20), it is necessary to define the concept of *consistency of a scheme with respect to a family of triangulations*.

Let $\mathbf{x}_K$ and $\mathbf{x}_L$ be the barycenters of finite volumes K and L, respectively, and $\mathbf{x}_{K|L}$ be the barycenter of the face $K|L$. Let

$$\delta_{K|L} = (\mathbf{x}_{K|L} - \mathbf{x}_K) - b_{K,L}(\mathbf{x}_L - \mathbf{x}_K),\ \ \Delta_K = \max_{1\le j\le 2}\sum_{i=1}^{2}\left|\sum_{L\in N(K)} m(K|L)(\delta_{K|L})_j(\mathbf{n}_{KL})_i\right|, \text{ and}$$

$$\mathbb{A}_K = \operatorname*{Sup}_{c\in\mathbb{R}}\frac{1}{\|\mathbf{f}'(c)\|}\sum_{i=1}^{2}\left|\sum_{L\in N(K)} m(K|L)\operatorname*{Sup}_{\substack{w\in[-r,r]\\K,L\in\mathcal{T}}}\left|\frac{\mathbf{f}(w)}{w}\cdot\mathbf{n}_{KL}\right|(\mathbf{x}_L - \mathbf{x}_K)_i\right|.$$

A numerical scheme of the form of (2.19), whose numerical flux, expressed in the form of (2.87), with

$$0 \le a_{K,L},\, b_{K,L},\, \alpha_{K|L} \le 1,$$

is conservative and consistent with nonlinearity $\mathbf{f}\cdot\mathbf{n}_{KL}$ and satisfies (2.89) and (2.90), is *consistent to the family of triangulations* $\mathcal{T}$ if $\Delta_K = \mathbb{A}_K \equiv 0$.

Remark 9 *The conditions for this new kind of consistency for the scheme, impose heavy restrictions on the grids and numerical fluxes. In fact, $\Delta_K = 0$ if $\mathbf{x}_{K|L} = (1-b_{K,L})\mathbf{x}_L + b_{K,L}\mathbf{x}_K$. This not only means that the value of scalar $b_{K,L}$ is determined, but that barycenters $\mathbf{x}_K$ and $\mathbf{x}_L$, as well as barycenter $\mathbf{x}_{K|L}$, must lie on the same line.*

In this work, we consider grids of equilateral triangles, as shown in (2.2). Thanks to (2.88), for all K in the equilateral triangulations considered and for all $L\in N(K)$, we have that $\delta_{K|L} = 0$ and $\mathbf{x}_K = \dfrac{1}{3}\displaystyle\sum_{L\in N(K)}\mathbf{x}_L$.

Thus, $\Delta_K = \mathbb{A}_K \equiv 0$, which means that the fully-discrete Lagrangian-Eulerian scheme (2.19)-(2.20) is **consistent with respect to equilateral triangulations**.

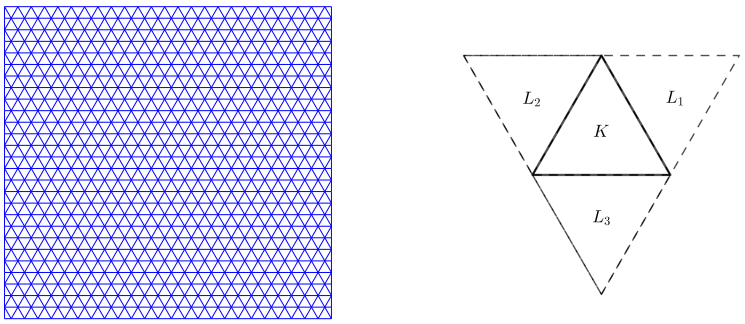

Figure 2.2: Equilateral triangular grid (left) and a grid cell with its neighbors (right).

The two grid-related quantities introduced below are also necessary.

Let $\varepsilon_h \equiv \bigcup \{K|L : K \in \mathcal{T},\ L \in N(K)\}$ be the set of edges of the triangles (K) in $\mathcal{T}$. For a face $K|L \in \varepsilon_h$, $C_{K|L}$ is defined as the convex hull of $K^+_{K|L} \cup K^-_{K|L}$, where $K^+_{K|L}$ denotes the cell above or to the right of $K|L$ and $K^-_{K|L}$ is the cell below or to the left of $K|L$; $D_{K|L}$ is defined as the diameter of $C_{K|L}$; and we set

$$\mathbb{D}_h = \operatorname*{Sup}_{K|L\in\varepsilon_h} \frac{m(K|L)D_{K|L}}{\max\left\{m(K^+_{K|L}), m(K^-_{K|L})\right\}}. \tag{2.91}$$

Furthermore, given finite volume K, the number of sets of $C_{K|L}$ for which $m(K \cap C_{K|L}) \neq 0$ for some $K|L \in \varepsilon_h$ is denoted by l_K, and we set

$$l_h = \operatorname*{Sup}_{K\in\mathcal{T}} l_K. \tag{2.92}$$

Now, we state the theorem that allows us to prove that, for the fully-discrete Lagrangian-Eulerian scheme (2.19)-(2.20), the $L^\infty(0,T;L^1(\mathbb{R}^2))-$norm of the error goes to zero as $h^{1/2}$ when h goes to zero.

Theorem 2.2.5 *Let assumption (2.90) be satisfied. Let u be the piecewise-constant solution provided by the fully-discrete Lagrangian-Eulerian scheme (2.19)-(2.20) to problem (1.1) on equilateral triangular grids and defined by (2.24). Let v be the entropy solution to such problem, and let $e(t) := \|u(t) - v(t)\|_{L^1(\mathbb{R}^2)}$ be the error. Then,*

$$e(t^N) \leq 2e(0) + 8\,|v_0|_{TV(\mathbb{R}^2)} \sqrt{2t^N \|\nu_v\|}\, h^{1/2} + |v_0|_{TV(\mathbb{R}^2)}\,(b_1 h^{3/4} + b_2 h), \tag{2.93}$$

where $|v_0|_{TV(\mathbb{R}^2)} = \displaystyle\int_{\mathbb{R}^2} \|\nabla_{\mathbf{x}} v_0(\mathbf{x})\|_1\, d\mathbf{x}$, $\|\nu_v\| = \displaystyle\operatorname*{Sup}_K \operatorname*{Sup}_{\substack{t\in(0,t^N)\\ \mathbf{x}\in\mathbb{R}^2}} \max_{1\leq i,j\leq 2} \left|\nu^{ij}_K(v(\mathbf{x},t)/h\right|$, *and the local viscosity coefficient, ν^{ij}_K, is given by*

$$\nu^{ij}_K(c) = \frac{\Delta t}{2} f_i'(c) f_j'(c) - \frac{1}{m(K)} \sum_{L\in\partial K} m(K|L) \left[\operatorname*{Sup}_{\substack{w\in[-r,r]\\ K,L\in\mathcal{T}}} \left| \frac{\mathbf{f}(w)}{w} \cdot \mathbf{n}_{KL} \right| + \frac{1}{2} \mathbf{f}'(c) \cdot \mathbf{n}_{KL} \right] \xi^{ij}_{K,L},$$

$$\xi^{ij}_{K,L} = \frac{1}{2}\left[(\mathbf{x}_L - \mathbf{x}_K)_i (\mathbf{x}_L - \mathbf{x}_K)_j + \mathbb{I}^{ij}_L - \mathbb{I}^{ij}_K \right], \qquad \mathbb{I}^{ij}_\Omega = \frac{1}{m(\Omega)} \int_\Omega (\mathbf{x}' - \mathbf{x}_\Omega)_i (\mathbf{x}' - \mathbf{x}_\Omega)_j d\mathbf{x}'.$$

Constants b_1 and b_2 are locally bounded functions that only depend on quantities $\|\mathbf{f}'(v)\|\,\Delta t/h$, $\|\mathbf{f}'(v)\|\,/\,\|\nu_v\|$, where $\|\mathbf{f}'(v)\| = \sup\limits_{\substack{t\in(0,t^N)\\ \mathbf{x}\in\mathbb{R}^2}} \|\mathbf{f}'(v(\mathbf{x},t))\|_{l^\infty}$, $\left\{t^N\,\|\nu_v\|\right\}^{1/2}$, and on $\mathbb{D}_h$ and l_h.

Proof.

a. The choice of the entropy dissipation form. Following [64], let us consider the entropy dissipation form

$$E(u,v;t^N) = \int_0^{t^N}\int_{\mathbb{R}^2}\sum_{n=0}^{N-1}\sum_{K\in\tau}\Psi_K^n(v(\mathbf{x},t))\phi(\mathbf{x},t,\mathbf{x}_K,t^{n+1})m(K)\Delta t d\mathbf{x}dt$$

where $U(\cdot)$ is the absolute value function $|\cdot|$, and Ψ_K^n is given by

$$\Psi_K^n(c) = U'(u_K^n - c)\left[\frac{u_K^{n+1}-u_K^n}{\Delta t} + \frac{1}{m(K)}\sum_{L\in N(K)} m(K|L)F_{KL}(u_K^n,u_L^n)\right]$$

It is clear that $\Psi_K^n \equiv 0$ and therefore $E(u,v;t^N) = 0$.

The term $\phi(\mathbf{x},t,\mathbf{x}_K,t^{n+1})$ is an averaged test function defined by

$$\phi(\mathbf{x},t,\mathbf{x}_K,t^{n+1}) = \frac{1}{m(K)}\int_K \varphi(\mathbf{x},t,\mathbf{x}',t^{n+1})d\mathbf{x}', \tag{2.94}$$

where the function $\varphi(\mathbf{x},t,\mathbf{x}',t')$ is defined as follows:

$$\varphi(\mathbf{x},t,\mathbf{x}',t') = w_{\epsilon_t}(t-t')\prod_{i=1}^{2}\eta_{\epsilon_\mathbf{x}}(x_i - x_i'), \tag{2.95}$$

$\mathbf{x},\mathbf{x}'$ and t, t' being respectively points in $\mathbb{R}^2$ and $\mathbb{R}^+$.

The functions w_{ϵ_t} and $\eta_{\epsilon_\mathbf{x}}$ are constructed as follows

$$w_{\epsilon_t}(s) = \frac{1}{\epsilon_t}w(\frac{s}{\epsilon_t}),\ \ \eta_{\epsilon_\mathbf{x}}(s) = \frac{1}{\epsilon_\mathbf{x}}\eta(\frac{s}{\epsilon_\mathbf{x}}),\ \ \forall s\in\mathbb{R}, \tag{2.96}$$

where ϵ_t and $\epsilon_\mathbf{x}$ are two arbitrary numbers. Both w and η satisfy the following conditions:

$$\begin{array}{l}(i)\quad w(t)\geq 0,\ \text{for } t>0\\ (ii)\quad w(t) = w(-t),\ \text{for } t>0\\ (iii)\ \text{the support of } w \text{ is } [-1,1]\\ (iv)\ \int_0^1 w(r)dr = 1/2\end{array} \tag{2.97}$$

Henceforth, we set

$$W(t) = \int_0^t w_{\epsilon_t}(s)\ ds. \tag{2.98}$$

Furthermore, we can find sequences of functions w and η, satisfying (2.97) and being nonincreasing on $(0,1)$, that converge pointwisely to

$$\chi(x) = \begin{cases}\frac{1}{2}, & \text{for } |x|<1,\\ 0, & \text{otherwise.}\end{cases}$$

and

$$\chi_\epsilon(x) = \begin{cases}(1+\epsilon)/2, & \text{for } |x|\leq(1-\epsilon)/(1+\epsilon),\\ (1+\epsilon)^2(1-|x|)/4\epsilon, & \text{for } |x|\in[(1-\epsilon)/(1+\epsilon),1],\\ 0, & \text{elsewhere.}\end{cases}$$

respectively.

In what follows, we denote these limit processes by $'w \to \chi'$ and it is easy to verify that $\lim_{w\to\chi} |w|_{TV(\mathbb{R})} = |\chi|_{TV(\mathbb{R})} = 1$ and

$$\lim_{\eta\to\chi_\epsilon} |\eta|_{TV(\mathbb{R})} = |\chi_\epsilon|_{TV(\mathbb{R})} = 1+\epsilon, \tag{2.99}$$

$$\lim_{\eta\to\chi_\epsilon} |\eta'|_{TV(\mathbb{R})} = |\chi'_\epsilon|_{TV(\mathbb{R})} = 2+\epsilon+1/\epsilon, \tag{2.100}$$

$$\lim_{\eta\to\chi_\epsilon} \|\eta\|_{L^\infty(\mathbb{R})} = \|\chi_\epsilon\|_{L^\infty(\mathbb{R})} = (1+\epsilon)/2. \tag{2.101}$$

b. The "divergence" and "dissipative" parts of $E(u,v;t^N)$

Proposition 2 *The entropy dissipation form, which measures how close from being an entropy solution the approximate solution is, can be expressed as the sum of its "divergence" and "dissipative" parts as follows:*

$$E(u,v;t^N) = E_{div}(u,v;t^N) + E_{diss}(u,v;t^N) \tag{2.102}$$

Proof. Defining $p_{KL}(s) = -m(K|L)[b_{KL}f(s)\cdot n_{KL} - \alpha_{K|L}N_{K|L}(s)]$ and taking into account that $\sum_{L\in N(K)} m(K|L)(f(u_K^n)\cdot n_{KL}) = 0$, we have that

$$\begin{aligned}
\sum_{L\in N(K)} (p_{KL}(u_K^n) - p_{KL}(u_L^n)) &= \sum_{L\in N(K)} \Bigg(- m(K|L)\left[\frac{1}{2}f(u_K^n)\cdot n_{KL} - \sup_{\substack{w\in[-r,r]\\K,L\in\mathcal{T}}} \left|\frac{\mathbf{f}(w)}{w}\cdot\mathbf{n}_{KL}\right| s u_K^n\right] \\
&\qquad + m(K|L)\left[\frac{1}{2}f(u_L^n)\cdot n_{KL} - \sup_{\substack{w\in[-r,r]\\K,L\in\mathcal{T}}} \left|\frac{\mathbf{f}(w)}{w}\cdot\mathbf{n}_{KL}\right| s u_L^n\right]\Bigg) \\
&= \sum_{L\in N(K)} m(K|L)\left[\frac{1}{2}\Big(f(u_K^n)+f(u_L^n)\Big)\cdot n_{KL}\right. \\
&\qquad \left. + \sup_{\substack{w\in[-r,r]\\K,L\in\mathcal{T}}} \left|\frac{\mathbf{f}(w)}{w}\cdot\mathbf{n}_{KL}\right| s(u_K^n - u_L^n)\right] \\
&= \sum_{L\in N(K)} m(K|L) F_{KL}^n(u_K^n, u_L^n).
\end{aligned}$$

Therefore, we can rewrite $\Psi_K^n(c)$ as:

$$\Psi_K^n(c) = \Psi_1(c) + \Psi_2(c)$$

where

$$\Psi_1(c) = \frac{1}{\Delta t}U'(u_K^n - c)(u_K^{n+1} - u_K^n)$$

and

$$\Psi_2(c) = \frac{1}{m(K)}\sum_{L\in N(K)} U'(u_K^n - c)(p_{KL}(u_K^n) - p_{KL}(u_L^n)).$$

Using the following simple identity

$$U'(a-c)(g(b)-g(a)) = \int_a^b g'(s)U'(s-c)ds - \int_a^b (g(b)-g(s))U''(s-c)ds,$$

with $g(s) = s$, we get

$$\begin{aligned}
\Psi_1(c) = \frac{1}{\Delta t}U'(u_K^n - c)(u_K^{n+1} - u_K^n) &= \frac{1}{\Delta t}\left[\int_{u_K^n}^{u_K^{n+1}} U'(s-c)ds - \int_{u_K^n}^{u_K^{n+1}} (u_K^{n+1} - s)U''(s-c)ds\right] \\
&= \frac{\left|u_K^{n+1} - c\right| - |u_K^n - c|}{\Delta t} - \frac{1}{\Delta t}\int_{u_K^n}^{u_K^{n+1}} (u_K^{n+1} - s))U''(s-c)ds.
\end{aligned}$$

Now, using the same identity with $g(s) = p_{KL}(s)$ and taking into account that

$$p'_{KL}(s) = -m(K|L)\left[\frac{1}{2}f'(s)\cdot n_{KL} - \frac{1}{2}N'_{K|L}(s)\right] = -m(K|L)\left[\frac{1}{2}f'(s)\cdot n_{KL} - \sup_{\substack{w\in[-r,r]\\K,L\in\mathcal{T}}}\left|\frac{\mathbf{f}(w)}{w}\cdot\mathbf{n}_{KL}\right| s\right],$$

we obtain

$$\begin{aligned}
\Psi_2(c) &= -\frac{1}{m(K)}\sum_{L\in N(K)} U'(u_L^n - c)(p_{KL}(u_K^n) - p_{KL}(u_L^n)) \\
&= -\frac{1}{m(K)}\sum_{L\in N(K)}\left(\int_{u_K^n}^{u_L^n} p'_{KL}(s)U'(s-c)ds - \int_{u_K^n}^{u_L^n}(p_{KL}(u_K^n) - p_{KL}(s))U''(s-c)ds\right) \\
&= \frac{1}{m(K)}\sum_{L\in N(K)}\int_{u_K^n}^{u_L^n} m(K|L)\left[\frac{1}{2}f'(s)\cdot n_{KL} - \sup_{\substack{w\in[-r,r]\\K,L\in\mathcal{T}}}\left|\frac{\mathbf{f}(w)}{w}\cdot\mathbf{n}_{KL}\right| s\right]U'(s-c)ds \\
&\qquad + \frac{1}{m(K)}\sum_{L\in N(K)}\int_{u_K^n}^{u_L^n}(p_{KL}(u_K^n) - p_{KL}(s))U''(s-c)ds \\
&= \frac{1}{m(K)}\Bigg(\sum_{L\in N(K)}\frac{1}{2}m(K|L)\left[\int_{u_K^n}^{u_L^n} f'(s)U'(s-c)ds\right]\cdot n_{KL} \\
&\qquad - \sum_{L\in N(K)}\frac{1}{2}m(K|L)\int_{u_K^n}^{u_L^n} N'_{K|L}(s)U'(s-c)ds\Bigg) \\
&\qquad + \frac{1}{m(K)}\sum_{L\in N(K)}\int_{u_K^n}^{u_L^n}(p_{KL}(u_K^n) - p_{KL}(s))U''(s-c)ds.
\end{aligned}$$

On the other hand, defining $p_K(s) = s - \dfrac{\Delta t}{m(K)}\displaystyle\sum_{L\in N(K)} p_{KL}(s)$, we get

$$\begin{aligned}
p_K(u_K^n) - p_K(s) &= u_K^n - \frac{\Delta t}{m(K)}\sum_{L\in N(K)} p_{K,L}(u_K^n) - s + \frac{\Delta t}{m(K)}\sum_{L\in N(K)} p_{KL}(s) \\
&= u_K^n - \frac{\Delta t}{m(K)}\sum_{L\in N(K)}(p_{KL}(u_K^n) - p_{KL}(u_L^n)) \\
&\qquad - \frac{\Delta t}{m(K)}\sum_{L\in N(K)}(p_{KL}(u_L^n) - p_{KL}(s)) - s \\
&= u_K^n - \frac{\Delta t}{m(K)}\sum_{L\in N(K)} m(K|L)F_{KL}^n(u_K^n, u_L^n) \\
&\qquad - \frac{\Delta t}{m(K)}\sum_{L\in N(K)}(p_{KL}(u_L^n) - p_{KL}(s)) - s \\
&= u_K^{n+1} - s - \frac{\Delta t}{m(K)}\sum_{L\in N(K)}(p_{KL}(u_L^n) - p_{KL}(s)).
\end{aligned}$$

Then,

$$\begin{aligned}
\Psi_1(c) = \frac{U(u_K^{n+1} - c) - U(u_K^n - c)}{\Delta t} &+ \frac{1}{\Delta t}\int_{u_K^{n+1}}^{u_K^n}(p_K(u_K^n) - p_K(s))U''(s-c)ds \\
&+ \frac{1}{m(K)}\sum_{L\in N(K)}\int_{u_K^{n+1}}^{u_K^n}(p_{KL}(u_L^n) - p_{KL}(s))U''(s-c)ds.
\end{aligned}$$

Finally,

$$\begin{aligned}\Psi_K^n(c) = \frac{U(u_K^{n+1}-c)-U(u_K^n-c)}{\Delta t} &+ \frac{1}{\Delta t}\int_{u_K^{n+1}}^{u_K^n}(p_K(u_K^n)-p_K(s))U''(s-c)ds \\ &+ \frac{1}{m(K)}\sum_{L\in N(K)}\int_{u_K^{n+1}}^{u_K^n}(p_{KL}(u_L^n)-p_{KL}(s))U''(s-c)ds \\ &+ \frac{1}{m(K)}\sum_{L\in N(K)}\int_{u_K^n}^{u_L^n}(p_{KL}(u_L^n)-p_{KL}(s))U''(s-c)ds \\ &+ \frac{1}{m(K)}\sum_{L\in N(K)}\frac{1}{2}m(K|L)(F(u_L^n,c)-F(u_K^n,c))\cdot n_{KL} \\ &- \frac{1}{m(K)}\sum_{L\in N(K)}\frac{1}{2}m(K|L)(\mathcal{N}(u_L^n,c)-\mathcal{N}(u_K^n,c)),\end{aligned}$$

where, $F(u,c)=\int_c^u f'(s)U'(s-c)ds$ and $\mathcal{N}(u,c)=\int_c^u N'_{K|L}(s)U'(s-c)ds$.

Remark 10 $F(u,c)=\int_c^u f'(s)U'(s-c)ds=\int_c^u f'(s)\mathrm{sign}(s-c)ds=\mathrm{sign}(u-c)(f(u)-f(c))$.

Therefore,

$$\begin{aligned}E(u,v;t^N) &= \int_0^{t^N}\int_{\mathbb{R}^2}\sum_{n=0}^{N-1}\sum_{K\in\tau}\Psi_K^n(v(\mathbf{x},t))\phi(\mathbf{x},t,\mathbf{x}_K,t^{n+1})m(K)\Delta t d\mathbf{x}dt \\ &= \int_0^{t^N}\int_{\mathbb{R}^2}\sum_{n=0}^{N-1}\sum_{K\in\tau}\Bigg[\frac{U(u_K^{n+1}-v(\mathbf{x},t))-U(u_K^n-v(\mathbf{x},t))}{\Delta t} \\ &\quad + \frac{1}{\Delta t}\int_{u_K^{n+1}}^{u_K^n}(p_K(u_K^n)-p_K(s))U''(s-v(\mathbf{x},t))ds \\ &\quad + \frac{1}{m(K)}\sum_{L\in N(K)}\int_{u_K^n}^{u_L^n}(p_{KL}(u_L^n)-p_{KL}(s))U''(s-v(\mathbf{x},t))ds \\ &\quad + \frac{1}{m(K)}\sum_{L\in N(K)}\frac{1}{2}m(K|L)(F(u_L^n,v(\mathbf{x},t))-F(u_K^n,v(\mathbf{x},t)))\cdot n_{KL} \\ &\quad - \frac{1}{m(K)}\sum_{L\in N(K)}\frac{1}{2}m(K|L)(\mathcal{N}(u_L^n,v(\mathbf{x},t))-\mathcal{N}(u_K^n,v(\mathbf{x},t)))\Bigg]\cdot \\ &\qquad \phi(\mathbf{x},t,\mathbf{x}_K,t^{n+1})m(K)\Delta t d\mathbf{x}dt.\end{aligned}$$

Defining, the local rate of entropy dissipation $LRED_K^n(c)$ as:

$$\begin{aligned}LRED_K^n(c) = \frac{1}{\Delta t}&\int_{u_K^{n+1}}^{u_K^n}(p_K(u_K^n)-p_K(s))U''(s-c)ds \\ &+ \frac{1}{m(K)}\sum_{L\in N(K)}\int_{u_K^{n+1}}^{u_L^n}(p_{KL}(u_L^n)-p_{KL}(s))U''(s-c)ds,\end{aligned}$$

and,

$$\begin{aligned} DIV_K^n(c) = & \frac{U(u_K^{n+1}-c)-U(u_K^n-c)}{\Delta t} \\ & + \frac{1}{m(K)} \sum_{L\in N(K)} \frac{1}{2} m(K|L)(F(u_L^n,c)-F(u_K^n,c))\cdot n_{KL} \\ & - \frac{1}{m(K)} \sum_{L\in N(K)} \frac{1}{2} m(K|L)(\mathcal{N}(u_L^n,c)-\mathcal{N}(u_K^n,c)), \end{aligned}$$

we have that, the "dissipative" part is

$$E_{diss}(u,v;t^N) = \int_0^{t^N} \int_{\mathbb{R}^2} \sum_{n=0}^{N-1} \sum_{K\in\tau} LRED_K^n(v(\mathbf{x},t))\phi(\mathbf{x},t,\mathbf{x}_K,t^{n+1}) m(K)\Delta t d\mathbf{x} dt,$$

and the "divergence" part is

$$E_{div}(u,v;t^N) = \int_0^{t^N} \int_{\mathbb{R}^2} \sum_{n=0}^{N-1} \sum_{K\in\tau} DIV_K^n(v(\mathbf{x},t))\phi(\mathbf{x},t,\mathbf{x}_K,t^{n+1}) m(K)\Delta t d\mathbf{x} dt.$$

This concludes the proof.

c. The dual form $E_{div}^\star(u,v;t^N)$ and the error term $T_{err}(u,v;t^N)$.

Proposition 3 *The "divergence" part $E_{div}(u,v;t^N)$ can be expressed as:*

$$E_{div}(u,v;t^N) = -E_{div}^\star(u,v;t^N) + T_{err}(u,v;t^N) \tag{2.103}$$

where the dual form $E_{div}^\star(u,v;t^N)$, the "truncation error" for the entropy/entropy pair U/F, is given by

$$\begin{aligned} E_{div}^\star(u,v;t^N) = & -\int_0^{t^N}\int_{\mathbb{R}^2}\int_0^{t^N}\int_{\mathbb{R}^2} U(u(\mathbf{x}',t')-v(\mathbf{x},t))\varphi_t(\mathbf{x},t,\mathbf{x}',t')d\mathbf{x}dtd\mathbf{x}'dt' \\ & + \int_0^{t^N}\int_{\mathbb{R}^2}\int_{\mathbb{R}^2} U(u(\mathbf{x}',t')-v(\mathbf{x},t^N))\varphi(\mathbf{x},t^N,\mathbf{x}',t')d\mathbf{x}d\mathbf{x}'dt' \\ & - \int_0^{t^N}\int_{\mathbb{R}^2}\int_{\mathbb{R}^2} U(u(\mathbf{x}',t')-v_0(\mathbf{x}))\varphi(\mathbf{x},0,\mathbf{x}',t')d\mathbf{x}d\mathbf{x}'dt' \\ & - \sum_{n=0}^{N-1}\sum_{K\in\mathcal{T}}\int_0^{t^N}\int_{\mathbb{R}^2}\sum_{L\in\partial K} m(K|L)b_{KL}[\phi(\mathbf{x},t,\mathbf{x}_K,t^{n+1})-\phi(\mathbf{x},t,\mathbf{x}_L,t^{n+1})] \\ & \qquad F(u_K^n,v)\cdot n_{KL}\Delta t d\mathbf{x}dt \\ & + \sum_{n=0}^{N-1}\sum_{K\in\mathcal{T}}\int_0^{t^N}\int_{\mathbb{R}^2}\sum_{L\in\partial K} m(K|L)\alpha_{KL}[\phi(\mathbf{x},t,\mathbf{x}_L,t^{n+1})-\phi(\mathbf{x},t,\mathbf{x}_K,t^{n+1})] \\ & \qquad \mathcal{N}_{K|L}(u_K^n,v)\Delta t d\mathbf{x}dt \end{aligned}$$

and $T_{err}(u,v;t^N)$, which contains the information of the distance between the functions u and v, is called the "error term", is given by

$$\begin{aligned} T_{err}(u,v;t^N) = & \int_0^{t^N}\int_{\mathbb{R}^2}\int_{\mathbb{R}^2} U(u(\mathbf{x}',t^N)-v(\mathbf{x},t))\varphi(\mathbf{x},t,\mathbf{x}',t^N)d\mathbf{x}d\mathbf{x}'dt \\ & + \int_0^{t^N}\int_{\mathbb{R}^2}\int_{\mathbb{R}^2} U(u(\mathbf{x}',t')-v(\mathbf{x},t^N))\varphi(\mathbf{x},t^N,\mathbf{x}',t')d\mathbf{x}d\mathbf{x}'dt' \\ & - \int_0^{t^N}\int_{\mathbb{R}^2}\int_{\mathbb{R}^2} U(u(\mathbf{x}',0)-v(\mathbf{x},t))\varphi(\mathbf{x},t,\mathbf{x}',0)d\mathbf{x}d\mathbf{x}'dt \\ & - \int_0^{t^N}\int_{\mathbb{R}^2}\int_{\mathbb{R}^2} U(u(\mathbf{x}',t')-v_0(\mathbf{x}))\varphi(\mathbf{x},0,\mathbf{x}',t')d\mathbf{x}d\mathbf{x}'dt'. \end{aligned}$$

Proof. After a standard integration by parts in time and another in space, we get

$$E_{div}(u,v;t^N) = E_{div,t}(u,v;t^N) + E_{div,x}(u,v;t^N)$$

where

$$\begin{aligned}
E_{div,t}(u,v;t^N) = &\sum_{n=0}^{N-1}\sum_{K\in\mathcal{T}}\int_0^{t^N}\int_{\mathbb{R}^2} U(u_K^n - v(\mathbf{x},t))[\phi(\mathbf{x},t,\mathbf{x}_K,t^n) - \phi(\mathbf{x},t,\mathbf{x}_K,t^{n+1})]m(K)d\mathbf{x}dt \\
&+ \sum_{K\in\mathcal{T}}\int_0^{t^N}\int_{\mathbb{R}^2} U(u_K(t^N) - v(\mathbf{x},t))\phi(\mathbf{x},t,\mathbf{x}_K,t^N)m(K)d\mathbf{x}dt \\
&+ \sum_{K\in\mathcal{T}}\int_0^{t^N}\int_{\mathbb{R}^2} U(u_K(0) - v(\mathbf{x},t))\phi(\mathbf{x},t,\mathbf{x}_K,0)m(K)d\mathbf{x}dt,
\end{aligned}$$

and

$$\begin{aligned}
E_{div,x}(u,v;t^N) = &-\sum_{n=0}^{N-1}\sum_{K\in\mathcal{T}}\int_0^{t^N}\int_{\mathbb{R}^2}\sum_{L\in\partial K} m(K|L)b_{KL}[\phi(\mathbf{x},t,\mathbf{x}_K,t^{n+1}) - \phi(\mathbf{x},t,\mathbf{x}_L,t^{n+1})] \\
&\qquad F(u_K^n,v)\cdot n_{KL}\Delta t d\mathbf{x}dt \\
&+\sum_{n=0}^{N-1}\sum_{K\in\mathcal{T}}\int_0^{t^N}\int_{\mathbb{R}^2}\sum_{L\in\partial K} m(K|L)\alpha_{KL}[\phi(\mathbf{x},t,\mathbf{x}_L,t^{n+1}) - \phi(\mathbf{x},t,\mathbf{x}_K,t^{n+1})] \\
&\qquad \mathcal{N}_{K|L}(u_K^n,v)\Delta t d\mathbf{x}dt.
\end{aligned}$$

Next, taking into account that $\phi(\mathbf{x},t,\mathbf{x}_K,t^n) - \phi(\mathbf{x},t,\mathbf{x}_K,t^{n+1}) = -\int_{t^n}^{t^{n+1}}\phi_{t'}(\mathbf{x},t,\mathbf{x}_K,t')dt'$ and u_K^n is equal to $u_K(t')$ on $[t^n,t^{n+1})$, we can rewrite $E_{div,t}(u,v;t^N)$ as follows:

$$\begin{aligned}
E_{div,t}(u,v;t^N) = &-\sum_{n=0}^{N-1}\sum_{K\in\mathcal{T}}\int_0^{t^N}\int_{\mathbb{R}^2} U(u_K^n - v(\mathbf{x},t))\int_{t^n}^{t^{n+1}}\phi_{t'}(\mathbf{x},t,\mathbf{x}_K,t')dt'm(K)d\mathbf{x}dt \\
&+ \sum_{K\in\mathcal{T}}\int_0^{t^N}\int_{\mathbb{R}^2} U(u_K(t^N) - v(\mathbf{x},t))\phi(\mathbf{x},t,\mathbf{x}_K,t^N)m(K)d\mathbf{x}dt \\
&+ \sum_{K\in\mathcal{T}}\int_0^{t^N}\int_{\mathbb{R}^2} U(u_K(0) - v(\mathbf{x},t))\phi(\mathbf{x},t,\mathbf{x}_K,0)m(K)d\mathbf{x}dt \\
= &-\int_0^{t^N}\sum_{K\in\mathcal{T}}\int_{\mathbb{R}^2}\int_0^{t^N} U(u_K(t') - v(\mathbf{x},t))\phi_{t'}(\mathbf{x},t,\mathbf{x}_K,t')d\mathbf{x}dtm(K)dt' \\
&+ \sum_{K\in\mathcal{T}}\int_0^{t^N}\int_{\mathbb{R}^2} U(u_K(t^N) - v(\mathbf{x},t))\phi(\mathbf{x},t,\mathbf{x}_K,t^N)m(K)d\mathbf{x}dt \\
&+ \sum_{K\in\mathcal{T}}\int_0^{t^N}\int_{\mathbb{R}^2} U(u_K(0) - v(\mathbf{x},t))\phi(\mathbf{x},t,\mathbf{x}_K,0)m(K)d\mathbf{x}dt
\end{aligned}$$

Now, taking into account that $\phi_{t'} = -\phi_t$, $\phi(\mathbf{x},t,\mathbf{x}_K,t') = \dfrac{1}{m(K)}\displaystyle\int_K \varphi(\mathbf{x},t,\mathbf{x}',t')d\mathbf{x}'$ and $u_K(t')$ is equal to $u(\mathbf{x}',t')$ on K, we get:

$$\begin{aligned}
E_{div,t}(u,v;t^N) = &\int_0^{t^N}\int_{\mathbb{R}^2}\int_0^{t^N}\int_{\mathbb{R}^2} U(u(\mathbf{x}',t') - v(\mathbf{x},t))\varphi_t(\mathbf{x},t,\mathbf{x}',t')d\mathbf{x}dtd\mathbf{x}'dt' \\
&+ \int_0^{t^N}\int_{\mathbb{R}^2}\int_{\mathbb{R}^2} U(u(\mathbf{x}',t^N) - v(\mathbf{x},t))\varphi(\mathbf{x},t,\mathbf{x}',t^N)d\mathbf{x}d\mathbf{x}'dt \\
&- \int_0^{t^N}\int_{\mathbb{R}^2}\int_{\mathbb{R}^2} U(u(\mathbf{x}',0) - v(\mathbf{x},t))\varphi(\mathbf{x},t,\mathbf{x}',0)d\mathbf{x}d\mathbf{x}'dt
\end{aligned}$$

Finally, adding and subtracting the terms

$$\int_0^{t^N}\int_{\mathbb{R}^2}\int_{\mathbb{R}^2} U(u(\mathbf{x}',t')-v(\mathbf{x},t^N))\varphi(\mathbf{x},t^N,\mathbf{x}',t')d\mathbf{x}d\mathbf{x}'dt'$$

and

$$\int_0^{t^N}\int_{\mathbb{R}^2}\int_{\mathbb{R}^2} U(u(\mathbf{x}',t')-v_0(\mathbf{x}))\varphi(\mathbf{x},0,\mathbf{x}',t')d\mathbf{x}d\mathbf{x}'dt'$$

in $E_{div,t}(u,v;t^N)$ and gathering it with $E_{div,x}(u,v;t^N)$, we obtain the result. This completes the proof.

Remark 11 *We expect the term $T_{err}(u,v;t^N)$ to converge to $e(t^N)-e(0)$ as the parameters ϵ_t and $\epsilon_{\mathbf{x}}$ defining φ go to zero, where the error $e(t)$ is given by*

$$e(t)=\int_{\mathbb{R}^2} U(u(\mathbf{x},t)-v(\mathbf{x},t))d\mathbf{x}$$

A lower bound for the error term is given in the following proposition.

Proposition 4 *We have*

$$T_{err}(u,v;t^N)\geq W(t^N)e(t^n)+\int_0^{t^N} w_{\epsilon_t}(t^N-t)e(t)dt-W(t^N)e(0)+\int_0^{t^N} w_{\epsilon_t}(t)e(t)dt \\ -4W(t^N)(\|f'(v)\|\,\epsilon_t+\epsilon_{\mathbf{x}})|v_0|_{TV(\mathbb{R})}.$$

Proof. From the definition of the error term, we can write $T_{err}=T_1+T_2+T_3+T_4$ with the obvious notation. Let us start by estimating T_1. Since

$$\begin{aligned}U(u(\mathbf{x}',t^N)-v(\mathbf{x},t)) &= U(u(\mathbf{x}',t^N)-v(\mathbf{x}',t^N)) \\ &\quad -[U(u(\mathbf{x}',t^N)-v(\mathbf{x}',t^N))-U(u(\mathbf{x}',t^N)-v(\mathbf{x},t^N))] \\ &\quad -[U(u(\mathbf{x}',t^N)-v(\mathbf{x},t^N))-U(u(\mathbf{x}',t^N)-v(\mathbf{x},t))] \\ &\geq U(u(\mathbf{x}',t^N)-v(\mathbf{x}',t^N))-|v(\mathbf{x},t^N))-v(\mathbf{x}',t^N)|-|v(\mathbf{x},t))-v(\mathbf{x},t^N)|,\end{aligned}$$

we get,

$$\begin{aligned}T_1 &= \int_0^{t^N}\int_{\mathbb{R}^2}\int_{\mathbb{R}^2} U(u(\mathbf{x}',t^N)-v(\mathbf{x},t))\varphi(\mathbf{x},t,\mathbf{x}',t^N)d\mathbf{x}d\mathbf{x}'dt \\ &\geq \int_0^{t^N}\int_{\mathbb{R}^2}\int_{\mathbb{R}^2} U(u(\mathbf{x}',t^N)-v(\mathbf{x}',t^N))\varphi(\mathbf{x},t,\mathbf{x}',t^N)d\mathbf{x}d\mathbf{x}'dt \\ &\quad -\int_0^{t^N}\int_{\mathbb{R}^2}\int_{\mathbb{R}^2} |v(\mathbf{x},t^N))-v(\mathbf{x}',t^N)|\varphi(\mathbf{x},t,\mathbf{x}',t^N)d\mathbf{x}d\mathbf{x}'dt \\ &\quad -\int_0^{t^N}\int_{\mathbb{R}^2}\int_{\mathbb{R}^2} |v(\mathbf{x},t))-v(\mathbf{x},t^N)|\varphi(\mathbf{x},t,\mathbf{x}',t^N)d\mathbf{x}d\mathbf{x}'dt.\end{aligned}$$

Now, since

$$|v(\mathbf{x},t^N))-v(\mathbf{x}',t^N)|=\left|\int_C \nabla_{\mathbf{x}}v(\cdot,t^N)\cdot d\overrightarrow{\gamma}\right|\leq\int_C \left\|\nabla_{\mathbf{x}}v(\cdot,t^N)\right\|d\gamma,$$

where C is the line joining the points $\mathbf{x}$ and $\mathbf{x}'$ and $\overrightarrow{\gamma}$ is a parametrization of C,

$$\begin{aligned}|v(\mathbf{x},t))-v(\mathbf{x},t^N)| &= \left|\int_t^{t^N} v_t(\mathbf{x},t')dt'\right|\leq\int_t^{t^N}|-f'(v)\cdot\nabla_{\mathbf{x}}v(\mathbf{x},t')|\,dt' \\ &\leq\|f'(v)\|\int_t^{t^N}\left\|\nabla_{\mathbf{x}}v(\mathbf{x},t^N)\right\|dt',\end{aligned}$$

$\int_{\mathbb{R}} w_{\epsilon_{\mathbf{x}}}(x_i - x_i')dx_i' = 1$ if $\|\mathbf{x} - \mathbf{x}'\| \le \epsilon_{\mathbf{x}}$ and $\int_0^{t^N} w_{\epsilon_t}(t - t^N)dt = W(t^N)$ if $|t - t^N| \le \epsilon_t$, we have:

$$\begin{aligned}
&\int_0^{t^N}\int_{\mathbb{R}^2}\int_{\mathbb{R}^2} U(u(\mathbf{x}',t^N) - v(\mathbf{x}',t^N))\varphi(\mathbf{x},t,\mathbf{x}',t^N)d\mathbf{x}d\mathbf{x}'dt \\
&\qquad = \int_0^{t^N}\int_{\mathbb{R}^2}\int_{\mathbb{R}^2} U(u(\mathbf{x}',t^N) - v(\mathbf{x}',t^N))w_{\epsilon_t}(t-t^N)\prod_{i=1}^{2} w_{\epsilon_{\mathbf{x}}}(x_i - x_i')d\mathbf{x}d\mathbf{x}'dt \\
&\qquad = \int_{\mathbb{R}^2} U(u(\mathbf{x}',t^N) - v(\mathbf{x}',t^N))\Big(\int_{\mathbb{R}}\prod_{i=1}^{2} w_{\epsilon_{\mathbf{x}}}(x_i - x_i')dx_i\Big)d\mathbf{x}'\Big(\int_0^{t^N} w_{\epsilon_t}(t-t^N)dt\Big) \\
&\qquad = W(t^N)\int_{\mathbb{R}^2} U(u(\mathbf{x}',t^N) - v(\mathbf{x}',t^N))d\mathbf{x}',
\end{aligned}$$

$$\begin{aligned}
&\int_0^{t^N}\int_{\mathbb{R}^2}\int_{\mathbb{R}^2} |v(\mathbf{x},t^N)) - v(\mathbf{x}',t^N)|\varphi(\mathbf{x},t,\mathbf{x}',t^N)d\mathbf{x}d\mathbf{x}'dt \\
&\qquad \le \int_0^{t^N}\int_{\mathbb{R}^2}\int_{\mathbb{R}^2}\Big(\int_C \big\|\nabla_{\mathbf{x}} v(\cdot,t^N)\big\|\,d\gamma\Big)w_{\epsilon_t}(t-t^N)\prod_{i=1}^{2} w_{\epsilon_{\mathbf{x}}}(x_i - x_i')d\mathbf{x}d\mathbf{x}'dt \\
&\qquad \le \int_C\int_{\mathbb{R}^2}\big\|\nabla_{\mathbf{x}} v(\cdot,t^N)\big\|\Big(\int_{\mathbb{R}}\prod_{i=1}^{2} w_{\epsilon_{\mathbf{x}}}(x_i - x_i')dx_i'\Big)d\mathbf{x}\;d\gamma\Big(\int_0^{t^N} w_{\epsilon_t}(t-t^N)dt\Big) \\
&\qquad \le W(t^N)|v_0|_{TV(\mathbb{R}^2)}\,\|\mathbf{x} - \mathbf{x}'\| \\
&\qquad \le W(t^N)|v_0|_{TV(\mathbb{R}^2)}\epsilon_{\mathbf{x}},
\end{aligned}$$

$$\begin{aligned}
&\int_0^{t^N}\int_{\mathbb{R}^2}\int_{\mathbb{R}^2} U(u(\mathbf{x}',t') - v_0(\mathbf{x}))\varphi(\mathbf{x},0,\mathbf{x}',t')d\mathbf{x}d\mathbf{x}'dt' \\
&\qquad \le \int_0^{t^N}\int_{\mathbb{R}^2}\int_{\mathbb{R}^2}\Big(\|f'(v)\|\int_t^{t^N}\big\|\nabla_{\mathbf{x}} v(\mathbf{x},t^N)\big\|\,dt'\Big)w_{\epsilon_t}(t-t^N)\prod_{i=1}^{2} w_{\epsilon_{\mathbf{x}}}(x_i - x_i')d\mathbf{x}d\mathbf{x}'dt \\
&\qquad \le \|f'(v)\|\Big(\int_0^{t^N} w_{\epsilon_t}(t-t^N)dt\Big)\int_t^{t^N}\int_{\mathbb{R}^2}\big\|\nabla_{\mathbf{x}} v(\mathbf{x},t^N)\big\|\Big(\int_{\mathbb{R}}\prod_{i=1}^{2} w_{\epsilon_{\mathbf{x}}}(x_i - x_i')dx_i'\Big)d\mathbf{x}dt' \\
&\qquad \le W(t^N)\,\|f'(v)\|\,|v_0|_{TV(\mathbb{R}^2)}\epsilon_t.
\end{aligned}$$

Thus,

$$T_1 \ge W(t^N)e(t^N) - W(t^N)(\|f'(v)\|\,\epsilon_t + \epsilon_{\mathbf{x}})|v_0|_{TV(\mathbb{R})}.$$

To estimate T_2, T_3 and T_4 we proceed in a similar way. We obtain:

$$T_2 \ge \int_0^{t^N} w_{\epsilon_t}(t'-t^N)\Big(\int_{\mathbb{R}^2} U(u(\mathbf{x}',t') - v(\mathbf{x}',t'))d\mathbf{x}'\Big)dt' - W(t^N)(\|f'(v)\|\,\epsilon_t + \epsilon_{\mathbf{x}})|v_0|_{TV(\mathbb{R})},$$

$$T_3 \ge -W(t^N)\int_{\mathbb{R}^2} U(u(\mathbf{x}',0) - v(\mathbf{x}',0))d\mathbf{x}' - W(t^N)(\|f'(v)\|\,\epsilon_t + \epsilon_{\mathbf{x}})|v_0|_{TV(\mathbb{R})},$$

and

$$T_4 \ge -\int_0^{t^N} w_{\epsilon_t}(t')\Big(\int_{\mathbb{R}^2} U(u(\mathbf{x}',t') - v(\mathbf{x}',t'))d\mathbf{x}'\Big)dt' - W(t^N)(\|f'(v)\|\,\epsilon_t + \epsilon_{\mathbf{x}})|v_0|_{TV(\mathbb{R})}.$$

This completes the proof.

Proposition 5 *The following approximation inequality holds:*

$$e(t^N) \leq 2e(0) + 8(\epsilon_{\mathbf{x}} + \epsilon_t \left\|f'(v)\right\|)|v_0|_{TV(\mathbb{R}^2)} + 2\left\|f'(v)\right\||v_0|_{TV(\mathbb{R}^2)}\Delta t \\ + 2\lim_{w\to\chi} \operatorname{Sup}_{1\leq n\leq N} \left\{E^{\star}_{div}(u,v;t^n)/W(t^n) - E_{diss}(u,v;t^n)/W(t^n)\right\},$$

where $W(t) = \displaystyle\int_0^t w_{\epsilon_t}(s)ds$.

To prove it, we need the following auxiliary Lemma.

Lemma 7 *Let* $\theta : [0,T] \to \mathbb{R}^+$ *be a nonnegative, measurable fuction such that* $\forall N \in \mathbb{N}$

$$W^{\infty}(t^N)\theta(t^N) + \int_0^{t^N} w^{\infty}_{\epsilon_t}(t^N - t)\theta(t)dt \leq C_1 W^{\infty}(t^N) + \int_0^{t^N} w^{\infty}_{\epsilon_t}(t)\theta(t)dt,$$

where $w^{\infty}(s) = \chi(s)$. *Moreover, assume that for* $t \in [t^n, t^{n+1})$,

$$\theta(t) \leq \theta(t^n) + C_2\Delta t.$$

Then, for $\tau \in [t^n, t^{n+1})$,

$$\theta(\tau) \leq 2C_1 + C_2\Delta t.$$

Proof. If $t \leq t^n \leq \epsilon_t$, we have that

$$w^{\infty}_{\epsilon_t}(t^N - t) = \frac{1}{\epsilon_t} w^{\infty}\left(\frac{t^n - t}{\epsilon_t}\right) = \frac{1}{\epsilon_t}\chi\left(\frac{t^n - t}{\epsilon_t}\right) = \frac{1}{2\epsilon_t} = w^{\infty}_{\epsilon_t}(t).$$

So, for the first hypothesis, $\theta(t^n) \leq C_1$.

By the second hypothesis, for $t^n \leq t \leq \epsilon_t$, $\theta(t) \leq C_1 + C_2\Delta t$.

To estimate $\theta(\tau)$ for $\tau \geq \epsilon_t$, we take into account that $w^{\infty}_{\epsilon_t}(t) = 0$, $\theta(t) \geq 0$ and rewrite the inequality satisfied by θ as follows:

$$\begin{aligned}\theta(\tau) &\leq C_1 + \frac{\int_0^{\tau}[w^{\infty}_{\epsilon_t}(t) - w^{\infty}_{\epsilon_t}(\tau - t)]\theta(t)dt}{W^{\infty}(\tau)} \\ &= C_1 + \frac{\int_0^{\epsilon_t}[w^{\infty}_{\epsilon_t}(t) - w^{\infty}_{\epsilon_t}(\tau - t)]\theta(t)dt + \int_{\epsilon_t}^{\tau}[w^{\infty}_{\epsilon_t}(t) - w^{\infty}_{\epsilon_t}(\tau - t)]\theta(t)dt}{W^{\infty}(\tau)} \\ &\leq C_1 + \frac{\int_0^{\epsilon_t}[w^{\infty}_{\epsilon_t}(t) - w^{\infty}_{\epsilon_t}(\tau - t)]\theta(t)dt}{W^{\infty}(\tau)}.\end{aligned}$$

Since for $t \in [0, \epsilon_t]$, $\theta(t) \leq C_1 + C_2\Delta t$,

$$\theta(\tau) \leq C_1 + \frac{\int_0^{\epsilon_t}[w^{\infty}_{\epsilon_t}(t) - w^{\infty}_{\epsilon_t}(\tau - t)]dt}{W^{\infty}(\tau)}(C_1 + C_2\Delta t).$$

Furthermore,

$$W^{\infty}(t) = \int_0^t w^{\infty}_{\epsilon_t}(s)ds = \int_0^t \frac{1}{\epsilon_t} w^{\infty}(\frac{s}{\epsilon_t})ds = \int_0^{\frac{t}{\epsilon_t}} \chi(r)dr = \begin{cases} t/2\epsilon_t & \text{if } t < \epsilon_t \\ 1/2 & \text{if } t \geq \epsilon_t \end{cases},$$

and $w^{\infty}_{\epsilon_t}(t) - w^{\infty}_{\epsilon_t}(\tau - t) \leq 1/2\epsilon_t$ for $t \in [0, \epsilon_t]$. Then,

$$\frac{\int_0^{\epsilon_t}[w^{\infty}_{\epsilon_t}(t) - w^{\infty}_{\epsilon_t}(\tau - t)]dt}{W^{\infty}(\tau)} \leq 1.$$

In consequence, $\theta(\tau) \leq 2C_1 + C_2\Delta t$. This completes the proof of Lemma 7.

Proof of Proposition 5. Taking into account that $v_t + \nabla_{\mathbf{x}} \cdot f(v) = 0$, we have:

$$\begin{aligned}
\int_{\mathbb{R}^2} |v(\mathbf{x}, t^n) - v(\mathbf{x}, t)| \, d\mathbf{x} &= \int_{\mathbb{R}^2} \left| \int_t^{t^n} v_t(\mathbf{x}, t) dt \right| \\
&\leq \int_{\mathbb{R}^2} \int_t^{t^n} |f'(v) \cdot \nabla_{\mathbf{x}} v(\mathbf{x}, t)| dt d\mathbf{x} \\
&\leq \|f'(v)\| \int_t^{t^n} \int_{\mathbb{R}^2} \|\nabla_{\mathbf{x}} v(\mathbf{x}, t)\| \, d\mathbf{x} dt \\
&\leq \|f'(v)\| \int_t^{t^n} |v_0|_{TV(\mathbb{R}^2)} dt \\
&\leq \|f'(v)\| \, |v_0|_{TV(\mathbb{R}^2)} \Delta t.
\end{aligned}$$

Thus,

$$\begin{aligned}
e(t) &= \int_{\mathbb{R}^2} |u(\mathbf{x}, t) - v(\mathbf{x}, t)| d\mathbf{x} \\
&\leq \int_{\mathbb{R}^2} |u(\mathbf{x}, t) - u(\mathbf{x}, t^n)| d\mathbf{x} + \int_{\mathbb{R}^2} |u(\mathbf{x}, t^n) - v(\mathbf{x}, t^n)| d\mathbf{x} + \int_{\mathbb{R}^2} |v(\mathbf{x}, t^n) - v(\mathbf{x}, t)| d\mathbf{x} \\
&\leq e(t^n) + 2 \|f'(v)\| \, |v_0|_{TV(\mathbb{R}^2)} \Delta t.
\end{aligned}$$

Furthermore, From Proposition 4, we get

$$\begin{aligned}
W^\infty(t^N) e(t^N) + \int_0^{t^N} w_{\epsilon_t}^\infty(t^N - t) e(t) dt \leq \\
W^\infty(t^N) \Bigg[\lim_{w \to \chi} \operatorname*{Sup}_{1 \leq n \leq N} \{ E_{div}^\star(u, v; t^n)/W(t^n) - E_{diss}(u, v; t^n)/W(t^n) \} \\
+ 4(\epsilon_{\mathbf{x}} + \epsilon_t \|f'(v)\|) |v_0|_{TV(\mathbb{R}^2)} + e(0) \Bigg] + \int_0^{t^N} w_{\epsilon_t}^\infty(t) e(t) dt.
\end{aligned}$$

Then, the result of Proposition 5 follows from the two above inequalities and Lemma 7 with

$\theta(t^n) = e(t^n)$,

$C_1 = e(0) + 4(\epsilon_{\mathbf{x}} + \epsilon_t \|f'(v)\|) |v_0|_{TV(\mathbb{R}^2)} + \lim_{w \to \chi} \operatorname*{Sup}_{1 \leq n \leq N} \left\{ \dfrac{E_{div}^\star(u, v; t^n) - E_{diss}(u, v; t^n)}{W(t^n)} \right\}$ and,

$C_2 = 2 \|f'(v)\| \, |v_0|_{TV(\mathbb{R}^2)}$.

This completes the proof.

Remark 12 *From Proposition 3 we have that, to obtain the error estimate, it is enough to estimate the forms $E_{div}^\star(u, v; t^n)$ and $E_{diss}(u, v; t^n)$.*

The following results give these estimates.

Proposition 6 *Under condition (2.26), and if condition (2.90) is satisfied, the local rate of entropy dissipation $LRED_j^n(c)$ is nonnegative. Hence*

$$-E_{diss}(u, v; t^n) \leq 0.$$

Proof. From (2.26), we have

$$p'_{KL}(s) = -m(K|L) \left[\frac{1}{2} f'(s) \cdot \mathbf{n}_{KL} - \operatorname*{Sup}_{\substack{w \in [-r, r] \\ K, L \in \mathcal{T}}} \left| \frac{\mathbf{f}(w)}{w} \cdot \mathbf{n}_{KL} \right| \right] \geq 0.$$

In addition, taking into account that

$$p'_K(s) = 1 - \frac{\Delta t}{m(K)} \sum_{L \in N(K)} p'_{KL}(s) \quad \text{and} \quad \sum_{L \in N(K)} p'_{KL}(s) = m(\partial K) \operatorname*{Sup}_{\substack{w \in [-r,r] \\ K,L \in \mathcal{T}}} \left| \frac{\mathbf{f}(w)}{w} \cdot \mathbf{n}_{KL} \right|,$$

from (2.90), we have $p'_K(s) \geq 0$. This means that functions $p_{KL}(s)$ and $p_K(s)$ are nondecreasing in s.

Now, for all s between u_K^n and u_K^{n+1}, the nondecreasing character of function $p_K(s)$ and the fact that $U''(\cdot) > 0$ imply

$$\int_{u_K^{n+1}}^{u_K^n} (p_K(u_K^n) - p_K(s)) U''(s-c)\, ds \geq 0. \tag{2.104}$$

In fact,

1) if $u_K^n > u_K^{n+1}$, $p_K(s) \leq p_K(u_K^n)$ and, hence, $\displaystyle\int_{u_K^{n+1}}^{u_K^n} (p_K(u_K^n) - p_K(s)) U''(s-c)\, ds \geq 0$, and

2) if $u_K^n < u_K^{n+1}$, $p_K(s) \geq p_K(u_K^n)$ and, hence,

$$\int_{u_K^{n+1}}^{u_K^n} (p_K(u_K^n) - p_K(s)) U''(s-c)\, ds = -\int_{u_K^n}^{u_K^{n+1}} (p_K(u_K^n) - p_K(s)) U''(s-c)\, ds \geq 0.$$

Similarly, the nondecreasing character of function $p_{KL}(s)$ and the fact that $U''(\cdot) > 0$ imply

$$\int_{u_K^{n+1}}^{u_L^n} (p_{KL}(u_L^n) - p_{KL}(s)) U''(s-c)\, ds \geq 0. \tag{2.105}$$

The result follows from (2.104) and (2.105) and the definition of $E_{diss}(u, v; t^n)$.

Proposition 7 *We have*

$$\lim_{w \to \chi} \operatorname*{Sup}_{1 \leq n \leq N} \{E^\star_{div}(u, v; t^n)/W(t^n)\} \leq TEW_{visc} + TEW_{h.o.t},$$

where

$$TEW_{visc}(u, v; t^n) \leq C_0 t^N \left[2 \frac{|\eta|_{TV(\mathbb{R})}}{\epsilon_{\mathbf{x}}} \left(1 + \frac{\Delta t}{\epsilon_t} \right) \right] \|\nu_v\|\, h,$$

$$\begin{aligned} TEW_{h.o.t}(u, v; t^n) \leq C_1 \Bigg[& \|f'(v)\| \frac{(\Delta t)^2 |\eta|_{TV(\mathbb{R})}}{\epsilon_t \epsilon_{\mathbf{x}}} t^N + 4 \left(1 + \frac{\Delta t}{\epsilon_t} \right) \Delta t \\ & + 32 \mathbb{D}_{\Delta \mathbf{x}} l_{\Delta \mathbf{x}} h^2 \left[\frac{4 |\eta|^2_{TV(\mathbb{R})}}{\epsilon_{\mathbf{x}}^2} + \frac{2 |\eta'|_{TV(\mathbb{R})}}{\epsilon_{\mathbf{x}}^2} \right] \left(1 + \frac{\Delta t}{\epsilon_t} \right) t^N \Bigg], \end{aligned}$$

with $h = \Delta \mathbf{x}$, $C_0 = 2|v_0|_{TV(\mathbb{R}^2)}$, $C_1 = C_0 \|f'(v)\|$ and $\|f'(v)\|$ is given by

$$\|f'(v)\| = \operatorname*{Sup}_{\substack{t \in (0, t^N) \\ \mathbf{x} \in \mathbb{R}^2}} \|f'(v(\mathbf{x}, t))\|_{l^\infty}.$$

Proof. To prove this result, we proceed in several steps.

First step: Relating the dual form $E^\star_{div}(u, v; t^n)$ to the truncation error.

Lemma 8 *The following upper bound for $E^{\star}_{div}(u,v;t^n)$ holds*

$$\begin{aligned}
E^{\star}_{div}(u,v;t^n) \leq & \sum_{n=0}^{N-1}\sum_{K\in\mathcal{T}}\int_0^{t^N}\int_{\mathbb{R}^2} F(u_K^n, v(\mathbf{x},t))\cdot\nabla_{\mathbf{x}}\overline{\phi}(\mathbf{x},t,\mathbf{x}_K,t^{n+1})m(K)\Delta t d\mathbf{x}dt \\
& - \sum_{n=0}^{N-1}\sum_{K\in\mathcal{T}}\int_0^{t^N}\int_{\mathbb{R}^2}\sum_{L\in\partial K} m(K|L)b_{L,K}[\phi(\mathbf{x},t,\mathbf{x}_K,t^{n+1})-\phi(\mathbf{x},t,\mathbf{x}_L,t^{n+1})] \\
& \qquad F(u_K^n, v(\mathbf{x},t))\cdot n_{K,L}\Delta t d\mathbf{x}dt \\
& + \sum_{n=0}^{N-1}\sum_{K\in\mathcal{T}}\int_0^{t^N}\int_{\mathbb{R}^2}\sum_{L\in\partial K} m(K|L)\alpha_{K|L}[\phi(\mathbf{x},t,\mathbf{x}_L,t^{n+1})-\phi(\mathbf{x},t,\mathbf{x}_K,t^{n+1})] \\
& \qquad \mathcal{N}_{K|L}(u_K^n, v(\mathbf{x},t))\Delta t d\mathbf{x}dt
\end{aligned}$$

Proof. By using the fact the v is the entropy solution and $u(\mathbf{x}',t') = u_K^n, \forall \mathbf{x}' \in K$ and $\forall t' \in [t^n, t^{n+1})$, we have:

$$\begin{aligned}
& -\int_0^{t^N}\int_{\mathbb{R}^2}\int_0^{t^N}\int_{\mathbb{R}^2} U(u(\mathbf{x}',t')-v(\mathbf{x},t))\varphi_t(\mathbf{x},t,\mathbf{x}',t')d\mathbf{x}dtd\mathbf{x}'dt' \\
& +\int_0^{t^N}\int_{\mathbb{R}^2}\int_{\mathbb{R}^2} U(u(\mathbf{x}',t')-v(\mathbf{x},t^N))\varphi(\mathbf{x},t^N,\mathbf{x}',t')d\mathbf{x}d\mathbf{x}'dt' \\
& -\int_0^{t^N}\int_{\mathbb{R}^2}\int_{\mathbb{R}^2} U(u(\mathbf{x}',t')-v_0(\mathbf{x}))\varphi(\mathbf{x},0,\mathbf{x}',t')d\mathbf{x}d\mathbf{x}'dt' \\
& \qquad \leq \int_0^{t^N}\int_{\mathbb{R}^2}\int_0^{t^N}\int_{\mathbb{R}^2} F(u(\mathbf{x}',t'),v(\mathbf{x},t))\cdot\nabla_{\mathbf{x}}\varphi(\mathbf{x},t,\mathbf{x}',t')d\mathbf{x}dtd\mathbf{x}'dt' \\
& \qquad = \int_0^{t^N}\int_{\mathbb{R}^2}\sum_{n=0}^{N-1}\sum_{K\in\mathcal{T}}\int_{t^n}^{t^{n+1}}\int_K F(u_K^n,v(\mathbf{x},t))\cdot\nabla_{\mathbf{x}}\varphi(\mathbf{x},t,\mathbf{x}',t')d\mathbf{x}'dt'd\mathbf{x}dt \\
& \qquad = \sum_{n=0}^{N-1}\sum_{K\in\mathcal{T}}\int_0^{t^N}\int_{\mathbb{R}^2} F(u_K^n,v(\mathbf{x},t))\cdot\nabla_{\mathbf{x}}\overline{\phi}(\mathbf{x},t,\mathbf{x}',t^{n+1})m(K)\Delta t d\mathbf{x}dt,
\end{aligned}$$

where, $\overline{\phi}(\mathbf{x},t,\mathbf{x}',t^{n+1}) = \dfrac{1}{m(K)\Delta t}\displaystyle\int_{t^n}^{t^{n+1}}\int_K \varphi(\mathbf{x},t,\mathbf{x}',t')d\mathbf{x}'dt'$.

Substituting this inequality in the definition of $E^{\star}_{div}(u,v;t^n)$, we get the result. This concludes the proof.

Next, a relation between the functions $\phi(\mathbf{x},\mathbf{x}_L)$ and $\phi(\mathbf{x},\mathbf{x}_K)$, defined by (2.94) is needed. That relation is displayed in the following lemma where, for the ske of clarity, we drop the dependence on t and t'. This simple result is a keystone of the proof of the Theorem 2.2.5.

Lemma 9 *The function ϕ defined by (2.94) satisfies the following equality:*

$$\phi(\mathbf{x},\mathbf{x}_L)-\phi(\mathbf{x},\mathbf{x}_K) = -(\mathbf{x}_L-\mathbf{x}_K)\cdot\nabla_{\mathbf{x}}\phi(\mathbf{x},\mathbf{x}_K) + \overline{H}_{K,L}(\mathbf{x},\mathbf{x}_K) + \overline{\overline{H}}_{K,L}(\mathbf{x}),$$

where

$$\overline{H}_{K,L}(\mathbf{x},\mathbf{x}_K) = \sum_{i,j=1}^{2}\xi_{K,L}^{ij}\partial^2_{x_i,x_j}\phi(\mathbf{x},\mathbf{x}_K),$$

$$\xi_{K,L}^{ij} = \frac{1}{2}\Big[(\mathbf{x}_L-\mathbf{x}_K)_i(\mathbf{x}_L-\mathbf{x}_K)_j + \mathbb{I}_L^{ij} - \mathbb{I}_K^{ij}\Big],$$

$$\mathbb{I}_{\Omega}^{ij} = \frac{1}{m(\Omega)}\int_{\Omega}(\mathbf{x}'-\mathbf{x}_{\Omega})_i(\mathbf{x}'-\mathbf{x}_{\Omega})_j d\mathbf{x},$$

and

$$\overline{\overline{H}}_{K,L}(\mathbf{x}) = \frac{1}{m(L)} \int_L \frac{1}{[m(K)]^3} \int_{K^3} \int_0^1 \int_0^1 \int_0^1 \Psi(\mathbf{x}) d\lambda d\mu d\nu d\mathbf{z}' d\mathbf{y}' d\mathbf{w}' d\mathbf{x}',$$

$$\Psi(\mathbf{x}) = \sum_{i,j,k=1}^{2} \zeta^{ijk} \partial^3_{x_i x_j x_k} \varphi(\mathbf{x}, \lambda(\mu(\nu\mathbf{x}' + (1-\nu)\mathbf{w}') + (1-\mu)\mathbf{y}') + (1-\lambda)\mathbf{z}'),$$

$$\zeta^{ijk} = (\mathbf{x}' - \mathbf{w}')_i (\nu\mathbf{x}' + (1-\nu)\mathbf{w}' - \mathbf{y}')_j (\mu(\nu\mathbf{x}' + (1-\nu)\mathbf{w}') + (1-\mu)\mathbf{y}') - \mathbf{z}')_k.$$

Proof. Recalling that $\nabla_{\mathbf{x}} \varphi = -\nabla_{\mathbf{x}'} \varphi$, we have that

$$-\int_0^1 (\mathbf{x}' - \mathbf{w}') \cdot \nabla_{\mathbf{x}} \varphi(\mathbf{x}, \nu\mathbf{x}' + (1-\nu)\mathbf{w}') d\nu = \int_0^1 \nabla_{\mathbf{x}'} \varphi(\mathbf{x}, \nu\mathbf{x}' + (1-\nu)\mathbf{w}') \cdot (\mathbf{x}' - \mathbf{w}') d\nu.$$

Let $r(\nu) = \nu\mathbf{x}' + (1-\nu)\mathbf{w}'$ then, $dr = (\mathbf{x}' - \mathbf{w}')d\nu$. So,

$$\begin{aligned} -\int_0^1 (\mathbf{x}' - \mathbf{w}') \cdot \nabla_{\mathbf{x}} \varphi(\mathbf{x}, \nu\mathbf{x}' + (1-\nu)\mathbf{w}') d\nu &= \int_0^1 \left(\nabla_{\mathbf{x}'} \varphi(\mathbf{x}, r(\nu)) \cdot \frac{dr}{d\nu} \right) \\ &= \int_0^1 d\varphi(\mathbf{x}, r(\nu)) \\ &= \varphi(\mathbf{x}, r(1)) - \varphi(\mathbf{x}, r(0)) \\ &= \varphi(\mathbf{x}, \mathbf{x}') - \varphi(\mathbf{x}, \mathbf{w}'). \end{aligned}$$

Therefore,

$$\varphi(\mathbf{x}, \mathbf{x}') = \varphi(\mathbf{x}, \mathbf{w}') - \int_0^1 (\mathbf{x}' - \mathbf{w}') \cdot \nabla_{\mathbf{x}} \varphi(\mathbf{x}, \nu\mathbf{x}' + (1-\nu)\mathbf{w}') d\nu.$$

Averaging the above equality over K with respect to $\mathbf{w}'$ yields

$$\begin{aligned} \frac{1}{m(K)} \int_K \varphi(\mathbf{x}, \mathbf{x}') d\mathbf{w}' = \frac{1}{m(K)} \int_K \varphi(\mathbf{x}, \mathbf{w}') d\mathbf{w}' \\ - \frac{1}{m(K)} \int_K \int_0^1 (\mathbf{x}' - \mathbf{w}') \cdot \nabla_{\mathbf{x}} \varphi(\mathbf{x}, \nu\mathbf{x}' + (1-\nu)\mathbf{w}') d\nu d\mathbf{w}'. \end{aligned}$$

From this equality and the definition of ϕ (2.94), we get

$$\varphi(\mathbf{x}, \mathbf{x}') = \phi(\mathbf{x}, \mathbf{x}_K) - \frac{1}{m(K)} \int_K \int_0^1 (\mathbf{x}' - \mathbf{w}') \cdot \nabla_{\mathbf{x}} \varphi(\mathbf{x}, \nu\mathbf{x}' + (1-\nu)\mathbf{w}') d\nu d\mathbf{w}'.$$

Using the above relation recursively twice, we obtain

$$\begin{aligned} \varphi(\mathbf{x}, \mathbf{x}') &= \phi(\mathbf{x}, \mathbf{x}_K) - \frac{1}{m(K)} \int_K \int_0^1 (\mathbf{x}' - \mathbf{w}') \cdot \nabla_{\mathbf{x}} \varphi(\mathbf{x}, \nu\mathbf{x}' + (1-\nu)\mathbf{w}') d\nu d\mathbf{w}' \\ &= \phi(\mathbf{x}, \mathbf{x}_K) - \frac{1}{m(K)} \sum_{i=1}^{2} \int_K \int_0^1 (\mathbf{x}' - \mathbf{w}')_i \partial_{x_i} \varphi(\mathbf{x}, \nu\mathbf{x}' + (1-\nu)\mathbf{w}') d\nu d\mathbf{w}' \\ &= \phi(\mathbf{x}, \mathbf{x}_K) - \frac{1}{m(K)} \sum_{i=1}^{2} \int_K \int_0^1 (\mathbf{x}' - \mathbf{w}')_i \partial_{x_i} \Big[\phi(\mathbf{x}, \mathbf{x}_K) \end{aligned}$$

$$
\begin{aligned}
&- \frac{1}{m(K)} \int_K \int_0^1 (\nu \mathbf{x}' + (1-\nu)\mathbf{w}' - \mathbf{y}') \cdot \\
&\qquad \nabla_{\mathbf{x}} \varphi(\mathbf{x}, \mu(\nu \mathbf{x}' + (1-\nu)\mathbf{w}') \\
&\qquad\qquad + (1-\mu)\mathbf{y}') d\mu d\mathbf{y}' \Big] d\nu d\mathbf{w}' \\
= \phi(\mathbf{x}, \mathbf{x}_K) &- \frac{1}{m(K)} \sum_{i=1}^2 \int_K \int_0^1 (\mathbf{x}' - \mathbf{w}')_i \partial_{x_i} \Big[\phi(\mathbf{x}, \mathbf{x}_K) \\
&\qquad - \frac{1}{m(K)} \partial_{x_i} \sum_{j=1}^2 \int_K \int_0^1 (\nu \mathbf{x}' + (1-\nu)\mathbf{w}' - \mathbf{y}')_j \\
&\qquad\qquad \partial_{x_j} \varphi(\mathbf{x}, \mu(\nu \mathbf{x}' + (1-\nu)\mathbf{w}') \\
&\qquad\qquad\qquad + (1-\mu)\mathbf{y}') d\mu d\mathbf{y}' \Big] d\nu d\mathbf{w}' \\
= \phi(\mathbf{x}, \mathbf{x}_K) &- \frac{1}{m(K)} \sum_{i=1}^2 \int_K \int_0^1 (\mathbf{x}' - \mathbf{w}')_i \partial_{x_i} \phi(\mathbf{x}, \mathbf{x}_K) d\nu d\mathbf{w}' \\
&+ \frac{1}{[m(K)]^2} \sum_{i=1}^2 \sum_{j=1}^2 \int_K \int_0^1 (\mathbf{x}' - \mathbf{w}')_i \int_K \int_0^1 (\nu \mathbf{x}' + (1-\nu)\mathbf{w}' - \mathbf{y}')_j \\
&\qquad \partial^2_{x_i x_j} \varphi(\mathbf{x}, \mu(\nu \mathbf{x}' + (1-\nu)\mathbf{w}') + (1-\mu)\mathbf{y}') d\mu d\mathbf{y}' d\nu d\mathbf{w}' \\
= \phi(\mathbf{x}, \mathbf{x}_K) &+ \sum_{i=1}^2 \Big(- \frac{1}{m(K)} \int_K (\mathbf{x}' - \mathbf{w}')_i d\mathbf{w}' \Big) \partial_{x_i} \phi(\mathbf{x}, \mathbf{x}_K) + \frac{1}{[m(K)]^2} \sum_{i=1}^2 \sum_{j=1}^2 \int_K \int_0^1 (\mathbf{x}' - \mathbf{w}')_i \\
&\qquad \int_K \int_0^1 (\nu \mathbf{x}' + (1-\nu)\mathbf{w}' - \mathbf{y}')_j \\
&\qquad \partial^2_{x_i x_j} \Big[\phi(\mathbf{x}, \mathbf{x}_K) - \frac{1}{m(K)} \int_K \int_0^1 [\mu(\nu \mathbf{x}' + (1-\nu)\mathbf{w}') + (1-\mu)\mathbf{y}' - \mathbf{z}'] \cdot \\
&\qquad \varphi(\mathbf{x}, \lambda(\mu(\nu \mathbf{x}' + (1-\nu)\mathbf{w}') + (1-\mu)\mathbf{y}') + (1-\lambda)\mathbf{z}') d\lambda d\mathbf{z}' \Big] d\mu d\mathbf{y}' d\nu d\mathbf{w}' \\
= \phi(\mathbf{x}, \mathbf{x}_K) &+ \sum_{i=1}^2 \Big(- \frac{1}{m(K)} \int_K (\mathbf{x}' - \mathbf{w}')_i d\mathbf{w}' \Big) \partial_{x_i} \phi(\mathbf{x}, \mathbf{x}_K) + \frac{1}{[m(K)]^2} \sum_{i=1}^2 \sum_{j=1}^2 \int_K \int_0^1 (\mathbf{x}' - \mathbf{w}')_i \\
&\qquad \int_K (\nu \mathbf{x}' + (1-\nu)\mathbf{w}' - \mathbf{y}')_j \partial^2_{x_i x_j} \phi(\mathbf{x}, \mathbf{x}_K) d\mathbf{y}' d\nu d\mathbf{w}' \\
&\qquad - \frac{1}{[m(K)]^3} \sum_{i=1}^2 \sum_{j=1}^2 (\mathbf{x}' - \mathbf{w}')_i \int_{K^2} \int_0^1 \int_0^1 (\nu \mathbf{x}' + (1-\nu)\mathbf{w}' - \mathbf{y}')_j \\
&\qquad\qquad \partial^2_{x_i x_j} \sum_{k=1}^2 [\mu(\nu \mathbf{x}' + (1-\nu)\mathbf{w}') + (1-\mu)\mathbf{y}' - \mathbf{z}']_k \\
&\qquad\qquad \partial_{x_k} \varphi(\mathbf{x}, \lambda(\mu(\nu \mathbf{x}' + (1-\nu)\mathbf{w}') + (1-\mu)\mathbf{y}') - (1-\lambda)\mathbf{z}') d\lambda d\mathbf{z}' d\mu d\mathbf{y}' d\nu d\mathbf{w}'
\end{aligned}
$$

Thus,

$$\varphi(\mathbf{x}, \mathbf{x}') = \phi(\mathbf{x}, \mathbf{x}_K) + \sum_{i=1}^2 A^i(\mathbf{x}') \partial_{x_i} \phi(\mathbf{x}, \mathbf{x}_K) + \sum_{i,j=1}^2 B^{ij}(\mathbf{x}') \partial^2_{x_i, x_j} \phi(\mathbf{x}, \mathbf{x}_K) + Res(\mathbf{x}, \mathbf{x}'), \quad (2.106)$$

where

$$A^i(\mathbf{x}') = -\frac{1}{m(K)} \int_K (\mathbf{x}' - \mathbf{w}')_i d\mathbf{w}',$$

$$B^{ij}(\mathbf{x}') = \frac{1}{m(K)} \int_K \int_0^1 (\mathbf{x}' - \mathbf{w}')_i \left\{ \frac{1}{m(K)} \int_K (\nu \mathbf{x}' + (1-\nu)\mathbf{w}' - \mathbf{y}')_j d\mathbf{y}' \right\} d\nu d\mathbf{w}',$$
$$Res(\mathbf{x}, \mathbf{x}') = \frac{1}{[m(K)]^3} \int_{K^3} \int_0^1 \int_0^1 \int_0^1 \Psi(\mathbf{x}) d\lambda d\mu d\nu d\mathbf{z}' d\mathbf{y}' d\mathbf{w}'.$$

Let $\mathbb{A}^i = \dfrac{1}{m(L)} \displaystyle\int_L A^i(\mathbf{x}') d\mathbf{x}'$ then,

$$\begin{aligned}
\mathbb{A}^i &= \frac{1}{m(L)} \int_L \Big(- \frac{1}{m(K)} \int_K (\mathbf{x}' - \mathbf{w}')_i d\mathbf{w}' \Big) d\mathbf{x}' \\
&= -\frac{1}{m(L)} \int_L (\mathbf{x}' - \mathbf{x_K})_i d\mathbf{x}' \\
&= -(\mathbf{x_L} - \mathbf{x_K})_i.
\end{aligned}$$

Now,

$$\begin{aligned}
B^{ij}(\mathbf{x}') &= \frac{1}{m(K)} \int_K \int_0^1 (\mathbf{x}' - \mathbf{w}')_i \left\{ \frac{1}{m(K)} \int_K (\nu \mathbf{x}' + (1-\nu)\mathbf{w}' - \mathbf{y}')_j d\mathbf{y}' \right\} d\nu d\mathbf{w}' \\
&= \frac{1}{m(K)} \int_K \int_0^1 (\mathbf{x}' - \mathbf{w}')_i (\nu \mathbf{x}' + (1-\nu)\mathbf{w}' - \mathbf{x_K})_j d\nu d\mathbf{w}' \\
&= \frac{1}{m(K)} \int_K (\mathbf{x}' - \mathbf{w}')_i \left(\frac{1}{2}(\mathbf{x}' - \mathbf{w}') - \mathbf{x_K} \right)_j d\mathbf{w}' \\
&= \frac{1}{2m(K)} \int_K ((\mathbf{x}' - \mathbf{x_K}) - (\mathbf{w}' - \mathbf{x_K}))_i ((\mathbf{x}' - \mathbf{x_K}) + (\mathbf{w}' - \mathbf{x_K}))_j d\mathbf{w}' \\
&= \frac{1}{2} \Big[\frac{1}{m(K)} \int_K ((\mathbf{x}' - \mathbf{x_K}) - (\mathbf{w}' - \mathbf{x_K}))_i (\mathbf{x}' - \mathbf{x_K})_j d\mathbf{w}' \\
&\qquad + \frac{1}{m(K)} \int_K ((\mathbf{x}' - \mathbf{x_K}) - (\mathbf{w}' - \mathbf{x_K}))_i (\mathbf{w}' - \mathbf{x_K})_j d\mathbf{w}' \Big] \\
&= \frac{1}{2} \Big[\frac{1}{m(K)} \int_K (\mathbf{x}' - \mathbf{x_K})_i (\mathbf{x}' - \mathbf{x_K})_j d\mathbf{w}' - \frac{1}{m(K)} \int_K (\mathbf{w}' - \mathbf{x_K})_i (\mathbf{x}' - \mathbf{x_K})_j d\mathbf{w}' \\
&\qquad + \frac{1}{m(K)} \int_K (\mathbf{x}' - \mathbf{x_K})_i (\mathbf{w}' - \mathbf{x_K})_j d\mathbf{w}' - \frac{1}{m(K)} \int_K (\mathbf{w}' - \mathbf{x_K})_i (\mathbf{w}' - \mathbf{x_K})_j d\mathbf{w}' \Big] \\
&= \frac{1}{2} \Big[(\mathbf{x}' - \mathbf{x_K})_i (\mathbf{x}' - \mathbf{x_K})_j - \mathbb{I}_K^{ij} \Big].
\end{aligned}$$

Defining $\mathbb{B}^{ij} = \dfrac{1}{m(L)} \displaystyle\int_L B^{ij}(\mathbf{x}') d\mathbf{x}'$ we have

$$\begin{aligned}
\mathbb{B}^{ij} &= \frac{1}{m(L)} \int_L \frac{1}{2} \Big[(\mathbf{x}' - \mathbf{x_K})_i (\mathbf{x}' - \mathbf{x_K})_j - \mathbb{I}_K^{ij} \Big] d\mathbf{x}' \\
&= \frac{1}{2} \Big[\frac{1}{m(L)} \int_L ((\mathbf{x}' - \mathbf{x_L}) - (\mathbf{x_K} - \mathbf{x_L}))_i ((\mathbf{x}' - \mathbf{x_L}) - (\mathbf{x_K} - \mathbf{x_L}))_j d\mathbf{x}' - \mathbb{I}_K^{ij} \Big] \\
&= \frac{1}{2} \Big[\frac{1}{m(L)} \int_L (\mathbf{x}' - \mathbf{x_L})_i (\mathbf{x}' - \mathbf{x_L})_j d\mathbf{x}' - \frac{1}{m(L)} \int_L (\mathbf{x}' - \mathbf{x_L})_i (\mathbf{x_K} - \mathbf{x_L})_j d\mathbf{x}' \\
&\qquad - \frac{1}{m(L)} \int_L (\mathbf{x_K} - \mathbf{x_L})_i (\mathbf{x}' - \mathbf{x_L})_j d\mathbf{x}' + \frac{1}{m(L)} \int_L (\mathbf{x_K} - \mathbf{x_L})_i (\mathbf{x_K} - \mathbf{x_L})_j d\mathbf{x}' - \mathbb{I}_K^{ij} \Big] \\
&= \frac{1}{2} \Big[(\mathbf{x_K} - \mathbf{x_L})_i (\mathbf{x_K} - \mathbf{x_L})_j + \mathbb{I}_L^{ij} - \mathbb{I}_K^{ij} \Big] = \xi_{K,L}^{ij}.
\end{aligned}$$

Averaging the equation (2.106) over L with respect to $\mathbf{x}'$ and using the definitions of ϕ (2.94), A^i and B^{ij} and the relations that these last two satisfy, we get the disired result.

With the Lemma 9, the upper bound of $E^{\star}_{div}(u,v;t^n)$ given by the Lemma 8 can be rewrite as follows:

Lemma 10

$$E^{\star}_{div}(u,v;t^n) \leq TE_{visc}(u,v;t^N) + TE_{h.o.t}(u,v;t^N),$$

where

$$\begin{aligned}
TE_{visc}(u,v;t^N) &= \sum_{n=0}^{N-1}\sum_{K\in\mathcal{T}}\int_0^{t^N}\int_{\mathbb{R}^2} VISC^n_K(v(\mathbf{x},t);\mathbf{x},t))d\mathbf{x}dt\Delta t \\
&- \sum_{n=0}^{N-1}\sum_{K\in\mathcal{T}}\int_{\mathbb{R}^2} F(u^n_K, v(\mathbf{x},t^N))\cdot\frac{\Delta t}{2}\nabla_{\mathbf{x}}\phi(\mathbf{x},t^N,\mathbf{x}_K,t^{n+1})d\mathbf{x}m(K)\Delta t \\
&+ \sum_{n=0}^{N-1}\sum_{K\in\mathcal{T}}\int_{\mathbb{R}^2} F(u^n_K, v(\mathbf{x},t^0))\cdot\frac{\Delta t}{2}\nabla_{\mathbf{x}}\phi(\mathbf{x},0,\mathbf{x}_K,t^{n+1})d\mathbf{x}m(K)\Delta t, \\
TE_{h.o.t}(u,v;t^N) &= \sum_{n=0}^{N-1}\sum_{K\in\mathcal{T}}\int_0^{t^N}\int_{\mathbb{R}^2} HOT^n_K(v(\mathbf{x},t);\mathbf{x},t))d\mathbf{x}dt\Delta t \\
&+ \sum_{n=0}^{N-1}\sum_{K\in\mathcal{T}}\int_{\mathbb{R}^2} F(u^n_K, v(\mathbf{x},t^N))\cdot\frac{\Delta t}{2}\nabla_{\mathbf{x}}\phi(\mathbf{x},t^N,\mathbf{x}_K,t^{n+1})d\mathbf{x}m(K)\Delta t \\
&- \sum_{n=0}^{N-1}\sum_{K\in\mathcal{T}}\int_{\mathbb{R}^2} F(u^n_K, v(\mathbf{x},t^0))\cdot\frac{\Delta t}{2}\nabla_{\mathbf{x}}\phi(\mathbf{x},0,\mathbf{x}_K,t^{n+1})d\mathbf{x}m(K)\Delta t.
\end{aligned}$$

The "viscosity" term $VISC^n_K(c;\mathbf{x},t)$ is given by

$$VISC^n_K(c;\mathbf{x},t) = \overset{time}{VISC}{}^n_K(c;\mathbf{x},t) + \overset{cent}{VISC}{}^n_K(c;\mathbf{x},t) + \overset{visc}{VISC}{}^n_K(c;\mathbf{x},t),$$

where

$$\begin{aligned}
\overset{time}{VISC}{}^n_K(c;\mathbf{x},t) &= F(u^n_K,c)\cdot\frac{\Delta t}{2}\nabla_{\mathbf{x}}\phi_t(\mathbf{x},t,\mathbf{x}_K,t^{n+1}), \\
\overset{cent}{VISC}{}^n_K(c;\mathbf{x},t) &= F(u^n_K,c)\cdot\sum_{L\in N(K)} m(K|L)b_{L,K}\overline{H}_{K,L}(\mathbf{x},t,\mathbf{x}_K,t^{n+1})n_{KL}, \\
\overset{visc}{VISC}{}^n_K(c;\mathbf{x},t) &= \sum_{L\in N(K)} m(K|L)\alpha_{K|L}\overline{H}_{K,L}(\mathbf{x},t,\mathbf{x}_K,t^{n+1})\mathcal{N}_{K|L}(u^n_K,c),
\end{aligned}$$

and the "high-order" term $HOT^n_K(c;\mathbf{x},t))$ is given by

$$HOT^n_K(c;\mathbf{x},t) = \overset{time}{HOT}{}^n_K(c;\mathbf{x},t) + \overset{cent}{HOT}{}^n_K(c;\mathbf{x},t) + \overset{visc}{HOT}{}^n_K(c;\mathbf{x},t),$$

where

$$\begin{aligned}
\overset{time}{HOT}{}^n_K(c;\mathbf{x},t) &= F(u^n_K,c)\cdot\Big[m(K)\nabla_{\mathbf{x}}\overline{\phi}(\mathbf{x},t,\mathbf{x}_K,t^{n+1}) - m(K)\nabla_{\mathbf{x}}\phi(\mathbf{x},t,\mathbf{x}_K,t^{n+1}) \\
&\qquad - \frac{\Delta t}{2}m(K)\nabla_{\mathbf{x}}\phi_t(\mathbf{x},t,\mathbf{x}_K,t^{n+1})\Big], \\
\overset{cent}{HOT}{}^n_K(c;\mathbf{x},t) &= F(u^n_K,c)\cdot\sum_{L\in N(K)} m(K|L)b_{L,K}\overline{\overline{H}}_{K,L}(\mathbf{x},t,t^{n+1})n_{KL}, \\
\overset{visc}{HOT}{}^n_K(c;\mathbf{x},t) &= \sum_{L\in N(K)} m(K|L)\alpha_{K|L}\overline{\overline{H}}_{K,L}(\mathbf{x},t,t^{n+1})\mathcal{N}_{K|L}(u^n_K,c).
\end{aligned}$$

Proof. Let $r \in \mathbb{R}^2$. The identity

$$m(K)r = \sum_{L \in N(K)} m(K|L)[r \cdot (\mathbf{x}_{K|L} - \mathbf{x}_K)]n_{KL}$$

is used in the proof. This identity can be proved as follows:

Since $\nabla_{\mathbf{x}'}[r \cdot (\mathbf{x}' - \mathbf{x}_K)] = r\mathbb{I}_2 = r$ then, the divergence theorem leads to:

$$\begin{aligned} m(K)r &= \int_K r d\mathbf{x}' = \int_K \nabla_{\mathbf{x}'}[r \cdot (\mathbf{x}' - \mathbf{x}_K)]d\mathbf{x}' \\ &= \sum_{L \in N(K)} \int_{K|L} [r \cdot (\mathbf{x}' - \mathbf{x}_K)]n_{KL} d\Gamma(\mathbf{x}') \\ &= \sum_{L \in N(K)} m(K|L)[r \cdot (\mathbf{x}_{K|L} - \mathbf{x}_K)]n_{KL}. \end{aligned}$$

Substituting Lemma 9 in Lemma 8 we get:

$$\begin{aligned} E^{\star}_{div}(u, v; t^n) \leq & \sum_{n=0}^{N-1} \sum_{K \in \mathcal{T}} \int_0^{t^N} \int_{\mathbb{R}^2} F(u_K^n, v(\mathbf{x}, t)) \cdot \nabla_{\mathbf{x}} \overline{\phi}(\mathbf{x}, t, \mathbf{x}_L, t^{n+1}) m(K) \Delta t d\mathbf{x} dt \\ & - \sum_{n=0}^{N-1} \sum_{K \in \mathcal{T}} \int_0^{t^N} \int_{\mathbb{R}^2} \sum_{L \in \partial K} m(K|L) b_{L,K} [-(\mathbf{x}_L - \mathbf{x}_K) \cdot \nabla_{\mathbf{x}} \phi(\mathbf{x}, \mathbf{x}_K) + \overline{H}_{K,L}(\mathbf{x}, \mathbf{x}_K) \\ & \qquad + \overline{\overline{H}}_{K,L}(\mathbf{x})] F(u_K^n, v(\mathbf{x}, t)) \cdot n_{K,L} \Delta t d\mathbf{x} dt \\ & + \sum_{n=0}^{N-1} \sum_{K \in \mathcal{T}} \int_0^{t^N} \int_{\mathbb{R}^2} \sum_{L \in \partial K} m(K|L) \alpha_{K|L} [-(\mathbf{x}_L - \mathbf{x}_K) \cdot \nabla_{\mathbf{x}} \phi(\mathbf{x}, \mathbf{x}_K) + \overline{H}_{K,L}(\mathbf{x}, \mathbf{x}_K) \\ & \qquad + \overline{\overline{H}}_{K,L}(\mathbf{x})] \mathcal{N}_{K|L}(u_K^n, v(\mathbf{x}, t)) \Delta t d\mathbf{x} dt. \end{aligned}$$

Using the above identity with $r = \nabla_{\mathbf{x}} \phi(\mathbf{x}, t, \mathbf{x}_K, t^{n+1})$ and rearranging terms, we obtain

$$\begin{aligned} E^{\star}_{div}(u, v; t^n) \leq & \sum_{n=0}^{N-1} \sum_{K \in \mathcal{T}} \int_0^{t^N} \int_{\mathbb{R}^2} \Bigg[F(u_K^n, c) \cdot \frac{\Delta t}{2} \nabla_{\mathbf{x}} \phi_t(\mathbf{x}, t, \mathbf{x}_K, t^{n+1}) \\ & + F(u_K^n, c) \cdot \sum_{L \in N(K)} m(K|L) b_{L,K} \overline{H}_{K,L}(\mathbf{x}, t, \mathbf{x}_K, t^{n+1}) n_{KL} \\ & + \sum_{L \in N(K)} m(K|L) \alpha_{K|L} \overline{H}_{K,L}(\mathbf{x}, t, \mathbf{x}_K, t^{n+1}) \mathcal{N}_{K|L}(u_K^n, c) \Bigg] d\mathbf{x} dt \Delta t \\ & + \sum_{n=0}^{N-1} \sum_{K \in \mathcal{T}} \int_0^{t^N} \int_{\mathbb{R}^2} \Bigg[F(u_K^n, c) \cdot \sum_{L \in N(K)} m(K|L) (\nabla_{\mathbf{x}} \phi(\mathbf{x}, t, \mathbf{x}_K, t^{n+1}) \cdot \\ & \qquad ((\mathbf{x}_{K|L} - \mathbf{x}_K) - b_{L,K}(\mathbf{x}_L - \mathbf{x}_K))) n_{KL} \\ & - \sum_{L \in N(K)} m(K|L) \alpha_{K|L} (\mathbf{x}_L - \mathbf{x}_K) \cdot \nabla_{\mathbf{x}} \phi(\mathbf{x}, t, \mathbf{x}_K, t^{n+1}) \mathcal{N}_{K|L}(u_K^n, c) \Bigg] d\mathbf{x} dt \Delta t \\ & + \sum_{n=0}^{N-1} \sum_{K \in \mathcal{T}} \int_0^{t^N} \int_{\mathbb{R}^2} \Bigg[F(u_K^n, c) \cdot \Bigg(m(K) \nabla_{\mathbf{x}} \overline{\phi}(\mathbf{x}, t, \mathbf{x}_K, t^{n+1}) - m(K) \nabla_{\mathbf{x}} \phi(\mathbf{x}, t, \mathbf{x}_K, t^{n+1}) \\ & \qquad - \frac{\Delta t}{2} m(K) \nabla_{\mathbf{x}} \phi_t(\mathbf{x}, t, \mathbf{x}_K, t^{n+1}) \Bigg) \\ & + F(u_K^n, c) \cdot \sum_{L \in N(K)} m(K|L) b_{L,K} \overline{\overline{H}}_{K,L}(\mathbf{x}, t, t^{n+1}) n_{KL} \\ & + \sum_{L \in N(K)} m(K|L) \alpha_{K|L} \overline{\overline{H}}_{K,L}(\mathbf{x}, t, t^{n+1}) \mathcal{N}_{K|L}(u_K^n, c) \Bigg] d\mathbf{x} dt \Delta t. \end{aligned}$$

Finally, the proof is concluded, adding and subtracting the terms

$$\sum_{n=0}^{N-1}\sum_{K\in\tau}\int_{\mathbb{R}^2} F(u_K^n, v(\mathbf{x},t^N))\cdot\frac{\Delta t}{2}\nabla_{\mathbf{x}}\phi(\mathbf{x},t^N,\mathbf{x}_K,t^{n+1})d\mathbf{x}m(K)\Delta t$$

and

$$\sum_{n=0}^{N-1}\sum_{K\in\tau}\int_{\mathbb{R}^2} F(u_K^n, v(\mathbf{x},t^0))\cdot\frac{\Delta t}{2}\nabla_{\mathbf{x}}\phi(\mathbf{x},0,\mathbf{x}_K,t^{n+1})d\mathbf{x}m(K)\Delta t,$$

in the last inequality.

Second step: Estimating $TE_{visc}(u,v;t^N)$.

Lemma 11

$$TE_{visc}(u,v;t^N)\leq 4C_0\frac{|\eta|_{TV(\mathbb{R})}}{\epsilon_{\mathbf{x}}}\left(1+\frac{\Delta t}{\epsilon_t}\right)\|\nu_v\|\,h,$$

where $C_0 = t^N|v_0|_{TV(\mathbb{R}^2)}W(t^N)$.

Proof. We have, by the definition of $TE_{visc}(u,v;t^N)$ in Lemma 9,

$$TE_{visc}(u,v;t^N)=\sum_{n=0}^{N-1}\sum_{K\in\mathcal{T}}\Xi(\mathbf{x}_K,t^{n+1})m(K)\Delta t$$

where

$$\begin{aligned}\Xi(\mathbf{x}_K,t^{n+1}) = \int_0^{t^N}\int_{\mathbb{R}^2}\Bigg[&F(u_K^n,v(\mathbf{x},t))\cdot\frac{\Delta t}{2}\nabla_{\mathbf{x}}\phi_t(\mathbf{x},t,\mathbf{x}_K,t^{n+1})\\ &+F(u_K^n,v(\mathbf{x},t))\cdot\frac{1}{m(K)}\sum_{L\in N(K)}m(K|L)b_{L,K}\overline{H}_{K,L}(\mathbf{x},t,\mathbf{x}_K,t^{n+1})n_{KL}\\ &+\frac{1}{m(K)}\sum_{L\in N(K)}m(K|L)\alpha_{K|L}\overline{H}_{K,L}(\mathbf{x},t,\mathbf{x}_K,t^{n+1})\mathcal{N}_{K|L}(u_K^n,v(\mathbf{x},t))\Bigg]d\mathbf{x}dt\\ &-\int_{\mathbb{R}^2}F(u_K^n,v(\mathbf{x},t^N))\cdot\frac{\Delta t}{2}\nabla_{\mathbf{x}}\phi(\mathbf{x},t^N,\mathbf{x}_K,t^{n+1})d\mathbf{x}\\ &+\int_{\mathbb{R}^2}F(u_K^n,v(\mathbf{x},t^0))\cdot\frac{\Delta t}{2}\nabla_{\mathbf{x}}\phi(\mathbf{x},0,\mathbf{x}_K,t^{n+1})d\mathbf{x}.\end{aligned}$$

Integrating by parts, we get:

$$\begin{aligned}\int_0^{t^N}F(u_K^n,v(\mathbf{x},t))\cdot\frac{\Delta t}{2}\nabla_{\mathbf{x}}\phi_t(\mathbf{x},t,\mathbf{x}_K,t^{n+1})dt =&F(u_K^n,v(\mathbf{x},t^N))\cdot\frac{\Delta t}{2}\nabla_{\mathbf{x}}\phi(\mathbf{x},t^N,\mathbf{x}_K,t^{n+1})\\ &-F(u_K^n,v(\mathbf{x},t^0))\cdot\frac{\Delta t}{2}\nabla_{\mathbf{x}}\phi(\mathbf{x},0,\mathbf{x}_K,t^{n+1})\\ &-\int_0^{t^N}F_t(u_K^n,v(\mathbf{x},t))\cdot\frac{\Delta t}{2}\nabla_{\mathbf{x}}\phi(\mathbf{x},t,\mathbf{x}_K,t^{n+1})dt\end{aligned}$$

Taking into account that $\phi\in C_c^\infty((\mathbb{R}^2\times\mathbb{R}^+)^2)$ and integrating again by parts, we obtain:

$$\begin{aligned}&\int_{\mathbb{R}^2}F(u_K^n,v(\mathbf{x},t))\cdot\frac{1}{m(K)}\sum_{L\in N(K)}m(K|L)b_{L,K}\overline{H}_{K,L}(\mathbf{x},t,\mathbf{x}_K,t^{n+1})n_{KL}d\mathbf{x}\\ &\quad=\int_{\mathbb{R}^2}\frac{1}{m(K)}\sum_{L\in N(K)}m(K|L)b_{L,K}\sum_{i,j=1}^{2}(F(u_K^n,v(\mathbf{x},t))\cdot n_{KL})\xi_{K,L}^{ij}\partial^2_{x_i,x_j}\phi(\mathbf{x},t,\mathbf{x}_K,t^{n+1})d\mathbf{x}\\ &\quad=-\int_{\mathbb{R}^2}\frac{1}{m(K)}\sum_{L\in N(K)}m(K|L)b_{L,K}\sum_{i,j=1}^{2}(\partial_{x_i}F(u_K^n,v(\mathbf{x},t))\cdot n_{KL})\xi_{K,L}^{ij}\partial_{x_j}\phi(\mathbf{x},t,\mathbf{x}_K,t^{n+1})d\mathbf{x}\end{aligned}$$

and

$$\int_{\mathbb{R}^2} \frac{1}{m(K)} \sum_{L\in N(K)} m(K|L)\alpha_{K|L}\overline{H}_{K,L}(\mathbf{x},t,\mathbf{x}_K,t^{n+1})\mathcal{N}_{K|L}(u_K^n,v(\mathbf{x},t))d\mathbf{x}$$
$$= -\int_{\mathbb{R}^2} \frac{1}{m(K)} \sum_{L\in N(K)} m(K|L)\alpha_{K|L} \sum_{i,j=1}^{2} \partial_{x_i}\mathcal{N}_{K|L}(u_K^n,v(\mathbf{x},t))\xi_{K,L}^{ij}\partial_{x_j}\phi(\mathbf{x},t,\mathbf{x}_K,t^{n+1})d\mathbf{x}.$$

Then,

$$\begin{aligned}\Xi(\mathbf{x}_K,t^{n+1}) = -\int_0^{t^N}\int_{\mathbb{R}^2}\Bigg(&F_t(u_K^n,v(\mathbf{x},t))\cdot\frac{\Delta t}{2}\nabla_{\mathbf{x}}\phi(\mathbf{x},t,\mathbf{x}_K,t^{n+1})\\ &+\frac{1}{m(K)}\sum_{L\in N(K)} m(K|L)b_{L,K}\sum_{i,j=1}^{2}\partial_{x_i}(F(u_K^n,v(\mathbf{x},t))\cdot n_{KL})\xi_{K,L}^{ij}\partial_{x_j}\phi(\mathbf{x},t,\mathbf{x}_K,t^{n+1})\\ &+\frac{1}{m(K)}\sum_{L\in N(K)} m(K|L)\alpha_{K|L}\sum_{i,j=1}^{2}\partial_{x_i}\mathcal{N}_{K|L}(u_K^n,v(\mathbf{x},t))\xi_{K,L}^{ij}\partial_{x_j}\phi(\mathbf{x},t,\mathbf{x}_K,t^{n+1})\Bigg)d\mathbf{x}dt\end{aligned}$$

Now, from the definition of F and $\mathcal{N}$ and the fact that $v_t + f(v)_{\mathbf{x}} = 0$, we have:

$$\partial_{x_i}F(u_K^n,v) = ((f(u_K^n)-f(v))\text{sign}(u_K^n-v))_{x_i} = -U'(u_K^n-v)f'(v)\partial_{x_i}v, \tag{2.107}$$

$$\begin{aligned}F_t(u_K^n,v) &= ((f(u_K^n)-f(v))\text{sign}(u_K^n-v))_t = -f'(v)v_t\text{sign}(u_K^n-v)\\ &= -U'(u_K^n-v)f'(v)(-f'(v)\cdot\nabla_{\mathbf{x}}v)\\ &= U'(u_K^n-v)f'(v)\sum_{i=1}^{2}f_i'(v)\partial_{x_i}v,\end{aligned} \tag{2.108}$$

$$\begin{aligned}&F_t(u_K^n,v(\mathbf{x},t))\cdot\frac{\Delta t}{2}\nabla_{\mathbf{x}}\phi(\mathbf{x},t,\mathbf{x}_K,t^{n+1})\\ &\qquad=\sum_{j=1}^{2}\left(U'(u_K^n-v)f'(v)\sum_{i=1}^{2}f_i'(v)\partial_{x_i}v\right)_j\left(\frac{\Delta t}{2}\partial_{x_j}\phi(\mathbf{x},t,\mathbf{x}_K,t^{n+1})\right)\\ &\qquad=\sum_{i,j=1}^{2}U'(u_K^n-v)\frac{\Delta t}{2}f_i'(v)f_j'(v)\partial_{x_i}v\,\partial_{x_j}\phi(\mathbf{x},t,\mathbf{x}_K,t^{n+1}),\end{aligned}$$

and

$$\partial_{x_i}\mathcal{N}(u_K^n,v) = ((N_{K|L}(u_K^n)-N_{K|L}(v))\text{sign}(u_K^n-v))_{x_i} = -U'(u_K^n-v)N_{K|L}'(v)\partial_{x_i}v.$$

So,

$$\begin{aligned}\Xi(\mathbf{x}_K,t^{n+1}) = -\int_0^{t^N}\int_{\mathbb{R}^2}\Bigg(&\sum_{i,j=1}^{2}U'(u_K^n-v)\frac{\Delta t}{2}f_i'(v)f_j'(v)\partial_{x_i}v\,\partial_{x_j}\phi(\mathbf{x},t,\mathbf{x}_K,t^{n+1})\\ &+\frac{1}{m(K)}\sum_{L\in N(K)}m(K|L)b_{L,K}\sum_{i,j=1}^{2}-U'(u_K^n-v)(f'(v)\cdot n_{KL})\partial_{x_i}v\,\xi_{K,L}^{ij}\partial_{x_j}\phi(\mathbf{x},t,\mathbf{x}_K,t^{n+1})\\ &+\frac{1}{m(K)}\sum_{L\in N(K)}m(K|L)\alpha_{K|L}\sum_{i,j=1}^{2}-U'(u_K^n-v)N_{K|L}'(v)\partial_{x_i}v\xi_{K,L}^{ij}\,\partial_{x_j}\phi(\mathbf{x},t,\mathbf{x}_K,t^{n+1})\Bigg)d\mathbf{x}dt.\end{aligned}$$

By making some algebraic manipulations, we get:

$$\Xi(\mathbf{x}_K,t^{n+1}) = -\sum_{i,j=1}^{2}\int_0^{t^N}\int_{\mathbb{R}^2}U'(u_K^n-v)\,\partial_{x_i}v\,\nu_K^{ij}(v(\mathbf{x},t))\,\partial_{x_j}\phi(\mathbf{x},t,\mathbf{x}_K,t^{n+1})d\mathbf{x}dt,$$

where the entries of the matrix ν are

$$\nu_K^{ij}(c) = \frac{\Delta t}{2} f_i'(c) f_j'(c) - \frac{1}{m(K)} \sum_{L \in N(K)} m(K|L)[b_{L,K} f'(c) \cdot n_{KL} + \alpha_{K|L} N'_{K|L}(c)] \xi_{K,L}^{ij}.$$

The following result is needed to complete the proof.

Lemma 12 *Let*

$$T_{aux} = \sup_{\substack{t \in (0,t^N) \\ x \in \mathbb{R}^2}} \left\{ \sum_{n=0}^{N-1} \sum_{K \in \mathcal{T}} \max_{1 \le i \le 2} \sum_{j=1}^{2} \nu_K^{ij}(v(\mathbf{x},t))\, \partial_{x_j} \phi(\mathbf{x}, t, \mathbf{x}_K, t^{n+1}) m(K) \Delta t \right\}$$

then,

$$T_{aux} \le 4 \frac{|\eta|_{TV(\mathbb{R})}}{\epsilon_{\mathbf{x}}} \left(1 + \frac{\Delta t}{\epsilon_t}\right) W(t^N) \, \|\nu_v\| \, h.$$

The proof of Lemma 12 requires the following result.

Lemma 13

$$\sup_{t \in (0,t^N)} \left\{ \sum_{n=0}^{N-1} w_{\epsilon_t}(t - t^{n+1}) \Delta t \right\} \le 2 \left(1 + \frac{\Delta t}{\epsilon_t}\right) W(t^N).$$

Proof. Integrating by parts, we have

$$\begin{aligned} \sum_{n=0}^{N-1} \int_{t^n}^{t^{n+1}} (s - t^n) w'_{\epsilon_t}(t-s) ds &= -\sum_{n=0}^{N-1} w_{\epsilon_t}(t - t^{n+1})\, \Delta t + \sum_{n=0}^{N-1} \int_{t^n}^{t^{n+1}} w_{\epsilon_t}(t-s) ds \\ &= -\sum_{n=0}^{N-1} w_{\epsilon_t}(t - t^{n+1})\, \Delta t + \int_0^{t^N} w_{\epsilon_t}(t-s) ds. \end{aligned}$$

Therefore,

$$\begin{aligned} \sum_{n=0}^{N-1} w_{\epsilon_t}(t - t^{n+1}) \Delta t &= \int_0^{t^N} w_{\epsilon_t}(t-s) ds - \sum_{n=0}^{N-1} \int_{t^n}^{t^{n+1}} (s - t^n) w'_{\epsilon_t}(t-s) ds \\ &\le \left| \int_0^{t^N} w_{\epsilon_t}(t-s) ds - \sum_{n=0}^{N-1} \int_{t^n}^{t^{n+1}} (s - t^n) w'_{\epsilon_t}(t-s) ds \right| \\ &\le \int_0^{t^N} w_{\epsilon_t}(t-s) ds + \sum_{n=0}^{N-1} \int_{t^n}^{t^{n+1}} |s - t^n| |w'_{\epsilon_t}(t-s)| ds \\ &\le \int_0^{t^N} w_{\epsilon_t}(t-s) ds + \Delta t \sum_{n=0}^{N-1} \int_{t^n}^{t^{n+1}} |w'_{\epsilon_t}(t-s)| ds. \end{aligned}$$

Now, since $w_{\epsilon_t}(-r) = w_{\epsilon_t}(r)$ and $t \le t^N$,

$$\begin{aligned} \int_0^{t^N} w_{\epsilon_t}(t-s) ds &= \int_{-t}^{t^N - t} w_{\epsilon_t}(t') dt' \\ &\le \int_{-t^N}^{t^N} w_{\epsilon_t}(t') dt' \\ &= 2 \int_0^{t^N} w_{\epsilon_t}(t') dt = 2 W(t^N). \end{aligned}$$

On the other hand,

$$\begin{aligned}\sum_{n=0}^{N-1}\int_{t^n}^{t^{n+1}}|w'_{\epsilon_t}(t-s)|ds &= \int_0^{t^N}|w'_{\epsilon_t}(t-s)|ds = \int_{-t}^{t^N-t}|w'_{\epsilon_t}(r)|dr\\ &= \frac{1}{\epsilon_t^2}\int_{-t}^{t^N-t}\left|w'\left(\frac{r}{\epsilon_t}\right)\right|dr = \frac{1}{\epsilon_t}\int_{-\frac{t}{\epsilon_t}}^{\frac{t^N-t}{\epsilon_t}}|w'(t')|\,dt'\\ &\leq \frac{1}{\epsilon_t}\int_{\mathbb{R}}|w'(t')|\,dt' = \frac{|w|_{TV(\mathbb{R})}}{\epsilon_t}\end{aligned}$$

Thus,

$$\sum_{n=0}^{N-1}w_{\epsilon_t}(t-t^{n+1})\Delta t \leq \left[2+\frac{\Delta t}{\epsilon_t}\left(\frac{|w|_{TV(\mathbb{R})}}{W(t^N)}\right)\right]W(t^N)$$

By taking a sequence of functions, $\{w\}$, satisfying (2.97), being nonincreasing on $(0,1)$ and that converges pointwisely to

$$\chi(s) = \begin{cases}\frac{1}{2}, & |s|<1\\ 0 & \text{otherwise}\end{cases}$$

and denoting this limit process by "$w\to\chi$", we have that

$$\begin{aligned}\lim_{w\to\chi}W(t^N) &= \lim_{w\to\chi}\int_0^{t^N}w_{\epsilon_t}(t')dt'\\ &= \int_0^{t^N}\lim_{w\to\chi}w_{\epsilon_t}(t')dt'\\ &= \int_0^{t^N}\chi_{\epsilon_t}(t')dt' = \frac{1}{2},\end{aligned}$$

and

$$\begin{aligned}\lim_{w\to\chi}|w|_{TV(\mathbb{R})} &= \lim_{w\to\chi}\mathrm{Sup}\sum_{k=1}^{N}|w(x_k)-w(x_{k-1})|\\ &= \mathrm{Sup}\sum_{k=1}^{N}\left|\lim_{w\to\chi}(w(x_k)-w(x_{k-1}))\right|\\ &= \mathrm{Sup}\sum_{k=1}^{N}|\chi(x_k)-\chi(x_{k-1})|\\ &= |\chi|_{TV(\mathbb{R})} = 1.\end{aligned}$$

Remark 13 *The supremum of above limit is taken over all subdivisions of the real line.*

Then,

$$\lim_{w\to\chi}\frac{|w|_{TV(\mathbb{R})}}{W(t^N)} = 2,$$

and with this, the proof is concluded.

Proof of the Lemma 12. Using the definitions of ϕ, φ and $\|\nu_v\|$ and the Lemma 13, we obtain

$$\begin{aligned}&\sum_{n=0}^{N-1}\sum_{K\in\tau}\max_{1\leq i\leq 2}\sum_{j=1}^{2}\nu_K^{ij}(v(\mathbf{x},t))\,\partial_{x_j}\phi(\mathbf{x},t,\mathbf{x}_K,t^{n+1})m(K)\Delta t\\ &\qquad=\sum_{n=0}^{N-1}\sum_{K\in\mathcal{T}}\max_{1\leq i\leq 2}\sum_{j=1}^{2}\frac{\nu_K^{ij}(v(\mathbf{x},t))}{h}\,\partial_{x_j}\left(\frac{1}{m(K)}\int_K\varphi(\mathbf{x},t,\mathbf{x}',t^{n+1})d\mathbf{x}'\right)m(K)\Delta t\,h\end{aligned}$$

$$
\begin{aligned}
&\leq \sum_{n=0}^{N-1}\sum_{K\in\mathcal{T}}\max_{1\leq i\leq 2}\sum_{j=1}^{2}\int_K \varphi_{x_j}(\mathbf{x},t,\mathbf{x}',t^{n+1})d\mathbf{x}'\Delta t\ \|\nu_v\|\ h\\
&= \sum_{n=0}^{N-1}\sum_{K\in\mathcal{T}}\max_{1\leq i\leq 2}\sum_{j=1}^{2}\int_K (-\varphi_{x'_j}(\mathbf{x},t,\mathbf{x}',t^{n+1}))d\mathbf{x}'\Delta t\ \|\nu_v\|\ h\\
&= \sum_{n=0}^{N-1}\sum_{K\in\mathcal{T}}\max_{1\leq i\leq 2}\sum_{j=1}^{2}\int_{K=K_1\times K_2}(-w_{\epsilon_t}(t-t^{n+1})\Big(\prod_{\substack{i=1\\ i\neq j}}^{2}\eta_{\epsilon_{\mathbf{x}}}(x_i-x'_i)\Big)\\
&\qquad\qquad (-\eta'_{\epsilon_{\mathbf{x}}}(x_i-x'_j))d\mathbf{x}'\Delta t\ \|\nu_v\|\ h\\
&= \Big(\sum_{n=0}^{N-1} w_{\epsilon_t}(t-t^{n+1})\Delta t\Big)\Big(\max_{1\leq i\leq 2}\prod_{\substack{i=1\\ i\neq j}}^{2}\prod_{\substack{l=1\\ l\neq j}}^{2}\sum_{l=1}^{2}\int_{K_l}\eta_{\epsilon_{\mathbf{x}}}(x_i-x'_l)dx'_l\Big)\\
&\qquad\qquad \Big(\sum_{j=1}^{2}\int_{K_j}\eta'_{\epsilon_{\mathbf{x}}}(x_i-x'_j)dx'_j\Big)\ \|\nu_v\|\ h\\
&\leq 2\Big(1+\frac{\Delta t}{\epsilon_t}\Big)W(t^N)\Big(\max_{1\leq i\leq 2}\prod_{\substack{i=1\\ i\neq j}}^{2}\prod_{\substack{l=1\\ l\neq j}}^{2}\sum_{l=1}^{2}\int_{K_l}\eta_{\epsilon_{\mathbf{x}}}(x_i-x'_l)dx'_l\Big)\\
&\qquad\qquad \Big(\sum_{j=1}^{2}\int_{K_j}\eta'_{\epsilon_{\mathbf{x}}}(x_i-x'_j)dx'_j\Big)\ \|\nu_v\|\ h.
\end{aligned}
$$

Thus, since $\eta_{\epsilon_{\mathbf{x}}}(\mathbf{x})=0$ if $\|\mathbf{x}\|>\epsilon_{\mathbf{x}}$, we have

$$
\begin{aligned}
\sum_{l=1}^{2}\int_{K_l}\eta_{\epsilon_{\mathbf{x}}}(x_i-x'_l)dx'_l &= \int_{\mathbb{R}}\eta_{\epsilon_{\mathbf{x}}}(x_i-x'_l)dx'_l\\
&= \int_{x_i-\epsilon_{\mathbf{x}}}^{x_i+\epsilon_{\mathbf{x}}}\eta_{\epsilon_{\mathbf{x}}}(x_i-x'_l)dx'_l\\
&= \int_{-\epsilon_{\mathbf{x}}}^{\epsilon_{\mathbf{x}}}\eta_{\epsilon_{\mathbf{x}}}(r)dr=1,
\end{aligned}
$$

and, taking into account the definition of $\eta_{\epsilon_{\mathbf{x}}}$, we also have

$$
\begin{aligned}
\sum_{j=1}^{2}\int_{K_j}\eta'_{\epsilon_{\mathbf{x}}}(x_i-x'_j)dx'_j &\leq \sum_{j=1}^{2}\int_{K_j}\left|\eta'_{\epsilon_{\mathbf{x}}}(x_i-x'_j)\right|dx'_j\\
&= \sum_{j=1}^{2}\int_{K_j}\frac{1}{\epsilon_{\mathbf{x}}^2}\left|\eta'_{\epsilon_{\mathbf{x}}}\Big(\frac{x_i-x'_j}{\epsilon_{\mathbf{x}}}\Big)\right|dx'_j\\
&\leq \sum_{j=1}^{2}\int_{\mathbb{R}}\frac{1}{\epsilon_{\mathbf{x}}}\left|\eta'_{\epsilon_{\mathbf{x}}}(r)\right|dr=\frac{2|\eta|_{TV(\mathbb{R})}}{\epsilon_{\mathbf{x}}}.
\end{aligned}
$$

In consequence,

$$
\sum_{n=0}^{N-1}\sum_{K\in\mathcal{T}}\max_{1\leq i\leq 2}\sum_{j=1}^{2}\nu_K^{ij}(v(\mathbf{x},t))\,\partial_{x_j}\phi(\mathbf{x},t,\mathbf{x}_K,t^{n+1})m(K)\Delta t\leq 4\frac{|\eta|_{TV(\mathbb{R})}}{\epsilon_{\mathbf{x}}}\Big(1+\frac{\Delta t}{\epsilon_t}\Big)W(t^N)\,\|\nu_v\|\,h,
$$

and with this, the proof is concluded.

From Lemma 12, we have now

$$TE_{visc}(u,v;t^N) \le \sum_{n=0}^{N-1}\sum_{K\in\mathcal{T}}\sum_{i,j=1}^{2}\int_0^{t^N}\int_{\mathbb{R}^2} |U'(u_K^n - v)|\,|\partial_{x_i} v|\,\nu_K^{ij}(v(\mathbf{x},t))\,\partial_{x_j}\phi(\mathbf{x},t,\mathbf{x}_K,t^{n+1}) \\ m(K)\Delta t d\mathbf{x} dt$$

$$\le T_{aux}\int_0^{t^N}\int_{\mathbb{R}^2}\max_{1\le i\le 2}|\partial_{x_i} v|\,d\mathbf{x}dt \le T_{aux}t^N\int_{\mathbb{R}^2}\|\nabla_{\mathbf{x}} v\|_1\,d\mathbf{x}$$

$$= T_{aux}t^N|v|_{TV(\mathbb{R}^2)} \le T_{aux}|v_0|_{TV(\mathbb{R}^2)}t^N$$
$$\le 4t^N|v_0|_{TV(\mathbb{R}^2)}W(t^N)\frac{|\eta|_{TV(\mathbb{R})}}{\epsilon_{\mathbf{x}}}\left(1+\frac{\Delta t}{\epsilon_t}\right)\|\nu_v\|\,h$$

This completes the poof.

Third step. Esimating $TE_{h.o.t}(u,v;t^N)$.

Lemma 14 *Let $\mathbb{D}_h$ and l_h be the quantities defined in (2.91) and (2.92) respectively. Let $\epsilon_{\mathbf{x}}$ and ϵ_t be the parameters used in (2.96). Let $W(t)$ be the function defined in (2.98) and let η be the function satisfying conditions (2.97). Asume that the conditions (2.26) and (2.90) are satisfied. Then,*

$$TE_{h.o.t}(u,v;t^N) \le C_0\Bigg[\|f'(v)\|\frac{(\Delta t)^2|\eta|_{TV(\mathbb{R})}}{\epsilon_t\epsilon_{\mathbf{x}}}t^N + 4\left(1+\frac{\Delta t}{\epsilon_t}\right)\Delta t \\ + 32\mathbb{D}_{\Delta\mathbf{x}}l_{\Delta\mathbf{x}}h^2\left(\frac{4|\eta|^2_{TV(\mathbb{R})}}{\epsilon_{\mathbf{x}}^2}+\frac{2|\eta'|_{TV(\mathbb{R})}}{\epsilon_{\mathbf{x}}^2}\right)\left(1+\frac{\Delta t}{\epsilon_t}\right)t^N\Bigg],$$

where $C_0 = W(t^N)\,\|f'(v)\|\,|v_0|_{TV(\mathbb{R}^2)}$.

To prove Lemma 14, we rewrite $TE_{h.o.t}(u,v;t^N)$ as the sum $\overset{time}{TE}_{h.o.t}(u,v;t^N)+\overset{cent}{TE}_{h.o.t}(u,v;t^N)+\overset{visc}{TE}_{h.o.t}(u,v;t^N)$, with the obvious notation (see Lemma 10), and estimate each of the above three terms.

Lemma 15

$$\overset{time}{TE}_{h.o.t}(u,v;t^N) \le C_0\Bigg[\|f'(v)\|\frac{(\Delta t)^2|\eta|_{TV(\mathbb{R})}}{\epsilon_t\epsilon_{\mathbf{x}}}t^N + 4\left(1+\frac{\Delta t}{\epsilon_t}\right)\Delta t\Bigg],$$

where $C_0 = W(t^N)\,\|f'(v)\|\,|v_0|_{TV(\mathbb{R}^2)}$.

Proof.

$$\overset{time}{TE}_{h.o.t}(u,v;t^N) = \sum_{n=0}^{N-1}\sum_{K\in\mathcal{T}}\int_0^{t^N}\int_{\mathbb{R}^2} F(u_K^n, v(\mathbf{x},t))\cdot\Big[m(K)\nabla_{\mathbf{x}}\overline{\phi}(\mathbf{x},t,\mathbf{x}_K,t^{n+1}) \\ - m(K)\nabla_{\mathbf{x}}\phi(\mathbf{x},t,\mathbf{x}_K,t^{n+1}) \\ - \frac{\Delta t}{2}m(K)\nabla_{\mathbf{x}}\phi_t(\mathbf{x},t,\mathbf{x}_K,t^{n+1})\Big]d\mathbf{x}dt\Delta t.$$

Taking into account the definition of ϕ and integrating by parts in time, we get:

$$\begin{aligned}
\overset{time}{TE}_{h.o.t}(u,v;t^N) &= \sum_{n=0}^{N-1}\sum_{K\in\mathcal{T}}\Bigg[\int_0^{t^N}\int_{\mathbb{R}^2}\Bigg(F(u_K^n,v(\mathbf{x},t))\cdot \\
&\qquad\qquad \int_K \nabla_{\mathbf{x}}(\overline{\varphi}(\mathbf{x},t,\mathbf{x}',t^{n+1})-\varphi(\mathbf{x},t,\mathbf{x}',t^{n+1}))d\mathbf{x}'\Bigg)d\mathbf{x}dt\Delta t \\
&\qquad + \frac{\Delta t}{2}\int_0^{t^N}\int_{\mathbb{R}^2} F_t(u_K^n,v(\mathbf{x},t))\cdot\left(\int_K \nabla_{\mathbf{x}}\varphi(\mathbf{x},t,\mathbf{x}',t^{n+1})d\mathbf{x}'\right)d\mathbf{x}dt\Delta t\Bigg] \\
&= \sum_{n=0}^{N-1}\int_0^{t^N}\int_{\mathbb{R}^2}\int_{\mathbb{R}^2}\Bigg[F(u(\mathbf{x}',t^n),v(\mathbf{x},t))\cdot\nabla_{\mathbf{x}}(\overline{\varphi}(\mathbf{x},t,\mathbf{x}',t^{n+1})-\varphi(\mathbf{x},t,\mathbf{x}',t^{n+1})) \\
&\qquad + \frac{\Delta t}{2}\int_0^{t^N}\int_{\mathbb{R}^2} F_t(u(\mathbf{x}',t^n),v(\mathbf{x},t))\cdot\nabla_{\mathbf{x}}\varphi(\mathbf{x},t,\mathbf{x}',t^{n+1}))\Bigg]d\mathbf{x}'d\mathbf{x}dt\Delta t \\
&= \sum_{n=0}^{N-1}\int_{\mathbb{R}^2}\Theta(\mathbf{x}',t^{n+1})d\mathbf{x}'\Delta t,
\end{aligned}$$

where

$$\begin{aligned}
\Theta(\mathbf{x}',t^{n+1}) &= \int_0^{t^N}\int_{\mathbb{R}^2} F(u(\mathbf{x}',t^n),v(\mathbf{x},t))\cdot\nabla_{\mathbf{x}}(\overline{\varphi}(\mathbf{x},t,\mathbf{x}',t^{n+1})-\varphi(\mathbf{x},t,\mathbf{x}',t^{n+1}))d\mathbf{x}dt \\
&\quad + \frac{\Delta t}{2}\int_0^{t^N}\int_{\mathbb{R}^2} F_t(u(\mathbf{x}',t^n),v(\mathbf{x},t))\cdot\nabla_{\mathbf{x}}\varphi(\mathbf{x},t,\mathbf{x}',t^{n+1}))d\mathbf{x}dt.
\end{aligned}$$

Remembering that $\varphi_t(t,t') = -\varphi_{t'}(t,t')$ and integrating by parts, we can note that,

$$\begin{aligned}
\frac{1}{\Delta t}\int_{t^n}^{t^{n+1}}(s-t^n)\varphi_t(t,s)ds &= \frac{1}{\Delta t}\int_{t^n}^{t^{n+1}}(s-t^n)(-\varphi_s(t,s))ds \\
&= -\frac{1}{\Delta t}\left[\Delta t\varphi(t,t^{n+1}) - \int_{t^n}^{t^{n+1}}\varphi(t,s)ds\right] \\
&= \frac{1}{\Delta t}\int_{t^n}^{t^{n+1}}\varphi(t,s)ds - \varphi(t,t^{n+1}) \\
&= \overline{\varphi}(t,t^{n+1}) - \varphi(t,t^{n+1}).
\end{aligned}$$

With this, one gets:

$$\begin{aligned}
\Theta(\mathbf{x}',t^{n+1}) &= \int_0^{t^N}\int_{\mathbb{R}^2} F(u(\mathbf{x}',t^n),v(\mathbf{x},t))\cdot\nabla_{\mathbf{x}}\left[\frac{1}{\Delta t}\int_{t^n}^{t^{n+1}}(s-t^n)\varphi_t(\mathbf{x},t,\mathbf{x}',s)ds\right]d\mathbf{x}dt \\
&\quad + \frac{\Delta t}{2}\int_0^{t^N}\int_{\mathbb{R}^2} F_t(u(\mathbf{x}',t^n),v(\mathbf{x},t))\cdot\nabla_{\mathbf{x}}\varphi(\mathbf{x},t,\mathbf{x}',t^{n+1}))d\mathbf{x}dt \\
&= -\int_0^{t^N}\int_{\mathbb{R}^2}\nabla_{\mathbf{x}}\cdot F(u(\mathbf{x}',t^n),v(\mathbf{x},t))\left[\frac{1}{\Delta t}\int_{t^n}^{t^{n+1}}(s-t^n)\varphi_t(\mathbf{x},t,\mathbf{x}',s)ds\right]d\mathbf{x}dt \\
&\quad + \frac{\Delta t}{2}\int_0^{t^N}\int_{\mathbb{R}^2} F_t(u(\mathbf{x}',t^n),v(\mathbf{x},t))\cdot\nabla_{\mathbf{x}}\varphi(\mathbf{x},t,\mathbf{x}',t^{n+1}))d\mathbf{x}dt \\
&= -\frac{1}{\Delta t}\int_{\mathbb{R}^2}\int_{t^n}^{t^{n+1}}\left[\int_0^{t^N}\nabla_{\mathbf{x}}\cdot F(u(\mathbf{x}',t^n),v(\mathbf{x},t))\varphi_t(\mathbf{x},t,\mathbf{x}',s)dt\right](s-t^n)dsd\mathbf{x} \\
&\quad + \frac{\Delta t}{2}\int_0^{t^N}\int_{\mathbb{R}^2} F_t(u(\mathbf{x}',t^n),v(\mathbf{x},t))\cdot\nabla_{\mathbf{x}}\varphi(\mathbf{x},t,\mathbf{x}',t^{n+1}))d\mathbf{x}dt
\end{aligned}$$

$$
\begin{aligned}
&= -\frac{1}{\Delta t}\int_{\mathbb{R}^2}\int_{t^n}^{t^{n+1}} \Big[\nabla_{\mathbf{x}}\cdot F(u(\mathbf{x}',t^n),v(\mathbf{x},t^N))\varphi(\mathbf{x},t^N,\mathbf{x}',s) \\
&\qquad\qquad - \nabla_{\mathbf{x}}\cdot F(u(\mathbf{x}',t^n),v(\mathbf{x},0))\varphi(\mathbf{x},0,\mathbf{x}',s)\Big](s-t^n)dsd\mathbf{x} \\
&+ \frac{1}{\Delta t}\int_{\mathbb{R}^2}\int_{t^n}^{t^{n+1}}\int_0^{t^N} (\nabla_{\mathbf{x}}\cdot F(u(\mathbf{x}',t^n),v(\mathbf{x},t)))_t\varphi(\mathbf{x},t,\mathbf{x}',s)(s-t^n)dtdsd\mathbf{x} \\
&+ \frac{\Delta t}{2}\int_0^{t^N}\int_{\mathbb{R}^2} F_t(u(\mathbf{x}',t^n),v(\mathbf{x},t))\cdot\nabla_{\mathbf{x}}\varphi(\mathbf{x},t,\mathbf{x}',t^{n+1})d\mathbf{x}dt.
\end{aligned}
$$

Now, since

$$
\int_{t^n}^{t^{n+1}}\frac{(s-t^n)^2}{2}\varphi_{t'}(\mathbf{x},t,\mathbf{x}',s)ds = \frac{\Delta t^2}{2}\varphi(\mathbf{x},t,\mathbf{x}',t^{n+1}) - \int_{t^n}^{t^{n+1}}(s-t^n)\varphi(\mathbf{x},t,\mathbf{x}',s)ds,
$$

$$
\begin{aligned}
&\frac{\Delta t}{2}\int_0^{t^N}\int_{\mathbb{R}^2} F_t(u(\mathbf{x}',t^n),v(\mathbf{x},t))\cdot\nabla_{\mathbf{x}}\varphi(\mathbf{x},t,\mathbf{x}',t^{n+1}))d\mathbf{x}dt \\
&\qquad = -\frac{\Delta t}{2}\int_0^{t^N}\int_{\mathbb{R}^2}\varphi(\mathbf{x},t,\mathbf{x}',t^{n+1})(\nabla_{\mathbf{x}}\cdot F(u(\mathbf{x}',t^n),v(\mathbf{x},t)))_t d\mathbf{x}dt \\
&\qquad = -\frac{\Delta t}{2}\int_0^{t^N}\int_{\mathbb{R}^2}\frac{2}{\Delta t^2}\Big(\int_{t^n}^{t^{n+1}}\Big[\frac{(s-t^n)^2}{2}\varphi_{t'}(\mathbf{x},t,\mathbf{x}',s) \\
&\qquad\qquad + \int_{t^n}^{t^{n+1}}(s-t^n)\varphi(\mathbf{x},t,\mathbf{x}',s)\Big]ds\Big)(\nabla_{\mathbf{x}}\cdot F(u(\mathbf{x}',t^n),v(\mathbf{x},t)))_t d\mathbf{x}dt \\
&\qquad = -\frac{1}{\Delta t}\int_0^{t^N}\int_{\mathbb{R}^2}\int_{t^n}^{t^{n+1}}\frac{(s-t^n)^2}{2}\varphi_{t'}(\mathbf{x},t,\mathbf{x}',s)(\nabla_{\mathbf{x}}\cdot F(u(\mathbf{x}',t^n),v(\mathbf{x},t)))_t dsd\mathbf{x}dt \\
&\qquad\quad - \frac{1}{\Delta t}\int_{\mathbb{R}^2}\int_{t^n}^{t^{n+1}}\int_0^{t^N}(\nabla_{\mathbf{x}}\cdot F(u(\mathbf{x}',t^n),v(\mathbf{x},t)))_t\varphi(\mathbf{x},t,\mathbf{x}',s)(s-t^n)dtdsd\mathbf{x} \\
&\qquad = \frac{1}{\Delta t}\int_0^{t^N}\int_{\mathbb{R}^2}\int_{t^n}^{t^{n+1}}\nabla_{\mathbf{x}}\Big(\frac{(s-t^n)^2}{2}\varphi_{t'}(\mathbf{x},t,\mathbf{x}',s)\Big)\cdot F_t(u(\mathbf{x}',t^n),v(\mathbf{x},t)dsd\mathbf{x}dt \\
&\qquad\quad - \frac{1}{\Delta t}\int_{\mathbb{R}^2}\int_{t^n}^{t^{n+1}}\int_0^{t^N}(\nabla_{\mathbf{x}}\cdot F(u(\mathbf{x}',t^n),v(\mathbf{x},t)))_t\varphi(\mathbf{x},t,\mathbf{x}',s)(s-t^n)dtdsd\mathbf{x}.
\end{aligned}
$$

So,

$$
\begin{aligned}
\Theta(\mathbf{x}',t^{n+1})\Delta t &= \int_0^{t^N}\int_{\mathbb{R}^2} F_t(u(\mathbf{x}',t^n),v(\mathbf{x},t)\cdot\nabla_{\mathbf{x}}\int_{t^n}^{t^{n+1}}\frac{(s-t^n)^2}{2}\varphi_{t'}(\mathbf{x},t,\mathbf{x}',s)dsd\mathbf{x}dt \\
&\quad - \int_{\mathbb{R}^2}\nabla_{\mathbf{x}}\cdot F(u(\mathbf{x}',t^n),v(\mathbf{x},t^N))\int_{t^n}^{t^{n+1}}(s-t^n)\varphi(\mathbf{x},t^N,\mathbf{x}',s)dsd\mathbf{x} \\
&\quad + \int_{\mathbb{R}^2}\nabla_{\mathbf{x}}\cdot F(u(\mathbf{x}',t^n),v_0(\mathbf{x}))\int_{t^n}^{t^{n+1}}(s-t^n)\varphi(\mathbf{x},0,\mathbf{x}',s)dsd\mathbf{x}.
\end{aligned}
$$

This allows us to rewrite $\overset{time}{TE}_{h.o.t}(u,v;t^N) = I - II + III$, with the obvious notation. Therefore, to obtain the result, we only need to estimate the terms I, II and III.

First, from (2.108) we have:

$$
|I| \le \sum_{n=0}^{N-1}\int_{\mathbb{R}^2}\int_0^{t^N}\int_{\mathbb{R}^2}|F_t(u(\mathbf{x}',t^n),v(\mathbf{x},t)|\int_{t^n}^{t^{n+1}}\frac{(s-t^n)^2}{2}|\varphi_{t'}(\mathbf{x},t,\mathbf{x}',s)|dsd\mathbf{x}dtd\mathbf{x}'
$$

$$
\begin{aligned}
&\leq \int_{\mathbb{R}^2}\int_0^{t^N}\int_{\mathbb{R}^2} \|f'(v)\|^2 |\nabla_{\mathbf{x}} v(\mathbf{x},t)| \left(\sum_{n=0}^{N-1}\int_{t^n}^{t^{n+1}} \frac{(s-t^n)^2}{2}|\varphi_{t'}(\mathbf{x},t,\mathbf{x}',s)|ds\right) d\mathbf{x}dtd\mathbf{x}' \\
&\leq \|f'(v)\|^2 \int_0^{t^N}\int_{\mathbb{R}^2} |\nabla_{\mathbf{x}} v(\mathbf{x},t)| \left(\frac{\Delta t^2}{2}\int_0^{t^N}\int_{\mathbb{R}^2} |\varphi_{t'}(\mathbf{x},t,\mathbf{x}',s)|d\mathbf{x}'ds\right) d\mathbf{x}dt \\
&\leq T_{aux} \|f'(v)\|^2 |v_0|_{TV(\mathbb{R}^2)},
\end{aligned}
$$

where

$$
\begin{aligned}
T_{aux} &= \frac{\Delta t^2}{2} \sup_{\substack{t\in(0,t^n)\\ \mathbf{x}\in\mathbb{R}^2}} \int_0^{t^N}\int_{\mathbb{R}^2} |\varphi_{t'}(\mathbf{x},t,\mathbf{x}',s)|d\mathbf{x}'ds \\
&\leq \frac{\Delta t^2}{2}\frac{2\,|\eta|_{TV(\mathbb{R})}}{\epsilon_{\mathbf{x}}\epsilon_{\mathbf{t}}} W(t^N).
\end{aligned}
$$

Next, we estimate the term II. From (2.107), we have:

$$
\begin{aligned}
|II| &\leq \sum_{n=0}^{N-1}\int_{(\mathbb{R}^2)^2} |\nabla_{\mathbf{x}}\cdot F(u(\mathbf{x}',t^n),v(\mathbf{x},t^N))| \int_{t^n}^{t^{n+1}} (s-t^n)|\varphi(\mathbf{x},t^N,\mathbf{x}',s)|ds d\mathbf{x}d\mathbf{x}' \\
&\leq \int_{(\mathbb{R}^2)^2} |f'(v)||\nabla_{\mathbf{x}} v(\mathbf{x},t^N)| \left[\sum_{n=0}^{N-1}\int_{t^n}^{t^{n+1}} (s-t^n)|\varphi(\mathbf{x},t^N,\mathbf{x}',s)|ds\right] d\mathbf{x}d\mathbf{x}'
\end{aligned}
$$

$$
\begin{aligned}
&\leq \Delta t \|f'(v)\| \int_0^{t^N}\int_{(\mathbb{R}^2)^2} |\nabla_{\mathbf{x}} v(\mathbf{x},t^N)| \sup_{\mathbf{x}\in\mathbb{R}^2}|\varphi(\mathbf{x},t^N,\mathbf{x}',s)|d\mathbf{x}d\mathbf{x}'ds \\
&\leq \Delta t \|f'(v)\| \int_0^{t^N}\int_{\mathbb{R}^2} \sup_{\mathbf{x}\in\mathbb{R}^2}|\varphi(\mathbf{x},t^N,\mathbf{x}',s)| \left(\int_{\mathbb{R}^2} |\nabla_{\mathbf{x}} v(\mathbf{x},t^N)|d\mathbf{x}\right) d\mathbf{x}'ds \\
&\leq \Delta t \|f'(v)\| |v_0|_{TV(\mathbb{R}^2)} \int_0^{t^N}\int_{\mathbb{R}^2} \sup_{\mathbf{x}\in\mathbb{R}^2}|\varphi(\mathbf{x},t^N,\mathbf{x}',s)|d\mathbf{x}'ds \\
&\leq \Delta t \|f'(v)\| |v_0|_{TV(\mathbb{R}^2)} T_{aux},
\end{aligned}
$$

where

$$
\begin{aligned}
T_{aux} &= \sup_{\mathbf{x}\in\mathbb{R}^2} \int_0^{t^N}\int_{\mathbb{R}^2} |\varphi(\mathbf{x},t^N,\mathbf{x}',s)|d\mathbf{x}'ds \\
&\leq 2\left(1+\frac{\Delta t}{\epsilon_t}\right) W(t^N).
\end{aligned}
$$

The term III is estimated in exactly the same way as II.

Before we estimate $\overset{cent}{TE}_{h.o.t}(u,v;t^N)$ and $\overset{visc}{TE}_{h.o.t}(u,v;t^N)$, we need to prove a couple of simple auxiliary results.

Lemma 16 *We have*

$$
\sum_{K\in\mathcal{T}}\sum_{L\in N(K)} m(K|L)d_{K|L}\mathcal{I}_{KL}(\Phi) \leq 2\mathbb{D}_h l_h \|\Phi\|_{L^1(\mathbb{R}^2)},
$$

where

$$
\begin{aligned}
&\mathcal{I}_{KL}(\Phi) = \frac{1}{m(L)}\int_L \frac{1}{[m(K)]^3}\int_{K^3}\int_0^1\int_0^1\int_0^1 \Phi d\lambda d\mu d\nu d\mathbf{z}'d\mathbf{y}'d\mathbf{w}'d\mathbf{x}', \\
&\Phi \equiv \Phi(\lambda(\mu(\nu\mathbf{x}'+(1-\nu)\mathbf{w}')+(1-\mu)\mathbf{y}')+(1-\lambda)\mathbf{z}').
\end{aligned}
$$

Proof.

$$\begin{aligned} m(C_{K|L})|\mathcal{I}_{KL}(\Phi)| &= \int_{C_{K|L}} |\mathcal{I}_{KL}(\Phi)| d\mathbf{x} \\ &\leq \int_{C_{K|L}} \frac{1}{m(L)} \int_L \frac{1}{[m(K)]^3} \int_{K^3} \int_0^1 \int_0^1 \int_0^1 |\Phi| d\lambda d\mu d\nu d\mathbf{z}' d\mathbf{y}' d\mathbf{w}' d\mathbf{x}' \\ &\leq \|\Phi\|_{L^1(C_{K|L})}. \end{aligned}$$

Hence,

$$|\mathcal{I}_{KL}(\Phi)| \leq \frac{1}{m(C_{K|L})} \|\Phi\|_{L^1(C_{K|L})} \leq \frac{1}{\max\{m(K), m(L)\}} \|\Phi\|_{L^1(C_{K|L})}.$$

Then, the above inequality along with the definitions of $\mathbb{D}_h$, l_K and l_h lead to:

$$\begin{aligned} \sum_{K\in\mathcal{T}} \sum_{L\in N(K)} m(K|L) d_{K|L} \mathcal{I}_{KL}(\Phi) &\leq \sum_{K\in\mathcal{T}} \sum_{L\in N(K)} \frac{m(K|L) d_{K|L}}{\max\{m(K), m(L)\}} \|\Phi\|_{L^1(C_{K|L})} \\ &\leq \mathbb{D}_h \sum_{K\in\mathcal{T}} \sum_{L\in N(K)} \|\Phi\|_{L^1(C_{K|L})} \\ &\leq 2\mathbb{D}_h \sum_{K|L\in\varepsilon_h} \|\Phi\|_{L^1(C_{K|L})} \\ &\leq 2\mathbb{D}_h \sum_{K\in\mathcal{T}} l_K \|\Phi\|_{L^1(K)} \\ &\leq 2\mathbb{D}_h \sum_{K\in\mathcal{T}} l_h \|\Phi\|_{L^1(K)} \\ &\leq 2\mathbb{D}_h l_h \|\Phi\|_{L^1(\mathbb{R}^2)}. \end{aligned}$$

This completes the proof.

Lemma 17 *Let*

$$\Theta_{aux} = \sum_{1\leq j,k\leq 2} \sum_{n=0}^{N-1} \sum_{K\in\mathcal{T}} \sum_{L\in N(K)} m(K|L) b_{KL} d_{K|L} \mathcal{I}_{KL}(|\partial^2_{x_j x_k} \varphi(\mathbf{x}, t)|) \Delta t.$$

Then,

$$\Theta_{aux} \leq 4t^N \mathbb{D}_h l_h \left(1 + \frac{\Delta t}{\epsilon_t}\right) W(t^N) \left(\frac{4|\eta|^2_{TV(\mathbb{R})}}{\epsilon^2_{\mathbf{x}}} + \frac{2|\eta'|_{TV(\mathbb{R})}}{\epsilon^2_{\mathbf{x}}}\right).$$

Proof. By the definition of the operator $\mathcal{I}_{KL}$ in Lemma 16 and the definition of φ, we get:

$$\begin{aligned} \Theta_{aux} &= \sum_{1\leq j,k\leq 2} \sum_{n=0}^{N-1} \sum_{K\in\mathcal{T}} \sum_{L\in N(K)} m(K|L) b_{KL} d_{K|L} \\ &\qquad \mathcal{I}_{KL}\left(|\partial^2_{x_j x_k} w_{\epsilon_t}(t - t^{n+1}) \prod_{i=1}^2 \eta_{\epsilon_{\mathbf{x}}}(x_i - x'_i)|\right) \Delta t \\ &= \left(\sum_{n=0}^{N-1} w_{\epsilon_t}(t - t^{n+1}) \Delta t\right) \left(\sum_{1\leq j,k\leq 2} \sum_{K\in\mathcal{T}} \sum_{L\in N(K)} m(K|L) b_{KL} d_{K|L} \mathcal{I}_{KL}(|\partial^2_{x_j x_k} \mathbb{R}^{jk}(\mathbf{x}, \mathbf{x}')|)\right) \\ &= \Theta_{aux,t} \Theta_{aux,\mathbf{x}}, \end{aligned}$$

where $\mathbb{R}^{jk}(\mathbf{x}, \mathbf{x}') = \prod_{i=1}^2 \eta_{\epsilon_{\mathbf{x}}}(x_i - x'_i)$.

From Lemma 13,

$$\Theta_{aux,t} \leq 2\Big(1+\frac{\Delta t}{\epsilon_t}\Big)W(t^N).$$

Since, by Lemma 16,

$$\Theta_{aux,\mathbf{x}} \leq \sum_{1\leq j,k\leq 2} 2\mathbb{D}_h l_h \left\|\partial^2_{x_jx_k}\mathbb{R}^{jk}(\mathbf{x},\cdot)\right\|_{L^1(\mathbb{R}^2)} = 2\mathbb{D}_h l_h \sum_{1\leq j,k\leq 2} \left\|\partial^2_{x_jx_k}\mathbb{R}^{jk}(\mathbf{x},\cdot)\right\|_{L^1(\mathbb{R}^2)},$$

and since,

$$\begin{aligned}
\sum_{1\leq j,k\leq 2} \left\|\partial^2_{x_jx_k}\mathbb{R}^{jk}(\mathbf{x},\cdot)\right\|_{L^1(\mathbb{R}^2)} &= \sum_{1\leq j,k\leq 2}\int_{\mathbb{R}^2} |\partial^2_{x_jx_k}\mathbb{R}^{jk}(\mathbf{x},\mathbf{x}')|d\mathbf{x}' \\
&= \sum_{1\leq j,k\leq 2}\left|\partial^2_{x_jx_k,j\neq k}\prod_{i=1}^2\eta_{\epsilon_\mathbf{x}}(x_i-x_i') + \partial^2_{x_j}\prod_{i=1}^2\eta_{\epsilon_\mathbf{x}}(x_i-x_i')\right| \\
&\leq \sum_{1\leq j,k\leq 2}\int_{\mathbb{R}^2}\left|\prod_{\substack{i=1\\ i\neq j\neq k}}^2\eta_{\epsilon_\mathbf{x}}(x_i-x_i')\eta'_{\epsilon_\mathbf{x}}(x_k-x_k')\eta'_{\epsilon_\mathbf{x}}(x_j-x_j')\right|d\mathbf{x}' \\
&\qquad + \sum_{1\leq j,k\leq 2}\int_{\mathbb{R}^2}\left|\prod_{\substack{i=1\\ i\neq j}}^2\eta_{\epsilon_\mathbf{x}}(x_i-x_i')\eta''_{\epsilon_\mathbf{x}}(x_j-x_j')\delta_{jk}\right|d\mathbf{x}' \\
&\leq \Big(\prod_{\substack{i=1\\ i\neq j\neq k}}^2\int_{\mathbb{R}}\eta_{\epsilon_\mathbf{x}}(x_i-x_i')dx_i'\Big)\Big(\sum_{k=1}^2\int_{\mathbb{R}}\left|\eta'_{\epsilon_\mathbf{x}}(x_k-x_k')\right|dx_k'\Big) \\
&\qquad \Big(\sum_{j=1}^2\int_{\mathbb{R}}\left|\eta'_{\epsilon_\mathbf{x}}(x_j-x_j')\right|dx_j'\Big) + \Big(\prod_{\substack{i=1\\ i\neq j\neq k}}^2\int_{\mathbb{R}}\eta_{\epsilon_\mathbf{x}}(x_i-x_i')dx_i'\Big) \\
&\qquad\qquad \Big(\sum_{j=1}^2\int_{\mathbb{R}}|\eta''_{\epsilon_\mathbf{x}}(x_j-x_j')|dx_j'\Big) \\
&= \frac{4|\eta|^2_{TV(\mathbb{R})}}{\epsilon_\mathbf{x}^2} + \frac{2|\eta'|_{TV(\mathbb{R})}}{\epsilon_\mathbf{x}^2},
\end{aligned}$$

we have that

$$\Theta_{aux,\mathbf{x}} \leq 2\mathbb{D}_h l_h\Big(\frac{4|\eta|^2_{TV(\mathbb{R})}}{\epsilon_\mathbf{x}^2} + \frac{2|\eta'|_{TV(\mathbb{R})}}{\epsilon_\mathbf{x}^2}\Big).$$

This concludes the proof.

We are now ready to estimate the remaining term $TE_{h.o.t}$.

Lemma 18

$$\begin{aligned}
\overset{cent}{TE}_{h.o.t}(u,v;t^N) &\leq C_2h^2\Big(\frac{4|\eta|^2_{TV(\mathbb{R})}}{\epsilon_\mathbf{x}^2} + \frac{2|\eta'|_{TV(\mathbb{R})}}{\epsilon_\mathbf{x}^2}\Big)\Big(1+\frac{\Delta t}{\epsilon_t}\Big), \\
\overset{visc}{TE}_{h.o.t}(u,v;t^N) &\leq C_2h^2\Big(\frac{4|\eta|^2_{TV(\mathbb{R})}}{\epsilon_\mathbf{x}^2} + \frac{2|\eta'|_{TV(\mathbb{R})}}{\epsilon_\mathbf{x}^2}\Big)\Big(1+\frac{\Delta t}{\epsilon_t}\Big)\|\alpha\|_{l^\infty(\varepsilon_h)},
\end{aligned}$$

where, $C_2 = 16t^N\mathbb{D}_h l_h W(t^N)\,\|f'(v)\|\,|v_0|_{TV(\mathbb{R}^2)}$ *and* $\|\alpha\|_{l^\infty(\varepsilon_h)} = \underset{K|L\in\varepsilon_h}{\mathrm{Sup}}\,|\alpha_{K|L}|\max_{1\leq j\leq 2}|(\mathbf{x}_L-\mathbf{x}_K)_j|$.

Proof. Using the definition of the terms $\overline{\overline{H}}_{K,L}$ and $\mathcal{I}_{KL}$, we have

$$
\begin{aligned}
\overset{cent}{TE}_{h.o.t}(u,v;t^N) &= \sum_{n=0}^{N-1}\sum_{K\in\mathcal{T}}\int_0^{t^N}\int_{\mathbb{R}^2} F(u_K^n, v(\mathbf{x},t))\cdot \\
&\qquad\qquad \sum_{L\in N(K)} m(K|L)b_{L,K}\overline{\overline{H}}_{K,L}(\mathbf{x},t,t^{n+1})n_{KL}d\mathbf{x}dt\Delta t \\
&= \sum_{n=0}^{N-1}\sum_{K\in\mathcal{T}}\int_0^{t^N}\int_{\mathbb{R}^2} F(u_K^n, v(\mathbf{x},t))\cdot \sum_{L\in N(K)} m(K|L)b_{L,K}\frac{1}{m(L)}\int_L \frac{1}{[m(K)]^3} \\
&\qquad\qquad \int_{K^3}\int_{[0,1]^3}\sum_{1\le i,j,k\le 2}\zeta^{ijk}\partial^3_{x_ix_jx_k}\varphi\; d\lambda d\mu d\nu d\mathbf{z}'d\mathbf{y}'d\mathbf{w}'d\mathbf{x}'n_{KL}\Delta t \\
&= \sum_{n=0}^{N-1}\sum_{K\in\mathcal{T}}\sum_{L\in N(K)} m(K|L)b_{L,K}\sum_{1\le i,j,k\le 2}\int_0^{t^N}\int_{\mathbb{R}^2} F(u_K^n, v(\mathbf{x},t))\cdot n_{KL} \\
&\qquad \left(\frac{1}{m(L)}\int_L\frac{1}{[m(K)]^3}\int_{K^3}\int_{[0,1]^3}\partial_{x_i}(\zeta^{ijk}\partial^2_{x_jx_k}\varphi)\; d\lambda d\mu d\nu d\mathbf{z}'d\mathbf{y}'d\mathbf{w}'d\mathbf{x}'\right)d\mathbf{x}dt\Delta t \\
&= \sum_{n=0}^{N-1}\sum_{K\in\mathcal{T}}\sum_{L\in N(K)} m(K|L)b_{L,K}\Bigg(\sum_{1\le i,j,k\le 2}\int_0^{t^N}\int_{\mathbb{R}^2} F(u_K^n, v(\mathbf{x},t))\cdot n_{KL} \\
&\qquad\qquad \partial_{x_i}\mathcal{I}_{KL}(\zeta^{ijk}\partial^2_{x_jx_k}\varphi)d\mathbf{x}dt\Bigg)\Delta t \\
&= \sum_{n=0}^{N-1}\sum_{K\in\mathcal{T}}\sum_{L\in N(K)} m(K|L)b_{L,K}\Theta^n_{KL}\Delta t.
\end{aligned}
$$

Performing integration by parts w.r.t x_i, we get

$$
\Theta^n_{KL} = -\sum_{1\le i,j,k\le 2}\int_0^{t^N}\int_{\mathbb{R}^2}(\partial_v F(u_K^n, v(\mathbf{x},t))\cdot n_{KL})\partial_{x_i}v(\mathbf{x},t)\mathcal{I}_{KL}(\Xi^{ijk}(\mathbf{x},t))d\mathbf{x}dt,
$$

where $\Xi^{ijk}(\mathbf{x},t) = \zeta^{ijk}\partial^2_{x_jx_k}\varphi$.

So,

$$
\begin{aligned}
|\Theta^n_{KL}| &= \sum_{1\le i,j,k\le 2}\int_0^{t^N}\int_{\mathbb{R}^2}|f'(v)|\,|\partial_{x_i}v(\mathbf{x},t)|\,\mathcal{I}_{KL}(\Xi^{ijk}(\mathbf{x},t))d\mathbf{x}dt \\
&\le \|f'(v)\|\sum_{1\le i,j,k\le 2}\int_0^{t^N}\int_{\mathbb{R}^2}|\partial_{x_i}v(\mathbf{x},t)|\,\mathcal{I}_{KL}(\Xi^{ijk}(\mathbf{x},t))d\mathbf{x}dt,
\end{aligned}
$$

and hence,

$$
\begin{aligned}
\overset{cent}{TE}_{h.o.t}(u,v;t^N) &\le \sum_{n=0}^{N-1}\sum_{K\in\mathcal{T}}\sum_{L\in N(K)} m(K|L)b_{L,K}\,\|f'(v)\| \\
&\qquad\qquad \sum_{1\le i,j,k\le 2}\int_0^{t^N}\int_{\mathbb{R}^2}|\partial_{x_i}v(\mathbf{x},t)|\,\mathcal{I}_{KL}(\Xi^{ijk}(\mathbf{x},t))d\mathbf{x}dt\Delta t \\
&= \|f'(v)\|\int_0^{t^N}\int_{\mathbb{R}^2}\sum_{i=1}^{2}|\partial_{x_i}v(\mathbf{x},t)|\sum_{1\le j,k\le 2}\sum_{n=0}^{N-1} \\
&\qquad\qquad \sum_{K\in\tau}\sum_{L\in N(K)} m(K|L)b_{L,K}\mathcal{I}_{KL}(\Xi^{ijk}(\mathbf{x},t))d\mathbf{x}dt\Delta t
\end{aligned}
$$

$$\leq \|f'(v)\| \, T_{aux} \int_0^{t^N} \int_{\mathbb{R}^2} \|v(\mathbf{x},t)\|_1 \, d\mathbf{x}dt$$
$$\leq \|f'(v)\| \, T_{aux} t^N \, |v_0|_{TV(\mathbb{R}^2)} \, ,$$

where

$$T_{aux} = \max_{1\leq i\leq 2} \operatorname*{Sup}_{\substack{t\in(0,t^N)\\ \mathbf{x}\in\mathbb{R}^2}} \sum_{1\leq j,k\leq 2} \sum_{n=0}^{N-1} \sum_{K\in\mathcal{T}} \sum_{L\in N(K)} m(K|L) b_{L,K} \mathcal{I}_{KL}(\Xi^{ijk}(\mathbf{x},t)) \Delta t.$$

Since, $\left|\zeta^{ijk}\right| \leq 4h^2 d_{K|L}$, we have that

$$\left|\mathcal{I}_{KL}(\Xi^{ijk}(\mathbf{x},t))\right| \leq \frac{1}{m(L)} \int_L \frac{1}{[m(K)]^3} \int_{K^3} \int_{[0,1]^3} \left|\zeta^{ijk}\right| \left|\partial^2_{x_j x_k} \varphi(\mathbf{x},t,\mathbf{x}',t^{n+1})\right| \, d\lambda d\mu d\nu d\mathbf{z}' d\mathbf{y}' d\mathbf{w}' d\mathbf{x}'$$
$$\leq 4h^2 d_{K|L} \mathcal{I}_{KL}(|\partial^2_{x_j x_k} \varphi(\mathbf{x},t,\mathbf{x}',t^{n+1})|),$$

and so, from Lemma 16

$$\sum_{1\leq j,k\leq 2} \sum_{n=0}^{N-1} \sum_{K\in\mathcal{T}} \sum_{L\in N(K)} m(K|L) b_{L,K} \mathcal{I}_{KL}(\Xi^{ijk}(\mathbf{x},t)) \Delta t$$
$$\leq 4h^2 \sum_{1\leq j,k\leq 2} \sum_{n=0}^{N-1} \sum_{K\in\mathcal{T}} \sum_{L\in N(K)} m(K|L) b_{L,K} d_{K|L} \mathcal{I}_{KL}(|\partial^2_{x_j x_k} \varphi(\mathbf{x},t,\mathbf{x}',t^{n+1})|) \Delta t = 4h^2 \Theta_{aux}$$
$$\leq 16 t^N h^2 \mathbb{D}_h l_h \left(1 + \frac{\Delta t}{\epsilon_t}\right) W(t^N) \left(\frac{4|\eta|^2_{TV(\mathbb{R})}}{\epsilon^2_{\mathbf{x}}} + \frac{2|\eta'|_{TV(\mathbb{R})}}{\epsilon^2_{\mathbf{x}}}\right).$$

Then,

$$T_{aux} \leq 16 t^N h^2 \mathbb{D}_h l_h \left(1 + \frac{\Delta t}{\epsilon_t}\right) W(t^N) \left(\frac{4|\eta|^2_{TV(\mathbb{R})}}{\epsilon^2_{\mathbf{x}}} + \frac{2|\eta'|_{TV(\mathbb{R})}}{\epsilon^2_{\mathbf{x}}}\right).$$

This leads to the first result of the Lemma.

Now we have

$$\overset{visc}{TE}_{h.o.t}(u,v;t^N)$$
$$= \sum_{n=0}^{N-1} \sum_{K\in\mathcal{T}} \int_0^{t^N} \int_{\mathbb{R}^2} \sum_{L\in N(K)} m(K|L) \alpha_{K|L} \overline{\overline{H}}_{K,L}(\mathbf{x},t,t^{n+1}) \mathcal{N}(u^n_K, v(\mathbf{x},t)) d\mathbf{x}dt\Delta t$$
$$= \sum_{n=0}^{N-1} \sum_{K\in\mathcal{T}} \int_0^{t^N} \int_{\mathbb{R}^2} \sum_{L\in N(K)} m(K|L) \alpha_{K|L} \Big(\frac{1}{m(L)} \int_L \frac{1}{[m(K)]^3}$$
$$\int_{K^3} \int_{[0,1]^3} \sum_{1\leq i,j,k\leq 2} \zeta^{ijk} \partial^3_{x_i x_j x_k} \varphi \, d\lambda d\mu d\nu d\mathbf{z}' d\mathbf{y}' d\mathbf{w}' d\mathbf{x}' \Big) \mathcal{N}(u^n_K, v(\mathbf{x},t)) d\mathbf{x}dt\Delta t$$
$$= \sum_{n=0}^{N-1} \sum_{K\in\mathcal{T}} \sum_{L\in N(K)} m(K|L) \alpha_{K|L} \sum_{1\leq i,j,k\leq 2} \int_0^{t^N} \int_{\mathbb{R}^2} \mathcal{N}(u^n_K, v(\mathbf{x},t))$$
$$\partial_{x_i} \mathcal{I}_{KL}(\Xi^{ijk}(\mathbf{x},t)) d\mathbf{x}dt\Delta t.$$

Performing an integration by parts w.r.t x_i, taking into account that

$$\begin{aligned}\partial_{x_i}\mathcal{N}(u_K^n, v(\mathbf{x},t)) &= \partial_v\mathcal{N}(u_K^n, v(\mathbf{x},t))\partial_{x_i}v(\mathbf{x},t)\\ &= \left(\partial_v\int_v^{u_K^n} N'_{K|L}(s)U'(s-v)ds\right)\partial_{x_i}v(\mathbf{x},t)\\ &= -N'_{K|L}(v(\mathbf{x},t))\partial_{x_i}v(\mathbf{x},t),\end{aligned}$$

and remembering that $N'_{K|L}(v) \leq \|f'(v)\|$, we get

$$\begin{aligned}\overset{visc}{TE}_{h.o.t}(u,v;t^N) &= -\sum_{n=0}^{N-1}\sum_{K\in\mathcal{T}}\sum_{L\in N(K)} m(K|L)\alpha_{K|L}\sum_{1\leq i,j,k\leq 2}\int_0^{t^N}\int_{\mathbb{R}^2}\partial_{x_i}\mathcal{N}(u_K^n, v(\mathbf{x},t))\\ &\qquad\qquad \mathcal{I}_{KL}(\Xi^{ijk}(\mathbf{x},t))d\mathbf{x}dt\Delta t\\ &= \sum_{n=0}^{N-1}\sum_{K\in\mathcal{T}}\sum_{L\in N(K)} m(K|L)\alpha_{K|L}\sum_{1\leq i,j,k\leq 2}\int_0^{t^N}\int_{\mathbb{R}^2} N'_{K|L}(v(\mathbf{x},t))\\ &\qquad\qquad \partial_{x_i}v(\mathbf{x},t)\mathcal{I}_{KL}(\Xi^{ijk}(\mathbf{x},t))d\mathbf{x}dt\Delta t\\ &\leq \|f'(v)\|\sum_{n=0}^{N-1}\sum_{K\in\mathcal{T}}\sum_{L\in N(K)} m(K|L)\alpha_{K|L}\int_0^{t^N}\int_{\mathbb{R}^2}\sum_{1\leq i\leq 2}\partial_{x_i}v(\mathbf{x},t)\\ &\qquad\qquad \sum_{1\leq j,k\leq 2}\mathcal{I}_{KL}(\Xi^{ijk}(\mathbf{x},t))d\mathbf{x}dt\Delta t\\ &\leq \|f'(v)\|\,T_{aux}t^N\,|v_0|_{TV(\mathbb{R}^2)}\operatorname*{Sup}_{K|L\in\varepsilon_h}\alpha_{K|L},\end{aligned}$$

where

$$T_{aux} = \max_{1\leq i\leq 2}\operatorname*{Sup}_{\substack{t\in(0,t^N)\\ \mathbf{x}\in\mathbb{R}^2}}\sum_{1\leq j,k\leq 2}\sum_{n=0}^{N-1}\sum_{K\in\mathcal{T}}\sum_{L\in N(K)} m(K|L)\mathcal{I}_{KL}(\Xi^{ijk}(\mathbf{x},t))\Delta t.$$

This last inequality leads to the second result of the Lemma and it completes the proof.

Now, we obtain the error estimate.

Inserting the estimates obtained in Propositions 6 and 7 into the approximation inequality obtained in Proposition 5 for $e(t^N)$ and taking the auxiliary function η as in (2.99), (2.100) and (2.101), we get

$$\begin{aligned}e(t^N) \leq 2e(0) &+ 8(\epsilon_{\mathbf{x}} + \epsilon_t\|f'(v)\|)|v_0|_{TV(\mathbb{R}^2)} + 2\|f'(v)\|\,|v_0|_{TV(\mathbb{R}^2)}\Delta t\\ &+ 2C_0t^N\left[4\frac{|\eta|_{TV(\mathbb{R})}}{\epsilon_{\mathbf{x}}}\left(1+\frac{\Delta t}{\epsilon_t}\right)\right]\|\nu_v\|\,h\\ &+ 2C_1\left[\|f'(v)\|\,\frac{(\Delta t)^2|\eta|_{TV(\mathbb{R})}}{\epsilon_t\epsilon_{\mathbf{x}}}t^N + 4\left(1+\frac{\Delta t}{\epsilon_t}\right)\Delta t\right.\\ &\left. + 32\mathbb{D}_{\Delta\mathbf{x}}l_{\Delta\mathbf{x}}h^2\left[\frac{4|\eta|^2_{TV(\mathbb{R})}}{\epsilon_{\mathbf{x}}^2} + \frac{2|\eta'|_{TV(\mathbb{R})}}{\epsilon_{\mathbf{x}}^2}\right]\left(1+\frac{\Delta t}{\epsilon_t}\right)t^N.\right.\end{aligned}$$

By eliminating the parameter Δt through the use of the CFL condition (2.90) and then taking the very same optimal values as those in [66], namely,

$$\epsilon_{\mathbf{x}}^\star = \sqrt{t^N\|\nu_v\|\,h/2},\ \ \epsilon_t = A_th^{3/4},\ \ \epsilon_{\mathbf{x}} = Ah^{1/4}.$$

we obtain

$$e(t^N) \leq 2e(0) + 8|v_0|_{TV(\mathbb{R}^2)}\sqrt{2t^N\|\nu_v\|}h^{1/2} + |v_0|_{TV(\mathbb{R}^2)}(b_1h^{3/4} + b_2h). \tag{2.109}$$

where the constant C is given by

$$C = 4\left\|f'(v)\right\|\left(t^N + \sqrt{2t^N/\left\|\nu_v\right\|}\right)(1 + b_0 h^{1/4}),$$

and the constants b_0, b_1 and b_2 are locally bounded functions that depend solely on the quantities $\left\|f'(v)\right\|\Delta t/h, \left\|f'(v)\right\|/\left\|\nu_v\right\|, (t^N\left\|\nu_v\right\|)^{1/2}, \mathbb{D}_h$ and l_h.

This concludes the proof.

2.2.4 Positivity Principle of the Triangular Fully-Dicrete Lagrangian-Eulerian Scheme for Multi-dimensional Systems

The Total Variation Diminishing (TVD) property, first introduced in [130,131], is a proper principle for designing numerical schemes to solve hyperbolic equations (or linear hyperbolic systems) in one space dimension. For multi-dimensional hyperbolic systems, due to the possibility of focusing, the TV norm is not bounded and hence no longer proper for such systems. The only functional known to be bounded for solutions of linear hyperbolic systems is L^2 norm [130]. Extending this result, the positivity principle was introduced for multi-dimensional hyperbolic systems in [131]. Positivity principle is a proper designing principle for solving multi-dimensional hyperbolic systems since schemes with this property are stable in the l^2 norm, i.e., the l^2 norm of their solutions has bounded growth.

Here, we consider (1.1) for the case of systems of n equations defined in 2D spatial domain Ω, i.e.,

$$\begin{cases} (u_i)_t(\mathbf{x},t) + \nabla\cdot\mathbf{f}_i(u(\mathbf{x},t) &= 0, & \forall\,\mathbf{x}=(x,y)\in\Omega,\ \forall\,t\in(0,T],\ i=1,\cdots,m,\\ u(0,\mathbf{x}) &= u_0(\mathbf{x}), & \forall\,\mathbf{x}=(x,y)\in\Omega, \end{cases} \tag{2.110}$$

where $T>0$, $u = u(\mathbf{x},t) = (u_1,\cdots,u_m)^T : \mathbb{R}_+\times\mathbb{R}^2\to\mathbb{R}^n$, $\mathbf{f} = (f_1,\cdots,f_n)$, for which each f_i for $i=1,\cdots,m$ satisfies $f_i:\mathbb{R}^n\to\mathbb{R}^2$. We say that a numerical scheme used to solve (2.110) is *positive* if it can be written in the following form:

$$U_j^n = \sum_K C_{J,K}U_{J+K}, \tag{2.111}$$

with coefficient matrices $C_{J,K}$ satisfying the following properties:

$$\begin{aligned} &(i)\quad C_{J,K} \text{ is symmetric and semipositive definite.}\\ &(ii)\quad \sum_K C_{J,K} = I, \text{ where } I \text{ is the identity matrix.}\\ &(iii)\quad C_{J,K} = 0, \text{ except for a finite set of } K. \end{aligned} \tag{2.112}$$

If, in addition to properties (i)–(iii) in (2.112), the numerical scheme satisfies the following condition:

$$(iv)\quad C_{J,K} \text{ depends Lipschitz continuously on } x, \tag{2.113}$$

scheme (2.111) satisfies, for the discrete l^2 norm (see [130, 131]),

$$||U^{n+1}||_2 \le (1+\text{const}\,\Delta)||U^n||_2, \quad \text{where} \quad ||U||_2 = \sqrt{\sum_J (U_J,U_J)}, \tag{2.114}$$

where (U_J,U_J) is the canonical inner product of R^n restrict to grid element; and Δ is the variation on the variables of $\mathbf{x}$.

The extension of the fully-discrete Lagrangian-Eulerian scheme (2.19)-(2.20) for systems can be written as, for $i=1,\cdots,m$:

$$\begin{cases} (u_i)_K^0 = \frac{1}{m(K)}\int_K (u_i)(\mathbf{x},0)d\mathbf{x},\\ (u_i)_K^{n+1} = (u_i)_K^n - \frac{\Delta t}{m(K)}\sum_{L\in N(K)} F_i(u_K^n, u_L^n), \end{cases} \tag{2.115}$$

where $u_L^n = ((u_1)_L^n, \cdots, (u_m)_L^n)^T$ for all L in the triangular grid. The numerical flux $F_i(u_K^n, u_L^n)$, for $i = 1, \cdots, m$, satisfies:

$$F_i(u_K^n, u_L^n) = \left[\frac{1}{2}\left(\mathbf{f}_i(u_K^n) + \mathbf{f}_i(u_L^n)\right)\cdot \mathbf{n}_{KL} - \operatorname*{Sup}_{w,K,L}\left|\frac{\mathbf{f}_i(w)}{w}\cdot \mathbf{n}_{KL}\right|\left((u_i)_L^n - (u_i)_K^n\right)\right] m(K|L). \quad (2.116)$$

To prove the positivity, we consider the supremum in (2.116) over all $\mathbf{f}_i$, i.e., we consider the numerical method written as:

$$F_i(u_K^n, u_L^n) = \left[\frac{1}{2}\left(\mathbf{f}_i(u_K^n) + \mathbf{f}_i(u_L^n)\right)\cdot \mathbf{n}_{KL} - C_{K,L}\left((u_i)_L^n - (u_i)_K^n\right)\right] m(K|L), \quad (2.117)$$

where

$$c_{K,L} = \operatorname*{Sup}_{w,K,L,i}\left|\frac{\mathbf{f}_i(w)}{w}\cdot \mathbf{n}_{KL}\right|. \quad (2.118)$$

Notice that the numerical scheme (2.117) is more restrictive than (2.116), since we consider the supremum of $\mathbf{f}_i$ over all $i = 1, \cdots, m$. However, in some simulations we can relax this condition considering only (2.116), i.e., the supremum for the i-th equation in the system depends only on the supremum of $\mho_i$.

We also can prove the positivity for the general numerical flux given by (2.22), namely,

$$F_i(u_K^n, u_L^n) = \left[\frac{1}{2}\left(\mathbf{f}_i(u_K^n) + \mathbf{f}_i(u_L^n)\right)\cdot \mathbf{n}_{KL} - Q_{LE}^i\left(\frac{\mathbf{f}_i(u_K^n)}{(u_i)_K^n}, \frac{\mathbf{f}_i(u_L^n)}{(u_i)_L^n}; \mathbf{n}_{KL}\right)\left((u_i)_L^n - (u_i)_K^n\right)\right] m(K|L), \quad (2.119)$$

Here, to prove the positivity for (2.119), it is necessary to consider that there is a $\tilde{c}_{K,L} > 0$ such that

$$Q_{LE}^i\left(\frac{\mathbf{f}_i(u_K^n)}{(u_i)_K^n}, \frac{\mathbf{f}_i(u_L^n)}{(u_i)_L^n}; \mathbf{n}_{KL}\right) \geq \tilde{c}_{K,L} \geq c_{K,L}, \quad (2.120)$$

where $C_{K,L}$ is given by (2.118).

To prove the positivity, we define the diagonal matrices $P_{K,L}$ and $C_{K,L}$

$$P_{K,L} = p_{K,L} I \quad \text{satisfying} \quad \sum_{L\in N(K)} P_{K,L} = I, \quad \text{and} \quad C_{K,L} = c_{K,L} I, \quad (2.121)$$

where I is the identity matrix. Thus, we can rewrite the numerical method (2.115) in the matricial form as:

$$u_K^{n+1} = \sum_{L\in N(K)} P_{K,L} u_K^n - \frac{\Delta t}{m(K)} F(u_K^n, u_L^n), \quad (2.122)$$

where $u_{K,L} = ((u_1)_{K.L}, \cdots, (u_m)_{K,L})^T$ and $F_{K,L} = ((F_1)_{K.L}, \cdots, (F_m)_{K,L})^T$.

We also use the following Lemma, which proof is very simple:

Lemma 19 *Given any triangle K, thus*

$$\sum_{L\in N(K)} \mathbf{n}_{KL} m(K|L) = 0, \quad (2.123)$$

where n_{KL} and $m(K|L)$ are the normal and the size of the side L of the triangle K and 0 is a vector of zeros.

Theorem 2.2.6 *Consider the numerical method (3.31), if the system is symmetric or simmetrizable, for the numerical flux $(F_i)_{K,L}$ given by (2.117), then the numerical scheme is positive.*

Proof: If we use $(F_i)_{K,L}$ given by (2.117) in Eq. (3.31) we obtain:

$$u_K^{n+1} = \sum_{L\in N(K)} P_{K,L}u_K^n - \frac{\Delta t}{m(K)}\left(\left[\frac{1}{2}\left(\mathbf{f}(u_K^n)+\mathbf{f}(u_L^n)\right)\cdot\mathbf{n}_{KL} - B_{K,L}\left(u_L^n-u_K^n\right)\right]m(K|L)\right). \tag{2.124}$$

By using (2.123), we know that

$$\sum_{L\in N(K)} \mathbf{f}(u_K^n)\cdot\mathbf{n}_{KL}m(K|L) = 0. \tag{2.125}$$

Subtrating (2.125) in Equation (2.124) it reads:

$$u_K^{n+1} = \sum_{L\in N(K)} P_{K,L}u_K^n - \frac{\Delta t}{m(K)}\left(\left[\frac{1}{2}\left(\mathbf{f}(u_L^n)-\mathbf{f}(u_K^n)\right)\cdot\mathbf{n}_{KL} - C_{K,L}\left(u_L^n-u_K^n\right)\right]m(K|L)\right). \tag{2.126}$$

Notice that $\mathbf{f} = (\mathbf{f}_1,\cdots,\mathbf{f}_n)$ and each $\mathbf{f}_i$ is a vector with two coordinates, which we denote as $\mathbf{f}_i = ((f_i)_1,(f_i)_2)$. We define $\mathbf{f}^1 = ((f_1)_1,(f_2)_1,\cdots,(f_n)_1)^T$, i.e., the first coordinate and $\mathbf{f}^2 = ((f_1)_2,(f_2)_2,\cdots,(f_n)_2)$. Using the Roe average construction, we can write:

$$\left(\mathbf{f}(u_L^n)-\mathbf{f}(u_K^n)\right)\cdot n_{kL} = A(\hat{u}_{K,L})\cdot\mathbf{n}_{KL}(u_L^n-u_K^n), \tag{2.127}$$

where $A=(A_1,A_2)$ and A_1 and A_2 are the Jacobian of $\mathbf{f}^1$ and $\mathbf{f}^2$, respectively. $A(\hat{u}_{K,L})\cdot\mathbf{n}_{KL}$ is a $n\times n$ matrix. If the system is symmetric, thus each A_i is also symmetric and $A(\hat{u}_{K,L})\cdot\mathbf{n}_{KL}$ is also symmetric.

Using (2.127) in Eq. (2.126), we obtain:

$$\begin{aligned} u_K^{n+1} &= \sum_{L\in N(K)} P_{K,L}u_K^n - \frac{\Delta t}{m(K)}\left[\left(\frac{1}{2}A(\hat{u}_{K,L})\cdot\mathbf{n}_{KL}(u_L^n-u_K^n) - C_{K,L}\left(u_L^n-u_K^n\right)\right]m(K|L)\right) \\ &= \sum_{L\in N(K)}\left(P_{K,L}+\frac{\Delta t}{m(K)}\left[\left(\frac{1}{2}A(\hat{u}_{K,L})\cdot\mathbf{n}_{KL}-C_{K,L}\right]m(K|L)\right)\right)u_K^n \\ &\qquad + \sum_{L\in N(K)}\frac{\Delta t}{m(K)}\left[C_{K,L}-\frac{1}{2}A(\hat{u}_{K,L})\cdot\mathbf{n}_{KL}\right]m(K|L)u_L^n. \end{aligned} \tag{2.128}$$

For the condition of positivity is necessary that each matrix multiplying u_K^n and u_L^n is positive defined, i.e., it is enough that

$$\left|\rho\big(A(\hat{u}_{K,L})\cdot\mathbf{n}_{KL}\big)\right| \le 2\,c_{K,L}\ (a) \quad \text{and} \quad \frac{\Delta t\, m(K|L)}{m(K)}\,c_{K,L} \le p_{K,L}\ (b), \tag{2.129}$$

where $\rho\big(A(\hat{u}_{K,L})\cdot\mathbf{n}_{KL}\big)$ is the spectral radius of matrix $A(\hat{u}_{K,L})\cdot\mathbf{n}_{KL}$. Notice that (2.129) generalizes for system the stability conditions (2.26) - (2.23) in the scalar case.

Since the system is symmetric (or symmetrizable, see [130,131]) conditions (i) -(iii) are satisfied and the scheme is positive. □

Remark 14 *Theorem* 2.2.6 *is valid for the numerical flux* (2.119) *satisfying* (2.120)*, with a very similar proof.*

2.2.5 Weak Positivity Principle of the Triangular Fully-Dicrete Lagrangian-Eulerian Scheme for Multi-Dimensional Systems

In [4] was introduced the concept of the *weak positivity* by following the same *positivity principle* as proposed in the seminal works of Lax and Liu (1996, [131]; 2003, [130]). Here, we prove that a bound on the no-flow curves, which is independent of the eigenvalues, is enough to guarantee the weak positivity for the triangular fully-dicrete scheme (2.124).

Theorem 2.2.7 *Assume that the no-flow condition*

$$\left|\frac{\mathbf{f_i}(u_L^n)}{(u_i)_L^n}\right| \leq 2c_{K,L}, \tag{2.130}$$

and the condition (2.129) *hold. Then, the numerical scheme* (3.31) *satisfies* ***positivity in the weak sense*** *if properties* (i) *and* (iii) *in* (2.112) *are satisfied. Furthermore, if* $u_i > 0$ *for all* i*, and the method satisfies the weak positivity, then the numerical method preserves the* L^1 *norm.*

Proof. To prove our statement, we notice that we can rewrite (2.124) in (2.126) that we can rearrange and obtain for each i:

$$\begin{aligned}(u_i)_K^{n+1} = &\sum_{L\in N(K)} (u_i)_K^n \left(p_{K,L} - \frac{\Delta t}{m(K)}\left[\frac{1}{2}\left(\frac{\mathbf{f_i}(u_K^n)}{(u_i)_K^n}\right)\cdot \mathbf{n}_{KL} - c_{K,L}\right] m(K|L)\right)\\ &+ (u_i)_L^n \frac{\Delta t}{m(K)}\left[c_{K,L} - \frac{1}{2}\left(\frac{\mathbf{f_i}(u_L^n)}{(u_i)_L^n}\right)\cdot \mathbf{n}_{KL}\right] m(K|L).\end{aligned} \tag{2.131}$$

Since (2.129) and (2.130) hold, the matrices are positive. Also, they are symmetric because they are diagonal matrices.

Finally, since $u_K > 0$ for all K, taking into account that $\sum_{L\in N(K)} P_{K,L} = I$ and using the fact that $\int_\Omega u_K^n d\mathbf{x} = \int_\Omega u_L^n d\mathbf{x}$, from (2.131) we get

$$\left\|u_K^{n+1}\right\|_1 = \left\|u_K^n\right\|_1.$$

That is, the numerical scheme (3.6) preserves the L^1– norm. □

Remark 15 *The numerical scheme* (3.31) *with numerical flux* (2.119) *also satisfies the weak positivity principle if the no-flow condition*

$$\left|\frac{\mathbf{f_i}(u_L^n)}{(u_i)_L^n}\right| \leq 2Q_{LE}^i, \tag{2.132}$$

and condition (2.129*b*) *hold.*

2.3 Numerical Tests

In this section we provide, using the fully-discrete Lagrangian-Eulerian scheme on triangular grids, numerical results for several nontrivial models of scalar conservation laws and systems. The time step is given by the weak CFL condition (2.23).

2.3.1 Linear Problem with Smooth Initial Data

We first consider the problem (1.1) with $f(u) = (u,u)^T$ and $u_0(x,y) = \exp\big(-\frac{x^2+y^2}{4}\big)$, $(x,y) \in [-6,6]^2$. This is a linear problem whose exact solution at $t = T$ is given by $u(x,y,T) = u_0(x - T, y - T)$.

Figure 2.3 shows the approximate solution at $t = 1.5$ for different refinements. As can be seen, the fully-discrete Lagrangian-Eulerian scheme (2.19)-(2.20) correctly captures the exact solution.

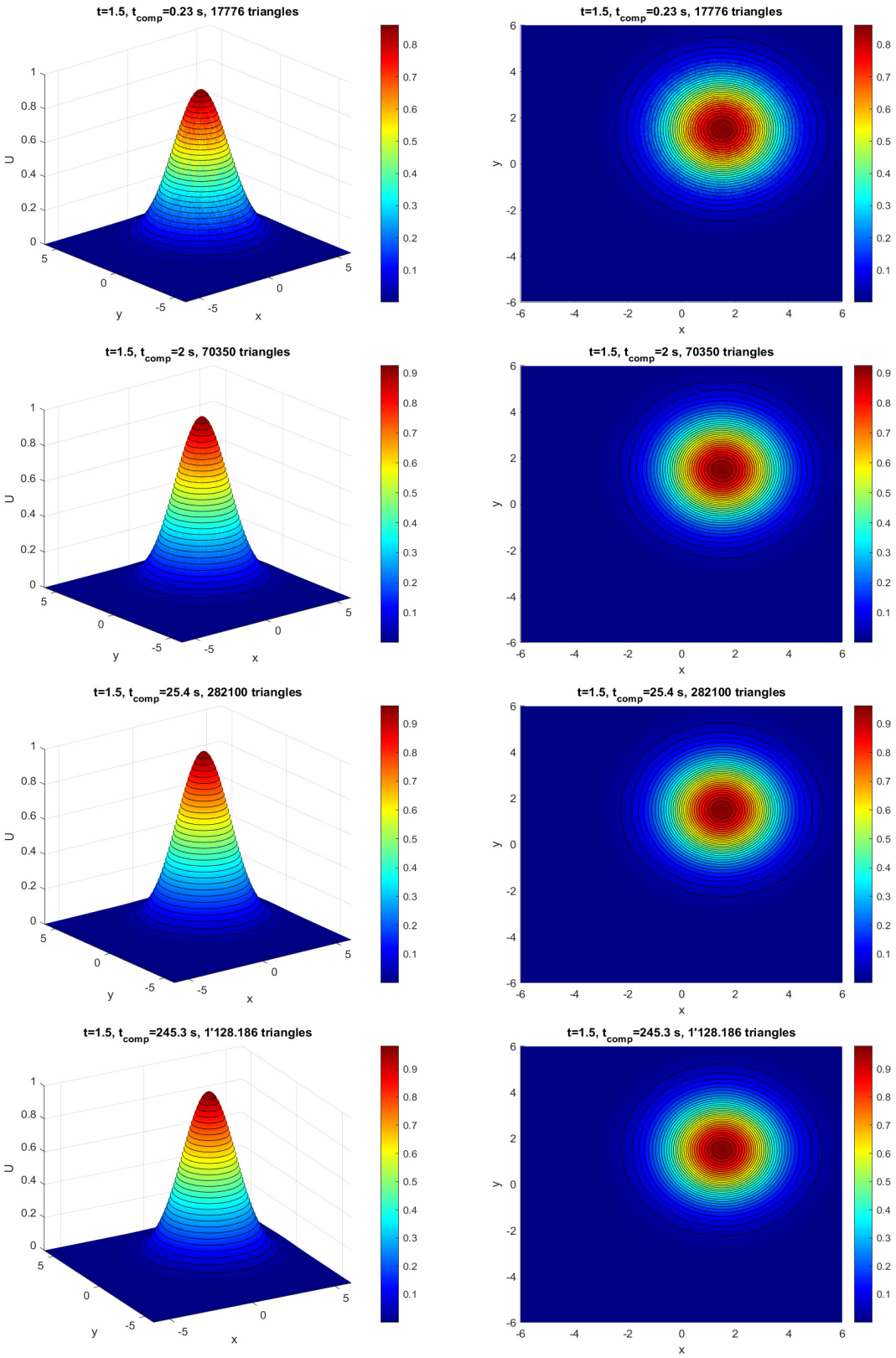

Figure 2.3: Solution to the linear problem at t=1.5. The CFL number is equal to 1/10.

Linear transport with nonsmooth solution.

Next, we solve the problem (1.1) in $D = \{(x,y) \in \mathbb{R}^2 \mid \|(x,y)\|_{l^2} < 1\}$ with the flux function $\mathbf{f}(u) = (-yu, xu)$ and initial data defined by

$$u(x,y,0) = \begin{cases} 1, & \|(x,y-0.5)\|_{l^2} \le 0.3 \quad \text{and} \quad (|x| \ge 0.05 \text{ or } |y| \ge 0.7), \\ 1 - \frac{10}{3}\|(x+0.5,y)\|_{l^2}, & \|(x+0.5,y)\|_{l^2} \le 0.3, \\ g(\|(x,y+0.5)\|_{l^2}), & \|(x,y+0.5)\|_{l^2} \le 0.3, \\ 0, & \text{otherwise}, \end{cases}$$

where $g(r) = \frac{1}{4}\left[1 + \cos\left(\frac{10\pi}{3}r\right)\right]$. This test problem is proposed in [104, 105].

The graph of u_0 consists of three solids: a slotted cylinder of height 1, a cone of height 1 and a smooth hump of height $\frac{1}{2}$.

We use four equilateral triangular grides with a total number of vertices in each grid equal to 9708, 29624, 99034 and 389270. Figure 2.4 shows the graph of the solution computed at $t = 1$ on each of these grids along with the computational time used by the fully-discrete Lagrangian-Eulerian scheme to obtain them. This solution is consistent with that reported in [104, 105].

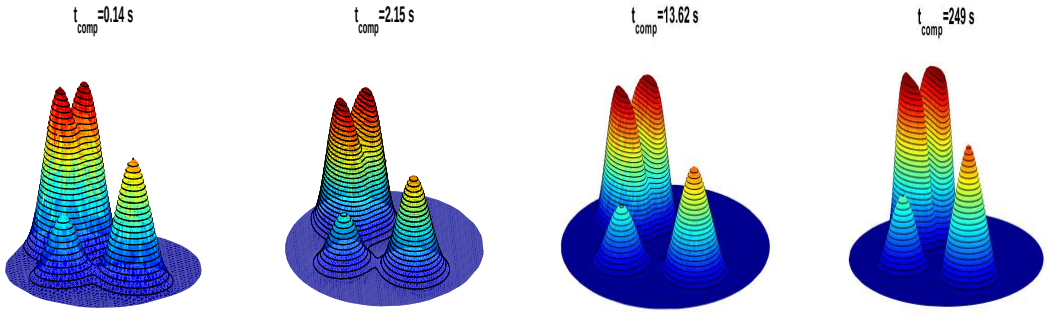

Figure 2.4: Solution to the linear transport equation with three body rotation at t=1; the CFL number is equal to 0.39.

2.3.2 Burgers' Equation with Smooth Initial data

In this section, we solve the Burgers' equation

$$u_t + \left(\frac{1}{2}u^2\right)_x + \left(\frac{1}{2}u^2\right)_y = 0, \tag{2.133}$$

subject to the initial condition: $u_0(x,y) = \exp\left(-\frac{x^2+y^2}{4}\right)$, $(x,y) \in [-5,5]^2$.

Burgers' equation is an important and basic partial differential equation from fluid mechanics that is used as a tool to describe the interaction between convection and diffusion.

The approximate solution is advanced at two different times. Figures 2.5 and 2.6 show the approximate solution obtained at a time before and after the formation of the shock, respectively.

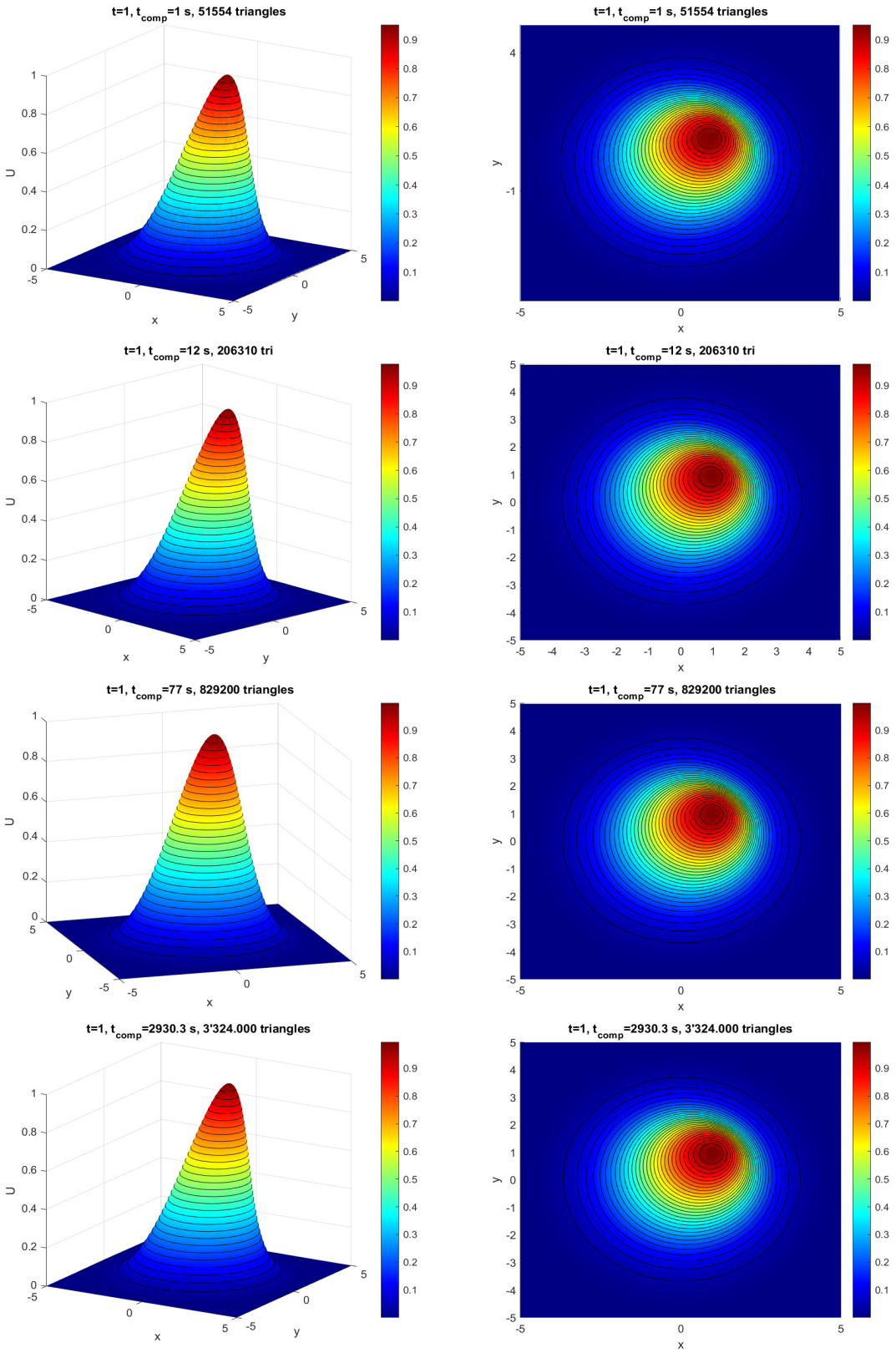

Figure 2.5: Solution to the Burger's equation at t=1 (Pre-Shock). The CFL number is equal to 1/10.

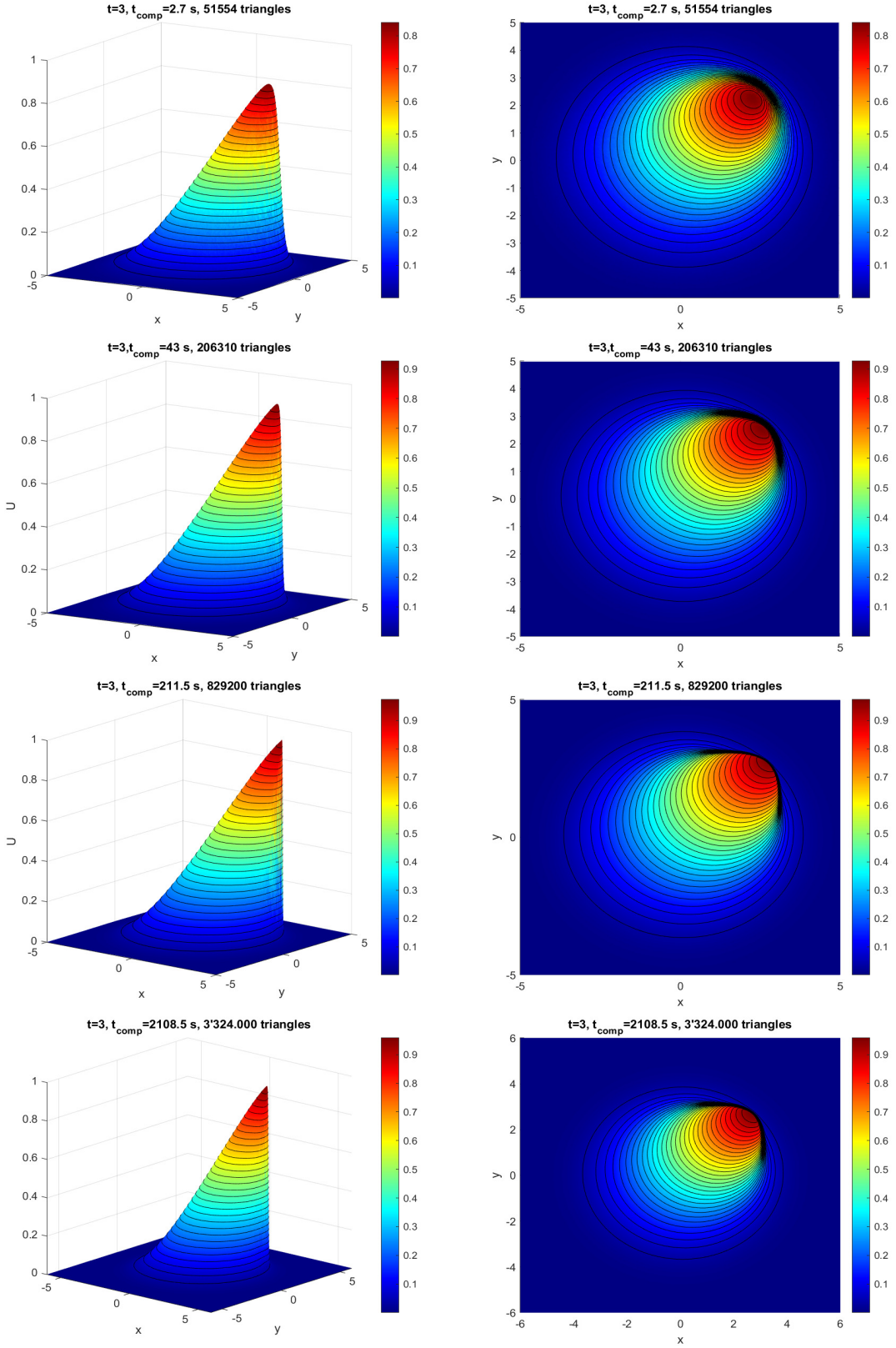

Figure 2.6: Solution to the Burger's equation at t=3 (Pos-Shock). The CFL number is equal to 1/10.

2.3.3 Nonlinear equation with non-convex flux

To demonstrate the robustness of the fully-discrete Lagrangian-Eulerian scheme (2.19)-(2.20), we now consider to solve the problem (1.1) in $D = [-2, 2] \times [-2.5, 1.5]$ with $\mathbf{f}(u) = (\sin u, \cos u)$ and

$$u_0(x, y) = \begin{cases} \frac{14\pi}{4}, & \sqrt{x^2 + y^2} \leq 1, \\ \frac{\pi}{4}, & \text{otherwise.} \end{cases}$$

It is a challenging test case because the solution has a two-dimensional composite wave structure that is difficult to capture correctly, and this can lead to the scheme producing shocks where there should be expansions (see [104]).

We show in Figures 2.7 and 2.8 simulations done at $t = 1$ on four equilateral triangular grids with 11600, 46000, 133672 and 535266 vertices in each one of them. The helicoidal composite wave is clearly visible. The computational time used to obtain them is also shown.

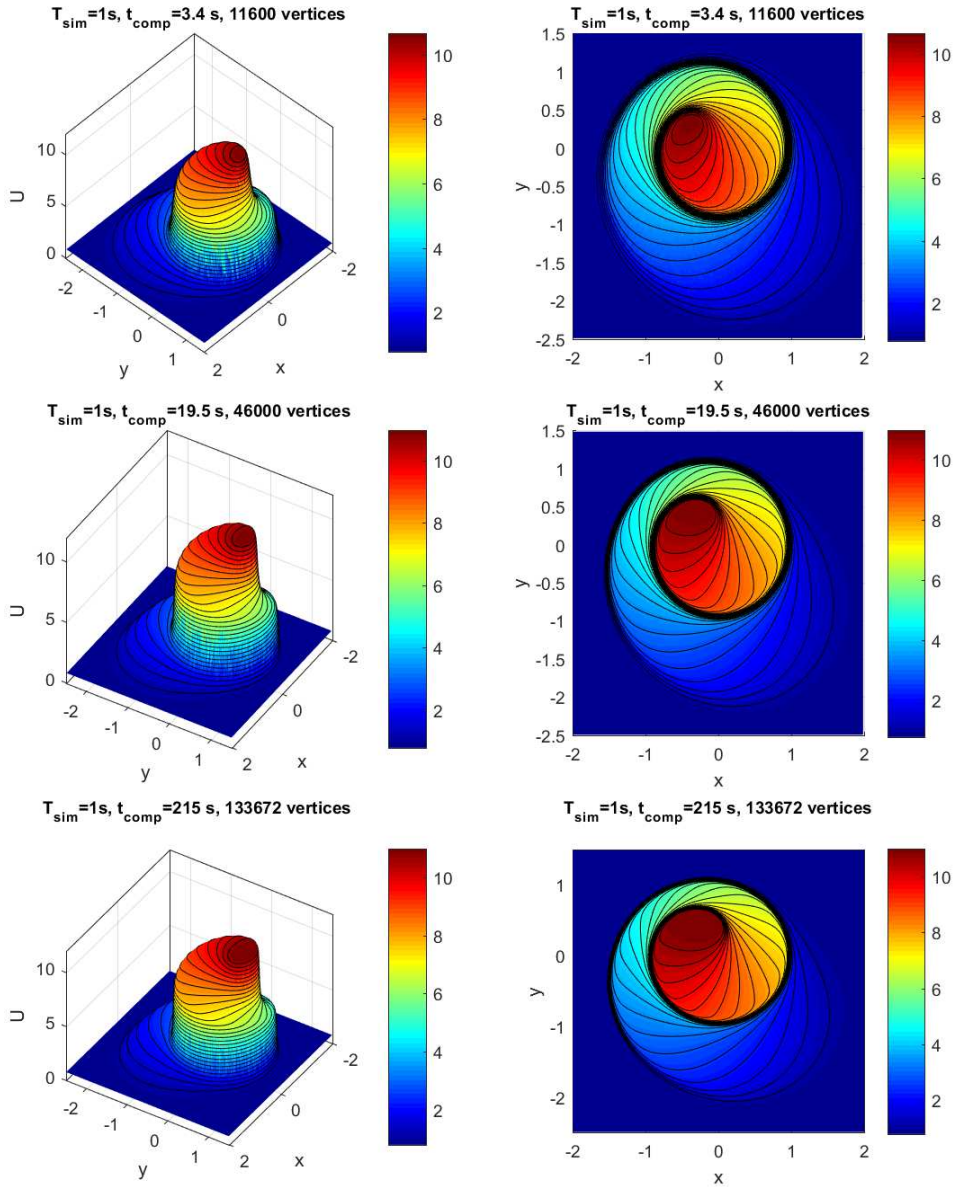

Figure 2.7: Solution to the nonconvex flux problem at t=1; the CFL number is equal to 1/10.

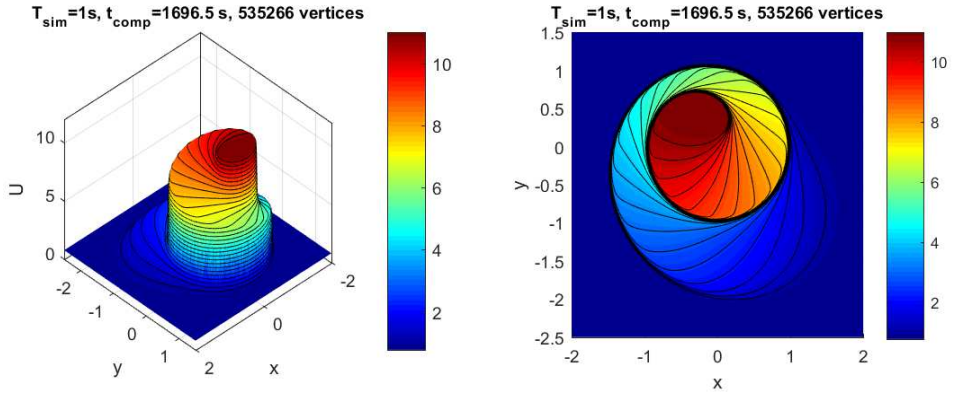

Figure 2.8: Solution to the nonconvex flux problem at t=1; the CFL number is equal to 1/10.

2.3.4 Buckley-Leverett equation with gravity

Next, we solve the problem (1.1) with $\mathbf{f}(u) = (f_1(u), f_2(u))$ where $f_1(u) = \dfrac{u^2}{u^2 + (1-u)^2}$ and $f_2(u) = f_1(u)[1 - 5(1-u)^2]$ and the initial data defined by $u_0(x,y) = \begin{cases} 1, & x^2 + y^2 \leq 0.5, \\ 0, & \text{otherwise}, \end{cases}$ which gives rise to a composite-wave solution.

The computacional domain $[-1.5, 1.5]^2$ is triangulated using equilateral triangular grids with 8330, 33320, 133280 and 535280 vertices. The solution is advanced up to $t = 0.5$ and it is shown along with the computational time used to obtain them in Figure 2.9 and 2.10. This solution agrees with the one reported in [63].

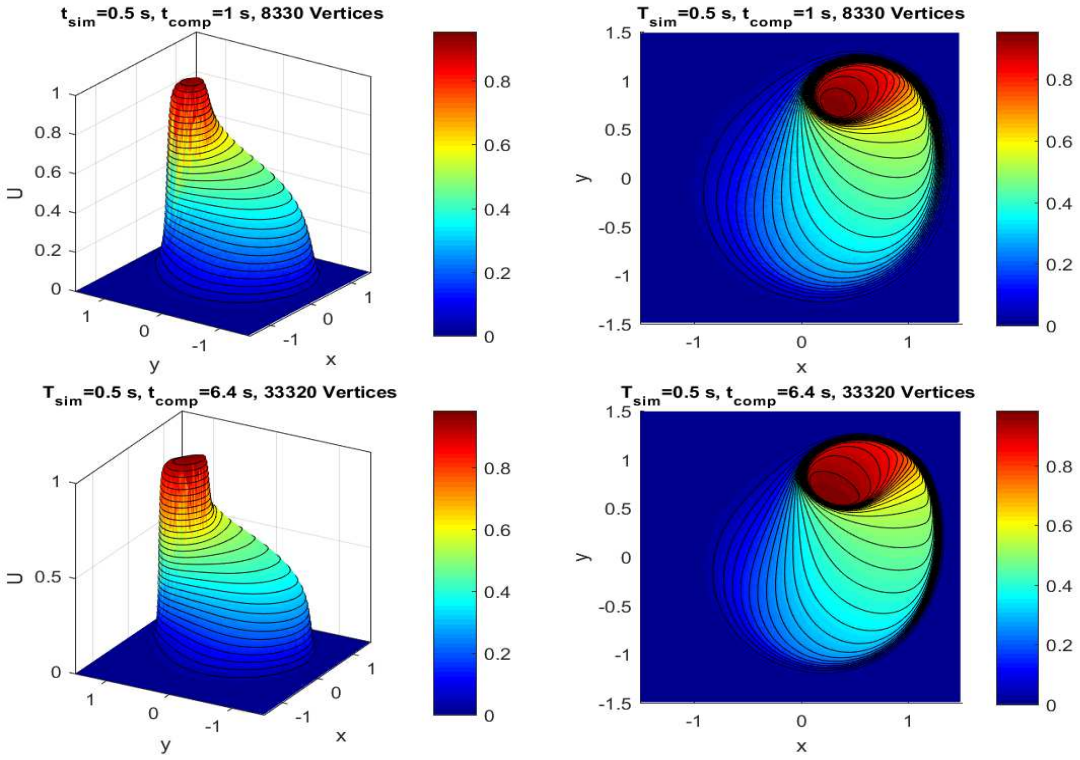

Figure 2.9: Solution to the Buckley-Leverett equation with gravity at t=0.5; the CFL number is equal to 1/10.

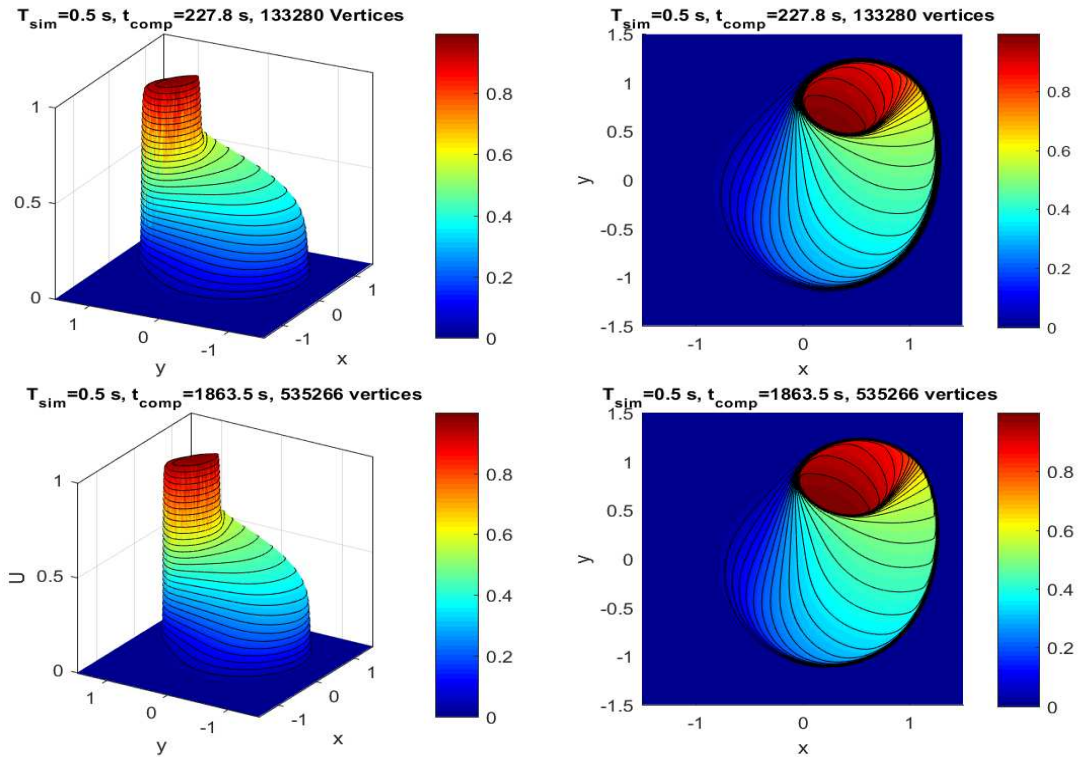

Figure 2.10: Solution to the Buckley-Leverett equation with gravity at t=0.5; the CFL number is equal to 1/10.

2.3.5 Inviscid Burgers equation

Now, we solve problem (1.1) with $\mathbf{f}(u) = (\frac{1}{2}u^2, \frac{1}{2}u^2)$ and the "oblique" Riemann problem initial condition $u_0(x,y) = \begin{cases} -1, & x > 0.5,\ y > 0.5, \\ -0.2, & x < 0.5,\ y > 0.5, \\ 0.5, & x < 0.5,\ y < 0.5, \\ 0.8, & x < 0.5,\ y < 0.5. \end{cases}$

The computacional domain $[-1,1]^2$ is also triangulated by using equilateral triangular grids with 11600, 46000, 133672 and 535266 vertices. The solution is advanced up to $t = 0.5$ and it is shown in Figures 2.12 along with the computational time used to obtain it.

As can be seen, the fully-discrete Lagrangian-Eulerian scheme accurately captures the exact solution to this problem shown in Figure 2.11.

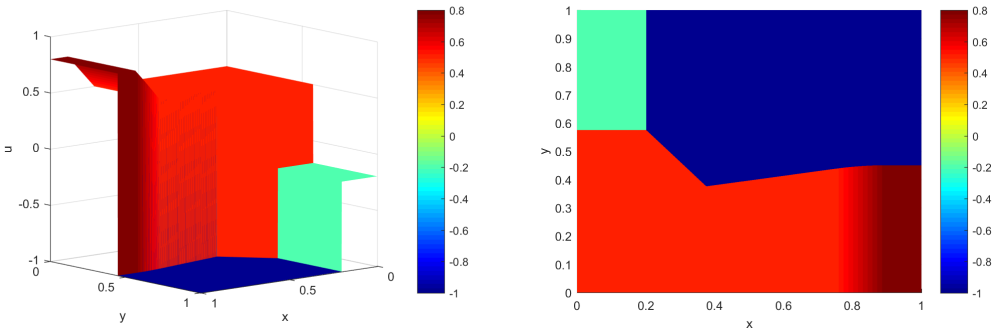

Figure 2.11: Exact analytical solution to the inviscid Burgers problem at t=0.5.

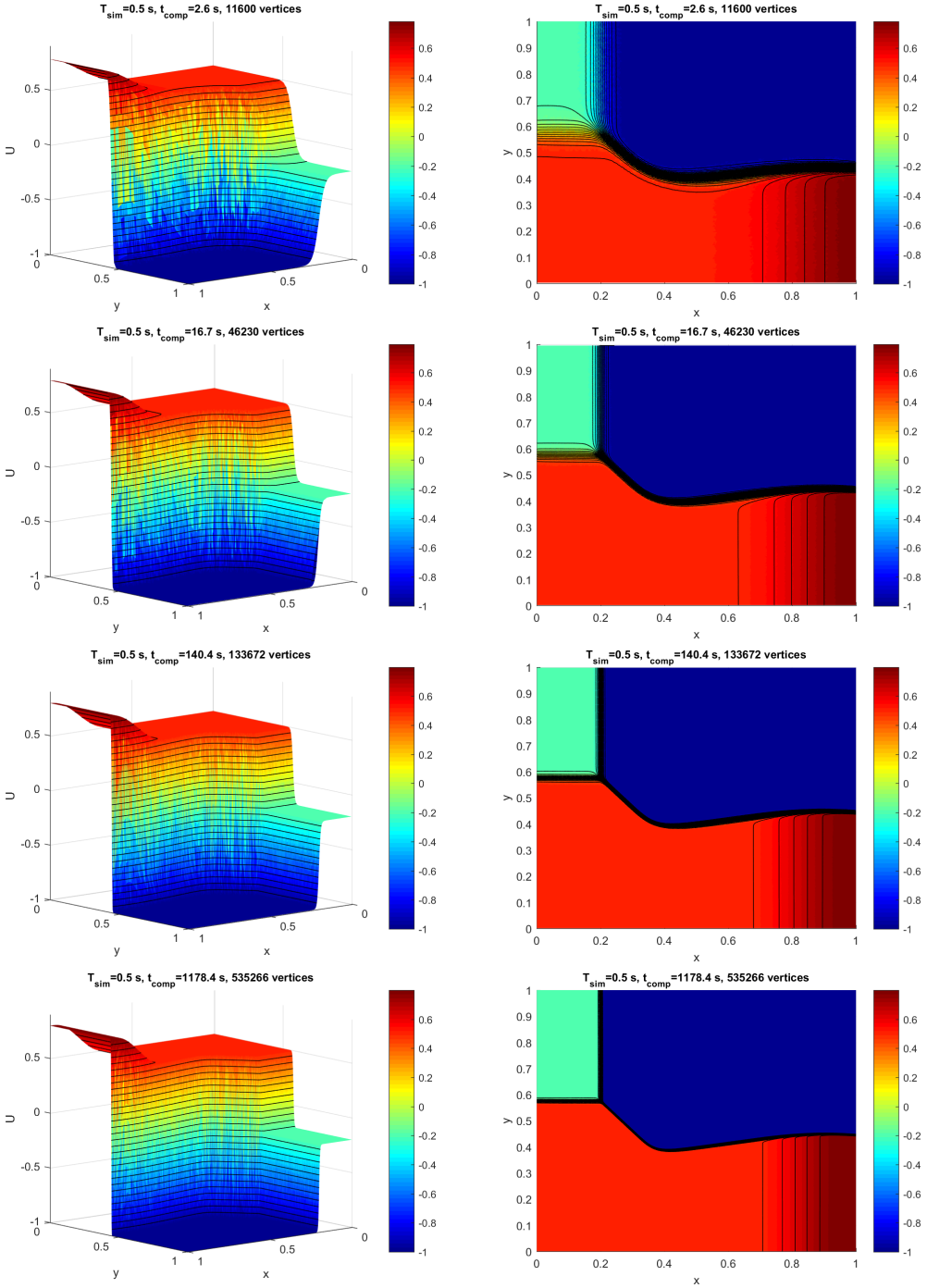

Figure 2.12: Solution to the inviscid Burgers problem at t=0.5; the CFL number is equal to 0.0833.

2.3.6 The sonic point for the inviscid Burgers' equation

We finish the 2D scalar tests by presenting a numerical experiment associated with the classical inviscid nonlinear Burgers' equation (2.133) subject to the initial condition

$$u_0(x,y) = \begin{cases} -1, & x < 0,\ -1.5 < y < 1.5, \\ 1, & x > 0,\ -1.5 < y < 1.5. \end{cases}$$

The sonic point, that the rarefaction wave finds at $(0,0)$, occurs due to the sign change in the

characteristic velocity. As Figure 2.13 shows, the fully-discrete Lagrangian-Eulerian scheme on triangular grids is able to capture both resonance and sonic effects with no spurious anomalies.

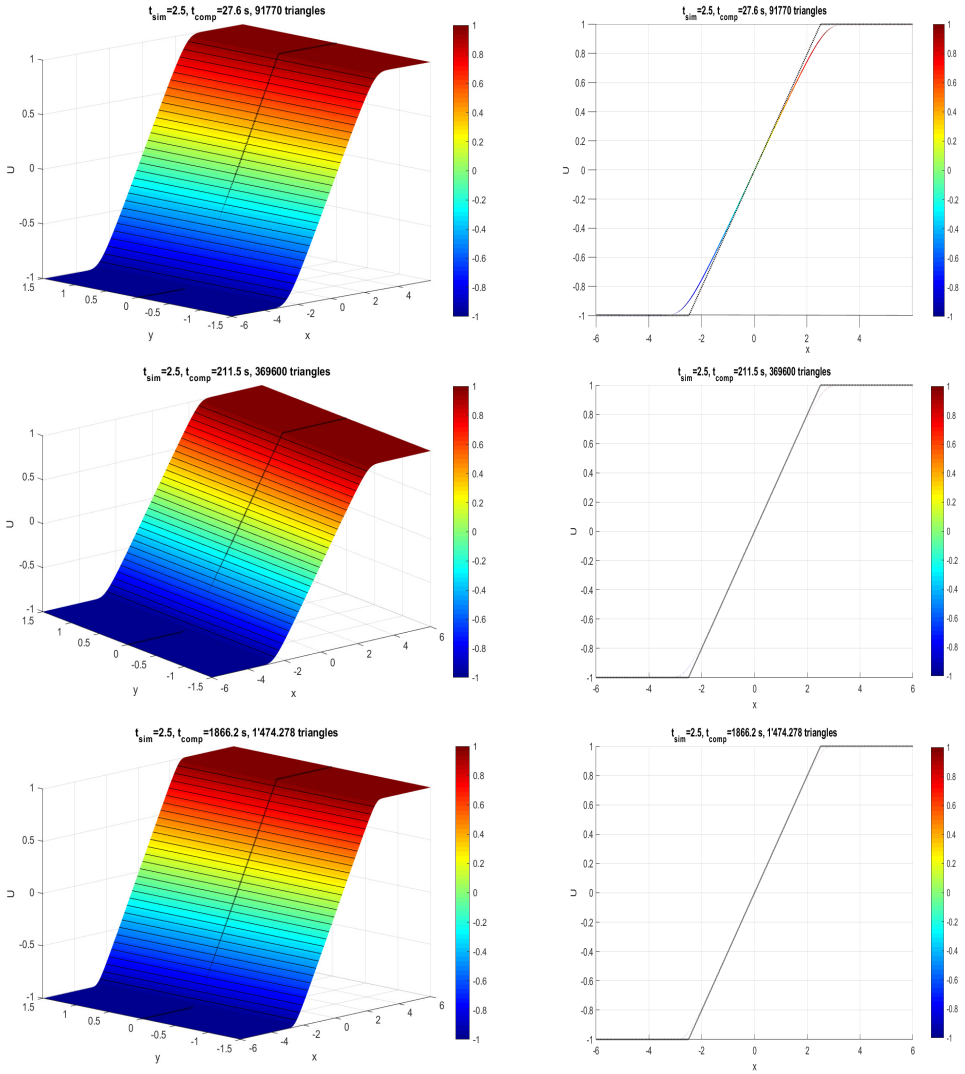

Figure 2.13: Solution to the sonic point for the inviscid Burgers' equation at t=2.5. The CFL number is equal to 1/10.

2.3.7 Non-strictly hyperbolic three-phase system of conservation laws in porous media applications

Below, we present the numerical results of the injection problems for Riemann data, namely RP_1 and RP_2, whose left and right states are given by

$$RP_1 : \begin{cases} S_w^L = 0.613 & \text{and} \quad S_w^R = 0.05, \\ S_g^L = 0.387 & \text{and} \quad S_g^R = 0.15, \end{cases} \quad RP_2 : \begin{cases} S_w^L = 0.721 & \text{and} \quad S_w^R = 0.05, \\ S_g^L = 0.279 & \text{and} \quad S_g^R = 0.15. \end{cases}$$

From [18, 135], we understand the correct structure of the solutions in the non-classical three-phase model under consideration. A transitional shock wave is present in the solution to RP_2 but not in the solution to RP_1.

To exhibit the effect of grid refinement in the numerical solution to (refeq:TPS) with Riemann data (RP_1 and RP_2), Figure 2.14 illustrates the water and gas saturation profiles and Figures 2.16

and 2.17, the oil saturation profile. The RP_1 problem is displayed on the top and the RP_2, on the bottom. Such computed saturation profiles are shown at dimensionless time: 2.50. From such figures, it is clear that, as the grid is refined, we obtain some evidence of the numerical convergence of our scheme.

Figures 2.15 and 2.18 depict the numerical simulations of water, gas, and oil distribution, respectively, at dimensionless time 200 in a reservoir with a size of 512 m $\times$ 128 m. In these simulations, $x = 0$ denotes the reservoir inflow; and $x = 512$, its outflow.

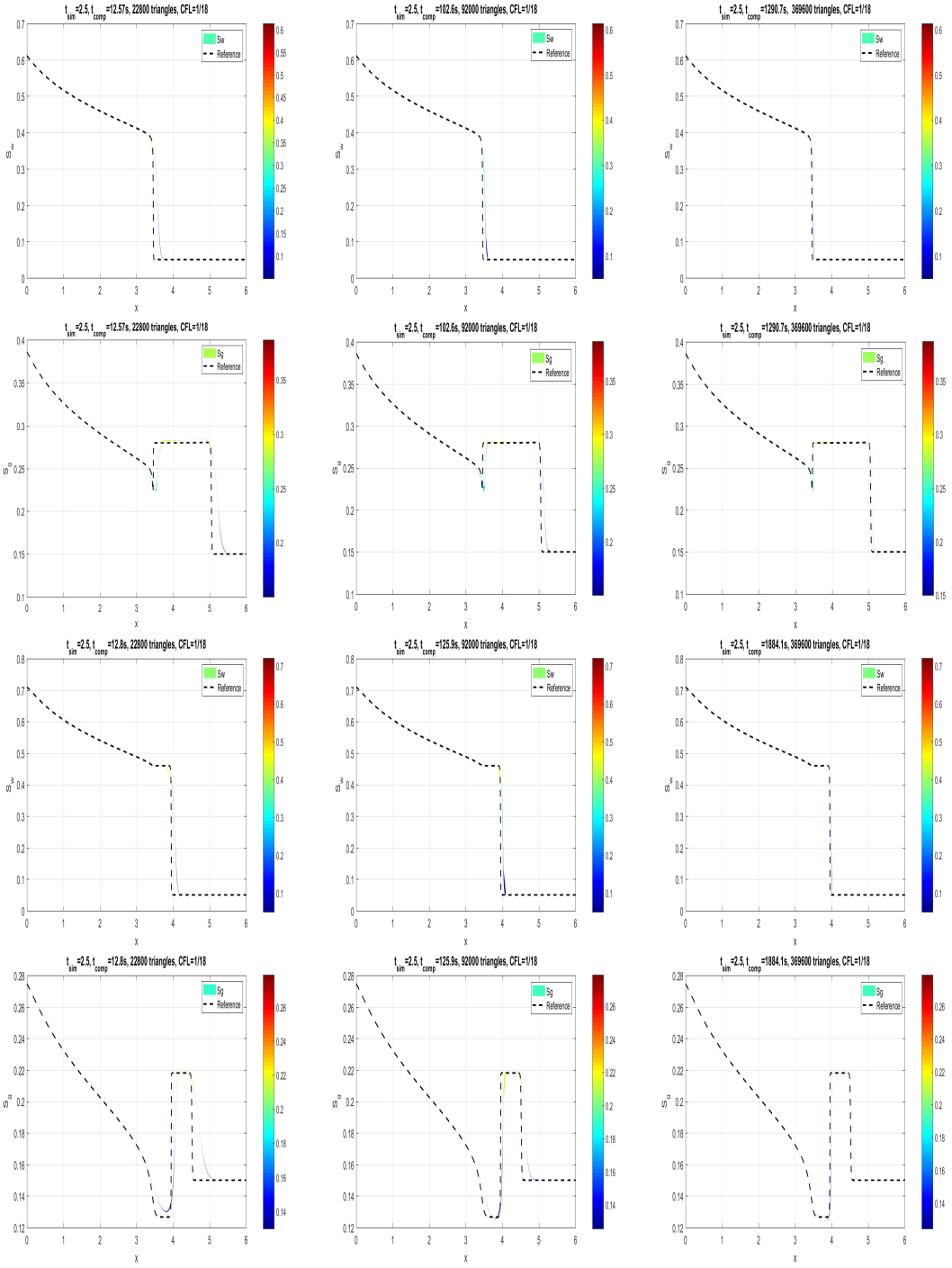

Figure 2.14: grid refinement study against a reference solution. Water and gas saturation profiles are shown as a function of distance. $RP1$ (on the top) and $RP2$ (on the bottom).

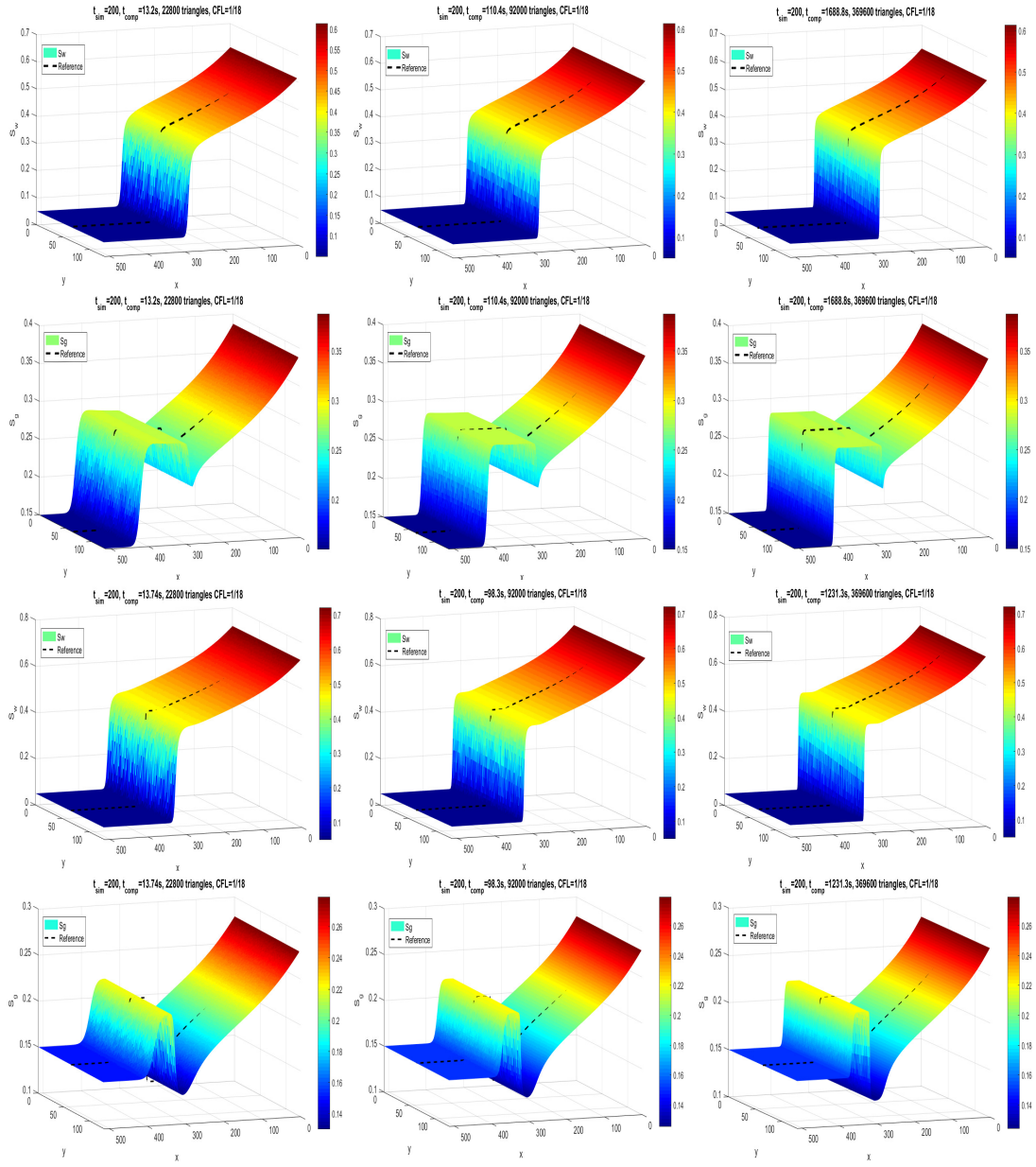

Figure 2.15: Numerical simulations of water and gas distribution in a reservoir with a size of 512 m × 128 m. $RP1$ (on the top) and $RP2$ (on the bottom).

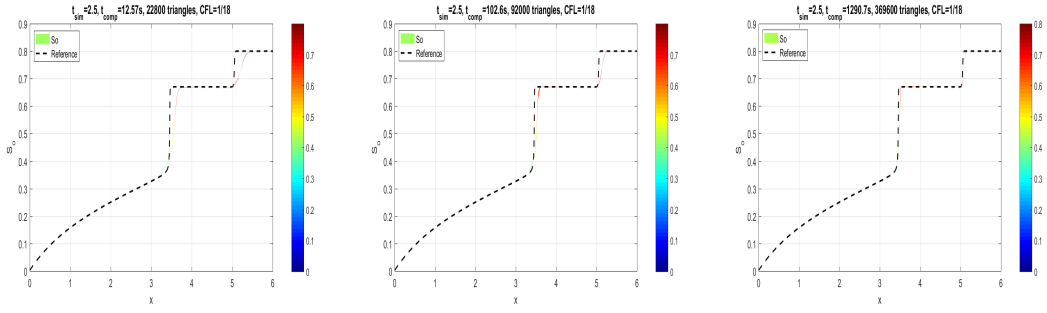

Figure 2.16: Grid refinement study against a reference solution. Oil saturation profiles are shown as a function of distance. $RP1$ (on the top) and $RP2$ (on the bottom).

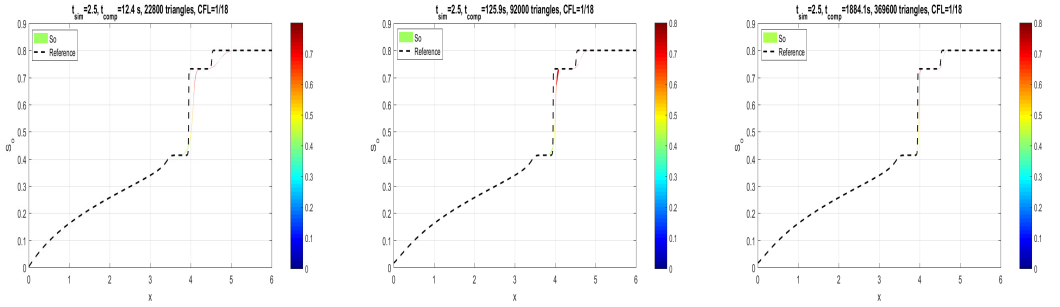

Figure 2.17: Grid refinement study against a reference solution. Oil saturation profiles are shown as a function of distance. $RP1$ (on the top) and $RP2$ (on the bottom).

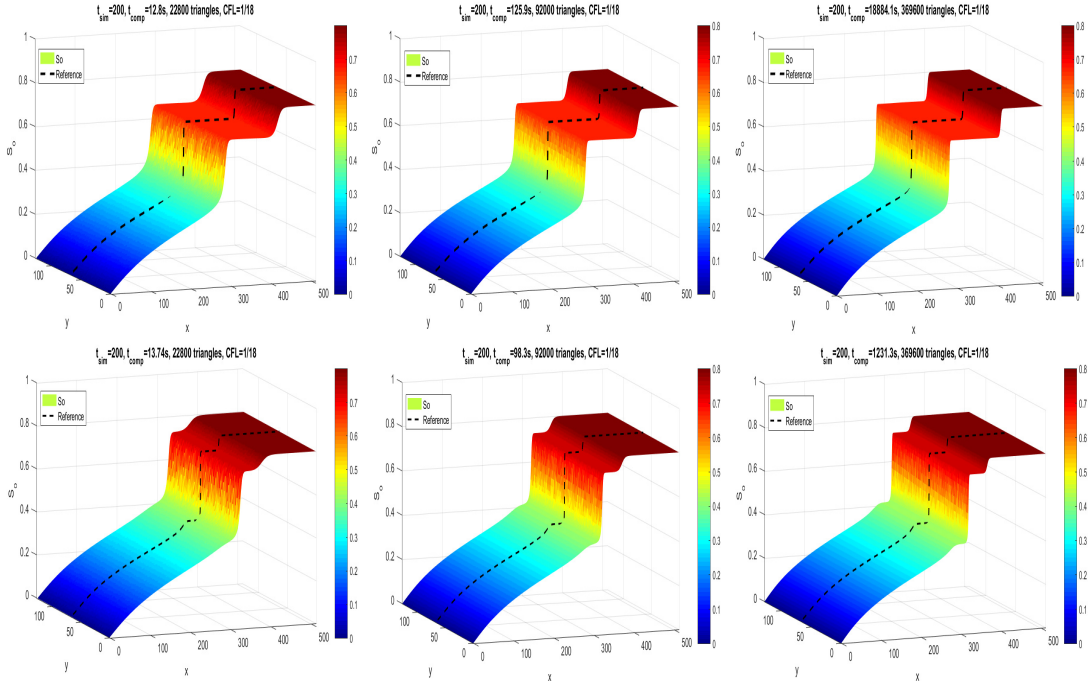

Figure 2.18: Numerical simulations of oil distribution in a reservoir with a size of 512 m $\times$ 128 m. $RP1$ (on the top) and $RP2$ (on the bottom).

2.3.8 Shallow water system with non-flat bottom and discontinuous topography

Continuing with hyperbolic systems of conservation laws, we discuss in this section, the shallow water problem. The shallow-water equations (1.2), which are derived from equations of conservation of mass and conservation of linear momentum, can be written as

$$\partial_t \begin{pmatrix} H \\ hu \\ hv \end{pmatrix} + \partial_x \begin{pmatrix} Hu \\ hu^2 + \frac{1}{2}gh^2 \\ huv \end{pmatrix} + \partial_y \begin{pmatrix} Hv \\ huv \\ hv^2 + \frac{1}{2}gh^2 \end{pmatrix} = \begin{pmatrix} (Zu)_x + (Zv)_y \\ -ghZ_x \\ -ghZ_y \end{pmatrix}. \tag{2.134}$$

We shall study the 2D system (2.134) subject to the initial conditions

$$h(x,y,0) = \begin{cases} 3.5 - Z(x,y), & x < 5, \\ 2.5 - Z(x,y), & x > 5, \end{cases}, \quad u(x,y,0) = v(x,y,0) = 0,$$

on the square domain $[0,10] \times [0,10]$. The gravitational constant g is taken equal to 1.

First, we perform numerical tests for purely hyperbolic shallow-water equations (2.134) (no bottom topography), i.e, $Z(x,y) \equiv 0$ and then, for the shallow water system (2.134) subject to the initial conditions with bottom topography, $Z(x,y) = 2-(x-5)^2-(y-5)^2$, $|x-5|<1$, $|y-5|<1$. In the second case, the source term is approximated by evaluating it at the approximate value of the conserved variables.

For both problems, we have two waves travelling in opposite directions on the $x-$ axis: a shock wave moving to the right, and a rarefaction wave moving to the left.

Fig. 2.19 provide numerical approximations with good resolution performed on relatively coarse grids allowing verify the capabilities of the fully-discrete Lagrangian-Eulerian scheme and to show numerical robustness of the flux separation strategy (see [10]).

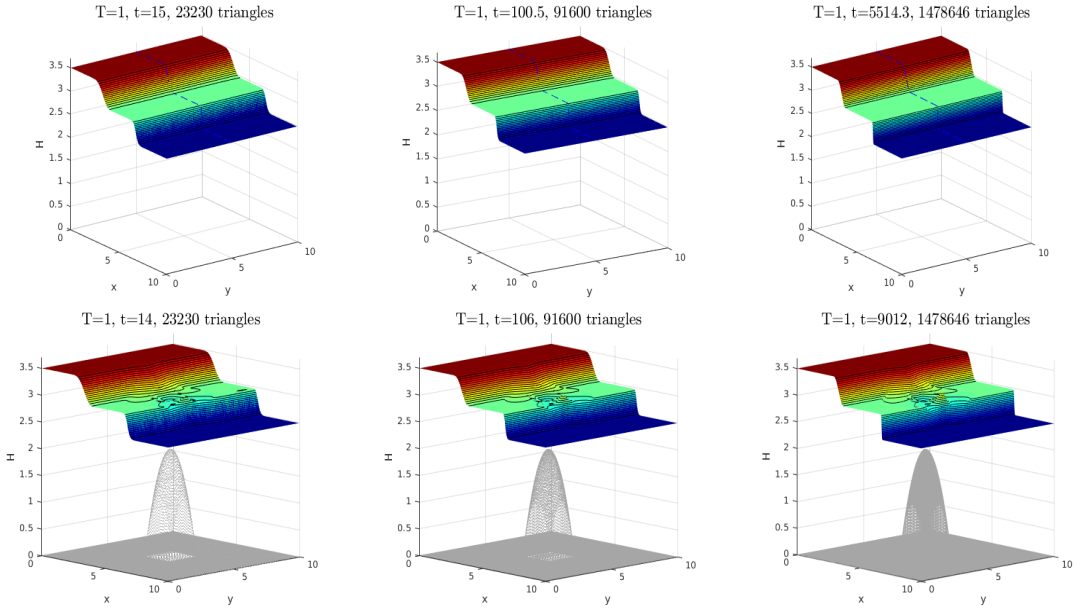

Figure 2.19: H pictures for Shallow water problem in $T = 1$. CFL=0.025. No bottom: 1st; with bottom: 2nd.

2.3.9 Two-dimensional Euler equations for gas dynamics

In this section, we solve the Euler equations (1.8) with different sets of initial conditions, via the fully-discrete Lagrangian-Eulerian scheme (2.19)-(2.20).

Using the flux separation strategy, system (1.8) takes the form

$$\partial_t \begin{pmatrix} \rho \\ \rho u \\ \rho v \\ E \end{pmatrix} + \partial_x \begin{pmatrix} \rho u \\ \rho u^2 \\ \rho uv \\ uE \end{pmatrix} + \partial_y \begin{pmatrix} \rho v \\ \rho uv \\ \rho v^2 \\ vE \end{pmatrix} = \begin{pmatrix} 0 \\ -p_x \\ -p_y \\ -(up)_x - (vp)_y \end{pmatrix}. \tag{2.135}$$

The equation of state of an ideal gas (1.10) is used to close the system.

• Involving slip line initial data

Fig. 2.20 shows the results obtained for two set of initial conditions shown in Table 2.1 (RP1 on the top and RP2 on the bottom), in which the unit square $[0,1]^2$ is divided in four quadrants by the lines $x = \frac{1}{2}$ and $y = \frac{1}{2}$. These initial data give rise to interacting contact discontinuities. The RP1 features slip lines that enter a subsonic area and end in a spiral (in the center), while the

$\begin{pmatrix}\rho_2\\u_2\\v_2\\p_2\end{pmatrix} = \begin{pmatrix}2\\-0.75\\-0.5\\1\end{pmatrix}$	$\begin{pmatrix}\rho_1\\u_1\\v_1\\p_1\end{pmatrix} = \begin{pmatrix}1\\-0.75\\0.5\\1\end{pmatrix}$
$\begin{pmatrix}\rho_3\\u_3\\v_3\\p_3\end{pmatrix} = \begin{pmatrix}1\\0.75\\0.5\\1\end{pmatrix}$	$\begin{pmatrix}\rho_4\\u_4\\v_4\\p_4\end{pmatrix} = \begin{pmatrix}3\\0.75\\-0.5\\1\end{pmatrix}$
$\begin{pmatrix}\rho_2\\u_2\\v_2\\p_2\end{pmatrix} = \begin{pmatrix}1.0222\\-0.6179\\0.1\\1\end{pmatrix}$	$\begin{pmatrix}\rho_1\\u_1\\v_1\\p_1\end{pmatrix} = \begin{pmatrix}0.5313\\0.1\\0.1\\0.4\end{pmatrix}$
$\begin{pmatrix}\rho_3\\u_3\\v_3\\p_3\end{pmatrix} = \begin{pmatrix}0.8\\0.1\\0.1\\1\end{pmatrix}$	$\begin{pmatrix}\rho_4\\u_4\\v_4\\p_4\end{pmatrix} = \begin{pmatrix}1\\0.1\\0.8276\\1\end{pmatrix}$

Table 2.1: Initial conditions. P1: left and P2: right

RP2 features four subsonic area slip lines that bend and end in two spirals. As can be seen in the figure, these features are accurately captured by the fully-discrete Lagrangian-Eulerian scheme.

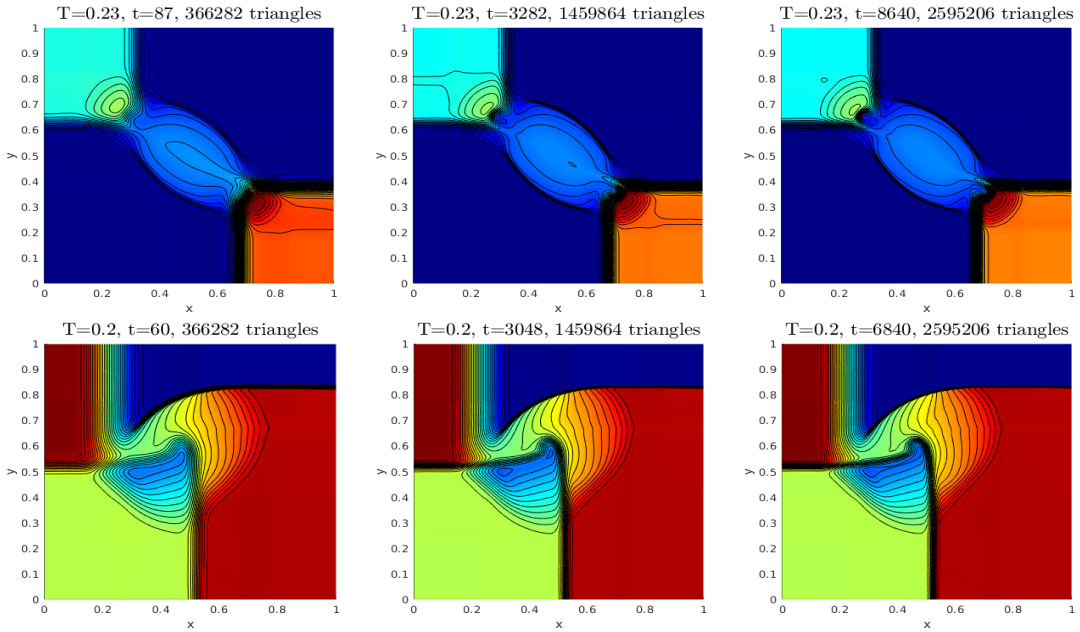

Figure 2.20: Slip line initial data simulations at $T = 0.23$ and $T = 0.2$. CFL=0.15 (P1); CFL=0.175 (P2). P1: top; P2: bottom.

- **Mach Reflection Problem**

The double Mach reflection (DMR) problem is a benchmark test that consits of a shock wave sent diagonally into a reflecting rigid wall.
The DMR problem is modeled by (1.8) and defined in the rectangular region $[0, 4] \times [0, 1]$. Initially a shock moves diagonally with a Mach 10 forming an angle of $\pi/3$ with the $x-$axis. The pre- and

post- shock conditions corresponding to the initial conditions are:

$$(\rho, u, v, p)(x, y, 0) = \begin{cases} (1.4, 0, 0, 1), & x > 1/6 + y/\tan(\pi/3) \\ (8, 8.25\cos(\pi/6), -8.25\sin(\pi/6), 116.5), & x < 1/6 + y/\tan(\pi/3) \end{cases} \quad (2.136)$$

The boundary conditions are as follows. At the left (the inflow boundary), we impose post-shock values; at the right (the outflow boundary), Neumann conditions. At the bottom ($y = 0$), we impose reflecting boundary conditions on $[1/6, 4]$ and exact post-shock conditions otherwise. At the top ($y = 1$) we set the pre- and post-shock conditions in a time dependent manner ($x_s(t) = 10t/\sin(\pi/3) + 1/6 + 1/\tan(\pi/3)$) by tracking the shock exactly.
We display in Fig. 2.21 the density and the pressure obtained by the numerical solution with the fully-discrete Lagrangian-Eulerian scheme. As can be seen, the main aspects of the simulation, such as the formation of the jet and the incident shock are well captured by the fully-discrete Lagrangian-Eulerian scheme.

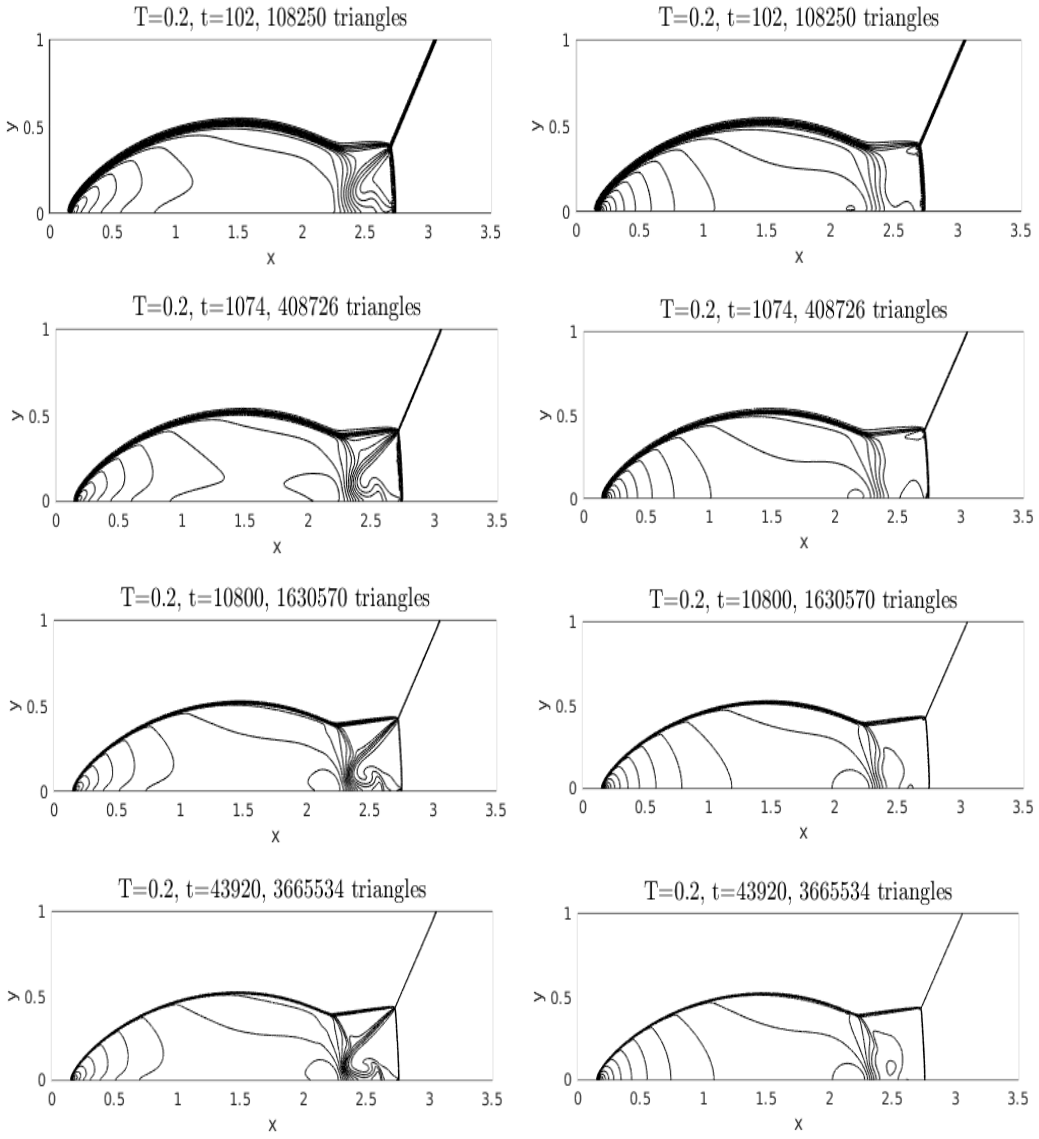

Figure 2.21: DMR simulations at $T = 0.2$. CFL=0.03. Density: left; Pressure: right

• 3 wind tunnel with a step

The 2D wind tunnel is 3 units long and 1 unit wide with a step of 0.2 units high located at 0.6 units from the tunnel inlet. The initial condition is a Mach 3 right-going uniform flow. Reflective boundary conditions are specified on the solid walls of the tunnel, i.e $(u, v)^T \cdot \mathbf{n} = 0$, where $\mathbf{n}$ is the outward unit normal to $\partial\Omega$, while inflow and outflow boundary conditions are used at the inlet and the outlet. Initially, the wind tunnel is filled with a gamma-law gas, with $\gamma = 1.4$, which everywhere has density 1.4, pressure 1.0 and velocity 3.

In an attempt to minimize numerical errors generated at the corner of the step and obtain a good quality solution, in our tests, as in [151], an additional boundary condition is applied in this corner, in order to maintain a steady flow around this singular point. In the first row of zones above the step we will reset the first four zones starting just to the right of the comer of the step; in the row above we will reset the first two zones. In these zones we reset the density so that the entropy has the same value as in the zone just to the left and below the comer of the step. We also reset the magnitudes of the velocities, not their directions, so that the sum of enthalpy and kinetic energy per unit mass has the same value as in the same zone used to set the entropy.

A mesh grid refinement study is shown in Fig. 2.22. In these simulations, it can be observed that our scheme well captures the front shock as well as the rarefaction near the singular point. Also, no noise or a boundary layer is observed along the top of the step. In short, all the main characteristics of the wave patterns are shown.

2.3.10 Orszag-Tang MHD turbulence problem

The Orszag-Tang problem (See [31, 32, 98, 139, 152, 154, 155]), which is a model to study MHD turbulence, is a compressible vortex system that involves the interaction between several shock waves travelling at various speed regimes, which makes the problem useful to validate the robustness of numerical schemes.

Here, we use the fully-discrete Lagrangian-Eulerian scheme to calculate the evolution of the equations (1.3)-(1.6) in two space dimensions with the initial data,

$$\begin{aligned} &\rho(x, z, 0) = \gamma^2,\ v_x(x, z, 0) = -\sin z,\ v_z(x, z, 0) = \sin x, \\ &p(x, z, 0) = \gamma,\ B_x(x, z, 0) = -\sin z,\ B_z(x, z, 0) = \sin 2x, \end{aligned}$$

where $\gamma = 5/3$. With these data, the average magnitude of the velocities and the magnetic fields are both 1; the initial average Mach number is 1; and the average plasma beta is 10/3.

We solve the problem in $[0, 2\pi] \times [0, 2\pi]$ with periodic boundary conditions in both x and $z-$directions.

System (1.3)-(1.6) is written in conservative form as

$$\partial_t \begin{pmatrix} \rho \\ \rho v_x \\ \rho v_y \\ \rho v_z \\ B_x \\ B_y \\ B_z \\ e \end{pmatrix} + \partial_x \begin{pmatrix} \rho v_x \\ \rho v_x^2 + p^* - B_x^2 \\ \rho v_x v_y - B_x B_y \\ \rho v_x v_z - B_x B_z \\ 0 \\ B_y v_x - B_x v_y \\ B_z v_x - B_x v_z \\ (e + p^*) v_x - B_x (v \cdot B) \end{pmatrix} + \partial_y \begin{pmatrix} \rho v_z \\ \rho v_z v_x - B_z B_x \\ \rho v_z v_y - B_z B_y \\ \rho v_z^2 + p^* - B_z^2 \\ B_x v_z - B_z v_x \\ B_z v_y - B_z v_y \\ 0 \\ (e + p^*) v_z - B_z (v \cdot B) \end{pmatrix} = 0, \tag{2.137}$$

where $p^* = p + \frac{1}{2} B^2$.

To apply our fully-discrete Lagrangian-Eulerian scheme, again we use the flux separation strategy as in Section 10.10. In short, in this approach we rewrite system (2.137) in an equivalent conservative form viewed as a generalized hyperbolic balance law as $\mathbf{q}_t + \mathbf{F}_1(\mathbf{q})_x + \mathbf{G}_1(\mathbf{q})_z =$

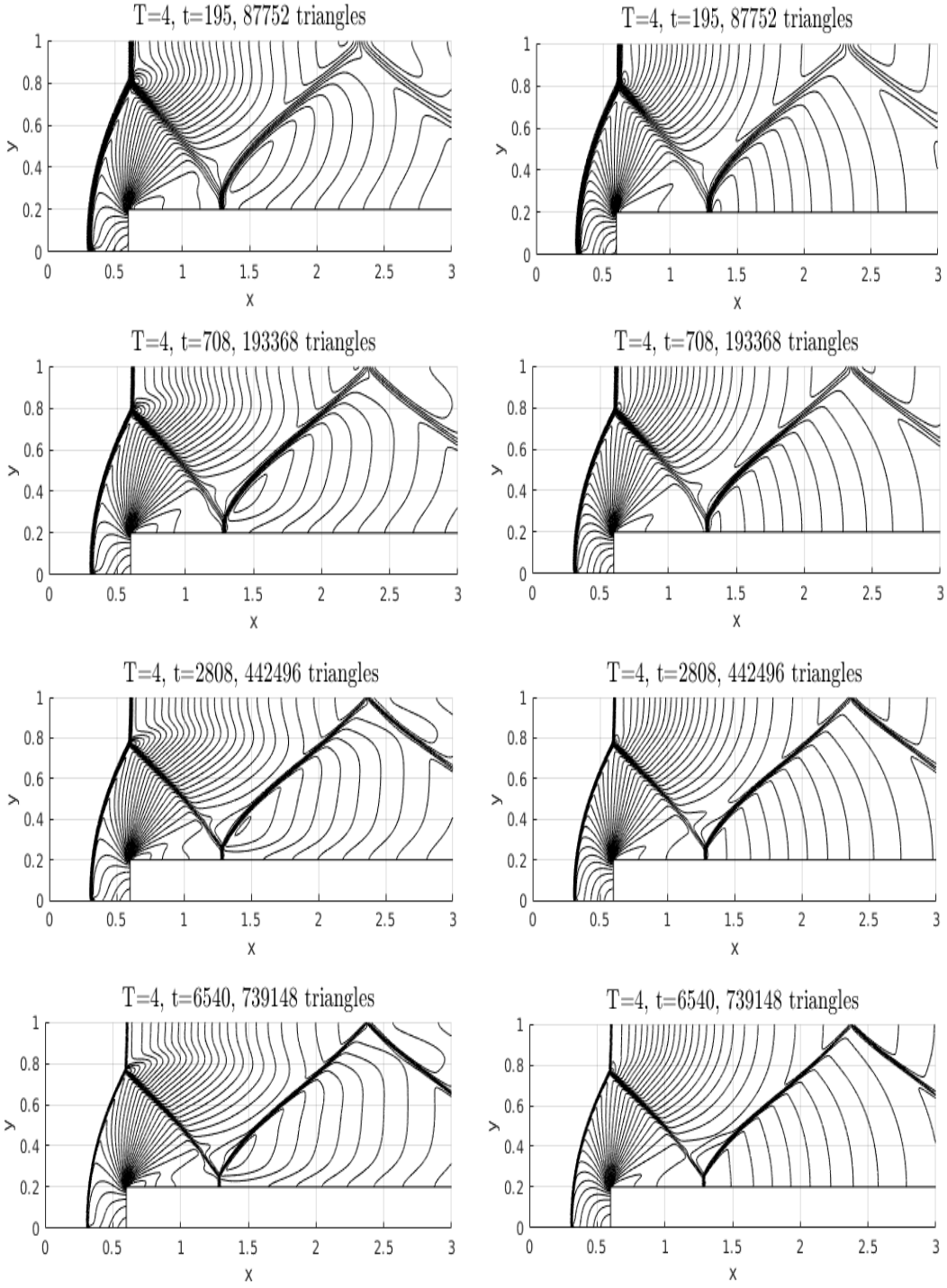

Figure 2.22: M3WT simulations at $T = 4$. CFL=0.15. Density: left; Pressure: right

$-\mathbf{F}_2(\mathbf{q})_x - \mathbf{G}_2(\mathbf{q})_z$ where $\mathbf{F}_1(\mathbf{q}) + \mathbf{F}_2(\mathbf{q}) = \mathbf{F}(\mathbf{q})$ and $\mathbf{G}_1(\mathbf{q}) + \mathbf{G}_2(\mathbf{q}) = \mathbf{G}(\mathbf{q})$ with

$$\mathbf{F}_1(\mathbf{q}) = \begin{pmatrix} \rho v_x \\ \rho v_x^2 \\ \rho v_x v_y \\ \rho v_x v_z \\ 0 \\ B_y v_x \\ B_z v_x \\ e v_x \end{pmatrix}, \mathbf{F}_2(\mathbf{q}) = \begin{pmatrix} 0 \\ p^* - B_x^2 \\ -B_x B_y \\ -B_x B_z \\ 0 \\ -B_x v_y \\ -B_x v_z \\ p^* v_x - B_x (v \cdot B) \end{pmatrix}, \mathbf{G}_1(\mathbf{q}) = \begin{pmatrix} \rho v_z \\ \rho v_z v_x \\ \rho v_z v_y \\ \rho v_z^2 \\ B_x v_z \\ B_z v_y \\ 0 \\ e v_z \end{pmatrix}, \mathbf{G}_2(\mathbf{q}) = \begin{pmatrix} 0 \\ -B_z B_x \\ -B_z B_y \\ p^* - B_z^2 \\ -B_z v_x \\ -B_z v_y \\ 0 \\ p^* v_z - B_z (v \cdot B) \end{pmatrix}$$

Figures 2.23, 2.24, and 2.25 display the solution of the Orszag-Tang vortex system at $t = 0.5$, $t = 2$, and $t = 3$, respectively. These results demonstrate the capability and effectiveness of fully-discrete Lagrangian-Eulerian scheme to resolve the shocks developed by the vortex system without the need of adding some correction technique to prevent divergence errors from increasing with time as in [31] (see also [98]) while maintaining the simplicity and ease of implementation.

Following [32], we quantitatively study the divergence error in the numerical magnetic field $\mathbf{B_h}$. Based in this paper, a standard way to measure the global divergence error is as follows

$$\|\nabla \cdot \mathbf{B}_h\|_{*,h} := \sum_{L \in N(K)} \int_{K|L} \big| \left[\mathbf{n}_{KL} \cdot \mathbf{B}_h\right] \big| ds + \sum_K \int_K |\nabla \cdot \mathbf{B}_h| \, d\mathbf{x}, \tag{2.138}$$

where $[\mathbf{n}_{KL} \cdot \mathbf{B}_h]$ denotes the jump of the normal component of $\mathbf{B}_h$ on the edge $K|L$. Then, the global relative divergence error is defined by

$$\xi_{div} := \frac{\|\nabla \cdot \mathbf{B}_h\|_{*,h}}{\|\mathbf{B}_h\|_{*,h}}, \text{ with } \|\mathbf{B}_h\|_{*,h} := \sum_{L \in N(K)} \int_{K|L} |\mathbf{B}_h| \, ds + \sum_K \int_K |\mathbf{B}_h| \, d\mathbf{x}. \tag{2.139}$$

In Fig. 2.26, we plot ξ_{div} against time t. It is observed that, during the entire simulation, the magnitude of ξ_{div} is kept at order $\mathcal{O}(10^{-4})$. Finally, Fig. 2.27 depicts the discrete divergence operator (2.138) and the corresponding magnetic field for two different grid refinements.

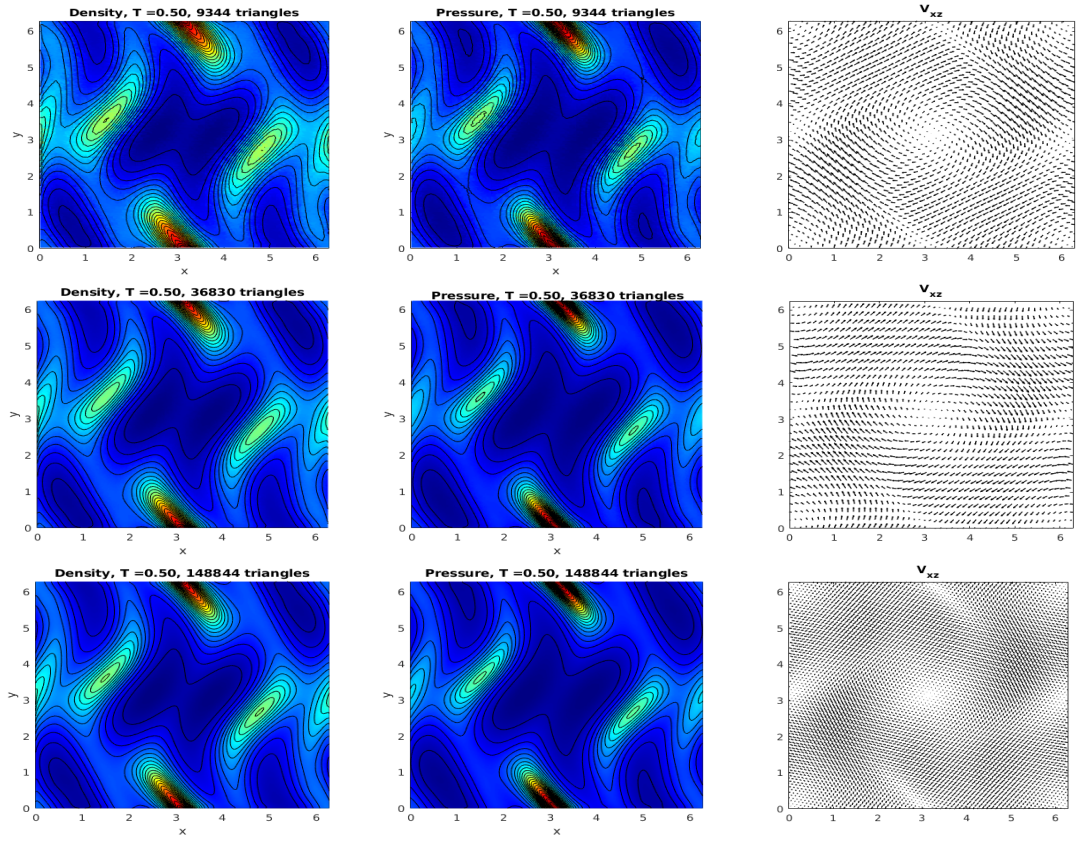

Figure 2.23: Simulations of the Orszag–Tang problem at $T = 0.5$. CFL=0.125. Density (left); pressure (center); velocity field (right).

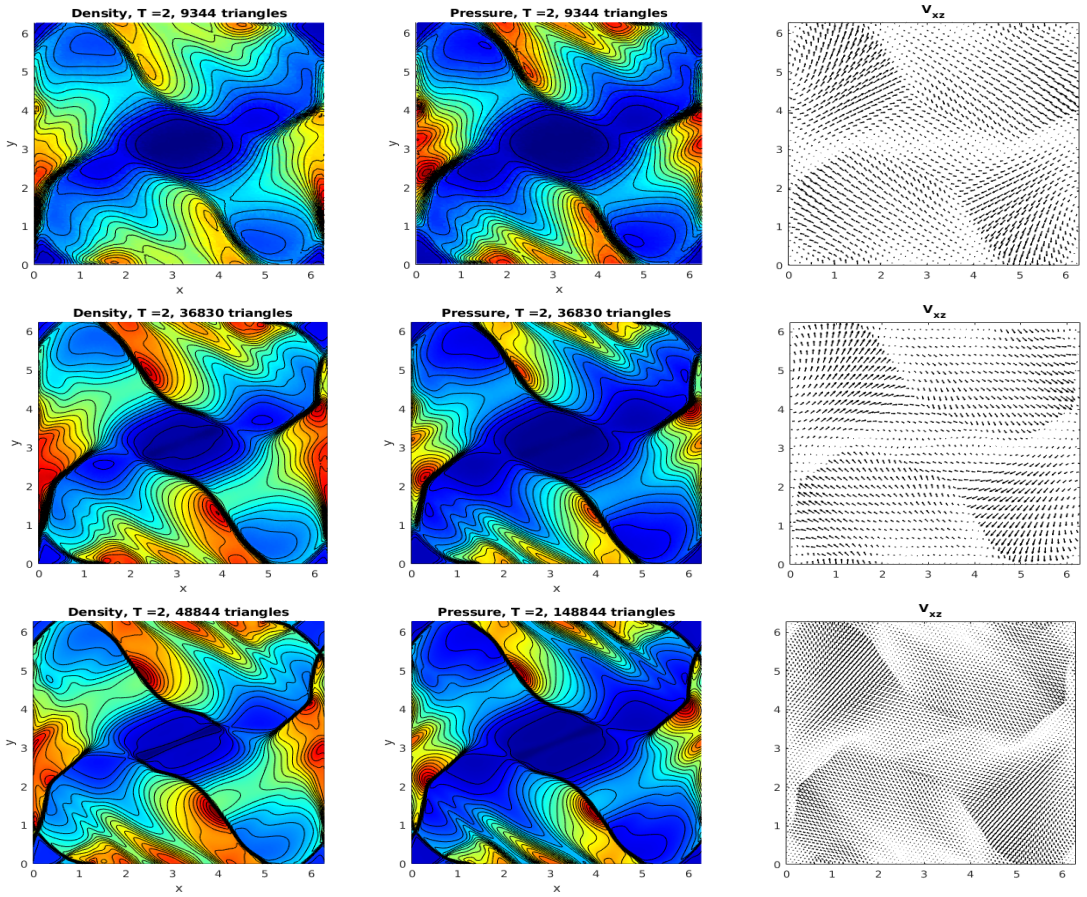

Figure 2.24: Simulations of the Orszag–Tang problem at $T = 2$. CFL=0.125. Density (left); pressure (center); velocity field (right).

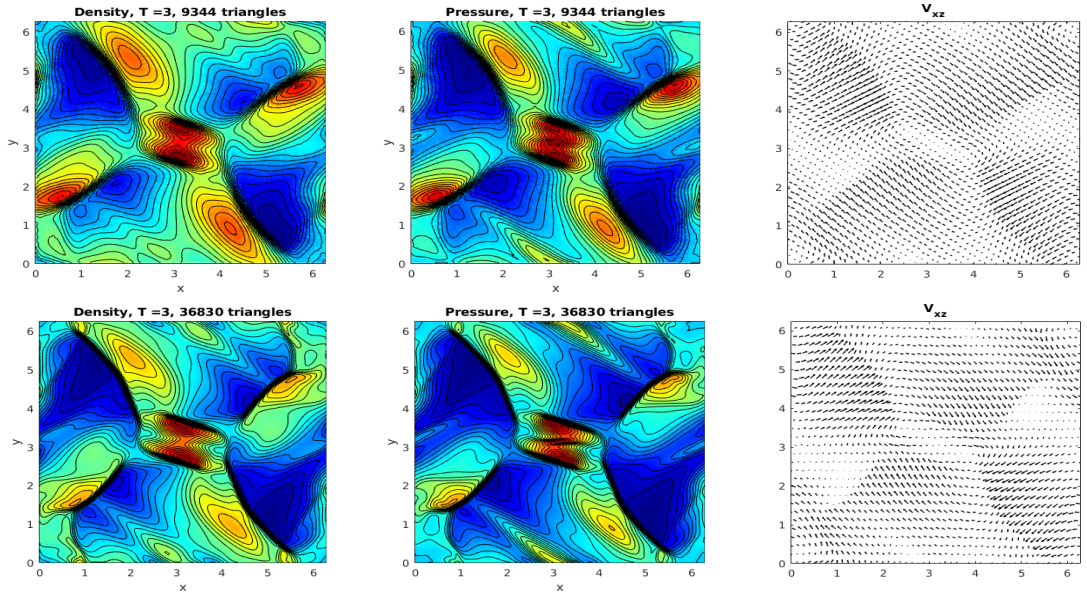

Figure 2.25: Simulations of the Orszag–Tang problem at $T = 3$. CFL=0.125. Density (left); pressure (center); velocity field (right).

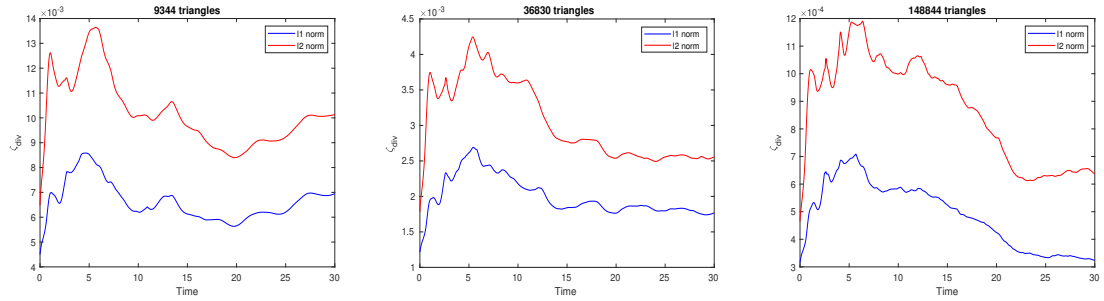

Figure 2.26: Global Relative Divergence Error.

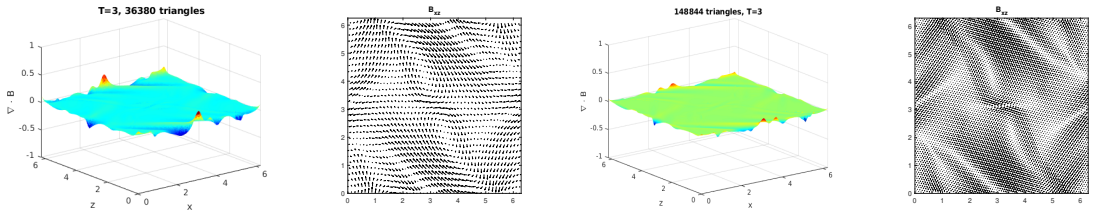

Figure 2.27: Magnetic field divergence (1st and 3st) and Magnetic field (2nd and 4th) at $t = 3$.

2.4 Experimental Order of Convergence of the Fully-Discrete Lagrangian-Eulerian Scheme on Triangular Grids

This section include the experimental order of convergence (EOC) of the fully-discrete scheme defined by,

$$EOC = \frac{\log(e_i/e_{i+1})}{\log(N_{i+1}/N_i)}, \tag{2.140}$$

where e_i is the relative error in the L_1-norm given by

$$e_i = \frac{\|U_i - U_{i+1}\|_{L^1}}{\|U_{i+1}\|_{L^1}}. \tag{2.141}$$

In Eq. (2.141), i stands for the refinement number (so, i and $i+1$ are consecutive refinement numbers) and for the refinement i, N_i stand for the number of triangles.

The reported results in the tables below are consistent with the theoretical order of convergence obtained in Theorem 2.2.5.

i	N_i	e_i	EOC
1	4312	0.047982	-
2	17776	0.024888	0.4634
3	70350	0.013063	0.4686
4	282100	0.0065508	0.4970
5	1128200	0.0032486	0.5060
6	4522000	0.0016215	0.5005

Table 2.2: Error and order of convergence for linear Problem (see Figure 2.3)

i	N_i	e_i	EOC
1	3268	0.032160	-
2	12750	0.017531	0.4457
3	51554	0.0091389	0.4663
4	206310	0.0045024	0.5105
5	829200	0.0022133	0.4804
6	3324000	0.0011074	0.4987

Table 2.3: Error and order of convergence for Burger's equation in $t = 1$. Pre-shock (see Figure 2.5)

i	N_i	e_i	EOC
1	3268	0.032426	-
2	12750	0.017108	0.4697
3	51554	0.0088068	0.4753
4	206310	0.0044988	0.4844
5	829200	0.0023109	0.4789
6	3324000	0.001183	0.4822

Table 2.4: Error and order of convergence for Burger's equation in $t = 3$. Post-shock (see Figure 2.6)

i	N_i	e_i	EOC
1	3268	0.031831	-
2	12750	0.021269	0.2962
3	51900	0.011209	0.4563
4	207000	0.00576	0.4813
5	829200	0.003009	0.4676
6	3324000	0.0016102	0.4503

Table 2.5: Error and order of convergence for the Burgers oblique problem (see Figure 2.12)

i	N_i	e_i	EOC
1	3182	0.08922	-
2	12750	0.054955	0.3491
3	51900	0.034026	0.3415
4	207000	0.020484	0.3668
5	829200	0.01222	0.3723
6	3324000	0.007025	0.3987

Table 2.6: Error and order of convergence for BL's equation (see Figures 2.9 and 2.10)

i	N_i	e_i	EOC
1	1296	0.074561	-
2	5586	0.051852	0.2486
3	22770	0.029512	0.3636
4	91142	0.017824	0.3745
5	368800	0.010439	0.3827
6	1476800	0.006047	0.3935

Table 2.7: Error and order of convergence for Non-Convex's equation (see Figures 2.7 and 2.8)

i	N_i	e_i	EOC
1	350	0.041028	-
2	1500	0.027727	0.2693
3	5800	0.017888	0.3241
4	22800	0.01157	0.3183
5	92000	0.0069566	0.3647
6	369600	0.004215	0.3603

Table 2.8: Error and order of convergence for the three phase system $RP1$ (see Figures 2.14, 2.15, 2.16, 2.17, and 2.18)

i	N_i	e_i	EOC
1	540	0.020642	-
2	2142	0.013791	0.2927
3	8750	0.008299	0.3609
4	35500	0.005064	0.3527
5	145000	0.002883	0.4003
6	578000	0.001650	0.4035

Table 2.9: Error and order of convergence for sonic point (see Figure 2.13)

3. The Semi-Discrete Lagrangian-Eulerian Schemes on Triangular Grids: Design, Analysis, and Implementation

In this chapter, based on the same framework of the fully-discrete Lagrangian-Eulerian schemes, we introduce a new class of semi-discrete Lagrangian-Eulerian schemes on triangular grids (SDLET schemes), prove their convergence to the entropy solution for scalar problems, and show that they satisfy the posivity principle for systems.

3.1 Construction of the Semi-Discrete Lagrangian-Eulerian Schemes on Triangular Grids

The semi-discrete Lagrangian-Eulerian schemes on triangular grids proposed in this work are based on the novel concept of Lagrangian-Eulerian no-flow surfaces/curves (per time step), which has been previously implemented for fully-discrete Lagrangian-Eulerian schemes.

Formally, the explicit semi-discrete Lagrangian-Eulerian schemes on triangular grids are constructed from the fully-discrete Lagrangian-Eulerian schemes (2.19)–(2.22) as follows.

Thanks to the stability coefficient of the Lagrangian-Eulerian numerical flux function (2.22), $Q_{LE}\Big(\frac{\mathbf{f}(u_K^n)}{u_K^n}, \frac{\mathbf{f}(u_L^n)}{u_L^n}; \mathbf{n}_{KL}\Big)$, does not depend on $\mathcal{O}(1/\Delta t)$, it has no blow-up singularity as $\Delta t \to 0^+$. Therefore, the limit as $\Delta t \to 0^+$ in Eq. (2.19) leads to

$$\begin{cases} u_K^0 = \dfrac{1}{m(K)} \displaystyle\int_K u(0,\mathbf{x}) d\mathbf{x}, \\ \dfrac{d}{dt} u_K(t) = -\dfrac{1}{|K|} \displaystyle\sum_{L \in N(K)} \mathcal{F}(u_K(t), u_L(t); \mathbf{n}_{KL}) := \mathcal{L}(u_K(t), u_L(t)). \end{cases} \tag{3.1}$$

Eqs. (3.1) and (2.22) correspond to the semi-discrete Lagrangian-Eulerian schemes on triangular grids.

The stability coefficient linked to the no-flow curves, which is a powerful key ingredient for this class of semi-discrete schemes (3.1)–(2.22), produces an accurate approximation of the local speeds in the space-time Lagrangian-Eulerian control volumes and is subject to the following CFL stability condition,

$$\frac{\Delta t}{h} Q_{LE}\left(\frac{\mathbf{f}(u_K^n)}{u_K^n}, \frac{\mathbf{f}(u_L^n)}{u_L^n}; \mathbf{n}_{KL}\right) \leq \frac{1}{2}. \tag{3.2}$$

Using a two–stage explicit Runge–Kutta method to discretize the ODE in (3.1), the approximate solution of the conservation law, U_K^{n+1}, $\forall \mathbf{x} \in K$, $\forall t \in (t^n, t^{n+1}]$, is given by

$$\begin{aligned} U_K^* &= U_K^n + \Delta t\, \mathcal{L}(U_K^n, U_L^n), \\ U_K^{**} &= U_K^* + \Delta t\, \mathcal{L}(U_K^*, U_L^*), \\ U_K^{n+1} &= \frac{1}{2}(U_K^n + U_K^{**}), \end{aligned} \tag{3.3}$$

with Δt satisfying (3.2).

Remark 16 *In what follows from this work,* $Q_{LE}\Big(\frac{\mathbf{f}(u_K^n)}{u_K^n}, \frac{\mathbf{f}(u_L^n)}{u_L^n}; \mathbf{n}_{KL}\Big)$ *will be taken as* $\underset{u,K,L}{\mathrm{Sup}} \left|\frac{\mathbf{f}(u)}{u} \cdot \mathbf{n}_{KL}\right|$.

3.2 Convergence Proof of the Triangular Semi-Discrete Lagrangian-Eulerian Scheme via Weak Asymptotic Analysis

In this section, from the triangular semi-discrete Lagrangian-Eulerian scheme (3.1)–(2.20), following [17] and [14], we construct sequences of continuous functions that tend to satisfy the conservation law asymptotically. To be more accurate, by using the weak asymptotic method, we show weak convergence of these sequences towards the unique solution of the conservation law in the spatial variables and strong convergence in the time variable.

The weak asymptotic method consists of transforming a Partial Differential Equation (PDE) with a special flux (using parameter $\boldsymbol{\epsilon}$) into a family of Ordinary Differential Equation (ODE) for variable t. Then, from the theory of ODEs, demonstrate the existence and stability of the solutions of these ODEs, and prove that these solutions satisfy (1.16).

In our Lagrangian-Eulerian approach, we use the auxiliary function, $\hat{\mathbf{f}}(u) = \mathbf{f}(u)/u$ (i.e., *the no flow curves*), and assume that $u \neq 0$ to avoid technical details (we stress that the convergence of the scheme can be proven in this case).

We also assume that the flux function $\mathbf{f}$ is a continuous function in t, bounded on the bounded sets of $\mathbb{R} \times \mathbb{T}^2 \times \mathbb{R}_+$ and locally Lipschitz continuous in u in the sense

$\forall c > 0, \exists C_{\text{Lips}} > 0$ such that

$$|t| \leq c,\ |u| \leq c,\ |v| \leq c \Rightarrow \|\mathbf{f}(u) - \mathbf{f}(v)\| \leq C_{\text{Lips}} |u - v|\,,\ \forall \mathbf{x} \in \mathbb{T}^2. \tag{3.4}$$

Furthermore, in the sequel (and without loss of generality; see [3] for details), we suppose that there exists a $a > 0$ such that $u > a > 0$ and, for each $T > 0$, function $\mathbf{f}$ is bounded on $\mathbb{S}$ where $\mathbb{S} \subseteq \mathbb{R}$ is the set of values $\{u_K(\mathbf{x}, t, \boldsymbol{\epsilon})\}_{t\in[0,T],\ \mathbf{x}\in K,\ \epsilon_1,\epsilon_2>0}$ of the approximate solutions $(u^{\boldsymbol{\epsilon}})$ constructed.

As a consequence, $\hat{\mathbf{f}}(u)$ is a locally Lipschitzian function in u with Lipschitz constant $\hat{C}_{\text{Lips}} = C_{\text{Lips}}/a + M/a^2$ where

$$M = \operatorname*{Sup}_{u\in\mathbb{S}} \|\mathbf{f}(u)\| < \infty. \tag{3.5}$$

From the triangular semi-discrete Lagrangian-Eulerian scheme (3.1)–(2.20), we obtain the following PDE in the weak asymptotic framework:

$$\partial_t(u_K^{\boldsymbol{\epsilon}}) = -\frac{1}{|K|} \sum_{L\in N(K)} \mathcal{F}(u_K^{\boldsymbol{\epsilon}}, u_L^{\boldsymbol{\epsilon}}; \mathbf{n}_{KL}),\ \ u^{\boldsymbol{\epsilon}}(0, \mathbf{x}) = u_0(\mathbf{x}), \tag{3.6}$$

where the numerical flux function $\mathcal{F}$ is given by Eq. (2.20), $u_K^{\boldsymbol{\epsilon}}(\mathbf{x}, t) = u_K(\mathbf{x}, t, \boldsymbol{\epsilon})$ is the approximate solution, $u_L^{\boldsymbol{\epsilon}}(\mathbf{x}, t) = u_K^{\boldsymbol{\epsilon}}(\mathbf{x}, t + \boldsymbol{\epsilon}_{K,L})$, and $\boldsymbol{\epsilon}_{K,L} = |\boldsymbol{\epsilon} \cdot \mathbf{n}_{KL}|\, \mathbf{n}_{KL}$.

Since we use estimates for $\hat{\mathbf{f}}(u)$, we obtain a global estimate bounded estimate for this quantity. For this, we assume that there exists $\xi > 0$ such that

$$\operatorname*{Sup}_{K,L} \left|\hat{\mathbf{f}}(u_K) \cdot \mathbf{n}_{K,L}\right| \leq \xi M, \tag{3.7}$$

where M is defined in (3.5).

Theorem 3.2.1 *For $\boldsymbol{\epsilon} = (\epsilon_1, \epsilon_2) \in (0, \infty)^2$, we construct, as solution to (3.6), a family of functions $(\mathbf{x}, t) \mapsto u_K(\mathbf{x}, t, \boldsymbol{\epsilon}) : \mathbb{R}_+ \times \mathbb{T}^2 \to \mathbb{R}$ which, for a fixed $\boldsymbol{\epsilon}$ with $\|\boldsymbol{\epsilon}\| << 1$, are of class $\mathcal{C}^1$ in t and of class L^∞ in $\mathbf{x}$ and satisfy (1.16). Moreover, if*

$$\left|(\hat{\mathbf{f}}(u_K^{\boldsymbol{\epsilon}}) + \hat{\mathbf{f}}(u_L^{\boldsymbol{\epsilon}})) \cdot \mathbf{n}_{K,L}\right| \leq \operatorname*{Sup}_{K,L} \left|\hat{\mathbf{f}}(u_K) \cdot \mathbf{n}_{K,L}\right|, \tag{3.8a}$$

$$3\frac{|K|L|}{|K|} \left(\operatorname*{Sup}_{K,L} \left|\hat{\mathbf{f}}(u_K^{\boldsymbol{\epsilon}}) \cdot \mathbf{n}_{K,L}\right| + \frac{1}{4}(\hat{\mathbf{f}}(u_K^{\boldsymbol{\epsilon}}) + \hat{\mathbf{f}}(u_L^{\boldsymbol{\epsilon}})) \cdot \mathbf{n}_{K,L}\right) dt \leq 1,\ L \in N(K),\ dt > 0, \tag{3.8b}$$

then family $(u^{\boldsymbol{\epsilon}}(\mathbf{x},t))_{\boldsymbol{\epsilon}}$ *is bounded in* $L^1(\mathbb{T}^2)$ *uniformly in* $\boldsymbol{\epsilon}$. *In fact,* $\|u(t,\cdot,\boldsymbol{\epsilon})\|_{L^1(\mathbb{T}^2)} \leq \|u(0,\cdot,\boldsymbol{\epsilon})\|_{L^1(\mathbb{T}^2)}$, $\forall t>0$. *Furthermore, if initial condition* $u_{0,\boldsymbol{\epsilon}}$ *and* $\mathbf{f}$ *are continuous, then* $u(\mathbf{x},t,\boldsymbol{\epsilon})$ *is also continuous in* $\mathbf{x}$.

Proof. For fixed $\boldsymbol{\epsilon}=(\epsilon_1,\epsilon_2)\in(0,\infty)^2$ with $\|\boldsymbol{\epsilon}\| << 1$ from (3.6), we consider the linear ODE in variable t and parameter $\mathbf{x}$ as follows:

$$\frac{d}{dt}u_K(\mathbf{x},t,\boldsymbol{\epsilon}) = F_{\boldsymbol{\epsilon}}(u_K(\mathbf{x},t,\boldsymbol{\epsilon}),\mathbf{x},t),\ u_K(0,\mathbf{x},\boldsymbol{\epsilon}) = u_0(\mathbf{x}). \tag{3.9}$$

By using notation $u_K(\mathbf{x}) = u_K(\mathbf{x},t,\boldsymbol{\epsilon})$, the function $F_{\boldsymbol{\epsilon}}:\ L^\infty(\mathbb{T}^2)\times[0,\infty)\times\mathbb{T}^2 \to L^\infty(\mathbb{T}^2)$ is defined as:

$$F_{\boldsymbol{\epsilon}}(u_K(\mathbf{x}),\mathbf{x},t) = -\frac{1}{|K|}\sum_{L\in N(K)}\mathcal{F}(u_K(\mathbf{x}),u_L(\mathbf{x}),\mathbf{x},t;\mathbf{n}_{KL}), \tag{3.10}$$

with

$$\begin{aligned}\mathcal{F}(u_K(\mathbf{x}),u_L(\mathbf{x}),\mathbf{x},t;\mathbf{n}_{KL}) = \Bigg[&\frac{1}{4}(u_K(\mathbf{x})+u_L(\mathbf{x}))(\hat{\mathbf{f}}(u_K(\mathbf{x}),\mathbf{x},t)+\hat{\mathbf{f}}(u_L(\mathbf{x}),\mathbf{x},t)))\cdot\mathbf{n}_{KL}\\ &+\sup_{K\in\mathcal{T},\ u_K\in\mathbb{S}}\left|\hat{\mathbf{f}}(u_K)\cdot\mathbf{n}_{KL}\right|(u_K(\mathbf{x})-u_L(\mathbf{x}))\Bigg]|K|L|\,.\end{aligned} \tag{3.11}$$

From the assumption (3.4), it follows that $F_{\boldsymbol{\epsilon}}$ is continuous in t and Lipschitz continuous in u. The Lipschitz constants of each $F_{\boldsymbol{\epsilon}}$ can be chosen uniform on the bounded sets of $L^\infty(\mathbb{T}^2)\times[0,\infty)\times\mathbb{T}^2$. Therefore from the classical theory of ODEs in Banach spaces in the Lipschitz case there is a local solution for $t\in[0,\delta(\|\boldsymbol{\epsilon}\|))$ and for some $\delta(\|\boldsymbol{\epsilon}\|)$ depending on $\boldsymbol{\epsilon}$.

The existence of a global in time solution is obtained by proving that, for fixed fixed $\boldsymbol{\epsilon}=(\epsilon_1,\epsilon_2)$, there exists a $\eta_{\boldsymbol{\epsilon}}(t)<\infty$ such that $\|u(t,\cdot)\|\leq\eta_{\boldsymbol{\epsilon}}(t)<\infty$ where $\eta_{\boldsymbol{\epsilon}}$ is a continuous function on $[0,\infty)$ without uniforminess in $\boldsymbol{\epsilon}$.

From (3.7) and (3.8a), the ODE (3.9) satifies

$$\left|\frac{d}{dt}u_K(\mathbf{x},t,\boldsymbol{\epsilon})\right| \leq C_2M\left\|u_K(\cdot,t,\boldsymbol{\epsilon})\right\|_\infty,\ C_2\sim\mathcal{O}(|K|L|\,/\,|K|)\sim\mathcal{O}(1/\left\|\boldsymbol{\epsilon}\right\|). \tag{3.12}$$

(3.12) implies that

$$\left\|u_K(\mathbf{x},t,\boldsymbol{\epsilon})\right\|_\infty \leq \left\|u_0(\mathbf{x},\boldsymbol{\epsilon})\right\|_\infty + C_2M\int_0^t\left\|u_K(\cdot,\tau,\boldsymbol{\epsilon})\right\|_\infty\,d\tau. \tag{3.13}$$

From Gronwall's formula, we get

$$\left\|u_K(\cdot,t,\boldsymbol{\epsilon})\right\|_\infty \leq \left\|u_{0,\boldsymbol{\epsilon}}\right\|_\infty e^{C_2Mt}. \tag{3.14}$$

Bound (3.14) shows that the ODE (3.9) has a global solution for every fixed $\boldsymbol{\epsilon}$. Even so, since C_2 depends on $\boldsymbol{\epsilon}$, there is no uniforminess in $\boldsymbol{\epsilon}$. Proving that the solutions to the ODE (3.9) satisfy a L^1 bound which is uniform in $\boldsymbol{\epsilon}$, we will prove that these solutions provide a weak asymptotic solution to (1.15). The proof is as follows.

Let $T>0$. For $dt>0$ and $t+dt>0$, from the mean value theorem applied to the function $t\mapsto u_K(\cdot,t,\boldsymbol{\epsilon})$, it follows that

$$\begin{aligned}u_K(\mathbf{x},t+dt,\boldsymbol{\epsilon}) &= u_K^{\boldsymbol{\epsilon}} + \frac{du_K^{\boldsymbol{\epsilon}}}{dt}\,dt + dt\,r(\mathbf{x},t,\boldsymbol{\epsilon},dt)\\ &= u_K^{\boldsymbol{\epsilon}} - \frac{dt}{|K|}\sum_{L\in N(K)}\Bigg[\frac{1}{4}(u_K^{\boldsymbol{\epsilon}}(\mathbf{x})+u_L^{\boldsymbol{\epsilon}}(\mathbf{x}))(\hat{\mathbf{f}}(u_K^{\boldsymbol{\epsilon}})+\hat{\mathbf{f}}(u_L^{\boldsymbol{\epsilon}}))\cdot\mathbf{n}_{KL}\\ &\qquad+\sup_{K\in\mathcal{T},\ u_K^{\boldsymbol{\epsilon}}\in\mathbb{S}}\left|\hat{\mathbf{f}}(u_K^{\boldsymbol{\epsilon}})\cdot\mathbf{n}_{KL}\right|(u_K^{\boldsymbol{\epsilon}}(\mathbf{x})-u_L^{\boldsymbol{\epsilon}}(\mathbf{x}))\Bigg]|K|L|\\ &\qquad+dt\,r(\mathbf{x},t,\boldsymbol{\epsilon},dt),\end{aligned} \tag{3.15}$$

where $\|r(\mathbf{x},t,\boldsymbol{\epsilon},dt)\|_\infty \underset{u}{\longrightarrow} 0$ in $t\in[0,T]$ for fixed $\boldsymbol{\epsilon}$ (no uniformness in $\boldsymbol{\epsilon}$) as $dt\to 0$ becuase the map $t\mapsto u(t,\cdot,\boldsymbol{\epsilon})$ is continuously differentiable for fixed $\boldsymbol{\epsilon}$.

Through some algebraic manipulations, we rewrite (3.15) as

$$u_K(\mathbf{x},t+dt,\boldsymbol{\epsilon}) = u_K^{\boldsymbol{\epsilon}} \sum_{L\in N(K)} \left(\frac{1}{3} - \frac{A_{K,L}\,|K|L|\,dt}{|K|}\right) + \sum_{L\in N(K)} u_L^{\boldsymbol{\epsilon}} \frac{B_{K,L}\,|K|L|\,dt}{|K|} + dt\; r(\mathbf{x},t,\boldsymbol{\epsilon},dt), \quad (3.16)$$

where

$$A_{K,L} = \underset{K\in\mathcal{T},\, u_K^{\boldsymbol{\epsilon}}\in\mathbb{S}}{\mathrm{Sup}} \left|\hat{\mathbf{f}}(u_K^{\boldsymbol{\epsilon}})\cdot\mathbf{n}_{KL}\right| + \frac{1}{4}(\hat{\mathbf{f}}(u_K^{\boldsymbol{\epsilon}}) + \hat{\mathbf{f}}(u_L^{\boldsymbol{\epsilon}}))\cdot\mathbf{n}_{KL}, \quad (3.17a)$$

$$B_{K,L} = \underset{K\in\mathcal{T},\, u_K^{\boldsymbol{\epsilon}}\in\mathbb{S}}{\mathrm{Sup}} \left|\hat{\mathbf{f}}(u_K^{\boldsymbol{\epsilon}})\cdot\mathbf{n}_{KL}\right| - \frac{1}{4}(\hat{\mathbf{f}}(u_K^{\boldsymbol{\epsilon}}) + \hat{\mathbf{f}}(u_L^{\boldsymbol{\epsilon}}))\cdot\mathbf{n}_{KL}. \quad (3.17b)$$

From (3.8a) and (3.8b), $\dfrac{1}{3} - \dfrac{A_{K,L}\,|K|L|\,dt}{|K|} \geq 0$ and $B_{K,L}\geq 0$. Then, by taking the absolute value of (3.16) we get

$$\begin{aligned} |u_K(\mathbf{x},t+dt,\boldsymbol{\epsilon})| \leq |u_K^{\boldsymbol{\epsilon}}| \sum_{L\in N(K)} &\left(\frac{1}{3} - \frac{A_{K,L}\,|K|L|\,dt}{|K|}\right) \\ &+ \sum_{L\in N(K)} |u_L^{\boldsymbol{\epsilon}}|\,\frac{B_{K,L}\,|K|L|\,dt}{|K|} + dt\,|r(\mathbf{x},t,\boldsymbol{\epsilon},dt)|\,. \end{aligned} \quad (3.18)$$

Integrating (3.18) in $\mathbf{x}$ and simplifying, we obtain

$$\|u_K(\mathbf{x},t+dt,\boldsymbol{\epsilon})\|_1 \leq \|u_K(t,\cdot,\boldsymbol{\epsilon})\|_1 + dt\; r_1(t,\boldsymbol{\epsilon},dt), \quad (3.19)$$

where $r_1(t,\boldsymbol{\epsilon},dt) = \int_K |r(\mathbf{x},t,\boldsymbol{\epsilon},dt)|\; d\mathbf{x} \underset{u}{\longrightarrow} 0$ in $t\in[0,T]$ for fixed $\boldsymbol{\epsilon}$ (no uniformness in $\boldsymbol{\epsilon}$) as $dt\to 0$.

By dividing the interval $[0,T]$ into subintervals $[idt,(i+1)dt]$, $0\leq i\leq n-1$, n as large as necessary so that $dt=T/n$ is small enough, and applying the bound (3.19) in each subinterval, we obtain

$$\int_K |u_K(\mathbf{x},(i+1)dt,\boldsymbol{\epsilon})|\; d\mathbf{x} \leq \int_K |u_K(\mathbf{x},idt,\boldsymbol{\epsilon})|\; d\mathbf{x} + dt\; r_2(\boldsymbol{\epsilon},dt), \quad (3.20)$$

where $r_2(\boldsymbol{\epsilon},dt) = \underset{t}{\mathrm{Sup}}\; r_1(t,\boldsymbol{\epsilon},dt)$.

Summing over all i, we obtain

$$\begin{aligned} &\sum_{i=0}^{n}\int_K |u_K(\mathbf{x},(i+1)dt,\boldsymbol{\epsilon})|\; d\mathbf{x} \leq \sum_{i=0}^{n}\int_K |u_K(\mathbf{x},idt,\boldsymbol{\epsilon})|\; d\mathbf{x} + dt\sum_{i=0}^{n} r_2(\boldsymbol{\epsilon},dt) \\ \Leftrightarrow\quad &\int_K |u_K(\mathbf{x},ndt,\boldsymbol{\epsilon})|\; d\mathbf{x} \leq \int_K |u(0,\mathbf{x},\boldsymbol{\epsilon})|\; d\mathbf{x} + n\;dt\; r_2(\boldsymbol{\epsilon},dt). \end{aligned} \quad (3.21)$$

Since $ndt=T$ and $r_2(\boldsymbol{\epsilon},dt)\to 0$ as $dt\to 0$, it follows that,

$$\|u_K(T,\cdot,\boldsymbol{\epsilon})\|_1 \leq \|u_0(\cdot,\boldsymbol{\epsilon})\|_1 = \|u_0(\cdot)\|_1\,. \quad (3.22)$$

By proving the approximation property (1.16), the proof of Theorem 3.2.1 is completed.

First, taking into account that

$$
\begin{aligned}
&\int_\Omega [(u_K^{\boldsymbol{\epsilon}})_t\psi - \mathbf{f}(u_K^{\boldsymbol{\epsilon}})\cdot\nabla\psi]\,d\mathbf{x}\\
&\quad= \int_\Omega \Bigg\{ -\frac{1}{|K|}\sum_{L\in N(K)} \Bigg[\frac{1}{4}(u_K^{\boldsymbol{\epsilon}}(\mathbf{x})+u_L^{\boldsymbol{\epsilon}}(\mathbf{x}))(\hat{\mathbf{f}}(u_K^{\boldsymbol{\epsilon}})+\hat{\mathbf{f}}(u_L^{\boldsymbol{\epsilon}}))\cdot\mathbf{n}_{KL}\\
&\qquad\qquad + \sup_{K\in\mathcal{T},\, u_K^{\boldsymbol{\epsilon}}\in\mathbb{S}} \left|\hat{\mathbf{f}}(u_K^{\boldsymbol{\epsilon}})\cdot\mathbf{n}_{KL}\right| (u_K^{\boldsymbol{\epsilon}}(\mathbf{x})-u_L^{\boldsymbol{\epsilon}}(\mathbf{x}))\Bigg] |K|L|\ \psi(\mathbf{x}) - \mathbf{f}(u_K^{\boldsymbol{\epsilon}})\cdot\nabla\psi(\mathbf{x})\Bigg\} \qquad (3.23)\\
&\quad= \int_\Omega \Bigg\{ -\frac{1}{|K|}\int_{\partial K} \mathbf{f}(u_K^{\boldsymbol{\epsilon}})\cdot\mathbf{n}_{KL}\ d(K|L)\psi(\mathbf{x}) + \mathcal{O}(\|\boldsymbol{\epsilon}\|)\\
&\qquad\qquad + \sup_{K\in\mathcal{T},\, u_K^{\boldsymbol{\epsilon}}\in\mathbb{S}} \left|\hat{\mathbf{f}}(u_K^{\boldsymbol{\epsilon}})\cdot\mathbf{n}_{KL}\right| (u_K^{\boldsymbol{\epsilon}}(\mathbf{x})-u_L^{\boldsymbol{\epsilon}}(\mathbf{x}))\,|K|L|\ \psi(\mathbf{x}) - \mathbf{f}(u_K^{\boldsymbol{\epsilon}})\cdot\nabla\psi(\mathbf{x})\Bigg\}\, d\mathbf{x}.
\end{aligned}
$$

Now, by using the mean value theorem, there exits $\widetilde{u}_K^{\boldsymbol{\epsilon}} \in \mathbb{S}$ such that

$$
\frac{1}{|K|}\int_{\partial K} \mathbf{f}(u_K^{\boldsymbol{\epsilon}})\cdot\mathbf{n}_{KL}\ d(K|L) = \frac{1}{|K|}\int_K \nabla\cdot\mathbf{f}(u_K^{\boldsymbol{\epsilon}})\ dK = \nabla\cdot\mathbf{f}(\widetilde{u}_K^{\boldsymbol{\epsilon}}). \qquad (3.24)
$$

So, Eq. (3.23) writes

$$
\begin{aligned}
&\int_\Omega [(u_K^{\boldsymbol{\epsilon}})_t\psi - \mathbf{f}(u_K^{\boldsymbol{\epsilon}})\cdot\nabla\psi]\,d\mathbf{x}\\
&\qquad= \int_\Omega [-\nabla\cdot\mathbf{f}(\widetilde{u}_K^{\boldsymbol{\epsilon}})\ \psi(\mathbf{x}) - \mathbf{f}(u_K^{\boldsymbol{\epsilon}})\cdot\nabla\psi(\mathbf{x})\\
&\qquad\qquad + \sup_{K\in\mathcal{T},\, u_K^{\boldsymbol{\epsilon}}\in\mathbb{S}} \left|\hat{\mathbf{f}}(u_K^{\boldsymbol{\epsilon}})\cdot\mathbf{n}_{KL}\right| (u_K^{\boldsymbol{\epsilon}}(\mathbf{x})-u_L^{\boldsymbol{\epsilon}}(\mathbf{x}))\,|K|L|\ \psi(\mathbf{x})\Bigg]\, d\mathbf{x} + \mathcal{O}(\|\boldsymbol{\epsilon}\|) \qquad (3.25)\\
&\qquad= \int_\Omega [\mathbf{f}(\widetilde{u}_K^{\boldsymbol{\epsilon}})\cdot\nabla\psi(\mathbf{x}) - \mathbf{f}(u_K^{\boldsymbol{\epsilon}})\cdot\nabla\psi(\mathbf{x})\\
&\qquad\qquad + \sup_{K\in\mathcal{T},\, u_K^{\boldsymbol{\epsilon}}\in\mathbb{S}} \left|\hat{\mathbf{f}}(u_K^{\boldsymbol{\epsilon}})\cdot\mathbf{n}_{KL}\right| (u_K^{\boldsymbol{\epsilon}}(\mathbf{x})-u_L^{\boldsymbol{\epsilon}}(\mathbf{x}))\,|K|L|\ \psi(\mathbf{x})\Bigg]\, d\mathbf{x} + \mathcal{O}(\|\boldsymbol{\epsilon}\|)
\end{aligned}
$$

Finally, from the definition of $u_L^{\boldsymbol{\epsilon}}$, it is clear that $u_L^{\boldsymbol{\epsilon}} \to u_K^{\boldsymbol{\epsilon}}$ as $\boldsymbol{\epsilon}\to\mathbf{0}$. So, $\lim_{\boldsymbol{\epsilon}\to\mathbf{0}}(u_K^{\boldsymbol{\epsilon}} - u_L^{\boldsymbol{\epsilon}}) = 0$, and

$$
\lim_{\boldsymbol{\epsilon}\to\mathbf{0}} \frac{1}{4}(u_K^{\boldsymbol{\epsilon}}+u_L^{\boldsymbol{\epsilon}})(\hat{\mathbf{f}}(u_K^{\boldsymbol{\epsilon}})+\hat{\mathbf{f}}(u_L^{\boldsymbol{\epsilon}}))\cdot\mathbf{n}_{KL} = u_K^{\boldsymbol{\epsilon}}\hat{\mathbf{f}}(u_K^{\boldsymbol{\epsilon}})\cdot\mathbf{n}_{KL} = \mathbf{f}(u_K^{\boldsymbol{\epsilon}})\cdot\mathbf{n}_{KL}.
$$

In consequence, the limit as $\boldsymbol{\epsilon}$ goes to zero of (3.25) leads to (1.16) and thus, the proof of Theorem (3.2.1) is concluded.

Remark 17 *It can be proved that when the function* $\mathbf{f}$ *depends only on* u *and is locally Lipschitz continuous in* u*, and when* $u_0 \in L^\infty(\mathbb{R}^2)$*, the weak asymptotic solution we construct tends to the Kruzhkov solution when* $\boldsymbol{\epsilon}$ *goes to zero (see Theorem 4 in [17]). The proof can be carried out following the proof of Proposition Appendix A.5 (Kruzhkov entropy) in [4].*

3.3 Positivity Principle of the Triangular Semi-Discrete Lagrangian-Eulerian Scheme for Multidimensional Systems

In this section, we prove that the triangular semi-discrete Lagrangian-Eulerian scheme (3.1)-(3.3) satisfies the properties of positivity $(i)-(iii)$ given in (2.112).

The scheme (3.6) to systems can be written, for $i = 1, \cdots, m$, as

$$\partial_t((u_K^{\boldsymbol{\epsilon}})_i) = -\frac{1}{|K|}\sum_{L\in N(K)} \mathcal{F}_i(u_K^{\boldsymbol{\epsilon}}, u_L^{\boldsymbol{\epsilon}}; \mathbf{n}_{KL}), \quad u_i^{\boldsymbol{\epsilon}}(0,\mathbf{x}) = u_{0i}(\mathbf{x}), \tag{3.26}$$

with

$$\begin{aligned}\mathcal{F}_i(u_K^{\boldsymbol{\epsilon}}, u_L^{\boldsymbol{\epsilon}}; \mathbf{n}_{KL}) = \Big[\frac{1}{4}((u_K^{\boldsymbol{\epsilon}})_i + (u_L^{\boldsymbol{\epsilon}})_i)(\hat{\mathbf{f}}_i(u_K^{\boldsymbol{\epsilon}}) + \hat{\mathbf{f}}_i(u_L^{\boldsymbol{\epsilon}}))\cdot\mathbf{n}_{KL} \\ + \operatorname*{Sup}_{K,L,i}\Big|\hat{\mathbf{f}}_i(u_K^{\boldsymbol{\epsilon}})\cdot\mathbf{n}_{KL}\Big|\,((u_K^{\boldsymbol{\epsilon}})_i - (u_L^{\boldsymbol{\epsilon}})_i)\Big]\,|K|L|\,,\end{aligned} \tag{3.27}$$

and $\hat{\mathbf{f}}(u)$ the *no flow curves*.

Taking into account that,

$$\begin{aligned}\frac{1}{4}((u_K^{\boldsymbol{\epsilon}})_i + (u_L^{\boldsymbol{\epsilon}})_i)(\hat{\mathbf{f}}_i(u_K^{\boldsymbol{\epsilon}}) + \hat{\mathbf{f}}_i(u_L^{\boldsymbol{\epsilon}}))\cdot\mathbf{n}_{KL} = \frac{1}{4}((\hat{\mathbf{f}}_i(u_L^{\boldsymbol{\epsilon}}) - \hat{\mathbf{f}}_i(u_K^{\boldsymbol{\epsilon}}))\cdot\mathbf{n}_{KL})((u_K^{\boldsymbol{\epsilon}})_i + (u_L^{\boldsymbol{\epsilon}})_i) \\ + \frac{1}{2}(\hat{\mathbf{f}}_i(u_K^{\boldsymbol{\epsilon}})\cdot\mathbf{n}_{KL})((u_K^{\boldsymbol{\epsilon}})_i + (u_L^{\boldsymbol{\epsilon}})_i),\end{aligned} \tag{3.28}$$

and defining the quantities $\widetilde{c}_{K,L} = \frac{1}{2}(\hat{\mathbf{f}}_i(u_K^{\boldsymbol{\epsilon}})\cdot\mathbf{n}_{KL})$ and $c_{K,L} = \operatorname*{Sup}_{K,L,i}\Big|\hat{\mathbf{f}}_i(u_K^{\boldsymbol{\epsilon}})\cdot\mathbf{n}_{KL}\Big|$, (3.27) can be written as

$$\begin{aligned}\mathcal{F}_i(u_K^{\boldsymbol{\epsilon}}, u_L^{\boldsymbol{\epsilon}}; \mathbf{n}_{KL}) = \Big[\frac{1}{4}((\hat{\mathbf{f}}_i(u_L^{\boldsymbol{\epsilon}}) - \hat{\mathbf{f}}_i(u_K^{\boldsymbol{\epsilon}}))\cdot\mathbf{n}_{KL})((u_K^{\boldsymbol{\epsilon}})_i \\ + (u_L^{\boldsymbol{\epsilon}})_i) + \widetilde{c}_{K,L}((u_K^{\boldsymbol{\epsilon}})_i + (u_L^{\boldsymbol{\epsilon}})_i) + c_{K,L}((u_K^{\boldsymbol{\epsilon}})_i - (u_L^{\boldsymbol{\epsilon}})_i)\Big]\,|K|L|\,.\end{aligned} \tag{3.29}$$

To prove that the triangular semi-discrete Lagrangian-Eulerian scheme (3.1)-(2.20) satisfies the positivity principle, we solve an ODE in the variable t for the parameter $\boldsymbol{\epsilon}$ by using the second order accurate Runge–Kutta method (3.3) and define diagonal matrices $P_{K,L}$, $C_{K,L}$, $\widetilde{C}_{K,L}$ and $D_{K,L}$ as $P_{K,L} = p_{K,L}I$ satisfying $p_{K,L} > 0$, $\sum_{L\in N(K)} P_{K,L} = I$, $C_{K,L} = c_{K,L}I$, $\widetilde{C}_{K,L} = \widetilde{c}_{K,L}I$, where I is the $m \times m$ identity matrix and $D_{K,L} = C_{K,L} - \widetilde{C}_{K,L}$.

Lemma 20, stated bellow and whose proof is very simple, allows us to prove that

$$\sum_{L\in N(K)} \widetilde{C}_{K,L}\,|K|L| = 0. \tag{3.30}$$

Lemma 20 *Given any triangle K, then $\sum_{L\in N(K)} \mathbf{n}_{KL}\,|K|L| = \mathbf{0}$.*

Thus, we can rewrite U_K^* in (3.3) in the following matricial form:

$$U_K^{\boldsymbol{\epsilon},*} = \sum_{L\in N(K)}\Big[P_{K,L}U_K^{\boldsymbol{\epsilon},n} - \frac{\Delta t}{|K|}F(U_K^{\boldsymbol{\epsilon},n}, U_L^{\boldsymbol{\epsilon},n})\Big], \tag{3.31}$$

where $U_{K,L} = ((U_1)_{K,L}, \cdots, (U_m)_{K,L})^T$ and $F_{K,L} = ((F_1)_{K,L}, \cdots, (F_m)_{K,L})^T$.

Theorem 3.3.1 *The numerical scheme (3.6), solved by 2nd order Runge–Kutta method (3.3), is positive, if the system is symmetric or symmetrizable for numerical flux $(F_i)_{K,L}$ given by (3.29) and the following conditions*

$$\Big|\rho\big(A(\hat{U}_{K,L}^{\boldsymbol{\epsilon},n})\cdot\mathbf{n}_{KL}\big)\Big|\,(U_K^{\boldsymbol{\epsilon},n} + U_L^{\boldsymbol{\epsilon},n}) \le 4(c_{K,L} - \widetilde{c}_{K,L}) \ \text{ and } \ \frac{\Delta t\,|K|L|}{|K|}c_{K,L} \le p_{K,L}, \tag{3.32}$$

where $\rho\big(A(\hat{U}_{K,L}^{\boldsymbol{\epsilon},n})\cdot\mathbf{n}_{KL}\big)$ is the spectral radius of matrix $A(\hat{U}_{K,L}^{\boldsymbol{\epsilon},n})\cdot\mathbf{n}_{KL}$, are satisfied. Furthermore, if $U_K > 0$ for all $K \in \mathcal{T}$ then, the numerical scheme preserves the L^1– norm.

Proof.

Substituting (3.29) in (3.31), we get

$$U_K^{\boldsymbol{\epsilon},*} = \sum_{L\in N(K)} \left\{ P_{K,L} U_K^{\boldsymbol{\epsilon},n} - \frac{\Delta t}{|K|}\left[\frac{1}{4}((\hat{\mathbf{f}}(U_L^{\boldsymbol{\epsilon},n}) - \hat{\mathbf{f}}(U_K^{\boldsymbol{\epsilon},n}))\cdot \mathbf{n}_{KL})(U_K^{\boldsymbol{\epsilon},n} + U_L^{\boldsymbol{\epsilon},n}) \right.\right. \\ \left.\left. + \widetilde{C}_{K,L}(U_K^{\boldsymbol{\epsilon},n} + U_L^{\boldsymbol{\epsilon},n}) + C_{K,L}((U_K^{\boldsymbol{\epsilon},n} - U_L^{\boldsymbol{\epsilon},n})\right] |K|L| \right\}. \tag{3.33}$$

Remark 18 *Note that* $\hat{\mathbf{f}} = (\hat{\mathbf{f}}_1, \cdots, \hat{\mathbf{f}}_m)$ *and each* $\hat{\mathbf{f}}_i$ *is a vector with two coordinates, which we denote as* $\hat{\mathbf{f}}_i = ((\hat{f}_i)_1, (\hat{f}_i)_2)$. *We define* $\hat{\mathbf{f}}^1 = ((\hat{f}_1)_1, (\hat{f}_2)_1, \cdots, (\hat{f}_m)_1)^T$, *i.e., the first coordinate, and* $\hat{\mathbf{f}}^2 = ((\hat{f}_1)_2, (\hat{f}_2)_2, \cdots, (\hat{f}_m)_2)$.

Now, by using the Roe's matrix expansion,

$$(\hat{\mathbf{f}}(u_L^{\boldsymbol{\epsilon}}) - \hat{\mathbf{f}}(u_K^{\boldsymbol{\epsilon}}))\cdot \mathbf{n}_{kL} = (A(\hat{u}_{K,L}^{\boldsymbol{\epsilon}})\cdot \mathbf{n}_{KL})(u_L^{\boldsymbol{\epsilon}} - u_K^{\boldsymbol{\epsilon}}), \tag{3.34}$$

where $A = (A_1, A_2)$ with A_1 and A_2, the Jacobian of $\hat{\mathbf{f}}^1$ and $\hat{\mathbf{f}}^2$ respectively, and rearranging terms, (3.33) rewrites

$$U_K^{\boldsymbol{\epsilon},*} = \sum_{L\in N(K)} \left\{ \left(P_{K,L} + \frac{\Delta t\,|K|L|}{|K|}\left[\frac{1}{4}(A(\hat{U}_{K,L}^{\boldsymbol{\epsilon},n})\cdot \mathbf{n}_{KL})(U_K^{\boldsymbol{\epsilon},n} + U_L^{\boldsymbol{\epsilon},n}) - C_{K,L}\right]\right) U_K^{\boldsymbol{\epsilon},n} \right. \\ \left. + \frac{\Delta t\,|K|L|}{|K|}\left[D_{K,L} - \frac{1}{4}(A(\hat{U}_{K,L}^{\boldsymbol{\epsilon},n})\cdot \mathbf{n}_{KL})(U_K^{\boldsymbol{\epsilon},n} + U_L^{\boldsymbol{\epsilon},n})\right] U_L^{\boldsymbol{\epsilon},n} \right\}. \tag{3.35}$$

Remark 19 $A(\hat{U}_{K,L}^{\boldsymbol{\epsilon},n})\cdot \mathbf{n}_{KL}$ *corresponds to a* $m\times m$ *matrix and the product* $(A(\hat{U}_{K,L}^{\boldsymbol{\epsilon},n})\cdot \mathbf{n}_{KL})(U_K^{\boldsymbol{\epsilon},n} + U_L^{\boldsymbol{\epsilon},n})$ *denotes a* $m\times m$ *matrix whose* i*-th row is obtained by multiplying the* i*-th row of* $A(\hat{u}_{K,L})\cdot \mathbf{n}_{KL}$ *by the* i*-th element of the vector* $(U_K^{\boldsymbol{\epsilon},n} + U_L^{\boldsymbol{\epsilon},n})$. *Besides, if the system is symmetric, each* A_i *and* $A(\hat{U}_{K,L}^{\boldsymbol{\epsilon},n})\cdot \mathbf{n}_{KL}$ *are also symmetric.*

Since the system is symmetric—or symmetrizable (see [130,131])—, and from (3.30) and (3.32), conditions (i)–(iii) are satisfied, and the scheme is positive.

Now, considering that the numerical scheme satisfies $U_K > 0$, for all K, the integration of (3.35) w.r.t the spatial variable leads to

$$\begin{aligned}\int_\Omega |U_K^{\boldsymbol{\epsilon},*}|\,d\mathbf{x} &= \int_\Omega U_K^{\boldsymbol{\epsilon},*} d\mathbf{x} \\ &= \int_\Omega \sum_{L\in N(K)} \left\{ \left(P_{K,L} + \frac{\Delta t\,|K|L|}{|K|}\left[\frac{1}{4}(A(\hat{U}_{K,L}^{\boldsymbol{\epsilon},n})\cdot \mathbf{n}_{KL})(U_K^{\boldsymbol{\epsilon},n} + U_L^{\boldsymbol{\epsilon},n}) - C_{K,L}\right]\right) U_K^{\boldsymbol{\epsilon},n} \right. \\ &\qquad \left. + \frac{\Delta t\,|K|L|}{|K|}\left[D_{K,L} - \frac{1}{4}(A(\hat{U}_{K,L}^{\boldsymbol{\epsilon},n})\cdot \mathbf{n}_{KL})(U_K^{\boldsymbol{\epsilon},n} + U_L^{\boldsymbol{\epsilon},n})\right] U_L^{\boldsymbol{\epsilon},n} \right\}.\end{aligned} \tag{3.36}$$

Making the respective cancellations in (3.36), we get

$$\begin{aligned}\left\|U_K^{\boldsymbol{\epsilon},*}\right\|_1 &= \left(\sum_{L\in N(K)} P_{K,L}\right)\int_\Omega U_K^{\boldsymbol{\epsilon},n}\,d\mathbf{x} \\ &\quad - \frac{\Delta t}{|K|}\left(\sum_{L\in N(K)} \frac{1}{4}(A(\hat{U}_{K,L}^{\boldsymbol{\epsilon},n})\cdot \mathbf{n}_{KL})(U_K^{\boldsymbol{\epsilon},n} + U_L^{\boldsymbol{\epsilon},n})|K|L|\right)\int_\Omega U_K^{\boldsymbol{\epsilon},n} d\mathbf{x} \\ &\quad + \frac{\Delta t}{|K|}\left(\sum_{L\in N(K)} \frac{1}{4}(A(\hat{U}_{K,L}^{\boldsymbol{\epsilon},n})\cdot \mathbf{n}_{KL})(U_K^{\boldsymbol{\epsilon},n} + U_L^{\boldsymbol{\epsilon},n})|K|L|\right)\int_\Omega U_L^{\boldsymbol{\epsilon},n} d\mathbf{x}.\end{aligned} \tag{3.37}$$

Finally, taking into account that $\sum_{L\in N(K)} P_{K,L} = I$ and using the fact that $\int_\Omega U_K^{\boldsymbol{\epsilon},n} d\mathbf{x} = \int_\Omega U_L^{\boldsymbol{\epsilon},n} d\mathbf{x}$, we get

$$\left\|U_K^{\boldsymbol{\epsilon},*}\right\|_1 = \left\|U_K^{\boldsymbol{\epsilon},n}\right\|_1 .$$

That is, the numerical scheme (3.6) preserves the L^1– norm. □

3.4 Weak Positivity Principle of the Triangular Semi-Discrete Lagrangian-Eulerian Scheme for Multidimensional Systems

As in Section 2.2.5, following [4], here we prove that a bound that only depends on the no-flow curves ($\hat{\mathbf{f}}(u)$), which are independent of the eigenvalues, is enough to guarantee the stability of the triangular semi-discrete Lagrangian-Eulerian scheme.

Theorem 3.4.1 *Assume that the no flow curve condition*

$$\frac{\Delta t\ |K|L|}{|K|}\left[\frac{1}{4}(\hat{\mathbf{f}}(U_K^{\boldsymbol{\epsilon},n}) + \hat{\mathbf{f}}(U_L^{\boldsymbol{\epsilon},n}))_{K,L}\cdot\mathbf{n}_{KL} + c_{K,L}\right] \le p_{K,L}, \tag{3.38}$$

holds. Then, the numerical scheme (3.6)*, solved by 2nd order Runge-Kutta method* (3.3)*, satisfies* ***positivity in the weak sense*** *if properties* (*i*) *and* (*iii*) *in* (2.112) *are satisfied.*

Proof. To prove our statement, we notice that we can rewrite U_K^* in (3.3) as:

$$\begin{aligned} U_K^{\boldsymbol{\epsilon},*} = \sum_{L\in N(K)} \Bigg\{ &\left(P_{K,L} - \frac{\Delta t\ |K|L|}{|K|}\left[\frac{1}{4}(\hat{\mathbf{f}}(U_K^{\boldsymbol{\epsilon},n}) + \hat{\mathbf{f}}(U_L^{\boldsymbol{\epsilon},n}))\cdot\mathbf{n}_{KL} + C_{K,L}\right]\right) U_K^{\boldsymbol{\epsilon},n} \\ &+ \frac{\Delta t\ |K|L|}{|K|}\left[C_{K,L} - \frac{1}{4}(\hat{\mathbf{f}}(U_K^{\boldsymbol{\epsilon},n}) + \hat{\mathbf{f}}(U_L^{\boldsymbol{\epsilon},n}))\cdot\mathbf{n}_{KL}\right] U_L^{\boldsymbol{\epsilon},n}\Bigg\}. \end{aligned} \tag{3.39}$$

From the hypothesis (3.38) and, taking into account that the i-th entry of the diagonal matrix $C_{K,L}$ is $\underset{K,L,i}{\mathrm{Sup}}\left|\hat{\mathbf{f}}_i(u_K^{\boldsymbol{\epsilon}})\cdot\mathbf{n}_{KL}\right|$, the entries of the diagonal matrices in (3.39) are positive.

In consequence, the numerical scheme (3.6) is *positive in the weak sense.* □

3.5 Numerical Tests

First, numerical experiments involving scalar two-dimensional problems, that is (1.1) with $m = 1$ and $d = 2$, are presented. Then, some nontrivial two-dimensional systems of hyperbolic conservation laws are solved. In all tests, we use equilateral triangular grids.

3.5.1 2D-dimensional inviscid Burgers' equation: oblique Riemann problem

We solve here the "oblique" Riemann problem described in Section 2.3.5.

Figure 3.1 shows the approximate solution at $t = 0.5$, with very good resolution, with no spurious oscillations in sharp-front regions, and no grid orientation difficulties. As can be noted, the semi-discrete Lagrangian-Eulerian scheme accurately captures the exact solution of this problem.

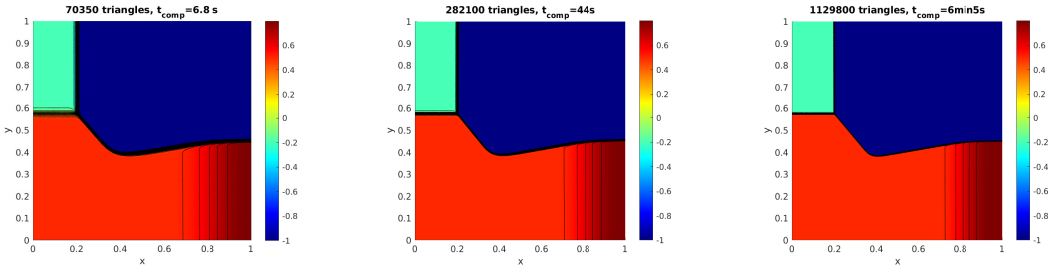

Figure 3.1: numerical solutions to the inviscid Burgers' problem at $T = 0.5$; CFL=0.125.

3.5.2 Nonlinear equation with non-convex flux

Next, we solve the model described in Section 2.3.3, whose solution has a two dimensional composite wave structure.

Figure 3.2 illustrates the simulations performed at $t = 1$ on three triangular grids with 65910, 265880 and 1067600 triangles, respectively. As a result, we were able to see the composite wave that is present in the solution. In addition, no undesirable numerical artifacts such as spurious oscillations are observed.

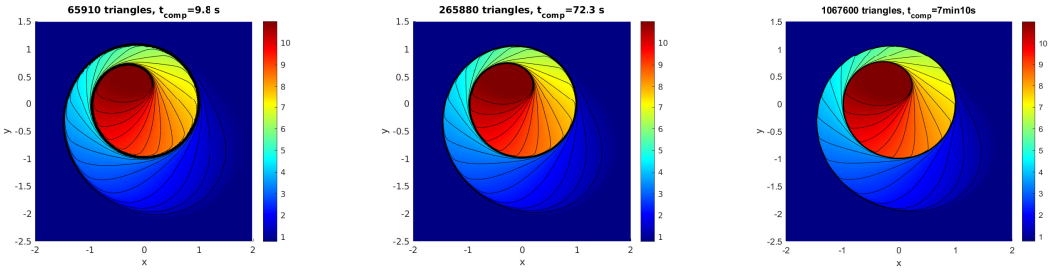

Figure 3.2: Solution to the nonconvex flux problem at $T = 1$; CFL=0.125.

3.5.3 Shallow water system with non-flat bottom

In this section, we perform numerical tests for shallow water system (2.134). The initial conditions and bottom topography are as described in Section 2.3.8.

Figure 3.3 illustrates a series of numerical approximations with good resolution performed on relatively coarse grids, which allows us to verify that the semi-discrete Lagrangian-Eulerian scheme adequately captures the expected behavior in the solutions of the dam–break flood with topography with no spurious noises or some undesired numerical artifacts.

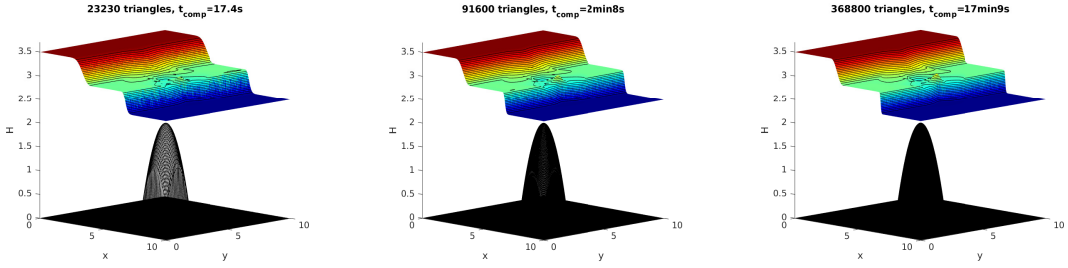

Figure 3.3: H pictures for the shallow-water problem at $T = 1$. CFL=0.1.

3.5.4 Orszag-Tang MHD turbulence problem

We now solve the Orszag-Tang problem described in Section 2.3.10.

Figures 3.4, 3.5, 3.6 and 3.7 display the density and pressure at $t = 2$ and $t = 3$, respectively. These results demonstrate the capability and effectiveness of semi-discrete Lagrangian-Eulerian scheme to resolve the shocks developed by the vortex system without the need of adding some correction technique to prevent divergence errors from increasing with time as in [31] (see also [98]) while maintaining the simplicity and ease of implementation.

As in Section 2.3.10, we also quantitatively study the divergence-free condition on the numerical magnetic field $\mathbf{B_h}$. Figure 3.8 depicts the discrete divergence operator (2.138) for three different grid refinements at $t = 2$ and $t = 3$ respectively.

Furthermore, we also study the global relative divergence error, ξ_{div}, defined by equations (2.139) and (2.138).

In Fig. 3.9, we plot ξ_{div} against time t. It is observed that, during the entire simulation, the magnitude of ξ_{div} is kept at order $\mathcal{O}(10^{-4})$ for refinements with 150000 triangles.

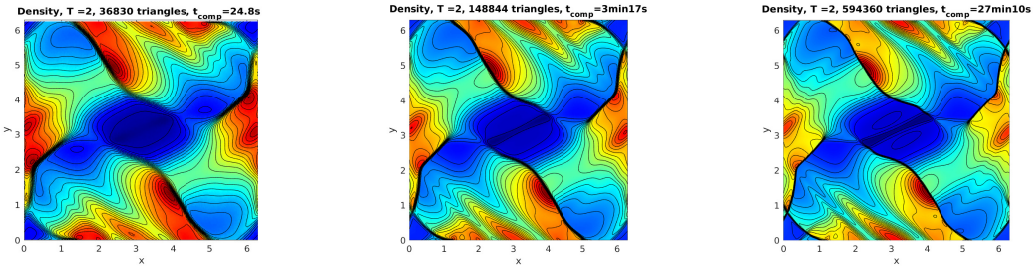

Figure 3.4: Density pictures of the Orszag–Tang problem at $T = 2$. CFL=0.2.

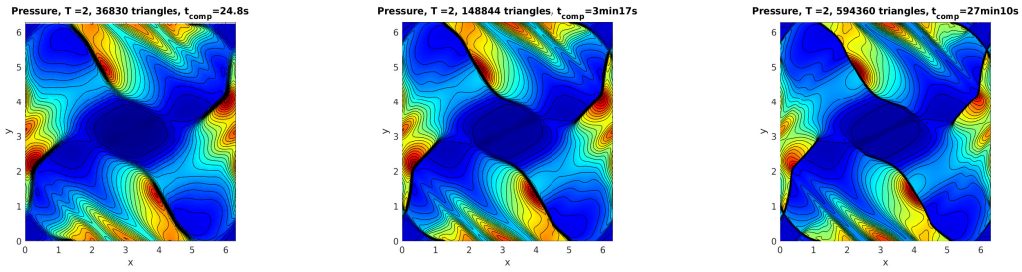

Figure 3.5: Pressure pictures of the Orszag–Tang problem at $T = 2$. CFL=0.2.

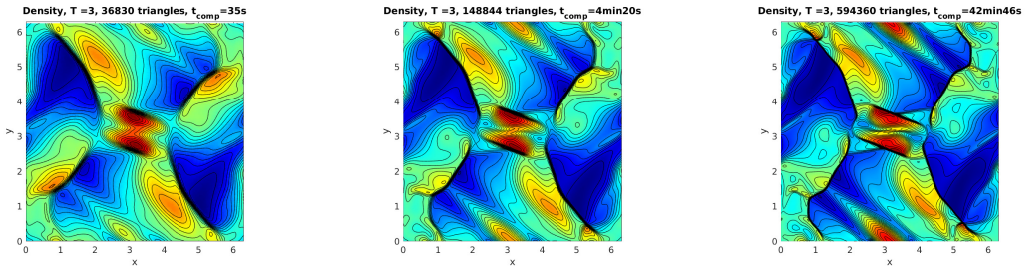

Figure 3.6: Density pictures of the Orszag–Tang problem at $T = 3$. CFL=0.2.

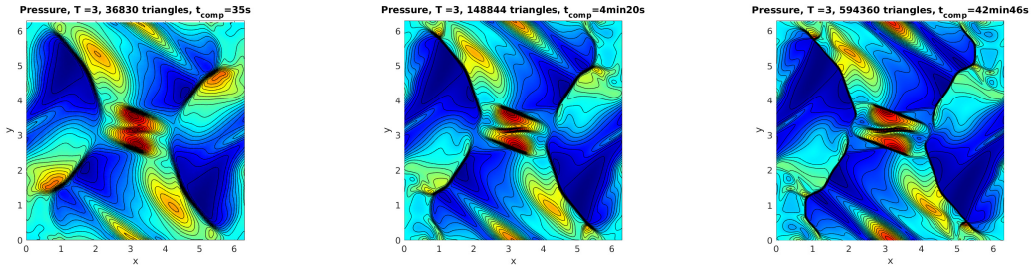

Figure 3.7: Pressure pictures of the Orszag–Tang problem at $T = 3$. CFL=0.2.

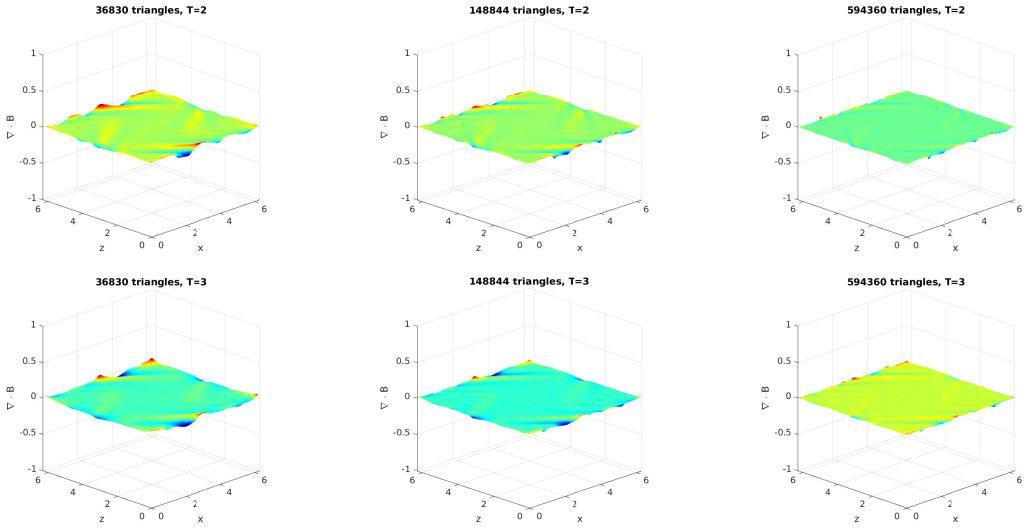

Figure 3.8: Magnetic field divergence.

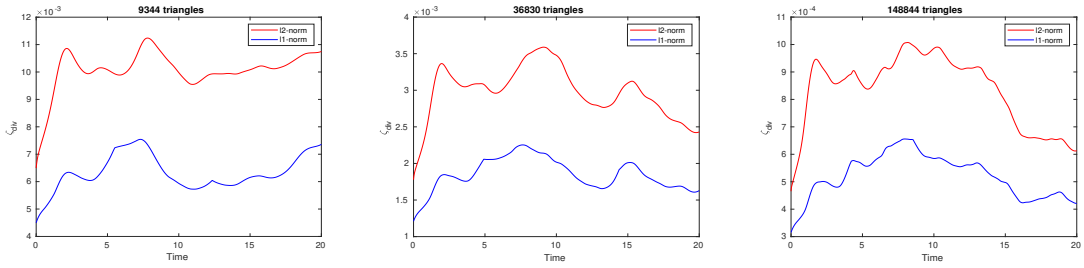

Figure 3.9: Global Relative Divergence Error.

3.5.5 Two-dimensional Euler equations for gas dynamics

In this section, we solve the Euler equations (1.8) with different sets of initial conditions, via the semi-discrete Lagrangian-Eulerian scheme.

- **Kelvin-Helmholtz problem 1**

We solve the two-dimensional Euler equations (1.8) by considering the following set of initial data:

$$w_0(x,y) = \begin{cases} w_L, & 0.25 < y < 0.75 \\ w_R, & y \le 0.25 \text{ or } y \ge 0.75, \end{cases} \quad (x,y) \in [0,1]^2. \tag{3.40}$$

with $\rho_L = 2,\ \rho_R = 1,\ u_L = -0.5,\ u_R = 0.5,\ v_L = v_R = 0$ and $p_L = p_R = 2.5$.

As in [91], we add the perturbation,

$$w_0^\varepsilon(x,y) = w_0(x,y) + \varepsilon X, \tag{3.41}$$

to the initial data (3.40) with $X_\rho = X_p = 0$, $X_u(x,y) = \sin(2\pi x)$, $X_v(x,y) = \sin(2\pi y)$ and compute approximate solutions for different refinements.

Figure 3.10 shows a series of approximate solutions using perturbation amplitude $\varepsilon = 0.01$. The results show that, with the refinement of the grid, different structures are formed at smaller and smaller scales, evidencing that there are no signs of convergence as the grid is refined.

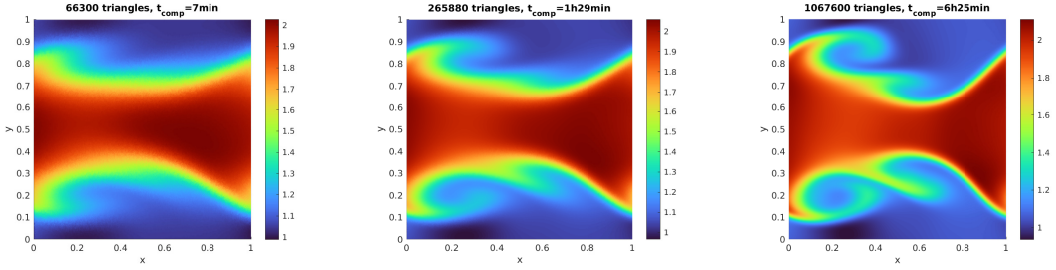

Figure 3.10: Density for the Kelvin-Helmholtz problem (3.40) with perturbation (3.41) and perturbation parameter $\varepsilon = 0.01$, at time $t = 1$

• **Kelvin-Helmholtz problem 2**

Following [91], we now consider the two-dimensional compressible Euler equations of gas dynamics (1.8) with the initial data

$$w_0(x,y,\omega) = \begin{cases} w_L, & I_1 < y < I_2 \\ w_R, & y \le I_1 \text{ or } y \ge I_2, \end{cases} \quad (x,y) \in [0,1]^2. \tag{3.42}$$

with $\rho_L = 2$, $\rho_R = 1$, $u_L = -0.5$, $u_R = 0.5$, $v_L = v_R = 0$ and $p_L = p_R = 2.5$. The interface profiles

$$I_j = I_j(\mathbf{x},\omega) := J_j + \varepsilon Y_j(\mathbf{x},\omega), \quad j = 1,2,$$

are chosen to be small perturbations around $J_1 := 0.25$ and $J_2 := 0.75$, respectively, with

$$Y_j(\mathbf{x},\omega) = \sum_{n=1}^{m} a_j^n(\omega)\cos(b_j^n + 2\pi x), \quad j = 1,2.$$

Here, $a_j^n = a_j^n(\omega) \in [0,1]$ and $b_j^n = b_j^n(\omega) \in [0,1]$, $j = 1,2$, $n = 1,...,m$ are randomly chosen numbers. The coefficients a_j^n have been normalized such that $\sum_{n=1}^m a_j^n = 1$ to guarantee that $|I_j(\mathbf{x},\omega) - J_j| \le \varepsilon$ for $j = 1,2$. We set $m = 10$.

The resulting Cauchy problem involves a random perturbation of the interfaces between the two streams (jets). This should be contrasted with initial value problem (3.40), where the amplitude was randomly perturbed (3.41).

Figure 3.11 shows the approximate solutions of density using perturbation amplitude $\varepsilon = 0.01$. Again, as in the initial problem (3.40), the results show that, with the refinement of the grid, different structures are formed at smaller and smaller scales, evidencing that there are no signs of convergence as the grid is refined.

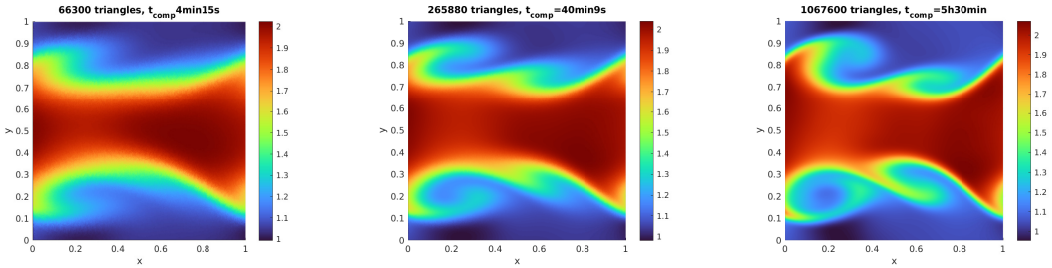

Figure 3.11: Approximate density for the Euler equations (1.8) with initial data (3.42), $\varepsilon = 0.01$ and for a fixed ω, computed with the SDLET, at time $t = 2$ at different grid refinements.

• Richtmeyer-Meshkov problem

Next, we solve the two-dimensional version of the Euler equations (1.8) with initial data:

$$p(x,y) = \begin{cases} 20, & x^2+y^2 < 0.01 \\ 1, & \text{otherwise,} \end{cases} \quad \rho(x,y) = \begin{cases} 2, & x^2+y^2 < I^2(x,y,\omega) \\ 1, & \text{otherwise,} \end{cases} \quad u = v = 0, \quad (x,y) \in [0,1]^2 \tag{3.43}$$

The radial density interface $I(x,y,\omega) = 0.25 + \varepsilon Y(\varphi(x,y),\omega)$ is perturbed with

$$Y(\varphi,\omega) = \sum_{n=1}^{m} a^n(\omega)\cos(\varphi + b^n(\omega)),$$

where $\varphi(x,y)$ is the angle of (x,y) with the positive x-axis, and a^n, b^n are the same as in the Kelvin-Helmholtz problem 2.

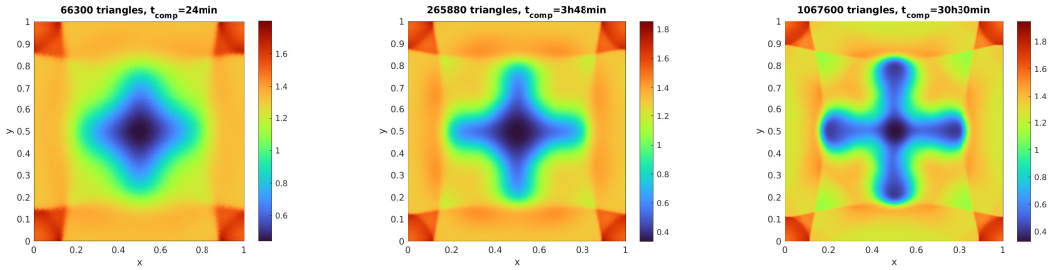

Figure 3.12: Approximate density for the Richtmeyer-Meshkov problem (3.43) for different grid refinements at time $t = 4$.

Figure 3.12 shows the effect of grid refinement on the density for at time $t = 4$. As in [91], the numerical results there seems to be no convergence as the grid is refined.

The findings of no convergence found with the semi-discrete Lagrangian-Eulerian scheme for the Kelvin-Helmholtz and Richtmeyer-Meshkov problems are consistent with those reported in [91].

• Two-dimensional vortex evolution problem for the Euler equations

Now, we consider the compressible Euler equations of gas dynamics (1.8) – (1.10). See [111] for a description of this problem. The mean flow density, velocities and pressure are $(\rho_\infty, u_\infty, v_\infty, p_\infty) = (1,1,1,1)$. At the initial time, the isentropic vortex has perturbations in u, v and temperature $T = p/\rho$ (no perturbation in the entropy $S = p/\rho^\gamma$) given by

$$\delta u = -\frac{b}{2\pi} e^{0.5(1-r^2)}(y - y_0), \tag{3.44}$$

$$\delta v = \frac{b}{2\pi} e^{0.5(1-r^2)}(x - x_0), \tag{3.45}$$

$$\delta T = -\frac{(\gamma-1)b^2}{8\gamma\pi^2} e^{0.5(1-r^2)}, \tag{3.46}$$

where $b = 5$ is the vortex strength, $(x_0, y_0) = (5, 5)$ is the vortex center and $r^2 = (x-x_0)^2+(y-y_0)^2$.

The initial condition is then given by $u_0 = u_\infty + \delta u$, $v_0 = v_\infty + \delta v$ and $\rho_0 = (T_\infty + \delta T)^{1/\gamma-1}$.

The computational domain is taken as $[0, 10] \times [0, 10]$, and periodic boundary conditions are used.

Fig. 3.13 and 3.14 show density simulation for three different refinements at $t = 2$ and $t = 10$ respectively. It is known that the exact solution at $t = T$ for this problem is the initial solution shifted by (uT, vT). As can be seen, at the end of each cycle that lasts 10 s, the vortex is back at its initial location (see Fig. 3.14).

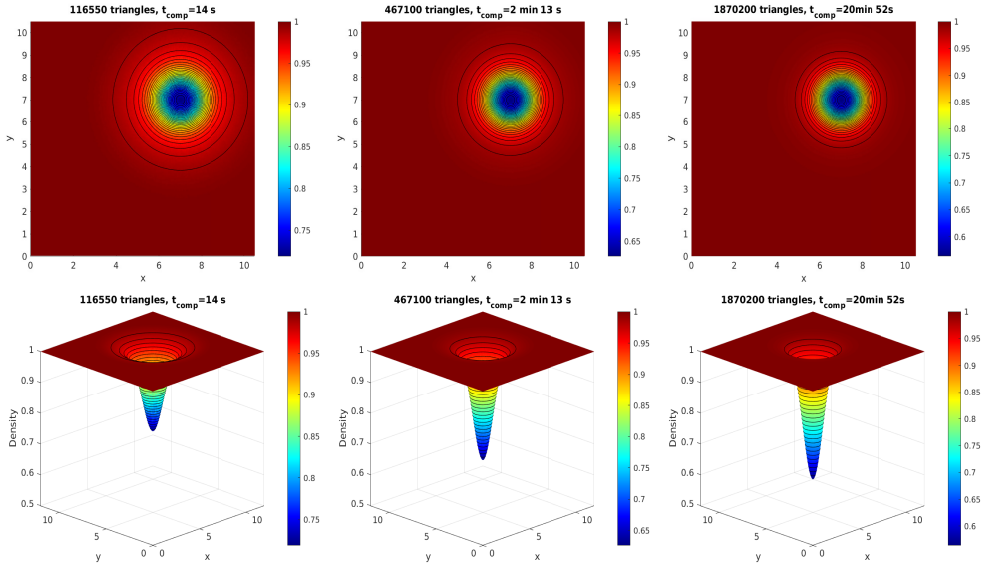

Figure 3.13: The density contours of isentropic vortex propagation at $T = 2$. CFL=0.125

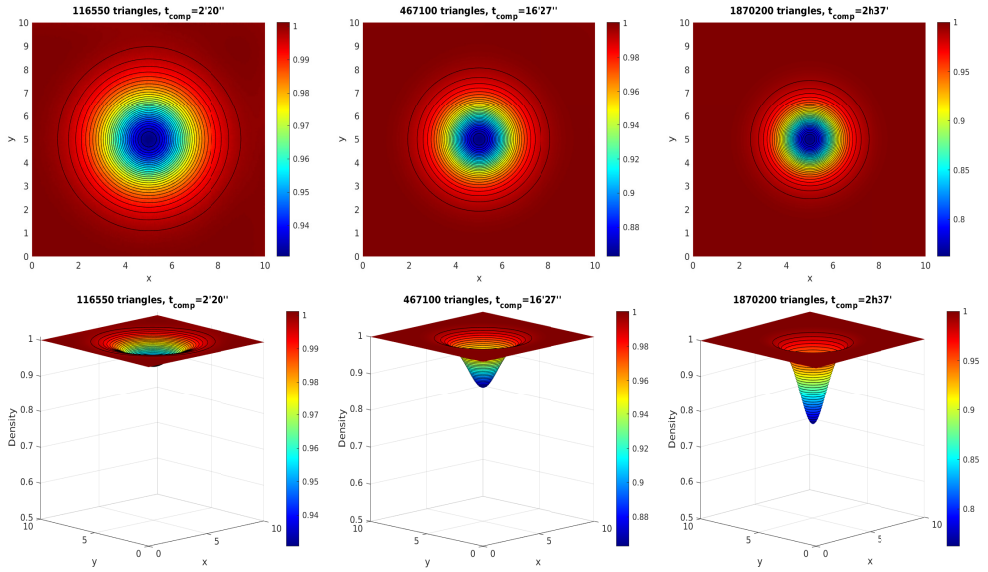

Figure 3.14: The density contours of isentropic vortex propagation at $T = 10$. CFL=0.125

3.6 Experimental Order of Convergence of the Triangular Semi-Discrete Lagrangian-Eulerian Scheme

In this section, we obtain the experimental order of convergence (EOC) of the semi-discrete Lagrangian-Eulerian scheme (3.1)–(3.3).

As in Section 2.4, the EOC (numerical convergence rate) is calculated by using equations (2.140) and (2.141).

Tables 3.1 and 3.2 show the error history via a set of numerical study of convergence in which it is evident that, as the grid grid is refined, the relative error e_i decays and the EOC remains consistent. That is, the numerical results obtained are shown to be very satisfactory even with relatively coarse grid discretizations.

i	N_i	e_i	EOC
1	4214	0.20291	-
2	17574	0.10953	0.4318
3	70350	0.057248	0.4678
4	282100	0.029202	0.4847
5	1128186	0.014769	0.4918
6	4518770	0.0074633	0.4919

i	N_i	e_i	EOC
1	12750	0.041982	-
2	51900	0.022011	0.4600
3	207000	0.012164	0.4287
4	829200	0.0068361	0.4153
5	3324000	0.0037145	0.4393
6	6667400	0.0028794	0.4425

Table 3.1: Linear problem(left); Burgers' oblique problem(right); see Figure 3.1.

i	N_i	e_i	EOC
1	51900	0.0295	-
2	105716	0.0224	0.3855
3	213408	0.0171	0.3843
4	425700	0.0128	0.4194
5	857660	0.0095	0.4256
6	1722816	0.00704	0.4296
7	3461850	0.00520	0.4341

i	N_i	e_i	EOC
1	23000	0.0064614	-
2	70350	0.0047015	0.2844
3	143500	0.003688	0.3406
4	323250	0.0027092	0.3798
5	829200	0.0018349	0.4136
6	1870200	0.0012837	0.4392
7	3607500	0.0009466	0.4637

Table 3.2: NonConvex flux problem (left); see Figure 3.2. Smooth Vortex Problem; see Figures 3.13–3.14.

4. Concluding Remarks and Perspectives for Future Work

4.1 Concluding Remarks

In order to approximate nonlinear multidimensional initial value problems for scalar hyperbolic equations and systems, in this thesis, based on the improved concept of multidimensional no-flow surfaces/curves, we constructed, analyzed, and implemented a new class of fully-discrete and semi-discrete positive Lagrangian-Eulerian schemes on triangular grids. The no-flow surfaces/curves allowed introducing an effective class of numerical fluxes over the interfaces of the triangulation elements, and finding a weak CFL-type condition (Eq. (2.23)), which guarantees the stability of these novel numerical schemes. These new numerical fluxes and the new weak CFL-type condition did not require constructing or evaluating the Jacobian matrix of the respective flux functions of the hyperbolic equation or the hyperbolic system of equations. The implementation of these novel fully-discrete and semi-discrete Lagrangian-Eulerian schemes on triangular grids in the solution of multidimensional scalar and system problems, besides being simple and efficient, has been Riemann-solver free without using any sophisticated and time-consuming tools, such as field-by-field decompositions, grid adaptivity, or upwinding techniques. As a matter of fact, the new Lagrangian-Eulerian schemes on triangular grids did not need high-resolution non-oscillating interpolation reconstructions (widely used in central differentiation schemes), which reduced the complexity of the algorithm design, and their extension to multidimensional systems has been easily carried out by a straightforward componentwise application of the scalar framework without the need to use any dimensional splitting strategies.

As proof of the validity of the proposed schemes, the following theoretical results were presented:

- Convergence proof of fully-discrete schemes towards the entropy solution of the scalar problem $u_t(\mathbf{x},t)+\text{div}(f(u(\mathbf{x},t)))=0$ with initial condition $u_0 \in L^\infty(\mathbb{R}^2)$, following the setting of the uniqueness and regularity properties of the entropy process solutions that are linked to the measure-valued solutions (Section 2.2.2).
- Convergence proof of semi-discrete schemes towards the entropy solution of the scalar problem $u_t(\mathbf{x},t)+\text{div}(f(u(\mathbf{x},t)))=0$ with initial condition $u_0 \in L^\infty(\mathbb{R}^2)$, by means of the weak asymptotic analysis (Section 3.2).
- Estimation of the optimal convergence rate of fully discrete schemes on equilateral triangular grids (Section 2.2.3).
- Proof of the stability of the numerical solutions of multidimensional systems obtained by fully-discrete (Section 2.2.4) and semi-discrete schemes (Section 3.3), by showing that they satisfy *the positivity principle* as proposed by P. Lax and X.-D. Liu [130, 131], and *the weak positivity principle* introduced in E. Abreu, J. François, W. Lambert and J. Pérez [4].

Finally, the robustness/reliability of the fully-discrete and semi-discrete Lagrangian-Eulerian schemes on triangular grids, in which the found CFL-type weak stability condition was used, was demonstrated by means of thorough and extensive numerical tests (Sections 2.3 and 3.5) such as 2D scalar equations with convex and non-convex flux functions (e.g. the sonic point for the inviscid Burgers' equation, and the Buckley-Leverett equation with gravity), the non-classical 2 by 2 three-phase flow system of nonstrictly hyperbolic conservation laws (with resonance/umbilic point), the 2D system of compressible Euler equations (Double Mach Reflection problem and Mach 3 wind tunnel flow), the 3 by 3 shallow-water system (with and without bottom topography), and the 8 by 8 system of Magnethohydrynamic equations (the Orzs-Tang problem). The results of the numerical tests, besides revealing that the new fully-discrete and semi-discrete locally conservative Lagrangian-Eulerian schemes are very effective and simple for users mainly interested in applications, confirming their effectiveness in the dynamic forward tracking of no-flow surfaces/curves on triangular grids per time step, and showed their capability of capturing correct

qualitative solutions, with a very good resolution, of nontrivial multidimensional models such as the shallow water system, the magnetohydrodynamics equations, the compressible Euler equations, the three-phase flow in porous media, among others.

4.2 Perspectives for Future Work

Considering the evolution of the state of the art, the following research topics, around the Lagrangian-Eulerian framework, are being developed or considered:

- Extension of fully-discrete and semi-discrete Lagrangian-Eulerian schemes to high-order schemes on unstructured Cartesian and triangular grids.
- Extension of fully-discrete and semi-discrete Lagrangian-Eulerian schemes to three spatial dimensions on cubic/tetrahedral grids.
- Study and feasibility of fully-discrete and semi-discrete Lagrangian-Eulerian schemes in parallel programming.
- Conducting numerical tests on other challenging hyperbolic problems in two and three dimensions, such as:
  - **Relativistic magnetohydrodynamics (RMHD) blast problem with strong magnetic field.** It describes the propagation of a circular strong fast magneto-sonic shock formulates and propagates into the ambient plasma with low plasma-beta. Its simulation with strong magnetic field is difficult, because nonphysical quantities, e.g., negative pressure, are very likely to be produced in the numerical simulation.
  - **Astrophysical jets problem: non-magnetized and the strongly magnetized cases.** Successfully simulating this type of jet flows is a challenge, because strong shock wave, shear flow and interface instabilities in high-speed jet flows there may exist. Moreover, negative pressure could be easily produced in numerical simulation.
  - **Shock cloud interaction problem.** This problem describes the disruption of a high density cloud by a strong shock wave and it is widely simulated in the literature.

Bibliography

[1] Abreu, E., Agudelo, J. & Pérez, J. *A Lagrangian-Eulerian method on regular triangular grids for hyperbolic problems: error estimates for the scalar case and a positive principle for multidimensional systems.* Journal of Dynamics and Differential Equations. Submitted.

[2] Abreu, E., Bachini, E., Pérez, J., & Putti, M. *A geometrically intrinsic lagrangian–Eulerian scheme for 2D shallow water equations with variable topography and discontinuous data.* Applied Mathematics and Computation, 443, 127776, 2023.

[3] Abreu, E., François, J., Lambert, W., & Pérez, J. *A semi-discrete Lagrangian–Eulerian scheme for hyperbolic-transport models. Journal of Computational and Applied Mathematics*, 406, 114011, 2022.

[4] Abreu, E., François, J., Lambert, W., & Pérez, J. *A Class of Positive Semi-discrete Lagrangian–Eulerian Schemes for Multidimensional Systems of Hyperbolic Conservation Laws.* Journal of Scientific Computing, 90(1), 1-79, 2022.

[5] Abreu, E., De la Cruz, R., Juajibioy, J. C., & Lambert, W. *Lagrangian-Eulerian Approach for Nonlocal Conservation Laws.* Journal of Dynamics and Differential Equations, 1-47, 2022.

[6] Abreu, E., Ferreira, L. C. F., Galeano, J., & Pérez, J. *On a 1D model with nonlocal interactions and mass concentrations: an analytical-numerical approach.* Nonlinearity 35(4), 1734, 2022.

[7] Abreu, E., Matos, V., Pérez, J., & Rodriguez-Bermudez, P. *A class of Lagrangian–Eulerian shock-capturing schemes for first-order hyperbolic problems with forcing terms.* Journal of Scientific Computing, 86(1), 1-47, 2021.

[8] Abreu, E., Diaz, C., Galvis, J., & Pérez, J. *On the Conservation Properties in Multiple Scale Coupling and Simulation for Darcy Flow with Hyperbolic-Transport in Complex Flows.* Multiscale Modeling & Simulation, 18(4), 1375-1408, 2020.

[9] Abreu, E., Diaz, C., Galvis, J., & Pérez, J. *On the conservation properties in multiple scale coupling and simulation for Darcy flow with hyperbolic-transport in complex flows.* Multiscale Modeling & Simulation, 18(4), 1375-1408, 2020.

[10] Abreu, E., & Pérez, J. *A fast, robust, and simple Lagrangian–Eulerian solver for balance laws and applications.* Computers & Mathematics with Applications, 77(9), 2310-2336, 2019.

[11] Abreu, E., Bustos, A., Ferraz, P., and Lambert, W. *A Relaxation Projection Analytical-Numerical Approach in Hysteretic Two-Phase Flows in Porous Media.* Journal of Scientific Computing, 79(3), 1936-1980, 2019.

[12] Abreu, E., Pérez, J., & Santo, A. *Lagrangian-Eulerian approximation methods for balance laws and hyperbolic conservation laws.* Revista UIS Ingenierías, 17(1), 191-200, 2018.

[13] Abreu, E., Pérez, J., & Santo, A. *A conservative Lagrangian-Eulerian finite volume approximation method for balance law problems.* Proceeding Series of the Brazilian Society of Computational and Applied Mathematics, 6(1), 2018.

[14] Abreu, E., Lambert, W., Pérez, J., & Santo, A. *A weak asymptotic solution analysis for a Lagrangian–Eulerian scheme for scalar hyperbolic conservation laws.* Hyperbolic Problems: Theory, Numerics, Applications. 223-230, 2018.

[15] Abreu, E., Lambert, W., Pérez, J., & Santo, A. *A new finite volume approach for transport models and related applications with balancing source terms.* Mathematics and Computers in Simulation, 137, 2-28, 2017.

[16] Abreu, E., Colombeau, M., & Panov, E. Y. *Approximation of entropy solutions to degenerate nonlinear parabolic equations*. Zeitschrift für angewandte Mathematik und Physik, 68(6), 133, 2017.

[17] Abreu, E., Colombeau, M., & Panov, E. *Weak asymptotic methods for scalar equations and systems*. Journal of mathematical analysis and applications, 444(2), 1203-1232, 2016.

[18] Abreu, E. *Numerical modelling of three-phase immiscible flow in heterogeneous porous media with gravitational effects*. Mathematics and Computers in Simulation, 97, 234-259, 2014.

[19] Abreu, E., & Conceição, D. *Numerical modeling of degenerate equations in porous media flow*. Journal of Scientific Computing, 55(3), 688-717, 2013.

[20] Abreu, E., & Lambert, W. *Computational modeling technique for numerical simulation of immiscible two-phase flow problems involving flow and transport phenomena in porous media with hysteresis*. AIP Conference Proceedings 4. American Institute of Physics, 1453(1), 2012.

[21] Alibaud, N., Andreianov, B., & Ouédraogo, *A. Nonlocal dissipation measure and L 1 kinetic theory for fractional conservation laws*. Communications in Partial Differential Equations, 45(9), 1213-1251, 2020.

[22] Almeida, C. G., Douglas Jr, J., & Pereira, F. *A new characteristics-based numerical method for miscible displacement in heterogeneous formations*. Computational and Applied Mathematics, 21, 573–605, 2002.

[23] Ambrosio, L., Bressan, A., Helbing, D., Klar, A., Zuazua, E., & Bressan, A. *Hyperbolic conservation laws: an illustrated tutorial*. Modelling and Optimisation of Flows on Networks, 157-245, 2013.

[24] Ancona, F., & Marson, A. *Sharp convergence rate of the Glimm scheme for general nonlinear hyperbolic systems*. Communications in mathematical physics, 302(3), 581-630, 2011.

[25] Aquino, J., Francisco, A. S., Pereira, F., Pereira, T. J., & Souto, H. A. *A Lagrangian strategy for the numerical simulation of radionuclide transport problems*. Progress in Nuclear Energy, 52(3), 282-291, 2010.

[26] Aquino, J., Francisco, A. S., Pereira, F., & Souto, H. A. *An overview of Eulerian–Lagrangian schemes applied to radionuclide transport in unsaturated porous media*. Progress in Nuclear Energy, 50(7):774-787, 2008.

[27] Aquino, J., Pereira, F., Amaral Souto, H. P., & Francisco, A. S. *A forward tracking scheme for solving radionuclide advective problems in unsaturated porous media*. International Journal of Nuclear Energy Science and Technology, 3(2), 196-205, 2007.

[28] Arbogast, T., Huang, C. S., & Russell, T. F. *A Locally Conservative Eulerian–Lagrangian Method for a Model Two-Phase Flow Problem in a One-Dimensional Porous Medium*. SIAM Journal on Scientific Computing, 34(4), A1950-A1974, 2012.

[29] Arbogast, T., & Wheeler, M. F. *A characteristics-mixed finite element method for advection-dominated transport problems*. SIAM Journal on Numerical analysis, 32(2), 404-424, 1995.

[30] Ascher, U. M., Ruuth, S. J., & Wetton, B. T. *Implicit-explicit methods for time-dependent partial differential equations*. SIAM Journal on Numerical Analysis, 32(3), 797-823, 1995.

[31] Balbás, J., Tadmor, E., & Wu, C. C. *Non-oscillatory central schemes for one-and two-dimensional MHD equations*. I. Journal of Computational Physics, 201(1), 261-285, 2004.

[32] Balbás, J., & Tadmor, E. *Nonoscillatory central schemes for one-and two-dimensional magnetohydrodynamics equations*. II: High-order semidiscrete schemes. SIAM Journal on Scientific Computing, 28(2), 533-560, 2006.

[33] Barth, T., & Ohlberger, M. *Finite volume methods: foundation and analysis*, 2003.

[34] Becker, S., Gess, B., Jentzen, A., & Kloeden, P. E. *Strong convergence rates for explicit space-time discrete numerical approximations of stochastic Allen-Cahn equations.* Stochastics and Partial Differential Equations: Analysis and Computations, 1-58, 2022.

[35] Benharbit, S., Chalabi, A., & Vila, J. P. *Numerical viscosity, entropy condition and convergence of finite volume schemes for general multidimensional conservation laws.* Nonlinear Hyperbolic Problems: Theoretical, Applied, and Computational Aspects, Springer, 48-55, 1993.

[36] Bianchini, S. *Hyperbolic limit of the Jin-Xin relaxation model.* Communications on pure and applied mathematics, 59(5), 688, 2006.

[37] Bianchini, S., & Bressan, A. *Vanishing viscosity solutions of nonlinear hyperbolic systems.* Annals of mathematics, 223-342, 2005.

[38] Bianchini, S. *BV solutions of the semidiscrete upwind scheme.* Archive for rational mechanics and analysis, 167(1), 1-81, 2003.

[39] Binning, P., & Celia, M. A. *Two-dimensional eulerian lagrangian localised adjoint method for the solution of the contaminant transport equation in the saturated and unsaturated zones.* International Conference on Computational Methods in Water Resources. Vol. 1, 165-172, 1994.

[40] Boscheri, W., Loubère, R., & Maire, P. H. *A 3D cell-centered ADER MOOD Finite Volume method for solving updated Lagrangian hyperelasticity on unstructured grids.* Journal of Computational Physics, 449, 110-779, 2022.

[41] Bouchut, F., & Westdickenberg, M. *Gravity driven shallow water models for arbitrary topography.* Communications in Mathematical Sciences, 2(3), 359-389, 2004.

[42] Bréhier, C. E., Cui, J., & Hong, J. *Strong convergence rates of semidiscrete splitting approximations for the stochastic Allen–Cahn equation.* IMA Journal of Numerical Analysis, 39(4), 2096-2134, 2019.

[43] Bressan, A., Chiri, M. T., & Shen, W. *A posteriori error estimates for numerical solutions to hyperbolic conservation laws.* Archive for Rational Mechanics and Analysis, 241, 357-402, 2021.

[44] Bressan, A., & Shen, W. *Optimality conditions for solutions to hyperbolic balance.* Control Methods in PDE-Dynamical Systems Contemp. Math, 426, 129-152, 2007.

[45] Bressan, A., & Yang, T. *On the convergence rate of vanishing viscosity approximations.* Communications on Pure and Applied Mathematics: A Journal Issued by the Courant Institute of Mathematical Sciences, 57(8), 1075-1109, 2004.

[46] Bressan, A., & Jenssen, H. K. *On the convergence of Godunov scheme for nonlinear hyperbolic systems.* Chinese Annals of Mathematics, 21(03), 269-284, 2000.

[47] Bressan, A. *Hyperbolic systems of conservation laws: the one-dimensional Cauchy problem.* Oxford University Press on Demand, Vol. 20, 2000.

[48] Bressan, A., & Marson, A. *Error bounds for a deterministic version of the Glimm scheme.* Archive for rational mechanics and analysis, 142(2), 155-176, 1998.

[49] Bressan, A., *Unique solutions for a class of discontinuous differential equations.* Proceedings of the American Mathematical Society, 104(3), 772-778, 1988.

[50] Bressan, A., & Colombo, G. *Existence and continuous dependence for discontinuous ODEs.* Bollettino Della Unione Matematica Italiana, 4(2), 295-311, 1990.

[51] Buckmaster, T., & Vicol, V. *Nonuniqueness of weak solutions to the Navier-Stokes equation.* Annals of Mathematics, 189(1), 101-144, 2019.

[52] Carlino, M. G., & Gaburro, E. *Well balanced finite volume schemes for shallow water equations on manifolds.* Applied Mathematics and Computation, 441, 127676, 2023.

[53] Castañeda, P., Abreu, E., Furtado, F., & Marchesin, D. *On a universal structure for immiscible three-phase flow in virgin reservoirs.* Computational Geosciences, 20, 171-185, 2016.

[54] Celia, M. A. *Eulerian-Lagrangian localized adjoint methods for contaminant transport simulations.* Computational methods in water resources X, 1: 207-216, 1994.

[55] Celia, M. A., Russell, T. F., Herrera, I., & Ewing, R. E. *An Eulerian-Lagrangian localized adjoint method for the advection-diffusion equation.* Advances in Water Resources, 13(4), 187-206, 1990.

[56] Chainais-Hillairet, C. *Finite volume schemes for a nonlinear hyperbolic equation. Convergence towards the entropy solution and error estimate.* ESAIM: Mathematical Modelling and Numerical Analysis, 33(1), 129-156, 1999.

[57] Champier, S., Gallouët, T., & Herbin, R. *Convergence of an upstream finite volume scheme for a nonlinear hyperbolic equation on a triangular mesh.* Numerische Mathematik, 66(1), 139-157, 1993.

[58] Chen, W., Wang, Q., Hesthaven, J. S., & Zhang, C. *Physics-informed machine learning for reduced-order modeling of nonlinear problems.* Journal of Computational Physics 446, 110666, 2021.

[59] Chen, G. Q. G., & Glimm, J. *Kolmogorov-type theory of compressible turbulence and inviscid limit of the Navier-Stokes equations in R3.* Physica D: Nonlinear Phenomena, 400, 132138, 2019.

[60] Chiodaroli, E., De Lellis, C., & Kreml, O. *Global ill-posedness of the isentropic system of gas dynamics.* Communications on Pure and Applied Mathematics, 68(7), 1157-1190, 2015.

[61] Chorin, A. J. *Numerical study of slightly viscous flow. Journal of fluid mechanics*, 57(4), 785-796, 1973.

[62] Christoforou, C., & Trivisa, K. *Rate of convergence for vanishing viscosity approximations to hyperbolic balance laws.* SIAM journal on mathematical analysis, 43(5), 2307-2336, 2011.

[63] Christov, I., & Popov, B. *New non-oscillatory central schemes on unstructured triangulations for hyperbolic systems of conservation laws.* Journal of Computational Physics, 227(11), 5736-5757, 2008.

[64] Cockburn, B., Gremaud, P. A., & Yang, J. X. *A priori error estimates for numerical methods for scalar conservation laws part iii: Multidimensional flux-splitting monotone schemes on non-cartesian grids.* SIAM journal on numerical analysis, 35(5),1775-1803, 1998.

[65] Cockburn, B., & Gremaud, P. A. *A priori error estimates for numerical methods for scalar conservation laws. part ii: Flux-splitting monotone schemes on irregular cartesian grids.* Mathematics of computation, 66(218), 547-572, 1997.

[66] Cockburn, B., & Gremaud, P. A. *A priori error estimates for numerical methods for scalar conservation laws. Part I: The general approach.* Mathematics of Computation of the American Mathematical Society, 65(214), 533-573, 1996.

[67] Cockburn, B., Coquel, F., & LeFloch, P. G. *Convergence of the finite volume method for multidimensional conservation laws.* SIAM Journal on Numerical Analysis, 32(3), 687-705, 1995.

[68] Cockburn, B., Coquel, F., & LeFloch, P. *An error estimate for finite volume methods for multidimensional conservation laws.* Mathematics of computation, 63(207), 77-103, 1994.

[69] Cockburn, B., Coquel, F., LeFloch, P., & Shu, C. W. *Convergence of finite volume methods*, 1991.

[70] Cockburn, B., & Shu, C. W. *TVB Runge-Kutta local projection discontinuous Galerkin finite element method for conservation laws. II. General framework.* Mathematics of computation, 52(186), 411-435, 1989.

[71] Córdoba, D., Faraco, D., & Gancedo, F. *Lack of uniqueness for weak solutions of the incompressible porous media equation.* Archive for Rational Mechanics and Analysis, 200(3), 725-746, 2011.

[72] Dafermos, C. M. *Hyperbolic conservation laws in continuous physics.* Springer, 2016.

[73] Dahle, H. K., Ewing, R. E., & Russell, T. F. *Eulerian-lagrangian localized adjoint methods for a nonlinear advection-diffusion equation.* Computer methods in applied mechanics and engineering, 122(3-4), 223-250, 1995.

[74] Danilov, V. G., & Shelkovich, V. M. *Dynamics of propagation and interaction of δ-shock waves in conservation law systems.* Journal of Differential Equations 211(2), 333-381, 2005.

[75] Danilov, V., & Shelkovich, V. *Delta-shock wave type solution of hyperbolic systems of conservation laws.* Quarterly of Applied Mathematics 63(3), 401-427, 2005.

[76] Danilov, V. G., & Shelkovich, V. M. *Generalized solutions of nonlinear differential equation and the maslov algebras of distributions.* Integral Transforms and Special Functions, 6(1-4), 171-180, 1998.

[77] De Lellis, C., & Kwon, H. *On Non-uniqueness of Hö lder continuous globally dissipative Euler flows.* arXiv preprint arXiv:2006.06482, 2020.

[78] De Lellis, C., & Székelyhidi Jr, L. *The Euler equations as a differential inclusion.* Annals of mathematics, 1417-1436, 2009.

[79] DiPerna, R. J. *Measure-valued solutions to conservation laws.* Archive for Rational Mechanics and Analysis, 88, 223-270, 1985.

[80] Douglas Jr, J., Spagnuolo, A. M., & Yi, S. Y. *The convergence of a multidimensional, locally conservative Eulerian–Lagrangian finite element method for a semilinear parabolic equation.* Mathematical Models and Methods in Applied Sciences, 20(02), 315-348, 2010.

[81] Douglas, J., Pereira, F., & Yeh, L. M. *A locally conservative Eulerian–Lagrangian numerical method and its application to nonlinear transport in porous media.* Computational Geosciences, 4(1), 1-40, 2000.

[82] Douglas, J., Pereira, F., & Yeh, L. M. *A locally conservative eulerian-lagrangian method for flow in a porous medium of a mixture of two components having different densities.* Numerical Treatment of Multiphase Flows in Porous Media, Springer, 138-155, 2000.

[83] Douglas, J., Pereira, F., & Yeh, L. M. *Numerical methods for transport-dominated flows in heterogeneous porous media.* WIT Transactions on Ecology and the Environment, 23, 1998.

[84] Douglas Jr, J., Furtado, F., & Pereira, F. *On the numerical simulation of waterflooding of heterogeneous petroleum reservoirs.* Computational Geosciences, 1(2),155, 1997.

[85] Douglas Jr, J., Pereira, F., & Yeh, L. M. *A parallelizable method for two-phase flows in naturally-fractured reservoirs.* Computational Geosciences, 1(3-4), 333-368, 1997.

[86] Douglas, Jr, J., & Russell, T. F. *Numerical methods for convection-dominated diffusion problems based on combining the method of characteristics with finite element or finite difference procedures.* SIAM Journal on Numerical Analysis, 19(5), 871-885, 1982.

[87] Eymard, R., Gallouët, T., & Herbin, R. *Finite volume methods*. Handbook of numerical analysis, 7, 713-1018, 2000.

[88] Eymard, R., Gallouët, T., & Herbin, R. *Convergence of a finite volume scheme for a nonlinear hyperbolic equation*. Proceedings of the third colloquium on numerical analysis, 61-70, 1995.

[89] Eymard, R., Gallouët, T., & Herbin, R. *Existence and uniqueness of the entropy solution to a nonlinear hyperbolic equation*. Chinese Annals of Mathematics, 16(1), 1-14, 1995.

[90] Fjordholm, U. S., Lye, K., Mishra, S., & Weber, F. *Statistical solutions of hyperbolic systems of conservation laws: numerical approximation*. Mathematical Models and Methods in Applied Sciences, 30(03), 539-609, 2020.

[91] Fjordholm, U. S., Käppeli, R., Mishra, S., & Tadmor, E. *Construction of approximate entropy measure-valued solutions for hyperbolic systems of conservation laws*. Foundations of Computational Mathematics, 17(3), 763-827, 2017.

[92] Fjordholm, U. S., Käppeli, R., Mishra, S., & Tadmor, E. *Construction of approximate entropy measure-valued solutions for hyperbolic systems of conservation laws*. Foundations of Computational Mathematics, 17, 763-827, 2017.

[93] Fjordholm, U. S., Lanthaler, S., & Mishra, S. *Statistical solutions of hyperbolic conservation laws: foundations*. Archive for Rational Mechanics and Analysis, 226(2), 809-849, 2017.

[94] Fjordholm, U. S., Mishra, S., & Tadmor, E. *On the computation of measure-valued solutions*. Acta numerica, 25, 567-679, 2016.

[95] Fjordholm, U. S., Mishra, S., & Tadmor, E. *Arbitrarily high-order accurate entropy stable essentially nonoscillatory schemes for systems of conservation laws*. SIAM Journal on Numerical Analysis, 50(2), 544-573, 2012.

[96] Fjordholm, U. S., Mishra, S., & Tadmor, E. *Well-balanced and energy stable schemes for the shallow water equations with discontinuous topography*. Journal of Computational Physics, 230(14), 5587-5609, 2011.

[97] Fořt, J., Fürst, J., Halama, J., Herbin, R., & Hubert, F. (Eds.). Finite Volumes for Complex Applications VI Problems & Perspectives: FVCA 6, International Symposium. Springer Science & Business Media, Vol. 4, 6-10, 2011.

[98] Gábor, Tóth. *The $\nabla \cdot B = 0$ constraint in shock-capturing magnetohydrodynamics codes*. Journal of Computational Physics, 161(2), 605-652, 2000.

[99] Glimm, J. *Solutions in the large for nonlinear hyperbolic systems of equations*. Communications on pure and applied mathematics, 18(4), 697-715, 1965.

[100] Godlewski, E., & Raviart, P. A. *Numerical approximation of hyperbolic systems of conservation laws*. Springer Science & Business Media, Vol. 118, 2013.

[101] Godlewski, E., & Raviart, P. A. *Numerical approximation of hyperbolic systems of conservation laws*. Springer Science & Business Media, Vol. 118, 2013.

[102] Gosse, L. *Computing qualitatively correct approximations of balance laws*. Springer, Vol. 2, 2013.

[103] Gottlieb, D., & Hesthaven, J. S. *Spectral methods for hyperbolic problems*. Journal of Computational and Applied Mathematics, 128(1-2), 83-131, 2001.

[104] Guermond, J. L., & Popov, B. *Invariant domains and second-order continuous finite element approximation for scalar conservation equations*. SIAM Journal on Numerical Analysis, 55(6), 3120-3146, 2017.

[105] Guermond, J. L., Nazarov, M., Popov, B., & Yang, Y. *A second-order maximum principle preserving Lagrange finite element technique for nonlinear scalar conservation equations.* SIAM Journal on Numerical Analysis, 52(4), 2163-2182, 2014.

[106] Healy, R. W., & Russell, T. F. *A finite-volume Eulerian-Lagrangian localized adjoint method for solution of the advection-dispersion equation.* Water Resources Research, 29(7), 2399-2413, 1993.

[107] Heibig, A. *Existence and uniqueness of solutions for some hyperbolic systems of conservation laws.* Archive for rational mechanics and analysis, 126, 79-101, 1994.

[108] Hoel, H., Karlsen, K. H., Risebro, N. H., & Storrøsten, E. B. *Numerical methods for conservation laws with rough flux.* Stochastics and Partial Differential Equations: Analysis and Computations, 8(1), 186-261, 2020.

[109] Hou, T. Y. *Blow-up or no blow-up? A unified computational and analytic approach to 3D incompressible Euler and Navier-Stokes equations.* Acta Numerica, 18, 277-346, 2009.

[110] Hu, J., Qi, K., & Yang, T. *A New Stability and Convergence Proof of the Fourier-Galerkin Spectral Method for the Spatially Homogeneous Boltzmann Equation.* SIAM Journal on Numerical Analysis, 59(2), 613-633, 2021.

[111] Hu, C., & Shu, C. W. *Weighted essentially non-oscillatory schemes on triangular meshes.* Journal of Computational Physics, 150(1), 97-127, 1999.

[112] Huang, C. S., Arbogast, T., & Qiu, J. *An Eulerian-Lagrangian WENO finite volume scheme for advection problems.* Journal of Computational Physics, 231(11), 4028-4052, 2012.

[113] Jin, S., & Xin, Z. *The relaxation schemes for systems of conservation laws in arbitrary space dimensions.* Communications on pure and applied mathematics, 48(3), 235-276, 1995.

[114] Kroener, D. *Numerical schemes for conservation laws.* John Wiley & Sons, 1997.

[115] Kroener, D., Rokyta, M., & Wierse, M. *A Lax-Wendroff type theorem for upwind finite volume schemes in 2-D.* East West Journal of Numerical Mathematics, 4, 279-292, 1996.

[116] Kruzhkov, S. N. *First order quasilinear equations in several independent variables.* Matematicheskii Sbornik, 123(2), 228-255, 1970.

[117] Kuznetsov, N. N. *Accuracy of some approximate methods for computing the weak solutions of a first-order quasi-linear equation.* USSR Computational Mathematics and Mathematical Physics, 16(6), 105-119, 1976.

[118] Kurganov, A. *Third-order semi-discrete central scheme for conservation laws and convection-diffusion equations.* SIAM Journal on Scientific Computing, 22(4), 1999.

[119] Kurganov, A., Noelle, S., & Petrova, G. *Semidiscrete central-upwind schemes for hyperbolic conservation laws and Hamilton–Jacobi equations.* SIAM Journal on Scientific Computing, 23(3), 707-740, 2001.

[120] Kurganov, A., & Tadmor, E. *New high-resolution central schemes for nonlinear conservation laws and convection–diffusion equations.* Journal of computational physics, 160(1), 241-282, 2000.

[121] Lattanzio, C. & Serre, D. *Convergence of a relaxation scheme for hyperbolic systems of conservation laws.* Numerische Mathematik, 88(1), 121-134, 2001.

[122] Liu, X. D., & Lax, P. D. *Positive schemes for solving multi-dimensional hyperbolic systems of conservation laws II.* Journal of Computational Physics, 187(2), 428-440, 2003.

[123] Lax, P. D., & Liu, X. D. *Solution of two-dimensional Riemann problems of gas dynamics by positive schemes.* SIAM Journal on Scientific Computing, 19(2), 319-340, 1998.

[124] Lax, P. D. *Hyperbolic systems of conservation laws and the mathematical theory of shock waves*. Society for Industrial and Applied Mathematics, 1973.

[125] LeFloch, P. G. *Hyperbolic Systems of Conservation Laws: The theory of classical and nonclassical shock waves*. Springer Science & Business Media, 2002.

[126] LeVeque, R. J. *Finite volume methods for hyperbolic problems*. Cambridge university press, Vol. 31, 2002.

[127] LeVeque, R. J. *Numerical methods for conservation laws*. Basel: Birkhäuser, Vol. 214, 1992.

[128] Li, F., Xu, L., & Yakovlev, S. *Central discontinuous Galerkin methods for ideal MHD equations with the exactly divergence-free magnetic field*. Journal of Computational Physics, 230(12), 4828-4847, 2011.

[129] Liu, T. P. *The deterministic version of the Glimm scheme*. Communications in Mathematical Physics, 57, 135-148, 1977.

[130] Liu, X. D., & Lax, P. D. *Positive schemes for solving multi-dimensional hyperbolic systems of conservation laws II*. Journal of Computational Physics, 187(2), 428-440, 2003.

[131] Liu, X. D., & Lax, P. D. *Positive schemes for solving multi-dimensional hyperbolic systems of conservation laws*. Journal of Computational Physics, 5(2), 133-156, 1996.

[132] Loubere, R., Maire, P. H., Shashkov, M., Breil, J., & Galera, S. ReALE: *a reconnection-based arbitrary-Lagrangian–Eulerian method*. Journal of Computational Physics, 229(12), 4724-4761, 2010.

[133] Majda, A. Compressible Fluid Flow and Systems of Conservation Laws in Several Space Variables, Series: Applied Mathematical Sciences, Springer-Verlag New York, Vol. 53, 1984.

[134] Mancuso, S., Pereira, F., & de Souza, G. *Um Novo Método Euleriano-Lagrangeano para Aproximação de Leis de Conservação*. Trends in Computational and Applied Mathematics, 8(2), 277-286, 2007.

[135] Marchesin, D., & Plohr, B. J. *Wave structure in WAG recovery*. SPE journal, 6(2), 209-219, 2001.

[136] Mishra, S. *On the convergence of numerical schemes for hyperbolic systems of conservation laws*. In Proceedings of the International Congress of Mathematicians: Rio de Janeiro, 3641-3668, 2018.

[137] Modena, S., & Bianchini, S. *Convergence rate of the Glimm scheme*. Bull. Inst. Math. Acad. Sin, 11(1), 235-300, 2016.

[138] Natarajan, H., & Jacobs, G. B. *An explicit semi-Lagrangian, spectral method for solution of Lagrangian transport equations in Eulerian-Lagrangian formulations*. Computers & Fluids, 207, 104526, 2020.

[139] Orszag, S. A., & Tang, C. M. *Small-scale structure of two-dimensional magnetohydrodynamic turbulence*. Journal of Fluid Mechanics, 90(1), 129-143, 1979.

[140] Pérez, J. *Lagrangian-Eulerian approximate methods for balance laws and hyperbolic conservation law*. PhD thesis, 2015.

[141] Rossmanith, J. A., Bale, D. S., & LeVeque, R. J. *A wave propagation algorithm for hyperbolic systems on curved manifolds*. Journal of Computational Physics, 199(2), 631-662, 2004.

[142] Russell, T. F., & Celia, M. A. *An overview of research on Eulerian–Lagrangian localized adjoint methods (ELLAM)*. Advances in Water resources, 25(8-12), 1215-1231, 2002.

[143] Serre, D., & Silvestre, L. *Multi-dimensional Burgers equation with unbounded initial data: well-posedness and dispersive estimates*. Archive for Rational Mechanics and Analysis, 234, 1391-1411, 2019.

[144] Tadmor, E. *Entropy stable schemes*. Handbook of Numerical Analysis, Elsevier, Vol. 17, 467-493, 2016.

[145] Tadmor, E. *Entropy stability theory for difference approximations of nonlinear conservation laws and related time-dependent problems*. Acta Numerica, 12, 451-512, 2003.

[146] Toro, E. F. *Riemann solvers and numerical methods for fluid dynamics: a practical introduction*. Springer Science & Business Media, 2013.

[147] Vides, J., Audit, E., Guillard, H., & Nkonga, B. *Divergence-free MHD simulations with the HERACLES code*. In ESAIM: Proceedings EDP Sciences, Vol. 43, 180-194, 2013.

[148] Vila, J. P. *Convergence and error estimates in finite volume schemes for general multidimensional scalar conservation laws. I.* Explicite monotone schemes. ESAIM: Mathematical Modelling and Numerical Analysis, 28(3), 267-295, 1994.

[149] Wang, H., Liang, D., Ewing, R. E., Lyons, S. L., & Qin, G. *An ELLAM-MFEM solution technique for compressible fluid flows in porous media with point sources and sinks*. Journal of Computational Physics, 159(2), 344-376, 2000.

[150] Wintermeyer, N., Winters, A. R., Gassner, G. J., & Kopriva, D. A. *An entropy stable nodal discontinuous Galerkin method for the two dimensional shallow water equations on unstructured curvilinear meshes with discontinuous bathymetry*. Journal of Computational Physics, 340, 200-242, 2017.

[151] Woodward, P., & Colella, P. *The numerical simulation of two-dimensional fluid flow with strong shocks*. Journal of computational physics, 54(1), 115-173, 1984.

[152] Wu, K., & Shu, C. W. *Provably physical-constraint-preserving discontinuous Galerkin methods for multidimensional relativistic MHD equations*. Numerische Mathematik, 148(3), 699-741, 2021.

[153] Wu, K., & Shu, C. W. *Entropy symmetrization and high-order accurate entropy stable numerical schemes for relativistic MHD equations*. SIAM Journal on Scientific Computing, 42(4), A2230-A2261, 2020.

[154] Wu, K. *Positivity-preserving analysis of numerical schemes for ideal magnetohydrodynamics*. SIAM Journal on Numerical Analysis, 56(4), 2124-2147, 2018.

[155] Wu, K., & Shu, C. W. *A provably positive discontinuous Galerkin method for multidimensional ideal magnetohydrodynamics*. SIAM Journal on Scientific Computing, 40(5), B1302-B1329, 2018.

[156] Wu, K. *Positivity-preserving analysis of numerical schemes for ideal magnetohydrodynamics*. SIAM Journal on Numerical Analysis, 56(4), 2124-2147, 2018.

[157] Wu, K., & Shu, C. W. *A provably positive discontinuous Galerkin method for multidimensional ideal magnetohydrodynamics*. SIAM Journal on Scientific Computing, 40(5), B1302-B1329, 2018.

[158] Xiaxi, D., Gui-Qiang, C., & Peizhu, L. *Convergence of the fractional step Lax-Friedrichs scheme and Godunov scheme for the isentropic system of gas dynamics*. Communications in mathematical physics, 121, 63-84, 1989.

[159] Xing, Y., & Shu, C. W. *A survey of high order schemes for the shallow water equations. J. Math. Study*, 47(3), 221-249, 2014.